Bimodal antagonism of PKA by ARHGAP36

Thesis submitted in accordance with the requirements of the University of Liverpool for the degree of Doctor in Philosophy

By

Rebecca Louise Eccles

April 2016

Bimodal antagonism of PKA by ARHGAP36

Rebecca Louise Eccles

Abstract

PKA is a ubiquitous kinase whose activity is controlled by the second messenger cAMP downstream of GPCR signalling. PKA is a tetrameric holoenzyme composed of a homodimer of regulatory subunits (PKAR) which each bind and inhibit a catalytic subunit (PKAC). In this conformation the enzyme is inactive. Upon cAMP binding to the regulatory subunits, the catalytic subunits are released and can phosphorylate their substrates. Regulation of PKA is mainly centred around PKAR, in a large part via binding of the A-kinase anchoring proteins (AKAPs). Here I characterise a novel Rho GAP, ARHGAP36, and describe how it directly binds the PKA catalytic subunits. This binding is via a pseudosubstrate motif, which inhibits PKAC activity by blocking access to substrates. In addition to this, ARHGAP36 also mediates polyubiquitylation and degradation of PKAC. This is the first description of ubiquitin-mediated degradation of PKAC. Surprisingly for a cytosolic protein, degradation is not mediated by the proteasome but by the endolysosomal pathway, which is usually reserved for transmembrane proteins. This bimodal antagonism of PKAC by ARHGAP36 leads to suppression of a variety of PKA signalling responses downstream. I found that ARHGAP36 expression is developmentally regulated and restricted to embryonic skeletal muscle. It is, however, upregulated in neuroblastoma cell lines, where I could show that ARHGAP36 modulates PKAC activity and stability in an endogenous setting.

Table of Contents

List of Figures

List of Tables

Abbreviations

36i	ARHGAP36 inhibitor
AC	Adenyl cyclase
ACTH	Adrenocorticotropic hormone
ADP	Adenosine diphosphate
AKAP	A-kinase anchoring protein
AKAR	A-kinase activity reporter
ALK1	Anaplastic lymphoma kinase
APC	Anaphase promoting complex
AQP	Aquaporin
Arp2/3	Actin-related protein-2/3
atg	Autophagy related gene
ATP	Adenosine triphosphate
AVP	Arginine vasopressin
Baf	Bafilomycin
BSA	Bovine Serum Albumin
cAMP	Cyclic adenosine monophosphate
CASA	Chaperone-assisted selected autophagy
CBP	CREB binding protein
CFP	Cerulean Flourescent Protein
CHX	Cycloheximide
CK1	Casein kinase 1
CLN5	Ceroid lipofuscinosis neuronal protein 5
CMA	Chaperone mediated autophagy
CRE	cAMP response element
CREB	Cre Response Element Binding Protein
CREM	CRE modulator
CRH	Corticotropin-releasing hormone
DMSO	Dimethyl sulfoxide
DNA	Deoxyribonucleic acid
DUB	Deubiquitylating Enzyme
EEA1	Early Endocytic Antigen 1
EGFR	Epidermal growth factor receptor
eMI	Endosomal microautophagy
EMT	Epithelial-mesenchymal transition
EPAC	Exchange proteins acrivated by cAMP
Epo	Epoxomicin
ER	Endoplasmic reticulum
ESCRT	Endosomal complexes required for transport
EtOH	Ethanol
FBS	Fetal Bovine Serum
FL-HCC	Fibrolamellar hepatocellular carcinoma
FRET	Flourescence resonance energy transfer
GAP	GTPase activating protein
GDI	GTPase dissociation inhibitor
GDP	guanosine diphosphate
GEF	GTPase exchange factor
GFP	Green Flourescent Protein

GliA	Gli Activator
GliR	Gli Repressor
GPCR	G protein coupled receptor
GSK3	Glycogen synthase kinase 3
GST	Gluthathione S Transferase
GST	Glutathione S-transferase
GTP	Guanosine triphosphate
HECT	Homology to E6AP carboxy terminus
Hh	Hedgehog
HPA	Hypothalamus-Pituitary-Adrenal
iBAQ	Intensity based absolute quantitation
IBMX	3-isobutyl-1-methylxanthine
ICER	Inducible CRE repressor
IF	Immunofluorescence
IgG	Immunoglobulin G
IP	Immunoprecipitation
ITC	Isothermal titration calorimetry
KO	Knock out
Leu	Leupeptin
LIR	LC3 interacting region
MAP	Microtubule associated protein
MC2R	Melanocortin receptor 2
MET	Mesenchymal-epithelial transition
mTOR	Mammalian target of rapamycin
MVB	Multivesicular Bodies
NCL	Neuronal ceroid lipoduscinoses
NEM	N-Ethylmaleimide
NES	Nuclear exclusion signal
OTU	Ovarian tumour protease
P/S	Penicillin Streptomycin
PACT	Pericentrin-AKAP-450 centrosomal targeting
PAK	p21 activated kinase
PBS	Phosphate Buffered Saline
PBS++	Phosphate Buffered Saline supplemented with Ca and Mg
pCREB	Phosphorylated Cre Response Element Binding Protein
PDE	Phosphodiesterase
PFA	Paraformaldehyde
PI3K	Phosphoinositide 3-kinase
PKA	Protein Kinase A
PKAC	Protein Kinase A Catalytic Subunit
PKAR	Protein Kinase A Regulatory Subunit
PKI	Protein Kinase Inhibitor
RBR	Ring between ring
RING	Really interesting new gene
RSK1	p90 Ribosomal S6 kinase-1
sAC	Soluble adenyl cyclase
SAG	Smoothened AGonist
SCF	Skp Cullin F-box
SFRS17A	Splicing factor arginine/serine-rich 17A
Shh	Sonic Hedgehog

SILAC	Stable isotope labelling by amino acids in cell culture
Smo	Smoothened
SRM	Selected Reaction Monitoring
StAR	Steroidogenic acute regulatory protein
SuFu	Suppressor of Fused
UBD	Ubiquitin binding domain
UCH	Ubiquitin C terminal hydrolase
UIM	Ubiquitin interacting motif
USP	Ubiquitin specific peptidase
WASP	Wiskott-Aldrich syndrome protein
WAVE1	(WASP)-family verprolin homologous protein 1
WB	Western Blot
YFP	Yellow Flourescent Protein
ZO-1	Zona occuldens-1

Acknowledgements

Firstly, thanks to Oliver Rocks, for this project, for the freedom to develop as a scientist and for always having an open door. Thank you to Sylvie Urbé for taking a chance on me over six years ago, and to you and Mike Clague for setting me on this path and teaching me so much. Thanks also for rescuing me from German bureaucracy and continuing to supervise me.

Thanks go to our many collaborators. Especially to Oli Daumke and the Daumke lab members past and present, Stephan in particular. Thanks to Annette Hammes and Nora Mecklenburg for help with *in situs* and Hedgehog advice. Thanks to the Klussmann lab for PKA advice and the generous sharing of reagents. Special thanks to my mass spec guru Erik, for always being up for one more experiment, and to Patrick for coming through on my last minute requests. Thank you also to all the past and present Liverpool lab members, especially to Claire, Amos and Yvonne, for continued support.

Thank you to my ever-expanding AG Rocks family, for support both in and out of the lab, especially to the original Rock stars Caro, Markus, Matti and Juliane. I wouldn't have survived in Berlin without you. Thanks again to Markus and Caro who helped me massively with this project. Huge thanks also go to Maciej for all the help, for trying to be a cell biologist, and for continuing the ARHGAP36 story. To all the Rocks lab members past and present, thank you for making it such a great place to do science, especially Sreusch, Vicky, Linda, Lennart, Phillip, Laura R and Moritz. Thanks also to the many weird and wonderful people I met at the MDC who helped me along the way.

Thanks to John for imparting your post doc wisdom. To Laura and Vicky, thank you for always entertaining and supporting me, and making Berlin an even better place. Thank you to Heather for always being there for me and trying to understand the science!

Thank you to my family for their unwavering belief in me, I hope I made you proud. Last but not least thank you to James for putting up with my craziness and getting me through. I couldn't have done it without you.

Chapter 1. Introduction

1.1. Signal Transduction Pathways

Cellular behaviour is controlled by the concerted action of signal transduction pathways, which relay signals from the outside in. These pathways were once believed to be linear and unidirectional, however crosstalk between pathways and complex regulatory feedback loops are now known to be the norm. Amongst the key players in signal generation are kinases and GTPases. These signalling cascades are not just switched on or off; the signals these proteins propagate must also be precisely regulated in a spatiotemporal manner. Where, when and for how long these signalling proteins are active is of extreme importance. Thus they can be recruited to specific subcellular localisations and assembled in macromolecular complexes together with particular regulators that can tightly control their activity.

Signals must be generated, however they must also be dynamically regulated. The interplay of proteins controlling activation and attenuation is key. Reversible post-translational modification (PTM) of proteins is a versatile way to modify protein behaviour. PTMs can be used to initiate, terminate or tweak signalling responses. The best-studied PTM is phosphorylation, where the action of kinases is reversed by phosphatases.

A further layer of regulation is the degradation of signalling components themselves. This is controlled by another reversible PTM, ubiquitylation, which mediates subsequent targeting of proteins to the respective degradation machineries. This is also a tightly regulated, dynamic process. Phosphorylation can prime for ubiquitylation and ubiquitin itself can be phosphorylated, thus allowing further complexity in the regulation of protein turnover and thus signalling.

In this thesis I will describe the regulation of a signalling protein, Protein Kinase A (PKA), by both inhibitory and degradative mechanisms. I will begin by introducing first the regulation of Rho GTPases, second ubiquitylation and its roles in proteasomal and lysosomal degradation, and lastly phosphorylation and kinases with a particular focus on Protein Kinase A.

1.2. Rho GTPases

Rho GTPases are master regulators of the actin cytoskeleton. Like other small GTPases of the Ras-like superfamily, they are molecular switches that cycle between inactive GDP and active GTP bound states. Only in the latter state can they bind and relay signals to downstream signalling proteins.

Rho GTPases were first linked to the actin cytoskeleton through the pioneering studies by Anne Ridley and Alan Hall: Injection of RhoA, Rac1 and Cdc42 into Swiss 3T3 cells led to formation of stress fibres, lamellipodia and filopodia respectively (Hall, 1998; Ridley & Hall, 1992). However, in the last 20 years it has become increasingly obvious that Rho signalling is not so simple. In contrast to the classical models where RhoA, Rac1 and Cdc42 were thought to cause distinct cellular behaviours, and to be active in different parts of the migrating cell (Ridley, 2001; Raftopoulou & Hall, 2004), recent studies using FRET biosensors showed all three Rho proteins to be activated at the leading edge (Machacek *et al*, 2009). The Rho proteins have also been implicated in a wide range of other cellular processes, such as cell cycle progression, cell survival, vesicular trafficking and transcriptional regulation (Vega & Ridley, 2008). So how is signalling specificity achieved?

The GTPase cycle is tightly controlled by three main factors: GTPase activating proteins (GAPs), Guanine nucleotide exchange factors (GEFs), and Rho guanine dissociation inhibitors (GDIs) (Figure 1.1) (Bos *et al*, 2007). GEF proteins are positive regulators, catalysing GTP loading (Rossman *et al*, 2005), whereas GAP proteins and GDI proteins act as negative regulators. GAPs increase the rate of GTP hydrolysis, whilst GDIs extract the Rho proteins from the membrane competent signalling pool and keep them bound in the inactive GDP state (Tcherkezian & Lamarche-Vane, 2007; Garcia-Mata *et al*, 2011). Of the twenty Rho proteins, 12 of them are classically activated and can be differentially regulated by GAPs and GEFs. In contrast, eight of the Rho proteins are atypical and are mostly GTP bound (Heasman & Ridley, 2008). Spatio-temporal control of the Rho GTPases is required to achieve the right signalling outcome. Approximately 80 GAPs, 60 GEFs and three GDIs provide numerous possibilities for fine-tuning classical Rho protein activity (Figure 1.2). These multi-domain regulatory proteins have the potential to specify signalling by targeting Rho proteins to distinct cellular localisations, and act as molecular scaffolds to recruit further signalling proteins. Determining the GTPase specificity, localisation and binding partners of these proteins will help to establish

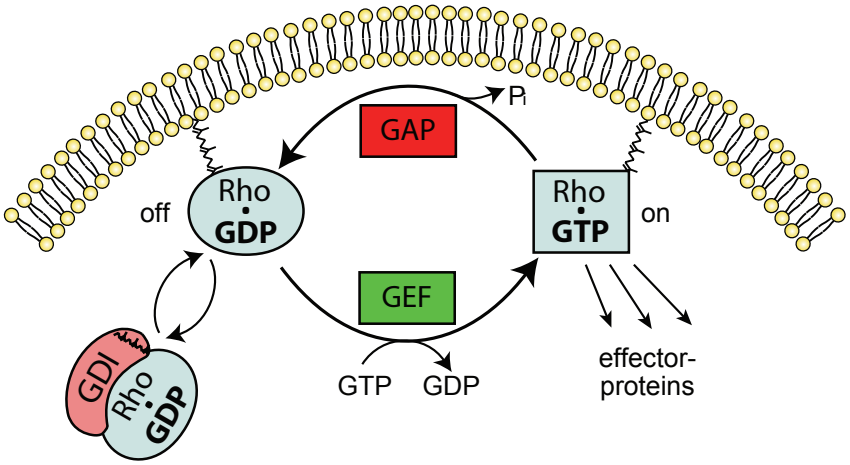

Figure 1.1 The Rho GTPase activation cycle
The Rho proteins are molecular switches which signal from membranes. They associate with membranes through their lipid anchors. The Rho GTPase cycle can be controlled negatively by GTPase activating proteins (GAPs) and positively by Guanine nucleotide exchange factors (GEFs). Guanine nucleotide dissociation inhibitors (GDIs) extract the Rho proteins from the membrane and and keep them in an inactive cytosolic complex.

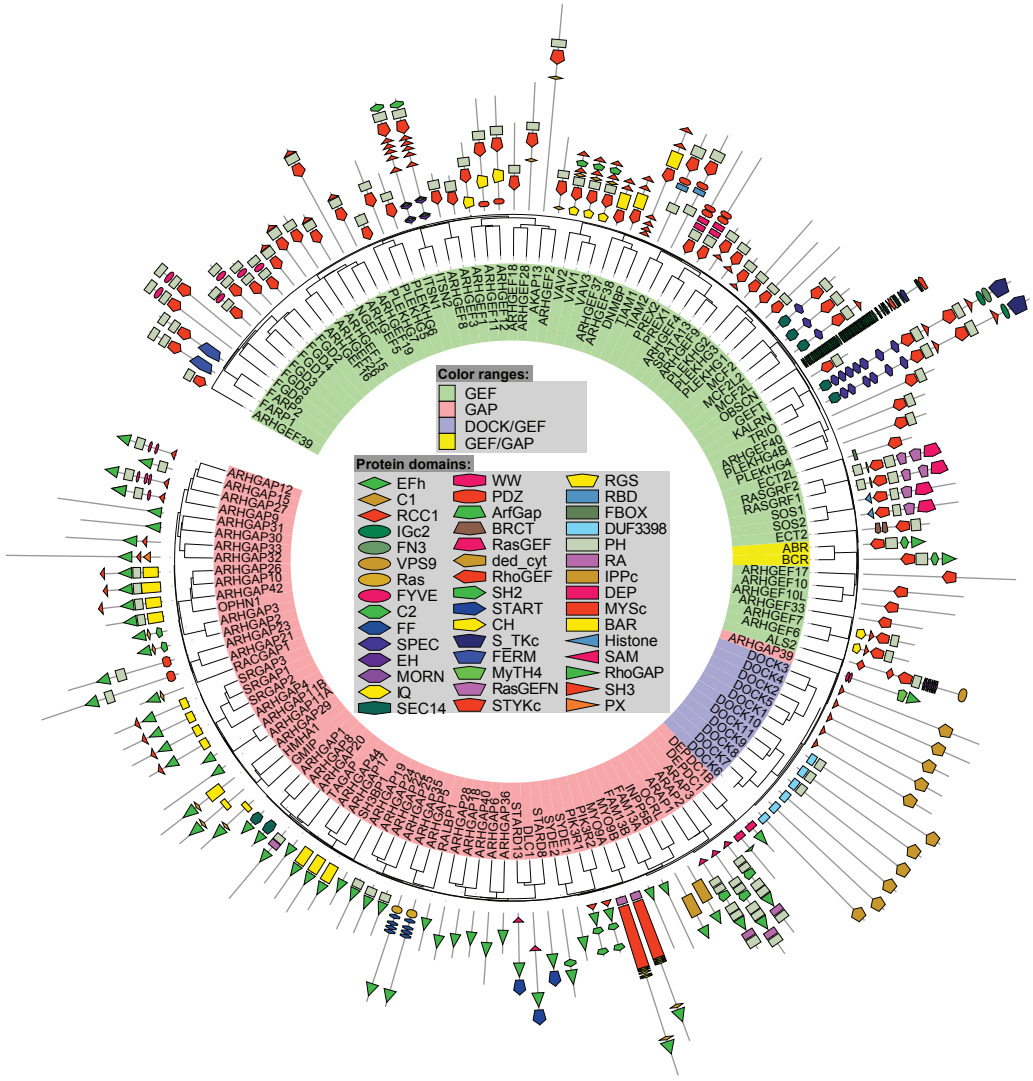

Figure 1.2 Modular domain architecture of the human RhoGEF and RhoGAP proteins. Rho guanine nucleotide exchange factors (RhoGEFs) and Rho GTPase activating proteins (RhoGAPs) are multi-domain scaffold proteins that provide subcellular targeting information and connect Rho GTPases to other signaling pathways, thereby specifying Rho signalling. Figure kindly provided by Oliver Rocks.

mechanisms of Rho regulation, and the crosstalk with other signalling pathways. Many of these proteins are uncharacterised.

Prior to the start of my PhD, my supervisor Oliver Rocks had carried out a systematic screen to characterise all the Rho GAP and GEF proteins, especially their binding proteins. This was done by mass spectrometry using epitope tagged GAP and GEF proteins as bait. In this interactome screen, an uncharacterised GAP, ARHGAP36, was found to interact with Protein Kinase A, as well as E3 ubiquitin ligases (Rocks and Pawson, manuscript in preparation). The regulation of PKAC activity and stability by ARHGAP36 will be the focus of this thesis.

1.3. Ubiquitylation and cellular degradation pathways

Nowadays it is widely accepted that protein lifetimes are dynamically regulated, however, this was not always the case. Seminal experiments by Rudolf Schoenheimer challenged the commonly held belief that proteins are stable entities and paved the way for modern day protein turnover experiments. He fed mice with stable isotope labelled amino acids and found that while some were excreted in urine others were incorporated into tissues. This was the first indication that protein turnover is dynamically regulated (Schoenheimer *et al*, 1939).

The lysosome was then discovered in 1953 (De Duve *et al*, 1953; De Duve & Wattiaux, 1966) and was thought to be responsible for all cellular protein degradation. However only a fraction of proteins were stabilised upon inhibition of the lysosome using weak bases (Poole *et al*, 1977). Reticulocytes were still able to degrade haemoglobin, despite being devoid of lysosomes (Rabinovitz & Fisher, 1964). This process also required ATP and took place at neutral pH as opposed to the acidic pH required for lysosomal degradation (Etlinger & Goldberg, 1977). It was thus hypothesised that another non-lysosomal mechanism for degradation must exist. This led to the eventual discovery of the proteasome (Tanaka *et al*, 1983; Hough *et al*, 1986; Hough & Rechsteiner, 1986; Ciechanover, 2005). Later on I will describe the three main pathways that eukaryotic cells use to degrade proteins: proteasomal degradation, endolysosomal degradation, and autophagy. But first I will turn to the unifying feature that is central to all of them: ubiquitin (Clague & Urbé, 2010).

1.3.1. Ubiquitin

Ubiquitylation involves the post-translational addition of the 76 amino acid protein ubiquitin to a lysine residue within the substrate protein. This results in the formation of an isopeptide bond between the lysine side chain and the exposed carboxyl terminal glycine tail of ubiquitin (Vijay-Kumar *et al*, 1987; Pickart & Eddins, 2004). Ubiquitylation was first recognised as a signal targeting proteins for proteasomal degradation, however, today it is known to regulate a variety of cellular events, by affecting protein activity, localisation and interaction (Komander & Rape, 2012).

Addition of one ubiquitin molecule to a substrate is termed monoubiquitylation. Complexity in the ubiquitin system is achieved by the ability of multiple ubiquitin molecules to be conjugated to a substrate. Multi-monoubiquitylation can occur via addition of single ubiquitin molecules to multiple different lysines within a substrate. Ubiquitin itself contains seven lysines: K6 K11, K27, K29, K33, K48, K63. Each of these lysines can be utilised for conjugation of further ubiquitin molecules. Linear ubiquitylation can also be achieved via a peptide bond between the C-terminal glycine of one ubiquitin and the N-terminal methionine (M1) of another (Walkzak et al 2012). Polyubiquitin chains can then be formed in a homotypic or heterotypic manner. Homotypic when the same linkage is utilised within a chain, heterotypic when differential linkage types are utilised. Heterotypic chains can be branched, if one ubiquitin is ubiquitylated at two or more sites (Ikeda and Dikic 2008, Behrends and Harper 2011) (Figure 1.3). The recent discovery that ubiquitin itself can be post-translationally modified, via phosphorylation or acetylation, further diversifies the ubiquitin code (Herhaus and Dikic 2015, Swatek and Komander 2016).

All chain linkages have been identified in HEK293 cells, with K48 (52%) and K63-linked chains (38%) being most abundant (Dammer *et al*, 2011). From the total ubiquitin pool in HEK293 cells, 26% was free ubiquitin, 11% incorporated in polyubiquitin chains, and the majority was identified as monoubiquitylated-conjugates (Kaiser *et al*, 2011).

Different ubiquitin chain linkages have different structural properties and thus allow differential recognition by ubiquitin binding domains (UBDs) of which there are over 20 different types in the human genome (Dikic *et al*, 2009; Scott *et al*, 2015). K48 and K11 linked chains are tightly packed together with the different ubiquitin molecules contacting each other (Cook *et al*, 1994; Bremm *et al*, 2010). In contrast, K63 and M1-linked chains are much more open with no contact between the

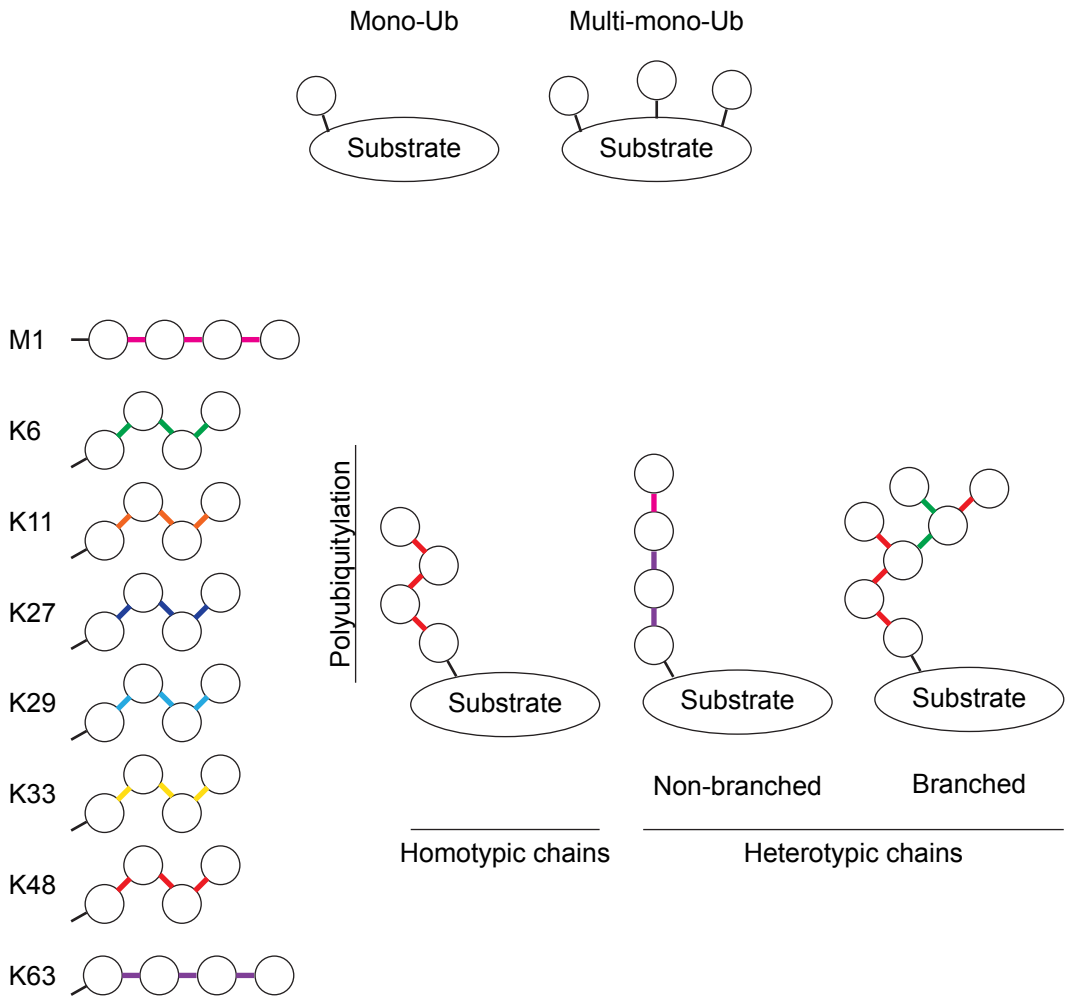

Figure 1.3 Types of ubiquitylation
Proteins can be mono- or multi-monoubiquitylated or polyubiquitylated. There are then eight different types of ubiquitin chain linkage, with different topologies that can be formed. Polyubiquitylation can be homotypic or heterotypic. Heterotypic chains can be nonbranched (shown is K63 and K11), or branched (shown is K48 and K6). Adapted from (Kulathu & Komander, 2012; Heride *et al*, 2014).

different ubiquitin molecules (Komander *et al*, 2009b). However even with these similarities, there are UBDs that have specificity for K63 or M1-linked chains (Husnjak & Dikic, 2012). Many UBDs bind a hydrophobic patch in ubiquitin around Ile44, which may suggest that binding of several ubiquitin binding proteins to the same ubiquitin is mutually exclusive.

1.3.2. The ubiquitylation cascade

Ciechanover, Hershko, Rose and colleagues characterised the machinery by which a chain of ubiquitin molecules are conjugated to a substrate leading to its degradation (Hershko *et al*, 1980). They discovered that ubiquitylation requires the action of three different classes of enzymes in a multistep process (Ciechanover *et al*, 1981, 1982; Hershko *et al*, 1983). The number of enzymes in each class increases dramatically; there are two E1 ubiquitin activating enzymes, around 40 E2 ubiquitin conjugating enzymes and over 600 E3 ubiquitin ligase enzymes. (Figure 1.4)

The two E1 enzymes, UBA1 and UBA2, catalyse the ATP dependent activation of the C-terminus of ubiquitin via acyl-adenylation. This is followed by the conjugation of the activated ubiquitin to the active site cysteine of the E1 via a thioester linkage. The ubiquitin is then transferred to a similar cysteine within the active site of the E2 via a *trans*-thioesterification reaction. The E3 ligase, in one way or another, then allows the transfer of ubiquitin to the substrate. The high number of E3 ligases is thought to allow substrate specificity.

E3 ligases can be split into three main families, HECT, RING or RING-like, and RBR. HECT (Homology to E6AP carboxy terminus) family E3 ligases have a two-step mechanism. They contain a catalytic cysteine, which accepts the ubiquitin from the E2 before transferring it to the substrate. They catalyse a wide range of chain linkages (Kim & Huibregtse, 2009).

RING (really interesting new gene) family E3 ligases transfer the ubiquitin directly from the E2 to the substrate. The same is true for RING-like U-box E3 ligases (Metzger *et al*, 2014). They therefore act mostly as scaffolds, and together with the E2 determine linkage specificity (David *et al*, 2011). As well as single functioning units, RING E3 ligases can also exist as multi-subunit E3 ligases (Li *et al*, 2008), such as the Cullin-Ring ligases, which associate with substrate receptors and

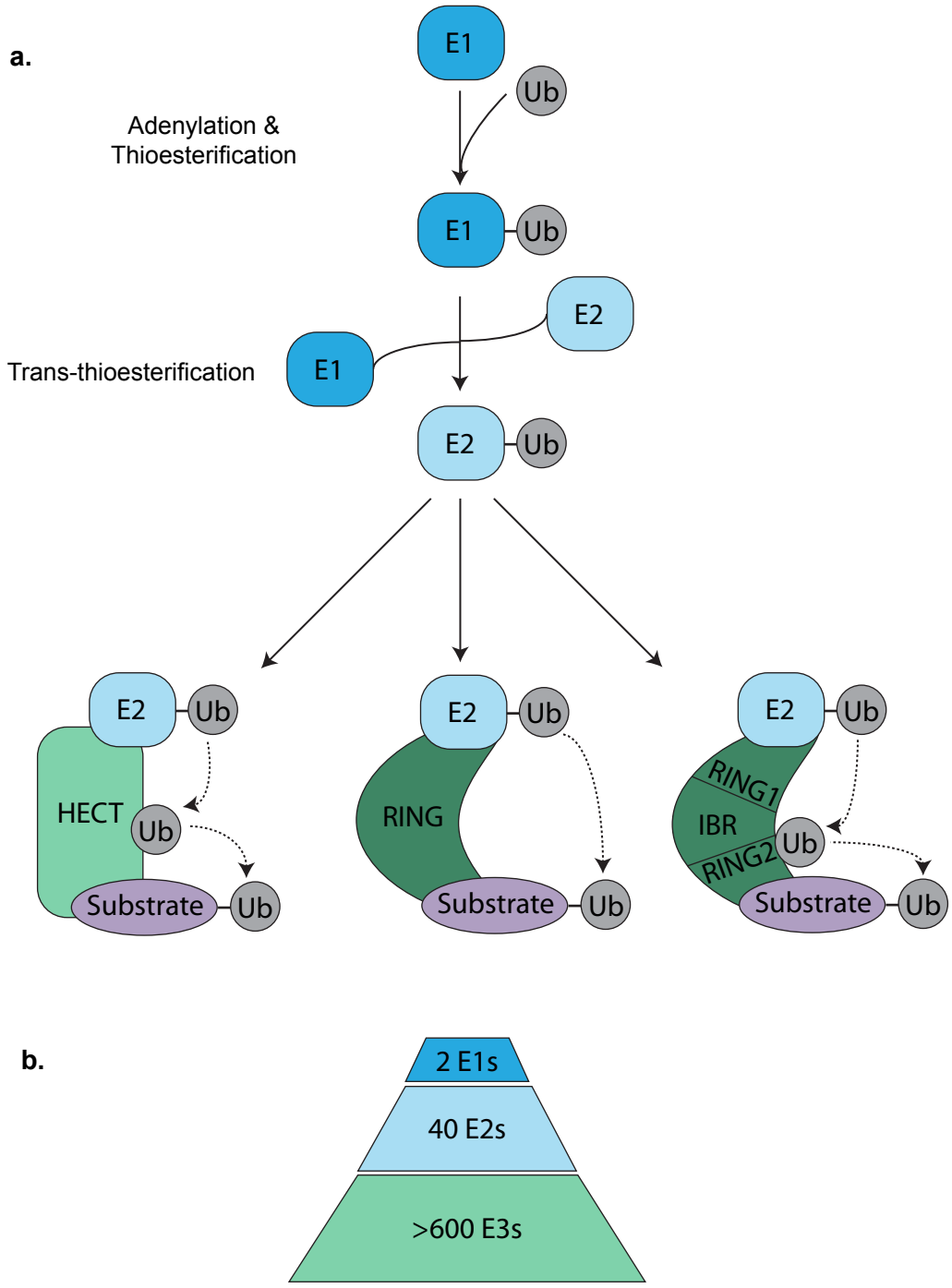

Figure 1.4 The ubiquitylation cascade
(**a**) E1 ubiquitin activating enzymes mediate adenylation and thioesterification of ubiquitin. Ubquitin is then transferred from the E1 to the E2 ubiquitin conjugating ezyme by a trans-thioesterification reaction. There are three different types of E3 ligase. HECT ligases accept the ubiquitin from the E2 before transferring it to the substrate. RING ligases transfer ubiquitin directly from the E2 to the substrate. Ring-between-RING (RBR) ligases bind E2s via a RING domain but also accept ubiquitin before transferring it to substrates in a HECT like manner. (**b**) The number of enzymes increases dramatically in each class. Adapted from (Winklhofer, 2014; Heride et al, 2014)

adapter proteins (Petroski & Deshaies, 2005). In the case of the SCF complex (Skp1, Cullin1, F-box), Skp1 acts as an adaptor between Cul1 and the F-box-protein, which then provides substrate specificity, whilst the Cullin protein links to the Ring E3 Rbx1 (Cardozo & Pagano, 2004). ßTRCP is one such F-box protein that mediates the degradation of a large number of signaling proteins, including the Gli and β-catenin transcription factors (see below 1.4.3.3 and 4.3.8).

RBR (RING-between-RING) family ligases, of which there are 18 in the human genome, were only recently identified as a distinct group (Eisenhaber *et al*, 2007). They have properties of both RING and HECT ligases (Aguilera *et al*, 2000). They bind E2s via a RING domain but also require a conserved catalytic cysteine to transfer ubiquitin to substrates (Wenzel *et al*, 2011).

1.3.3. Deubiquitylases

Ubiquitylation is a reversible process. Deubiquitylating enzymes (DUBs) oppose the action of E3 ligases. DUBs play various roles in ubiquitin regulation. Ubiquitin is transcribed from four different genes, and is expressed either as a linear fusion of multiple ubiquitin molecules, or ubiquitin fused to the ribosomal proteins (Wiborg *et al*, 1985; Baker & Board, 1991). DUB activity is thus required to generate free ubiquitin. DUBs are known to associate with the degradation machineries and recycle ubiquitin from substrates committed for degradation in order to contribute to ubiquitin homeostasis (Kimura *et al*, 2009; Clague *et al*, 2012). They can also rescue substrates from their fate by removing or editing ubiquitin chains. DUBs are known to associate with E3 ligases and these interactions may play a role in chain editing or protect E3s from degradation due to autoubiquitylation. The latter is the case for USP7 and the E3 ligase Mdm2, which is responsible for regulating p53 stability (Li *et al*, 2003).

There are around 80 active DUBs in the human genome that fall into five classes. Four of them are cysteine proteases: Ubiquitin C terminal hydrolases (UCH), Ubiquitin specific peptidases (USP), ovarian tumour proteases (OTU) and the Josephins (Komander *et al*, 2009a). The final class, the JAMM/MPN+ DUBs, are zinc metalloproteases. DUBs can cleave the isopeptide bond of the terminal ubiquitin of a chain (exopeptidase activity) or also cut within the chain (endopeptidase activity). DUBs have different specificities for chain linkages, with

some only cleaving one chain-type, whereas others will non-discriminately cleave all linkages (Clague *et al*, 2013; Mevissen *et al*, 2013).

Substrate specificity and roles of the DUBs can also be regulated by their subcellular localisation. Many have intrinsic localisation properties and can be found at distinct locations in the cell, such as the plasma membrane, nucleolus, centrosome, microtubules, ER, and mitochondria (Urbé *et al*, 2012). For example, USP33 is a DUB that is associated with the ER, COP coated vesicles and the *cis*-Golgi (Thorne *et al*, 2011). USP19 and USP30 are the only mammalian DUBs that contain transmembrane domains. USP19 is tethered at the ER and plays a role in ER associated degradation (ERAD) there (Hassink *et al*, 2009). USP30 is targeted to the outer mitochondrial membrane where it opposes ubiquitylation of Parkin substrates and can also regulate mitochondrial morphology (Nakamura & Hirose, 2008; Bingol *et al*, 2014; Liang *et al*, 2015).

1.3.4. The Proteasome

The majority of cytosolic proteins are degraded by the proteasome, a large multimeric complex that is essentially an assembly of proteases (Figure 1.5). It is composed of two subunits: the 20S core particle and the 19S regulatory particle. The core particle is made up of α and β subunits, arranged as a four-stacked ring structure $\alpha_7\beta_7\beta_7\alpha_7$. The β-rings form an inner hydrolytic chamber and the outer α-rings form a gate to the inner chamber where degradation occurs. The core particle combines three different proteolytic activities contributed by the β 1, β 2 and β5 subunits, which cleave proteins after acidic, basic or hydrophobic residues respectively (Finley *et al*, 2016). Proteasome activity can thus be inhibited by compounds targeting these subunits, such as epoxomicin, which inhibits the chymotrypsin-like activity (Meng *et al*, 1999; Kisselev & Goldberg, 2001). Bortezomib, another inhibitor of the chymotrypsin-like activity, has successfully been used in the clinic in the treatment of multiple myeloma (Goldberg, 2012).

The regulatory particle is composed of a hexameric ring of AAA-ATPases, which mediate the unfolding of substrates and control entry into the core particle. This unfolding is a key prerequisite for proteasomal substrates, and also prevents the non-discriminate degradation of cytosolic proteins. The core particle can be capped at one or both ends by a regulatory particle (Voges *et al*, 1999). Aside from the six AAA-ATPases the regulatory particle contains 13 other components. Three of these,

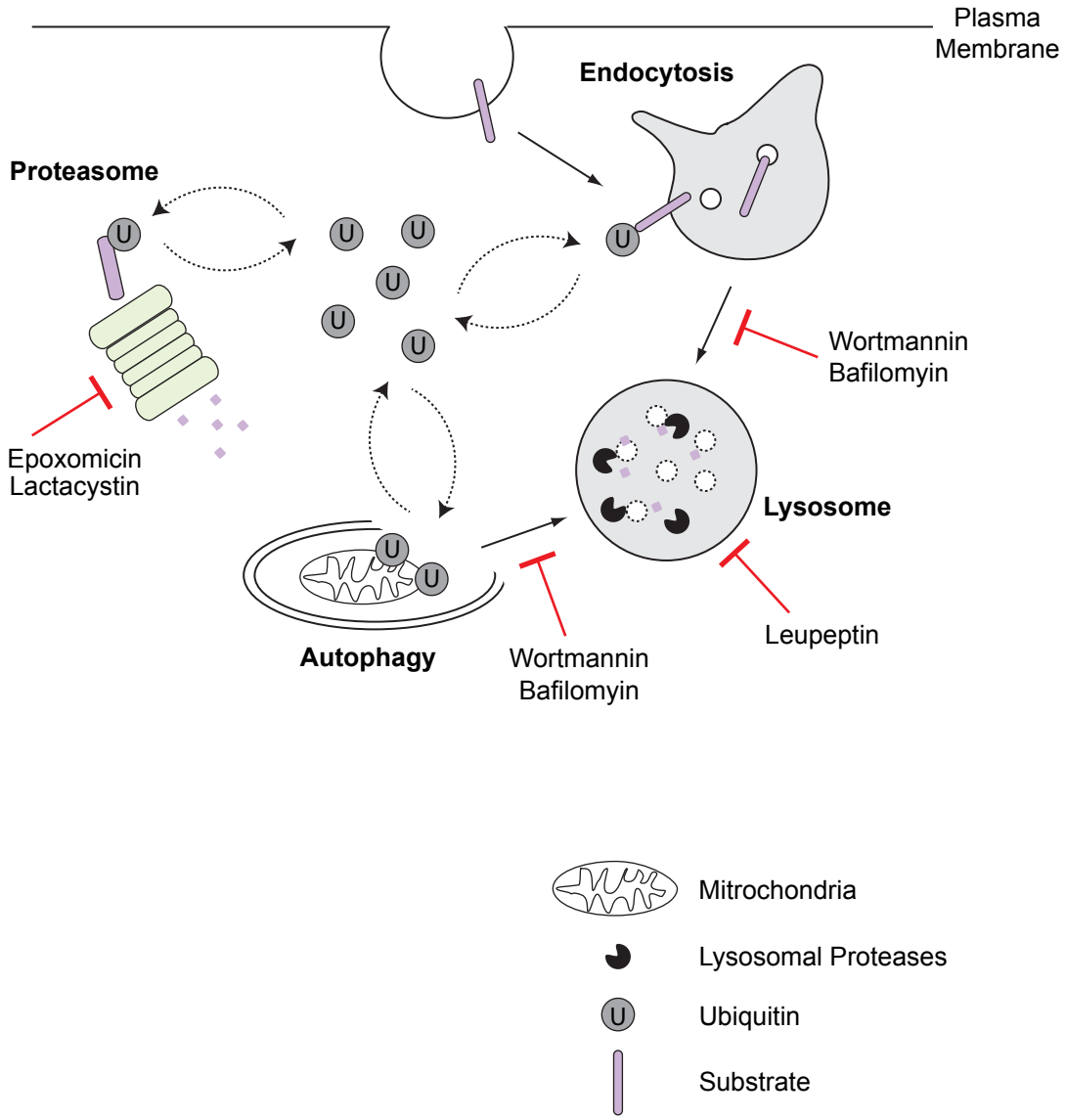

Figure 1.5 The main degradation pathways and their inhibitors
Ubiquitylation is a unifying feature of the different degradation pathways. Endocytosed and autophagosome engulfed cargo are both degraded in the lysosome and therefore inhibitors have an effect on both pathways. Adapted from (Clague & Urbé, 2010)

Rpn10, Rpn13 and Rpn1, have been shown to bind both polyubiquitin chains and a DUB each (van Nocker *et al*, 1996; Husnjak *et al*, 2008; Finley *et al*, 2016; Shi *et al*, 2016). Rpn11, a JAMM/MPN+ metalloprotease DUB, is also a component of the regulatory particle and associates with Rpn10. It is able to cleave the isopeptide bond between the substrate and the final ubiquitin and thus removes chains 'en bloc' from substrates before their degradation (Yao & Cohen, 2002). Two further DUBs are associated with the regulatory particle, USP14 and UCH37. These are thought to be involved in rescuing substrates from degradation via chain editing (Qiu *et al*, 2006; Lee *et al*, 2011; Finley, 2009). The receptor for UCH37 is Rpn13 (Qiu *et al*, 2006), whilst the yeast orthologue of USP14, Ubp6 is recruited to Rpn1, thus suggesting chain recognition is coupled to deubiquitylation (Husnjak *et al*, 2008; Chen & Walters, 2015; VanderLinden *et al*, 2015; Sahtoe *et al*, 2015; Shi *et al*, 2016).

The canonical ubiquitin chains associated with proteasomal degradation are linked via K48, and K48 linked tetra-ubiquitin is sufficient to target substrates for proteasomal degradation (Thrower *et al*, 2000). However, all chain linkages except for K63 were found to accumulate in HEK293T cells upon proteasome inhibition (Dammer *et al*, 2011). Interestingly all the DUBs of the proteasome can cleave K63 linked chains, which may provide a proof reading mechanism to prevent proteasomal degradation of substrates with this chain type (Jacobson *et al*, 2009).

K11 linked chains formed by the anaphase promoting complex (APC) E3 ligase in association with the K11-specific E2 UBE2S have been shown to mediate proteasomal degradation of cell cycle regulators during mitosis (Jin *et al*, 2008; Williamson *et al*, 2009; Matsumoto *et al*, 2010; Song & Rape, 2010). K27 linked chains have also been suggested to regulate proteasomal degradation of Parkin substrates during mitophagy (Geisler *et al*, 2010). K6 linked chains have been implicated in Parkin-mediated mitophagy (Durcan *et al*, 2014; Ordureau *et al*, 2015).

In addition to playing a clear role in endolysosomal degradation (see below), K63-linked chains have been shown to have non-degradative roles in some signal transduction pathways (Conze *et al*, 2008; Komander & Rape, 2012). This is particularly well established for the NFkB signaling cascade which also employs M1 linked chains (Iwai & Tokunaga, 2009; Tokunaga *et al*, 2009). K63 and K6-linked chains have also been implicated in DNA damage repair mechanisms (Morris & Solomon, 2004; Thorslund *et al*, 2015). K29 and K33 linked chains have been

shown to have an inhibitory effect on AMPK (AMP-activated protein kinase) (Al-Hakim *et al*, 2008). Finally, K33 linked chains have also been implicated in T cell receptor signalling and post-Golgi trafficking (Huang *et al*, 2010; Yuan *et al*, 2014).

1.3.5. Endolysosomal degradation

The endolysosomal pathway is the main route by which plasma membrane proteins, such as receptors and channels, are turned over by the cell. Endocytosed membrane proteins enter an early endosomal compartment from where they can either be recycled back to the plasma membrane or be sorted for degradation in the lysosome (Figure 1.6). The lysosome contains a collection of proteases, which require an acidic pH for their action (Haider & Segal, 1972). The acidic environment of the lysosome is achieved via the vacuolar H+-ATPase (v-ATPase) (Schneider, 1981). Lysosomal degradation can be inhibited in a variety of manners (Figure 1.5). Bafilomycin can be used to specifically inhibit the v-ATPase, thus preventing acidification of the lysosome (Yoshimori *et al*, 1991). Weak bases such as chloroquine and NH_4Cl which accumulate in the lysosome can also be used to abolish acidification (Poole *et al*, 1977). Alternatively, leupeptin can be used to inhibit lysosomal proteases (Libby & Goldberg, 1978).

Trafficking along the endocytic pathway is controlled by the endosomal sorting complexes required for transport (ESCRT) machinery, which can be split into four groups: ESCRT-0 –I –II –III. The first three ESCRT complexes all contain ubiquitin-binding motifs (UBD) with which they engage with ubiquitylated cargo (Williams & Urbé, 2007; Hurley & Stenmark, 2011).

ESCRT-0 is composed of two proteins, HRS and STAM, which initially select ubiquitylated cargo at the endosomal membrane. They bind to each other via coiled coil domains (Asao *et al*, 1997; Prag *et al*, 2007) and to ubiquitin via their ubiquitin interacting motifs (UIM) and VHS domains (Urbé *et al*, 2003; Mizuno *et al*, 2003; Hong *et al*, 2009; Ren & Hurley, 2010). Together they contain four (mammals) or five (yeast) ubiquitin binding modules. HRS is targeted to early endocytic compartments via its FYVE domain that binds with high specificity to Phosphatidylinositol 3-phosphate (PI3*P*), the main phosphoinositide on early endosomes (Gillooly *et al*, 2000; Raiborg *et al*, 2001). HRS then binds clathrin and mediates the sorting of proteins into clathrin-coated microdomains of early

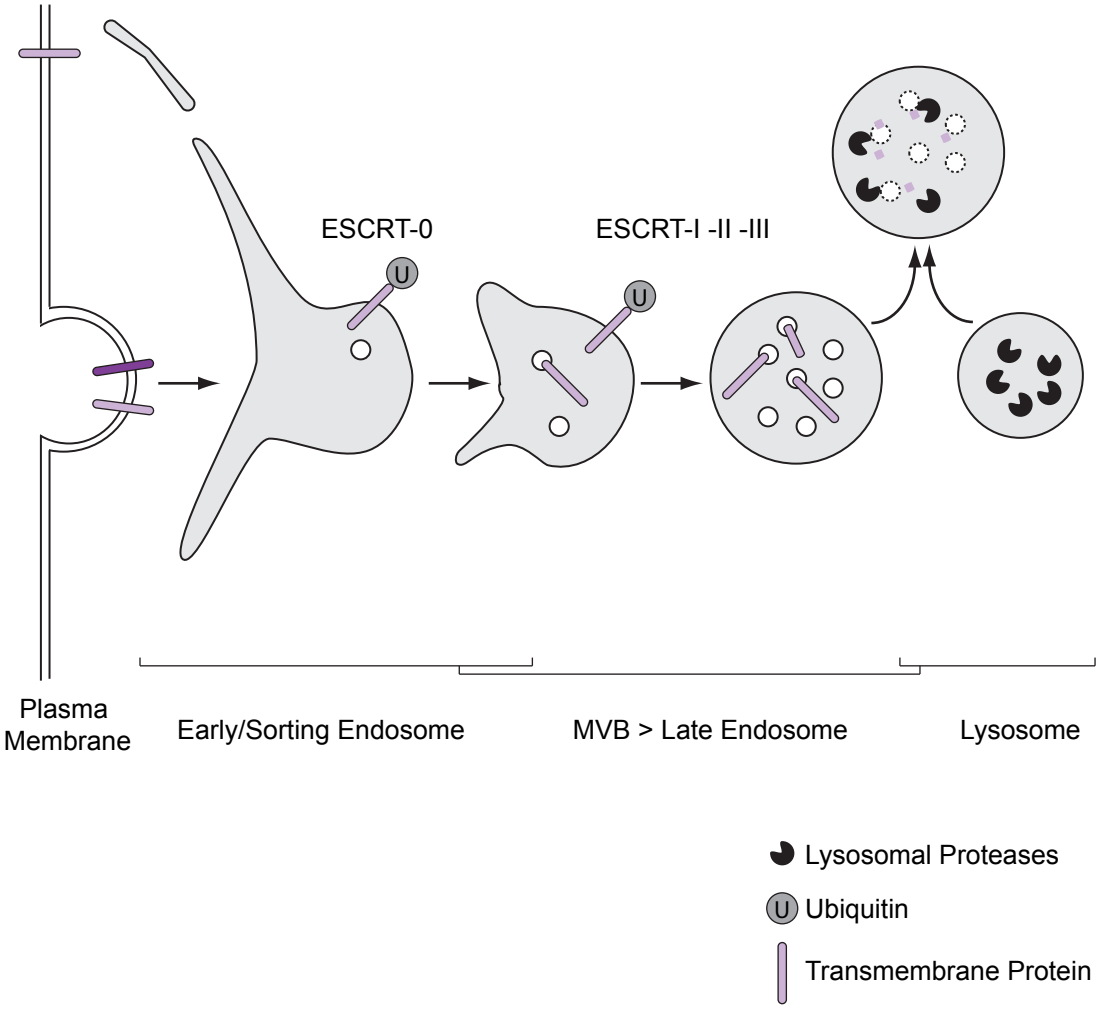

Figure 1.6 The Endolysosomal Pathway
Membrane proteins, such as activated transmembrane receptors, can be removed from the plasma membrane via endocytosis. From the early/sorting endosomes they can either be recycled back to the plasma membrane or trafficked along the endocytic pathway for eventual degradation in the lysosome. ESCRT-0 mediates the selection of ubiquitylated cargo, and the concerted action of ESCRT-I -II and -III leads to the internalisation of cargo into intraluminal vesicles of MVBs. The fusion of the lysosome and MVBs then allows the delivery of the lysosomal proteases which mediate subsequent degradation. Adapted from (Williams & Urbé, 2007).

endosomes (Raiborg *et al*, 2002; Lloyd *et al*, 2002; Clague, 2002). STAM is also thought to bind clathrin (McCullough *et al*, 2006). HRS then recruits the ESCRT-I complex via its interaction with Tsg101 (Lu *et al*, 2003; Bache *et al*, 2003).

ESCRT-I and ESCRT-II have been proposed to be involved in initial membrane deformation to form buds that confine cargo (Wollert & Hurley, 2010). ESCRT-II initiates the ordered assembly of the ESCRT-III complex (Teis *et al*, 2008; Henne *et al*, 2012). ESCRT-III proteins are found in an autoinhibited state in the cytoplasm, then upon recruitment to the endosome they have the ability to oligomerise (Zamborlini *et al*, 2006). ESCRT-III is thought to gather and confine ubiquitylated cargo and endosomal ubiquitin receptors at sites of internal vesicle formation and to initiate the scission of intraluminal vesicles (Wollert *et al*, 2009; Wollert & Hurley, 2010; Hurley & Hanson, 2010; Chiaruttini *et al*, 2015). The ESCRT-III component Vps2 recruits the AAA-ATPase Vps4, which is required for the recycling of ESCRT components and for the formation of intraluminal vesicles, two processes that may thus be coupled (Bishop & Woodman, 2000; Sachse *et al*, 2004). ESCRT-III does not contain an intrinsic UBD but rather engages with DUBs to deubiquitylate cargo prior to the inward budding of the intraluminal vesicles and thus allows ubiquitin recycling (Williams & Urbé, 2007). Multivesicular bodies (MVBs) can then fuse with lysosomes which deliver the acidic hydrolases responsible for degradation of the cargo (Luzio *et al*, 2010; Wartosch *et al*, 2015).

Lysosomal targeting is preferentially mediated via K63 linked polyubiquitylation. ESCRT-0 binds with slightly higher affinity to K63 than K48 linked chains (Ren & Hurley, 2010). K63 linked chains also accumulate rapidly upon lysosomal inhibition (Dammer *et al*, 2011). This linkage has been shown to be critical for degradation of the epidermal growth factor receptor (EGFR), TrkA and dopamine receptors (Geetha *et al*, 2005; Huang *et al*, 2006, 2013; Vina-Vilaseca & Sorkin, 2010). Monoubiquitylation is thought to be sufficient to promote internalization of membrane proteins like EGFR but K63 linked polyubiquitylation is required for lysosomal sorting by the ESCRT machinery (Huang *et al*, 2013). It has also been shown in yeast that monoubiquitylation of the Gap1 permease is sufficient for its internalization, but K63 linked polyubiquitylation is required for its sorting into MVBs (Lauwers *et al*, 2009). A combination of K11 and K63 chains have been implicated in the degradation of MHC-I (Boname *et al*, 2010), whilst K29 linked ubiquitin chains have been shown to regulate endolysomal trafficking of Notch pathway components (Chastagner *et al*, 2006).

DUBs are thought to play distinct roles at different stages of the endocytic pathway. As well as interacting with ESCRT-III, the K63-linkage specific DUB AMSH and the non-discriminating DUB USP8 can bind to the SH3 domain of STAM via their microtubule interacting and transport (MIT) domains (McCullough *et al*, 2006; Clague & Urbé, 2006; Komander *et al*, 2009a; Faesen *et al*, 2011). At this early stage they are thought to determine the fate of cargo between recycling and degradation. Depletion of AMSH has been shown to promote degradation of EGFR, suggesting that it usually favours receptor recycling (McCullough *et al*, 2004). USP8 has pleotropic roles including the stabilisation of ESCRT-0 (Row *et al*, 2006, 2007), and has been shown to promote recycling of some plasma membrane proteins including the Hedgehog receptor Smoothened (Li *et al*, 2012; Xia *et al*, 2012). USP8 has also recently been shown to be required for the correct trafficking of mannose-6-phosphate receptor and thus for the delivery of newly synthesised lysosomal proteases to the endocytic pathway (MacDonald *et al*, 2014).

1.3.6. Autophagy

The word autophagy literally means '*self-eating*': it is derived from the Greek words ‘auto’ meaning self and ‘phagein’ meaning eating. This was originally thought to be a non-specific process that mediates the bulk degradation of cytosolic material. However it is now known that there are many different types of autophagy which serve to sequester proteins in both non-selective and selective manners, including macroautophagy, microautophagy and chaperone-mediated autophagy (CMA) (Klionsky, 2005).

In classical macroautophagy cytosolic material is surrounded by a double-limiting membrane that then closes to form an autophagosome. The autophagosome then fuses with the lysosome, to degrade engulfed material. This involves over 30 autophagy-related genes (atg) that were originally identified in yeast and are mostly conserved in mammals (Klionsky *et al*, 2003; Reggiori & Klionsky, 2002). In contrast to the classical macroautophagy, microautophagy and CMA do not require the formation of an autophagosome nor do they involve the atg genes. However, all of these mechanisms rely on the lysosome to terminally degrade proteins.

CMA is mainly thought to be mediated by the cytosolic chaperone Hsc70, which recognises substrates with the sequence KFERQ (Chiang & Dice, 1988; Chiang *et al*, 1989). Through the action of LAMP-2A (lysosome-associated membrane protein

2A), the so-called CMA receptor, substrates are then unfolded and translocated through the lysosomal membrane with the aid of a luminal form of Hsc70 (Cuervo & Dice, 1996; Agarraberes *et al*, 1997; Salvador *et al*, 2000). This does not involve ubiquitylation of the cargo (Kaushik & Cuervo, 2012). Recently another process was described called chaperone-assisted selected autophagy (CASA). This also involves Hsc70, as well as other chaperones. However, it further requires ubiquitylation mediated by Stub1, the autophagic ubiquitin adaptor p62 and formation of an autophagosome (Arndt *et al*, 2010; Ulbricht & Höhfeld, 2013)

Microautophagy involves the sequestration of cargo directly into the lysosome via membrane invagination (Marzella *et al*, 1981; Kunz *et al*, 2004). This has only been described in yeast, however recently microautophagy by late endosomes has been postulated in mammals (endosomal microautophagy, e-MI) (Sahu *et al*, 2011). This is thought to require components of the ESCRT pathway, specifically Tsg101 and Vps4. This can occur in a selective manner via Hsc70 mediated recruitment of KFERQ motif containing proteins. In contrast to CMA, this does not involve LAMP-2A or cargo unfolding. Hsc70 is thought to associate with the endosomal limiting membrane via an electrostatic interaction mediated by a basic region in its C-terminus. This process is not thought to require ubiquitin. Apparently eMI can also occur in a non-selective fashion in which cytosolic proteins are incorporated passively and trapped in MVBs upon intraluminal vesicle budding (Sahu *et al*, 2011).

Macroautophagy can be either non-selective or selective. Non-selective autophagy occurs in response to different types of cellular stress and amino acid starvation, through inhibition of mammalian target of rapapmycin (mTOR). (Yang & Klionsky, 2010). Multiple selective macroautophagy pathways have now been identified and are named after their specific cargo: Mitophagy (mitochondria), aggrephagy (aggregates), proteophagy (proteasomes) among others (Khaminets *et al*, 2016).

General macroautophagy starts with the initiation of a phagopore, which then expands and closes to give the double-membrane autophagosome. Initiation and development of an autophagosome requires the sequential action of four different groups of proteins (Mizushima *et al*, 2011; Klionsky & Schulman, 2014). Nucleation of the phagopore is mediated by the ULK1-kinase complex, followed by the PtdIns-3-kinase (PI3K) complex composed of Vps34, p150, Beclin and ATG14L. A second Vps34, Beclin and UVRAG containing PI3K complex is thought to be involved in the autophagosome maturation process (Vanhaesebroeck *et al*, 2010). PI3K inhibitors

such as wortmannin can therefore be used to block the pathway, however this also inhibits progression along the endolysosomal pathway (Figure 1.5). The transmembrane protein Atg9 is thought to be involved in trafficking of membrane sources to the phagopore assembly site. Ubiquitin-like proteins (UBLs) are then involved in the autophagosome expansion process. Specifically, these are Atg8 (LC3 and GAPARAP in mammals) and Atg12. Atg12 is conjugated to Atg5 in a process that requires the action Atg7 and Atg10, which are E1 and E2 like enzymes. An Atg5-Atg12-Atg16 complex then acts in an E3-like manner to mediate the conjugation of Atg8 to the lipid phosphatidylethanolamine (PE). This process also requires the action of the E1 and E2 like enzymes Atg7 and Atg3 (Klionsky & Schulman, 2014).

For selective autophagy, recognition of cargo is achieved via a variety of autophagy receptors, which contain LC3 interacting regions (LIR) and can deliver cargo to the autophagic membrane (Stolz *et al*, 2014). Ubiquitin has now been widely implicated in the regulation of many selective autophagy mechanisms (Kirkin *et al*, 2009; Khaminets *et al*, 2016). This involves autophagic receptors which contain UBDs and thus can specifically recognize ubiquitylated cargo and also simultaneously bind the LC3/GABARAP proteins (Khaminets *et al*, 2016). For example, the UBDs of autophagy receptors OPTN and NDP52 are required for mitophagy (Lazarou *et al*, 2015). Most recently, phosphorylated ubiquitin has been shown to act as a signal to trigger mitophagy (Durcan & Fon, 2015). In aggrephagy, K63 linked ubiquitylation has been implicated in targeting of Tau and Sod1 aggregates for degradation by the autophagosome (Tan *et al*, 2008).

1.4. Phosphorylation and Kinases

Phosphorylation is a reversible post-translational modification. Kinases catalyse the transfer of the gamma-phosphate group from ATP onto substrates, usually onto Ser, Thr and Tyr residues. Phosphatases reverse this reaction. The first kinase was described in 1954 and was later identified as casein kinase 2 (Burnett & Kennedy, 1954). The seminal studies by Krebs and Fischer that later won them the Nobel Prize then described how phosphorylation was a reversible process and could modulate the activity of enzymes (Krebs & Fischer, 1956). It is now known that there are over 500 protein kinases encoded in the human genome (Manning *et al*, 2002), and a staggering 700,000 potential phosphorylation sites (Ubersax & Ferrell, 2007). The interplay of different kinases in regulating the same substrate by multi-step

phosphorylation processes is commonplace. Phosphorylation has now been shown to modulate all aspects of protein biology, affecting catalytic activity, protein-protein interaction, stability, and subcellular localisation. It is thus no surprise that phosphorylation plays a central role in a variety of signalling processes (Cohen, 2000).

1.4.1. PKA

Protein Kinase A (PKA) was the second ever kinase to be identified (Walsh *et al*, 1968). It is a broad spectrum Ser/Thr kinase of the AGC subfamily (PKA, PKG, PKC) (Pearce *et al*, 2010). PKA is a tetrameric holoenzyme comprised of a homodimer of regulatory (PKAR) subunits that each bind a catalytic (PKAC) subunit. In this conformation the enzyme is inactive, as PKAR binds PKAC via its catalytic domain, blocking access to substrates. PKA is then activated upon cAMP binding to PKAR, leading to the release of PKAC (Figure 1.7a) (Reimann *et al*, 1971; Corbin *et al*, 1975). PKA was thus initially known as the cAMP-dependent kinase.

1.4.1.1. PKAR

There are four PKAR isoforms PKARIα, PKARIβ, PKARIIα and PKARIIβ. Depending on the regulatory subunit makeup, the holoenzyme is termed either type I or type II PKA. PKARIα and PKARIIα are ubiquitously expressed. PKARIβ is expressed predominantly in the central nervous system. PKARIIβ is expressed mainly in the brain, as well as in neuroendocrine, adipose and reproductive tissues (Skalhegg & Tasken, 2000).

All PKAR subunits are composed of an N-terminal D/D domain for dimerization and two C-terminal cAMP binding domains (Taylor *et al*, 2012). A flexible linker region in between these N and C terminal domains contains the PKAC binding site. This resembles a peptide substrate of PKAC. Whereas the RI subunits are pseudosubstrate inhibitors, containing an Ala or a Gly, the RII subunits are actual substrates, containing an acceptor Ser (Johnson & Lewis, 2001). This site is auto-phosphorylated within the holoenzyme.

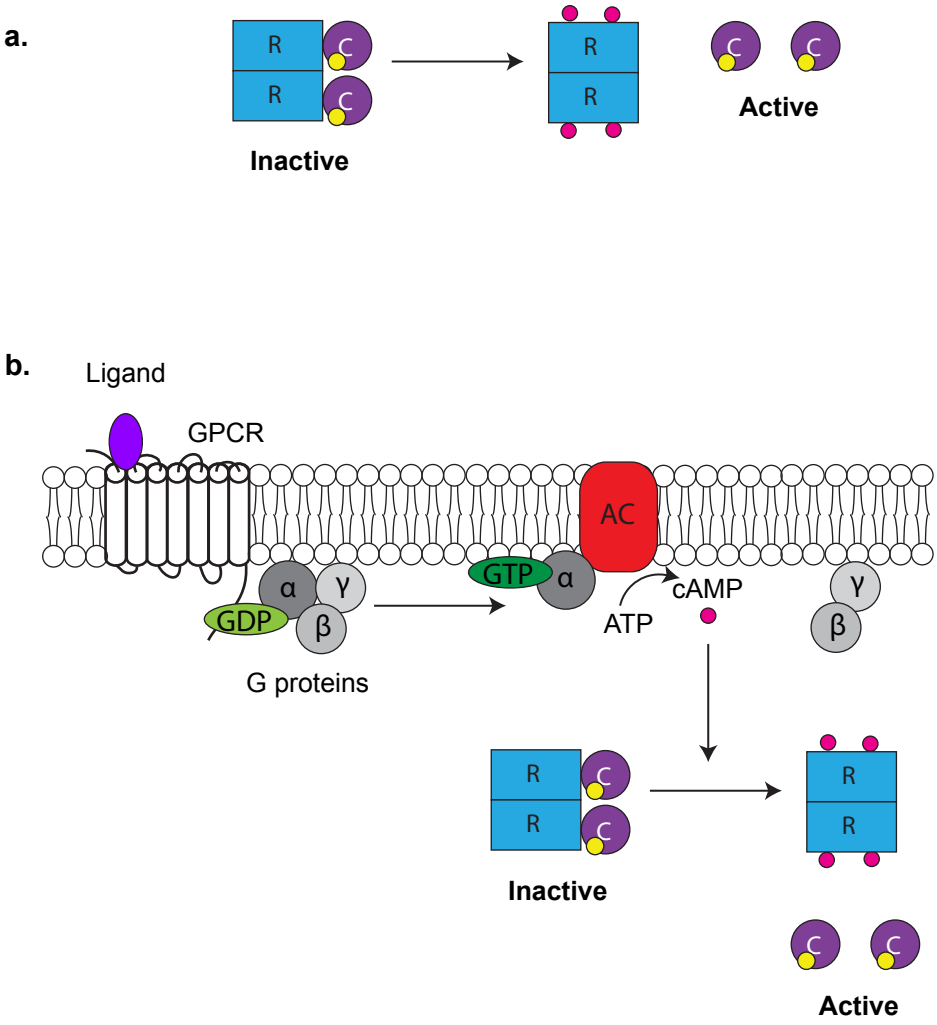

Figure 1.7 PKA activation and cAMP generation (**a**) PKA is a tetrameric holoenzyme composed of a heterodimer of regulatory subunits (R) which each bind and inhibit a catalytic subunit (C). cAMP (represented by the pink dots) binding to PKAR leads to the release of PKAC, which is already phosphorylated (represented by the yellow dots) in the catalytic site and thus active. (**b**) Ligand binding to GPCRs mediates dissociation of the heterotrimeric G proteins. Activated GTP bound Gαs stimulates the adenyl cyclase (AC) to produce cAMP. cAMP can then bind PKAR and thus release PKAC. Adapted from (Pearce *et al*, 2010)

1.4.1.2. PKAC

PKAC itself is constitutively active. Most protein kinases are regulated by dynamic phosphorylation of the activation loop, however for PKAC this activation loop phosphorylation occurs soon after synthesis, and is very stable (Steichen *et al*, 2010, 2012). Thr197 is phosphorylated by PDK1 or, *in trans*, by another PKAC molecule. PKAC activity is thus not regulated by turnover of this phosphorylation but solely by binding to PKAR.

PKAC also undergoes *cis*-autophosphorylation at Ser338, which occurs at the ribosome and is required for its maturation and subsequent activating Thr197 phosphorylation (Keshwani *et al*, 2012). PKAC is also myristoylated at its N-terminus. This enhances its structural stability (Yonemoto *et al*, 1993; Bastidas *et al*, 2012) and is also thought to contribute to membrane association of both the holoenzyme and the catalytic subunit alone (Gangal *et al*, 1999; Gaffarogullari *et al*, 2011).

PRKACα and PRKACβ are the two main isoforms of the PKAC subunits in human and are highly conserved. In humans another isoform was detected, PRKACγ, that is found specifically in the testis (Beebe *et al*, 1990). Two other related kinases have also been identified in humans, PRKX and PRKY, which are encoded on the X and Y chromosomes respectively. PRKX was found to bind the regulatory subunits and become activated by cAMP (Zimmermann *et al*, 1999), however it is unclear if the same is the case for PRKY (Schiebel *et al*, 1997). Interestingly PRKX is thought only to form holoenzyme complexes with RI subunits (Zimmermann *et al*, 1999).

PRKACα and PRKACβ can then be differentially spliced to give Cα1, Cα2, Cβ1 and Cβ2. For PRKACα the canonical Cα1 is ubiquitously expressed and the best studied. In contrast Cα2 is found only in male germ cells (also termed CaS). A third variant has also been described but has not been characterised (Strausberg *et al*, 2002). For PRKACβ, Cβ1 is ubiquitously expressed in mouse, albeit at much lower levels than Cα1. Cβ2 is predominantly found in the brain (Uhler *et al*, 1986). Additional PRKACβ splice variants are thought to exist in humans (Ørstavik *et al*, 2001).

1.4.2. PKA regulation

1.4.2.1. cAMP production

cAMP (cyclic adenosine monophosphate) was identified over 60 years ago (Sutherland & Rall, 1958). This discovery and the fact that cAMP production is coupled to hormone signalling led to Earl Sutherland receiving the Nobel Prize in 1971. cAMP is a ubiquitous second messenger. We now know its production is stimulated by ligand binding to G protein coupled receptors (GPCRs), of which there are over 800 in the genome (Figure 1.7a) (O'Hayre *et al*, 2013). They comprise seven transmembrane domains, as well as a N-terminal extracellular domain and a C-terminal intracellular domain. As their name suggests, they signal via heterotrimeric G proteins, which link the receptor to its downstream effectors. G proteins are made up of α, β, and γ subunits (Pierce *et al*, 2002). Ligand binding activates the receptor, which can then act as a Guanine nucleotide exchange factors (GEF) to mediate GDP dissociation from and GTP-binding to the Gα subunit, resulting in the dissociation of the beta-gamma subunits and recruitment of downstream effectors to the alpha subunits (Gilman, 1987; Johnston & Siderovski, 2007). There are four classes of α subunit: $G\alpha_s$, $G\alpha_i$, $G\alpha_q$ and $G\alpha_{12}$. $G\alpha_s$ stimulates activity of the adenyl cyclase whereas $G\alpha_i$ inhibits it (Gilman, 1987). $G\alpha_q$ and $G\alpha_{12}$ couple to phospholipase C and Rho GEFs respectively. Upon G protein activation the β and γ subunits remain associated as a heterodimer, and can also modulate adenyl cyclase activity as well as other downstream effectors (Tang & Gilman, 1991).

There are nine membrane-associated isoforms of the adenyl cyclase (AC1-9) (Sunahara & Taussig, 2002). These consist of 12 transmembrane passes, which are split into two tandem repeating domains of six transmembrane passes, each followed by a cytosolic catalytic loop (Krupinski *et al*, 1989). G proteins are thought to bind at the interface of these loops to stimulate activation (Hurley, 1999). The activity of some isoforms can also be differentially modulated by Ca^{2+} (Halls & Cooper, 2011). PKA itself can phosphorylate and inhibit AC5/6, which is thought to contribute to a refractory period (Iwami *et al*, 1995; Chen *et al*, 1997). PKA phosphorylation of the GPCR can also lead to inhibition of signalling via G protein switching. This has been shown for the β-adrenergic receptor and also the prostacyclin receptor (Daaka *et al*, 1997; Lawler *et al*, 2001).

It should also be noted that there is one soluble isoform of the adenyl cyclase (sAC/AC10), which is predominantly expressed in testis and is not responsive to G proteins (Braun & Dods, 1975; Buck *et al*, 1999). This is rather regulated by intracellular calcium and has been postulated to be a bicarbonate sensor (Chen *et al*, 2000; Steegborn *et al*, 2005).

cAMP levels are negatively regulated by phosphodiesterases. There are 11 different members of the phosphodiesterase family (Conti & Beavo, 2007; Omori & Kotera, 2007). These are encoded for by different genes and undergo differential splicing, leading to a large number of isoforms. Some are specific for cAMP (PDE4, PDE7, PDE8), some for cGMP (PDE5, PDE6, PDE9) while the rest catalyse the hydrolysis of both (Houslay, 2010).

cAMP synthesis can be stimulated by Forskolin, a natural compound isolated from the Indian medical plant *Coleus forskohlii* (Metzger & Lindner, 1981). It directly activates all membrane bound adenyl cyclases, except AC9. IBMX can also be used to increase cAMP levels, which inhibits phosphodiesterase activity in a non-selective manner (Costa *et al*, 1975). Maximal stimulation can be obtained by combined use of Forskolin and IBMX.

PKA is the main cellular effector of cAMP, however it was later found that the EPAC (Exchange proteins activated by cAMP) proteins are also activated by cAMP (de Rooij *et al*, 1998). These are GEFs for the small GTPase Rap (de Rooij *et al*, 1998). Specific cAMP analogues have been developed that can selectively activate EPAC proteins in order to dissect the distinct roles of PKA and EPAC proteins downstream of cAMP, such as 8-pCPT-2-O-Me-cAMP, also known as *007* (Gloerich & Bos, 2010).

1.4.2.2. AKAPs

Compartmentalised signalling by PKAC was first hypothesised in the 1970s. Prostaglandin and epinephrine stimulation both caused a similar increase in cAMP levels and PKA activity in the rat heart, however only epinephrine led to an increase in glycogen phosphorylase activity (Keely, 1977). This suggested differential activities of PKAC within the same cell. Cellular PKA activities were later shown to be compartmentalised by the action of A-kinase anchoring proteins (AKAPs). AKAPs bind R subunits and thus target the PKA holoenzyme to specific subcellular

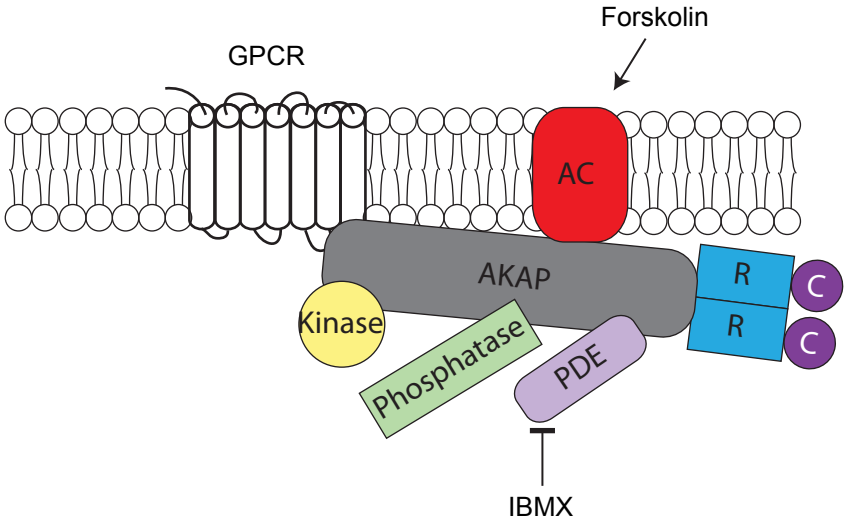

Figure 1.8 AKAPs provide tailored PKA signalling nodes
AKAPs bind PKAR and can thus target the holoenzyme to different subcellular locations, such as the plasma membrane, placing PKA close to particular substrates. They can also bind further proteins that can regulate PKA signalling. Such as GPCRs, the adenyl cyclase (AC) for cAMP production, phosphodiesterases (PDE) for cAMP hydrolysis, phosphateses to reverse substrate phosphorylation and other kinases allwoing for crosstalk with other pathways. cAMP levels can be modulated by Forskolin which stimulates the adenyl cyclase, and IBMX which inhibits phospodiesterases. Adapted from (Skroblin *et al*, 2010)

locations, providing spatial information and placing PKA in the vicinity of particular substrates (Skroblin *et al*, 2010). The first AKAP was identified in 1982, when Protein kinase A was found to co-purify with microtubule associated protein 2 (MAP2) from microtubule preparations isolated from rat brain (Vallee *et al*, 1981). It was subsequently shown that MAP2 binds RII subunits and thereby recruits PKA to microtubules (Theurkauf & Vallee, 1982).

Over 50 AKAPs have now been identified. They are similar only in the way they bind PKA regulatory subunits, whereas they target PKA to different subcellular compartments via distinct mechanisms. AKAPs bind the N-terminal D/D domain of PKA regulatory subunits via an amphipathic helix of 14-18 residues (Skroblin *et al*, 2010). AKAPs in general preferentially bind RII subunits, however both dual specificity and RI specific AKAPs have been described. These proteins also have numerous other binding partners and thus act as scaffolds to recruit other proteins that modulate PKA signalling (Figure 1.8). These include adenyl cyclases and phosphodiesterases for cAMP generation and turnover respectively, protein phosphatases to reverse PKA substrate phosphorylation and other protein kinases, allowing for the integration of other signalling pathways. AKAPs therefore provide different PKA signalling modules for particular signalling contexts, allowing for modular specialisation of this ubiquitously used pathway. The same AKAP can also bind different sets of proteins at different times, further adding to the complexity of their role in PKA signalling. Since the identification of MAP2 as a microtubule targeting AKAP, AKAPs have been found that target PKA to diverse cellular locations, such as the nucleus, centrosome, plasma membrane, Golgi and mitochondria (Skroblin *et al*, 2010). AKAP mediated PKA signalling is thought to be the key mechanism by which specific cAMP signalling outcomes are achieved.

1.4.2.3. PKAC binding proteins

In contrast there are few proteins that bind directly to the C subunits, as most regulation is thought to be via the regulatory proteins. The protein kinase inhibitor protein (PKI) is the most famous of these proteins, mainly as it is widely used experimentally to inhibit PKAC. PKI binds directly to PKAC and inhibits it via a pseudosubstrate motif, similar to that found in PKAR (Scott *et al*, 1985). This mechanism of pseudosubstrate inhibition rather than blocking the ATP pocket increases specificity for PKAC over other kinases. The ATP binding pocket is

extremely conserved across kinases, whereas the catalytic site is more diverse (Murray, 2008).

PKI cannot compete with PKAR for PKAC within the holoenzyme, but rather binds free PKAC (Herberg & Taylor, 1993). PKI proteins contain a nuclear export signal (Wen *et al*, 1995), which is hidden unless PKI is bound to PKAC (Dalton & Dewey, 2006). PKI proteins are thus thought to be involved in shuttling nuclear PKAC back to the cytoplasm. PKAR subunits that are not bound to cAMP can then compete for PKAC in order to reform the holoenzyme (Herberg & Taylor, 1993).

PDE7A1, a cAMP specific phosphodiesterase, also contains two PKAC pseudosubstrate sites in its N-terminus (Han *et al*, 2006). It thus inhibits PKAC directly via pseudosubstrate binding, and indirectly via hydrolysing cAMP.

Two PKAC binding proteins are involved in NFkB signalling. IkB, a negative regulator of the NFkB pathway, binds PKAC directly and blocks ATP binding, thus inhibiting kinase activity (Zhong *et al*, 1997). AKIP1 (A-kinase interacting protein 1), which can bind the transcription factor p65 subunit of NFkB (Gao *et al*, 2008), can also bind PKAC in the A-helix at its N-terminus. This does not affect PKA activity, but AKIP1 contains a nuclear localisation signal and is thought to play a role in nuclear shuttling of PKAC (Sastri *et al*, 2005). p65 is also a PKA substrate and thus AKIP1 helps to mediate its phosphorylation, which enhances NFkB pathway activation.

The G protein $G\alpha_o$ binds PKAC and prevents it from translocating to the nucleus. The binding mechanism is unknown, however $G\alpha_o$ does not affect PKAC activity (Ghil *et al*, 2006). The role of $G\alpha_o$ signalling is unclear. It belongs to the $G\alpha_i$ family, but does not seem to inhibit the adenyl cyclase.

A dual role of RSK1 (p90 ribosomal S6 kinase-1) in PKA regulation has been proposed based on work from the Patel laboratory. Active RSK1 binds PKAC to promote PKAR binding and inactivation. In contrast, inactive RSK1 binds PKAR and displaces PKAC. RSK1 is thought to bind PKAR in the cytoplasm, and PKAC in the nucleus (Chaturvedi *et al*, 2006, 2009; Gao & Patel, 2009; Gao *et al*, 2010, 2012).

Caveolin-1 is proposed to bind and inhibit PKAC, although the mechanism is not known (Razani *et al*, 1999). The binding site on PKAC has not been identified, but

the scaffolding domain and C-terminal portion of Caveolin-1 can both mediate the interaction. How Caveolin-1 inhibits PKAC is unclear; the binding domains do not resemble substrates. Interestingly upon Caveolin-1 overexpression PKAC was seen to translocate from the cytosol to Caveolin-rich microdomains at the plasma membrane (Razani *et al*, 1999; Razani & Lisanti, 2001).

1.4.2.4. Regulation of PKA protein levels

PKAC and PKAR are encoded on different chromosomes, however their expression is thought to be co-regulated to result in approximately equal protein levels. This ensures optimal responsiveness of the kinase to cAMP. This has been shown across a wide variety of cells types (Hofmann *et al*, 1977). Compensatory mechanisms have been demonstrated in mice where knock out of either PKARIβ and PKARIIβ led to an increase in PKARIα levels (Amieux *et al*, 1997). Previous experiments in PKAC null cells showed that PKAR was much less stable and also synthesised to a lesser degree (Steinberg & Agard, 1981a). In contrast, when PKAC is exogenously overexpressed, a corresponding increase in PKAR levels could be seen (Uhler & McKnight, 1987).

Conversely, degradation of PKAR has been shown to play a role in synaptic plasticity by causing persistent PKAC signalling (Sweatt & Kandel, 1989). PKAR degradation via the ubiquitin-proteasome system is thought to alter the R/C ratio and thus achieve continual and eventually autonomous PKAC activation, even in the presence of basal cAMP levels (Greenberg *et al*; Hegde *et al*, 1993; Chain *et al*, 1995, 1999). Until recently the E3 ubiquitin ligase involved in this turnover was unknown.

One of the more recent AKAPs to be discovered was Praja2, which is also a largely neuronal E3 ubiquitin ligase (Lignitto *et al*, 2011). Praja2 has dual specificity AKAP properties. It binds the D/D domain of both RI and RII subunits via an amphipathic helix located in its N-terminus. Interestingly it was identified as the E3 ligase that mediates the ubiquitylation and proteasomal degradation of the PKAR subunits (Lignitto *et al*, 2011). PKAC activation leads to Praja2 phosphorylation and enhanced E3 activity, causing ubiquitylation and degradation of PKAR, which in turn leads to more free and active PKAC. Praja2 thus mediates a positive feed forward loop. This was the first identification of an E3 ubiquitin ligase that regulates PKAR. There is currently no mechanism described for PKAC degradation, even though

degradation of activated kinases is a common mechanism of their regulation (Lu & Hunter, 2009; Liu *et al*, 2012). However some studies in the literature provide hints that PKAC is degraded upon chronic stimulation (Hemmings, 1986; Armstrong *et al*, 1995; Richardson *et al*, 1990).

1.4.3. PKA substrates

PKA is a serine/ threonine kinase, which phosphorylates substrates with the sequence R-R-X-S/T-Y, where X is variable and Y is a hydrophobic residue (Songyang *et al*, 1994). PKA phosphorylates a myriad of substrates with new targets constantly being identified (Shabb, 2001). Here I will outline a selection of these to highlight the diverse roles of PKA in a variety of cellular pathways.

1.4.3.1. Nuclear substrates

PKA mediates many of its long-term effects by modulating gene expression through regulation of transcription factors. CREB, cAMP response element binding protein, was the first transcription factor for which activity was shown to be regulated by phosphorylation (Gonzalez & Montminy, 1989). CREB becomes activated upon phosphorylation at Ser133 (Figure 1.9). Phospho-CREB (p-CREB) binds to palindromic CRE (cAMP response element) sequences within DNA (Montminy *et al*, 1986; Comb *et al*, 1986; Short *et al*, 1986). In this activated state p-CREB can recruit transcriptional co-activators such as CBP (CREB binding protein) and p300. These proteins are acetyl tansferases and are also thought to interact with RNA polymerase II complexes (Kee *et al*, 1996; Vo & Goodman, 2001). Upon activation, PKAC translocates to the nucleus to phosphorylate CREB. CREB activity peaks after approximately 30 minutes of stimulation, at which point maximal amounts of active PKAC have accumulated in the nucleus. Activity is then attenuated via the action of the phosphatases PP-1 and PP-2 on Ser-133 (Hagiwara *et al*, 1992; Wadzinski *et al*, 1993).

The CREB family contains two further transcription factors, CREM (CRE modulator) and ATF-1. CREM is highly expressed in neuroendocrine tissues, whereas CREB and ATF-1 are expressed ubiquitously. CREM proteins can also be alternatively spliced to produce ICER (inducible CRE repressor), which lacks an activation domain, and is thus a negative transcriptional regulator (Molina *et al*, 1993). Transient expression of ICER is induced by the binding of phosphorylated CREB family proteins to CRE elements. ICER then acts in a negative feedback loop to

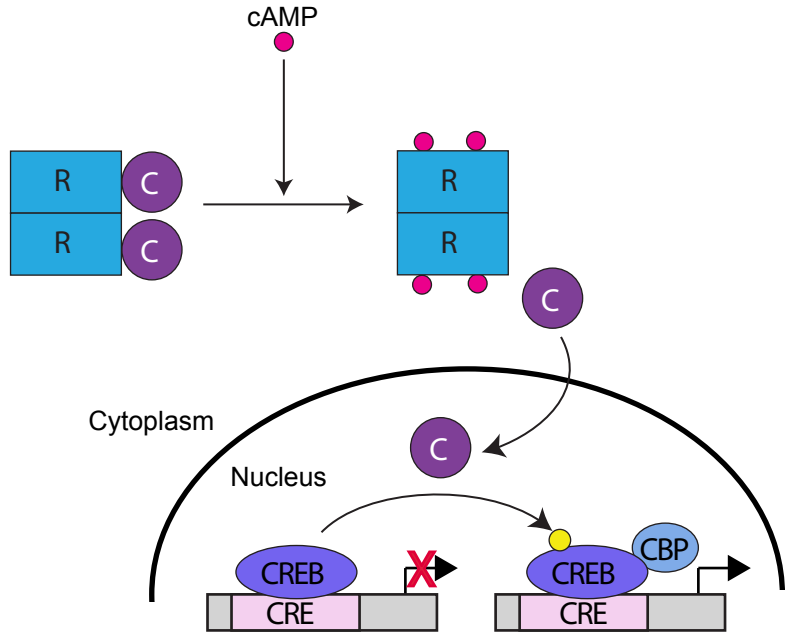

Figure 1.9 PKA mediated CREB activation
cAMP activation of PKA allows phosphorylation of CREB at Ser133. This mediates binding to cofactors, such as CREB binding protein (CBP) and allows the activation of transcription from CRE sequences. Adapted from (Altarejos & Montminy, 2011).

switch off other CRE genes, which is of particular importance for hormone secretion in the pituitary gland (Mazzucchelli & Sassone-Corsi, 1999).

Although CREB is clearly regulated by PKA, this is not the only mechanism for its activation. It has been shown in recent years that phosphorylation of CREB family proteins can also be stimulated by a vast array of stimuli and multiple different kinases (Johannessen *et al*, 2004).

PKA has many other nuclear substrates that can affect transcription. I have described above how p65, the NFkB subunit and transcription factor is also activated by PKA phosphorylation (Gao *et al*, 2008). PKA has also been shown to phosphorylate many different nuclear hormone receptors in order to mediate their transcriptional activity (Shao & Lazar, 1999). However, PKA does not just affect transcription factors. Histone H1 was the first PKA substrate for which the phosphorylation site was identified (Langan, 1969). This was initially found upon glucagon stimulation in liver cells, and was also later observed in mouse neuroblastoma cells (Ajiro *et al*, 1990). PKA was later shown to also phosphorylate Histone H3 (Wei *et al*, 1999; DeManno *et al*, 1999).

Recently a role for PKA phosphorylation has been identified in the regulation of splicing (Kvissel *et al*, 2007). SFRS17A (splicing factor arginine/serine-rich 17A) was also recently found to be an AKAP that can target PKA to splicing factor compartments within the nucleus (Jarnaess *et al*, 2009). Whereas previous models hypothesised that only free activated PKAC translocates to the nucleus, it has recently been shown that functional holoenzyme complexes also exist in the nucleus (Sample *et al*, 2012). They hypothesised that cAMP produced at the plasma membrane would normally not be able to activate nuclear PKA holoenzymes due to cytosolic phosphodiesterase activity. Consequently, PKAC translocation from the activated cytoplasmic pool would normally be responsible for nuclear activity. However once a certain cAMP threshold is overcome, cAMP may directly activate this nuclear pool, leading to faster signalling kinetics. The soluble adenyl cyclase (sAC) has also been localised to the nucleus in some cells, and may play a role in nuclear PKA activation (Zippin *et al*, 2004).

Through these nuclear substrates it becomes apparent how PKA can mediate long-term effects and widely affect gene transcription.

1.4.3.2. PKA in cell migration and Rho protein regulation

PKA can both positively and negatively regulate cell migration, through the phosphorylation of a variety of proteins, including Integrins and Rho proteins, which I will discuss below (Howe, 2011). PKA activity during cell migration is spatially regulated and this is thought to be mediated by AKAP-Lbc (Howe *et al*, 2005; Paulucci-Holthauzen *et al*, 2009). AKAP-Lbc is, as the name suggests, an AKAP, however it is also a Rho GEF protein (Diviani *et al*, 2001, 2006). AKAP-Lbc GEF activity can be stimulated by activated $G\alpha_{12}$ and is thought to play a role in stress fibre formation (Diviani *et al*, 2001). Phosphorylation of AKAP-Lbc by PKA mediates 14-3-3 binding, which inhibits its GEF activity (Diviani *et al*, 2004; Jin *et al*, 2004).

Integrins play an important role in cell migration as they mediate cell-extracellular matrix contacts (Harburger & Calderwood, 2009). PKA can phosphorylate α4 -integrin at Ser988, which inhibits its interaction with Paxillin (Han *et al*, 2001). Dynamic paxillin binding to the cytoplasmic tail of α4-integrin is required for proper cell migration. Phosphorylated α4-integrin is spatially restricted to the leading edge of the migrating cell, in order to enhance lamellipodia formation there, and restrict formation elsewhere (Goldfinger *et al*, 2003). It was later shown that α4-integrins are actually non-canonical AKAPs which specifically bind the type I holoenzyme (Lim *et al*, 2007). Integrins are also hypothesised to activate PKA in response to mechanical stress, which is thought to be via integrin-mediated activation of $G\alpha_s$ (Lim *et al*, 2008; Alenghat *et al*, 2009).

Rac1 has been shown to be sequestered in AKAP complexes mediated by AKAP220 and WAVE1. AKAP220 anchors PKA close to cortical actin. In response to high calcium levels AKAP220 further recruits IQGAP2, a Ras-GAP-like scaffolding protein (Logue *et al*, 2011b, 2011a). PKA phosphorylation of IQGAP2 then leads to recruitment of active Rac1 to influence actin remodelling. WAVE1, is an AKAP that mediates subcellular targeting of two different PKA complexes, one at the mitochondria and one on actin (Wong & Scott, 2004). WAVE1 is a member of the Wiskott-Aldrich syndrome protein (WASP) family of scaffolding proteins that coordinate actin reorganization (Machesky & Insall, 1998). Actin associated WAVE1 binds Rac as well as SRGAP3/WRP, a WAVE-associated Rac-GAP, and the Arp2/3 complex (Miki *et al*, 1998; Westphal *et al*, 2000; Soderling *et al*, 2002).

Rac1 itself was also shown to act in an AKAP manner, by interacting with PKAR via an amphipathic helix in its C-terminus (Bachmann *et al*, 2013). Rac1 interacts

preferentially with PKAR in the holoenzyme context, and dissociates from PKAR upon PKAC release. Rac1 is not thought to be a PKA substrate itself, however its downstream effector PAK (p21 activated kinase) is regulated by PKA phosphorylation (Howe & Juliano, 2000).

PKA phosphorylation has been implicated in regulating the association of Rho and GDI proteins. GDI proteins extract the Rho proteins from the membrane competent signalling pool and thus binding leads to termination of signalling (Garcia-Mata *et al*, 2011). Phosphorylation of GDI by PKA at Ser174 was shown to inhibit its interaction with RhoA (Qiao *et al*, 2008). Conversely PKA was also found to phosphorylate RhoA at Ser188 and Cdc42 at Ser185, in proximity of their lipid anchors causing enhanced GDI binding (Lang *et al*, 1996; Forget *et al*, 2002; Ellerbroek *et al*, 2003).

Interestingly, Tkachenko and colleagues found that PKA governs a RhoA-RhoGDI protrusion-retraction pacemaker in migrating cells (Tkachenko *et al*, 2011). By using activity sensors for both proteins in live migrating cells, they found PKA and RhoA activation correlated both temporally and spatially. RhoA activation led to protrusion of the leading edge, where PKA activation closely followed. This activation was proposed to be via mechanical stimulation due to the formation of adhesions within the protrusion. PKA is then thought to phosphorylate RhoA at Ser188, and thus cause displacement of RhoA from the membrane via enhanced GDI binding. This leads to termination of protrusions and in turn adhesions, forming a self-inhibiting feedback loop. This is an intriguing new insight into how PKA activity is dynamically regulated at the leading edge. PKA inhibition via PKI significantly increases both duration and amplitude of the protrusions. This additional intersection of the Rho and PKA signalling pathways further supports the notion that this crosstalk is critical for controlled migration.

Other cytoskeleton related AKAPs include Pericentrin and AKAP350, which are both targeted to the centrosome via PACT domains (Diviani *et al*, 2000; Gillingham & Munro, 2000), and MAP2, the first identified AKAP, which is localised to microtubules (Theurkauf & Vallee, 1982). Multiple AKAPs localise to the plasma membrane, including AKAPP79/150, Gravin and AKAP18. This is mediated via a basic region in AKAPP79/150 that binds phospholipids. Gravin requires myristolylation and phospholipid binding, whereas AKAP18 requires both myristoylation and palmitoylation for membrane association (Dell'Acqua *et al*, 1998; Trotter *et al*, 1999; Malbon *et al*, 2004).

1.4.3.3. PKA phosphorylation in the Hedgehog signalling pathway

PKA is emerging as a negative master regulator of the Hedgehog (Hh) signalling pathway in mammals (Figure 1.10) (Chen & Jiang, 2013). Hh signalling responses are mediated by the Gli transcription factors. There are three Gli proteins in mammals Gli1, Gli2 and Gli3. Gli2 and Gli3 respond first to signalling and induce the expression of Gli1, which amplifies the response (Dai *et al*, 1999). In the absence of a stimulus, Gli3, and to a lesser extent Gli2, undergo partial cleavage from transcriptional activators (GliA) into transcriptional repressors (GliR) (Tian *et al*, 2005; Hui & Angers, 2011). Binding of Hh ligands to the twelve-transmembrane-pass receptor Ptch1 relieves its suppression of the GPCR Smoothened (Smo) leading to the accumulation of transcriptionally active GliA.

PKA initiates the multistep phosphorylation of a cluster of sites within Gli2/3 (Pan *et al*, 2009; Wang *et al*, 1999, 2000). PKA phosphorylation primes for further phosphorylation by GSK3 and CK1, generating a so-called phosphodegron (Tempé *et al*, 2006). This leads to recognition of Gli2 and Gli3 by the $SCF^{\beta TRCP}$ ubiquitin E3 ligase complex (Tempé *et al*, 2006; Wang & Li, 2006). They are then subsequently ubiquitylated and partially cleaved by the proteasome, resulting in the loss of the transcriptional activation domain. PKA is often used as a priming kinase for the generation of phospho-degrons. Within the phosphorylated cluster, PKA directly phosphorylates six sites (termed p1-6) (Niewiadomski *et al*, 2014). Loss of phosphorylation at p1-4 is enough to inhibit GliR production. However loss of phosphorylation at all six sites is required for full GliA activity and nuclear accumulation. PKA thus not only mediates GilR formation but also inhibits the generation of GliA.

Sufu is a negative regulator of the pathway that is thought to bind and sequester Gli proteins in the cytosol and promote their conversion into transcriptional repressors (Humke *et al*, 2010). Upon pathway activation by Hedgehog, the Gli proteins translocate to the tip of the primary cilium and dissociate from Sufu, before translocating to the nucleus to activate transcription (Tukachinsky *et al*, 2010). Activation of signalling also promotes the proteasomal degradation of Sufu (Yue *et al*, 2009). In an additional negative regulatory feedback loop PKA, and GSK3β, are thought to phosphorylate Sufu and thus stabilise it (Chen *et al*, 2011).

PKA thus tonically suppresses Hh pathway activation, but how is PKA activated in this context? Recently an orphan GPCR was characterised, GPR161, which

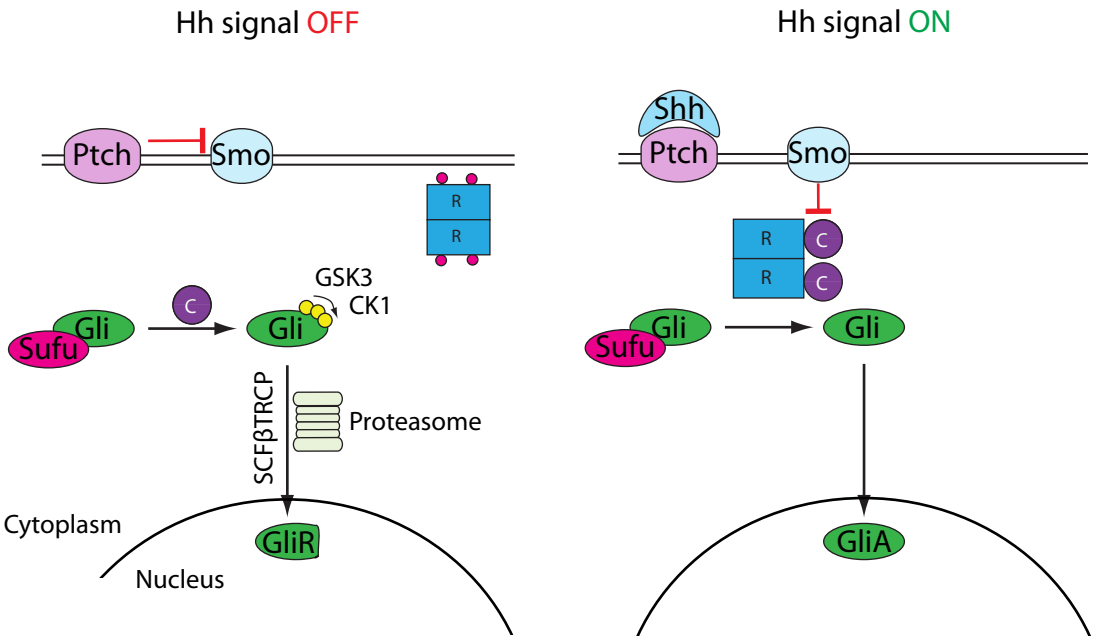

Figure 1.10 PKA regulation of Gli repressor formation
In the absence of Hh ligand, Ptch represses Smo. PKA phosphorylates Gli2/3, initiating further phosphorylation by GSK3 and CK1. This leads to recognition of Gli2/3 by the SCF βTRCP E3 ligase complex, ubiquitylation and partial processing by the proteasome into a Gli repressor form (GliR). Shh binding to Ptch relieves its suppression of Smo and allows Gli activator formation (GliA). Adapted from (Niewiadomski *et al*, 2014)

localises specifically to cilia. GPR161 is thought to be constitutively basally active, and coupled to $G\alpha_s$ which thus leads to constant cAMP production (Mukhopadhyay *et al*, 2013). Interestingly Shh signalling leads to GPR161 internalisation and removal from the cilium, which would reduce cAMP levels and contribute to suppressing PKA signalling in the cilium (Mukhopadhyay *et al*, 2013; Pal *et al*, 2016). Furthermore, upon stimulation, Smo has been proposed to couple to $G\alpha_i$ in order to inhibit adenyl cyclase activation (Ogden *et al*, 2008; Barzi *et al*, 2011; Riobo *et al*, 2006).

Complete PKAC knockout mice arrest at E9 with complete ventralisation of the neural tube (Tuson *et al*, 2011). This phenotype is strikingly similar to null mutants of Ptch1 and Sufu, both negative regulators of the Hh pathway. This phenotype suggests that a primary function of PKA in the early embryo is to restrain Hh pathway activity.

A role of PKA phosphorylation of the fly homologue of Gli, Ci, has long been proposed (Chen *et al*, 1998). Drosophila mutants that lack PKA catalytic activity also show a gain of Hh pathway activity (Chen *et al*, 1999). In the fly, PKA phosphorylation also leads to formation of a Ci repressor form (Dai *et al*, 1999). However, upon pathway activation in the fly, PKA has been proposed to switch substrates and instead phosphorylate and activate Smo (Ranieri *et al*, 2014). PKA is thus hypothesised to have a dual function in the fly Hh pathway, suppressing the pathway in the absence of Hh and supporting activation upon Hh stimulation.

Hh is a classic morphogen and its diffusion creates a graded signal to control cell patterning and differentiation in various embryonic tissues (Jiang & Hui, 2008). Hh signalling also regulates stem cell maintenance in adult tissues (Beachy *et al*, 2004). This perhaps explains why aberrant Hh signalling is found in a variety of cancers (Teglund & Toftgård, 2010). Thus tight regulation of this pathway is critical.

1.4.3.4. The role of PKA in water homeostasis

The water channel aquaporin-2 (AQP2) is important in water homeostasis in the distal collecting duct cells of the kidney. The subcellular localisation of AQP2 is controlled by the hormone vasopressin and subsequent activation of PKA. In the absence of a stimulus, AQP2 is located on vesicles in the cytoplasm. Upon

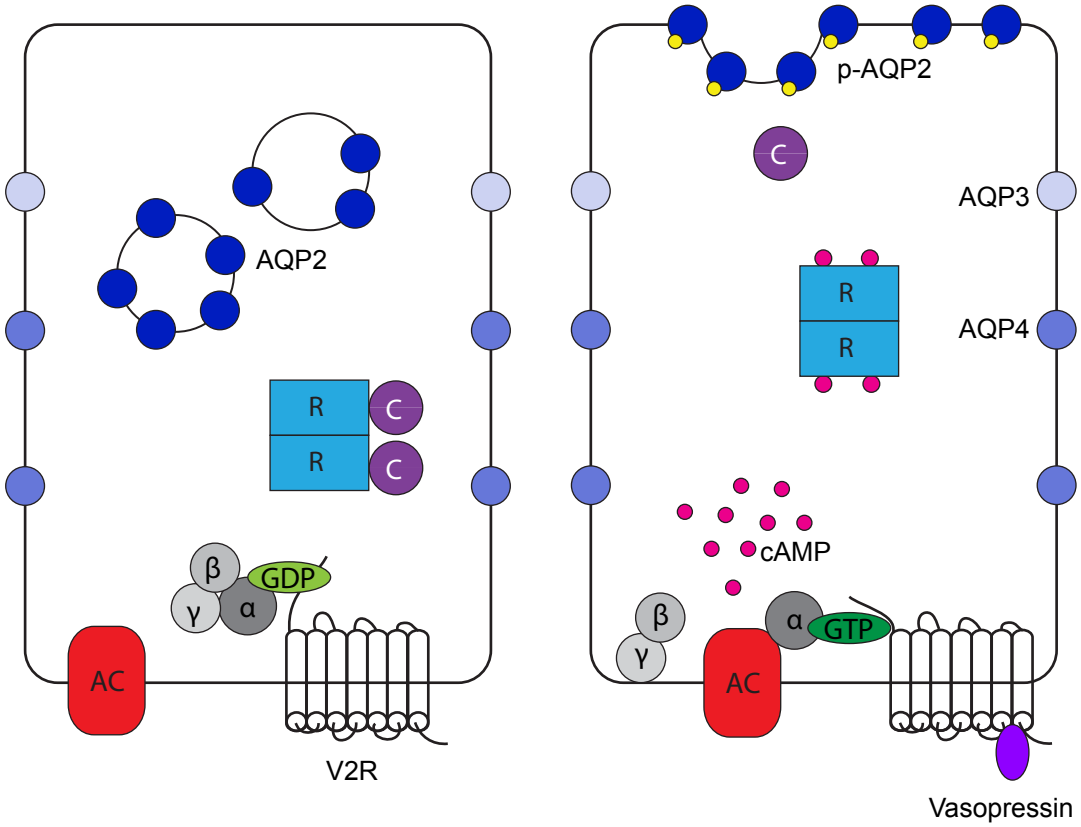

Figure 1.11 PKA regulation of AQP2 trafficking
In the proximal cells of the kidney, in the absence of stimulus AQP2 is located on vesicles in the cytoplasm. Vasopressin binding to its receptor V2R, leads to dissociation of the heterotrimeric G proteins (α, β, γ), activation of the adenyl cyclase (AC), and subsequent cAMP production. Activated PKA then mediates the phosphorylation of AQP2 at Ser256 (p-AQP2), which directs its insertion into the apical membrane, in order to increase water reabsorption. Water can then leave the proximal cells through AQP3 and AQP4 located in the basolateral membrane.

vasopressin stimulation of the V2 receptor, which is located in the basolateral membrane, PKA is activated and phosphorylates AQP2 at Ser256 (Katsura *et al*, 1997; Fushimi *et al*, 1997). This leads to translocation and insertion of AQP2 into the apical plasma membrane (Figure 1.11). As each AQP2 monomer forms an independent pore this leads to a significant increase in permeability and reabsorption of water from the urine. Reabsorbed water can then exit the principal cells via AQP3 and AQP4 that are located in the basolateral membrane (Nedvetsky *et al*, 2009). This PKA activity is thought to be AKAP dependent, as peptide disrupters of AKAP-PKAR D/D domain binding abolished this effect (Klussmann *et al*, 1999). A potential AKAP, described as a 90 kDa RII binding protein was identified on AQP2 vesicles (Jo *et al*, 2001). Another AKAP, AKAP11δ also colocalised together with AQP2 on vesicles, as well as with PDE4D (Stefan *et al*, 2007). This suggests PKA is specifically targeted to AQP2 containing vesicles, ready to respond to vasopressin. PDE4D may keep local cAMP levels low under basal conditions in order to prevent aberrant trafficking and excessive water reabsorption. Precise regulation of this process is required, as aberrations are associated with disease. Excess water retention stimulated by abnormally high levels of vasopression can lead to chronic heart failure (Schrier, 2011). Loss of vasopressin secretion leads to central diabetes insipidus, whereas mutations in both AQP2 and the vasopressin V2 receptor can lead to nephrogenic diabetes insipidus (Deen & Knoers, 1998).

1.4.4. PKA in disease

Clearly perturbations of the PKA pathway can have vast implications, and not surprisingly lead to various diseases, some of which are already mentioned above. Here I will discuss a few examples of particular interest.

1.4.4.1. PKA in diseases of the Endocrine System relating to Cushing's Syndrome

A recurring theme is the deregulation of PKA in cancers of endocrine origin, especially those of the HPA axis (hypothalamus-pituitary-adrenal gland). Stress leads to the release of corticotropin-releasing hormone (CRH) by the hypothalamus, which stimulates the pituitary gland to release adrenocorticotropic hormone (ACTH). ACTH binds its receptor at the adrenal gland, the melanocortin receptor 2 (MC2R). This leads to stimulation of the adenyl cyclase, cAMP production and thus activation of PKA (Ramachandran *et al*, 1987; Simpson & Waterman, 1988). PKA is thought to

be involved in both short and long term responses in the regulation of steroidogenesis. In the short term PKA phosphorylates and stabilises the mitochondrial protein StAR (steroidogenic acute regulatory protein) (Arakane *et al*, 1997; Clark *et al*, 2001). StAR then mediates the transport of cholesterol from the outer to the inner mitochondrial membrane, and thus regulates cortisol production (Epstein & Orme-Johnson, 1991; Clark *et al*, 1994; Artemenko *et al*, 2001; Manna *et al*, 2015). In the long term, PKA upregulates the transcription of genes involved in cortisol production (Simpson & Waterman, 1988).

Overproduction of cortisol can lead to Cushing's syndrome, characterised by metabolic aberrations including central obesity, myopathy, hypertension and osteoporosis (Hatipoglu, 2012). Cushing's syndrome has a variety of causes, some of which I will detail below, all leading to excessive cortisol secretion. This can be due to adrenal tumours autonomously producing cortisol, or tumours producing ACTH or CRH (Lodish & Stratakis, 2016). Overproduction of cortisol due to pituitary tumours that secrete ACTH is classified as Cushing's disease.

Deregulated PKA signalling was first implicated in cortisol-producing tumours of the adrenal cortex in patients with McCune Albright Syndrome (Weinstein *et al*, 1991). This is a rare disease that occurs sporadically, characterised by multiple tumours of the endocrine system. Weinstein and colleagues identified mutations in the gene coding for the G protein $G\alpha_S$, GNAS, as the cause for this syndrome. These mutations caused constitutive activation of $G\alpha_S$, thus leading to increased adenyl cyclase activity and cAMP production.

Carney Complex is another rare disorder that leads to multiple neoplasms including those of the adrenal and pituitary gland that can lead to Cushing's syndrome (Correa *et al*, 2015). It can be both inherited and sporadic. Carney Complex is caused by a variety of mutations in PKARIα; over 120 have been identified so far (Salpea & Stratakis, 2014). Most of these lead to haplo-insufficiency of PKARIα and thus defects in PKA signalling (Kirschner *et al*, 2000; Correa *et al*, 2015). Some mutations have also been identified that inhibit PKAC binding (Greene *et al*, 2008). Both Carney Complex and McCune Albright Syndrome are ultimately caused by uncontrolled PKA signalling.

Inactivating mutations in phosphodiesterases, PDE11A and PDE8B, were later identified in adrenal hyperplasia that also leads to Cushing's syndrome (Horvath *et*

al, 2006, 2008). Most recently mutation of PKAC itself have been identified in adrenal tumours that lead to Cushing's syndrome (Beuschlein *et al*, 2014; Cao *et al*, 2014; Goh *et al*, 2014; Sato *et al*, 2014). This mutation, L206R, is thought to inhibit PKAR binding (Cheung *et al*, 2015), again leading to uncontrolled PKA signalling.

1.4.4.2. PKA in other cancers

As in normal physiology PKA plays a variety of roles in a wide range of cancers (Sapio *et al*, 2014).

Around the same time as the PKAC mutants were described in adrenal tumours, a fusion protein of PKAC was identified in fibrolamellar hepatocellular carcinoma (FL-HCC) (Honeyman *et al*, 2014). PKAC is fused to the C-terminus of DNAJB1, a molecular chaperone. It was initially hypothesised that this fusion protein has lost the ability to bind PKAR, however, further studies showed that this was not the case (Cheung *et al*, 2015). This chimeric PKAC is thought to be overexpressed under the control of the DNAJB1 promoter and is also intrinsically more active, leading to enhanced signalling (Cheung *et al*, 2015).

Increased PKAR1α expression has been observed in a wide variety of cancers, including colorectal, ovarian, breast, melanoma and cholangiocarcinoma (a cancer of the bile ducts) (Bradbury *et al*, 1994; McDaid *et al*, 1999; Miller, 2002; Mantovani *et al*, 2008; Loilome *et al*, 2011). This has led to the hypothesis that type II PKAR is preferentially expressed in non-proliferating tissues, and type I PKAR is transiently upregulated in proliferating cells, and constitutively upregulated in cancer (Cho-Chung *et al*, 1995; Sapio *et al*, 2014). Type I PKAR binds cAMP with higher affinity than type II, and thus is thought to be able to activate PKA signalling in the presence of lower cAMP levels (Rannels *et al*, 1985; Robinson-Steiner *et al*, 1984). It has thus been speculated that 'isozyme switching' may be a potential strategy for cancer therapy (Cho-Chung & Nesterova, 2005). Overexpression of RIIβ led to growth arrest in colon cancer cells (Nesterova *et al*, 1996). Furthermore, treatment of cells with RIα antisense oligonucleotides caused a decrease in RIα levels, and led to stabilisation and increased RII levels. This led to differentiation in leukaemia cells, and induced growth arrest in a variety of epithelial cancer cell lines (Cho-Chung *et al*, 1999; Nesterova *et al*, 2000). A single subcutaneous injection of RIα antisense given to mice with colon carcinomas led to decreased RIα expression and a striking suppression of tumour growth for up to 14 days (Nesterova & Cho-Chung, 1995).

As mentioned above perturbation of Hh signalling has been found in a range of cancers. Given the role of PKA as a negative master regulator in this pathway, PKA has unsurprisingly been implicated as a tumour suppressor in both medulloblastoma and basal-cell carcinoma, two tumour-types that are driven by Hh signalling (He *et al*, 2014; Iglesias-Bartolome *et al*, 2015).

PKA has most recently been implicated as a mediator of mesenchymal-epithelial transition (MET) in a variety of cancer cell lines. This is thought to be through phosphorylation and activation of the histone demethylase PHF2, which enhances the expression of epithelial genes (Pattabiraman *et al*, 2016). Importantly PKA-induced MET made cells much more susceptible to chemotherapeutics, as well as causing a dramatic reduction in their potential to metastasise. This is thus a further mechanism by which PKA can convey tumour suppressive qualities, as the mesenchymal state is associated with increased tumourigenic potential.

1.5. Project Summary

Previous mass spectrometry data from a systematic screen, aimed at characterising Rho regulatory proteins, identified ARHGAP36 as a novel interacting partner of PKAC (Rocks and Pawson manuscript in preparation). The initial aim of this thesis was to confirm and characterise the interaction between ARHGAP36 and PKAC, and investigate a potential interplay between the Rho and PKA signalling pathways. In this thesis, I found that ARHGAP36 interacts with PKAC via a pseudosubstrate inhibition motif, akin to those found in the PKA regulatory subunits and the PKI proteins. Furthermore and unexpectedly, ARHGAP36 promotes polyubiquitylation of PKAC at a single lysine, K285. Surprisingly for a cytosolic protein, this mediates its degradation via the endolysosomal pathway. This bimodal antagonism of PKAC by ARHGAP36 results in a suppression of a wide variety of PKA signalling responses, including CREB activation and AQP2 trafficking. The ability of ARHGAP36 to inhibit PKAC and promote its degradation was independent of its Rho GAP domain.

Chapter 2. Materials and Methods

2.1. Molecular Biology

2.1.1. Creator Reactions

cDNAs for overexpression of ARHGAP36 were available as donor plasmids of the Creator system described previously from the Pawson Lab Toronto (Colwill *et al*, 2006). The full-length sequence refers to human ARHGAP36 UniProt ID: Q6ZRI8-2. Subcloning into acceptor expression plasmids was then done by Creator Reaction as shown in Table 2.1. The reaction was pipetted at room temperature and incubated for 15 min before heat inactivation of the Cre enzyme for 10 min at 70 °C. After cooling the total reaction was transformed into DH5α and plated onto sucrose chloramphenicol plates. If possible three colonies were picked to be screened. Colonies were then grown overnight in approximately 5 ml LB media containing kanamycin. Purified DNA was digested at 37 °C for 1 h with the restriction enzymes AscI and PacI, to cut out the insert from the backbone. Resulting fragments were then assessed by agarose gel electrophoresis. Where necessary clones were sequenced by Source Bioscience with primers O19, O20 or RE.

Component	Amount
Donor Plasmid	500 ng
Acceptor Plasmid	500 ng
BSA	1 µl
Cre 10x Buffer	1 µl
Cre Enzyme	0.5 µl
Water	Up to 10 µl
Total	10 µl

Table 2.1 Standard Creator Reaction

Clone Number	Acceptor Plasmid
v180	Triple Flag
v3531	Cerulean (CFP)
v3534	Citrine (YFP)
v3535	Cherry

Table 2.2 Creator Acceptor Plasmids

2.1.2. Gifted Plasmids

Mouse PKAC-Venus YFP was provided by Manuela Zaccolo (Zaccolo & Pozzan, 2002). Human PRKACA (GenBank: BC039846.1) was cloned into the Gateway system (Life Technologies). K285R mutants were generated by site directed

mutagenesis. Human PRKAR1α (GenBank: BC036285) was cloned into the gateway system. Praja2, Stub1 and Huwe1 were also available as Gateway donors and cloned into the Gateway expression system. Cerulean CFP-PKI was kindly provided by Susan Taylor (University of California, San Diego). AKAR-4-NES and PKI-Cherry were provided by Jin Zhang (Johns Hopkins) and were described previously (Herbst *et al*, 2011). LAMP1-YFP was a gift from Lee Haynes (University of Liverpool). GFP-HRS was described previously (Urbé *et al*, 2003). GFP-Vps4 and the EQ mutant were a gift from Phil Woodman (Bishop & Woodman, 2000), GFP-Rab5-Q79L was a gift from Volker Haucke (FMP, Berlin).

2.1.3. Site-directed mutagenesis

Subsequent mutation and deletion constructs of ARHGAP36 and PKAC were created by site-directed mutagenesis (QuikChange, Agilent Technologies) according to manufacturer's guidelines using the Pfu polymerase. Following the reaction DNA was incubated with Dpn1, to digest methylated bacterial template DNA, leaving only unmethylated mutant DNA. Part of the reaction was then transformed into XL10 Gold bacteria (Invitrogen). All primers were purchased from Sigma.

ARHGAP36	Primer	Sequence	Template
N	F R	cttctgggatccaaaaggaagttaattaaccaggtaagttcc ggaacttacctggttaattaacttccttttggatcccagaag	dC
N1	F R	cggtcaggctgcgggcttaattaaccaggtaag cttacctggttaattaagcccgcagcctgaccg	dC
N2	F R	cttctgggatccaaaaggaagttaattaaccaggtaagttcc ggaacttacctggttaattaacttccttttggatcccagaag	Iso3
ARG	F R	tcgccgtgggcgtcgattaattaaccaggtaag cttacctggttaattaatcgacgcccacggcga	N2
dARG	F R	tcaggctgcgggcggtgcagtgtctg cagacactgcaccgcccgcagcctga	WT
dN	F R	ccaggggcgcgccatgagtctcaatcc ggattgagactcatggcgcgcccctgg	WT
dC	F R	gataactgggatgtcctcttcttaattaaccaggtaagttcc ggaacttacctggttaattaagaagaggacatcccagttatc	WT
GAP	F R	gataactgggatgtcctcttcttaattaaccaggtaagttcc ggaacttacctggttaattaagaagaggacatcccagttatc	dN
dGAP	F R	gggatccaaaaggaagcaggtgcctccccata tatggggaggcacctgcttccttttggatccc	WT
Linker	F R	agacactgcaccggcgcgcccctg caggggcgcgccggtgcagtgtct	N2
RRV	F R	tcagccagactatccacagaatctgcaccatcatccccacggcgagtg gggagttcactcgccgtggggatgatggtgcagattctgtggatagtc	WT
Iso3 (delN1)	F R	ggggcgcgcccgtcgtcggg cccgacgacgggcgcgcccc	WT

Table 2.3 ARHGAP36 Mutagenesis Primers

PKAC	F	R
K286R	atcgttgaccccattcctgaggttcccaaagcg	cgctttgggaacctcaggaatggggtcaacgat
E127A	ggtgggagaacatcgcgccaccagctaca	tgtagctggtggcgcgatgttctcccacc
E170A	tcgatgagaagattcgcgggcttcaggtccc	gggacctgaagcccgcgaatcttctcatcga
E230A	ggagtcctcatctacgcgatggctgctggttac	gtaaccagcagccatcgcgtagatgaggactcc

Table 2.4 PKAC Mutagenesis Primers

2.1.4. 36i Cloning

36i was amplified with the primers below and inserted into pmCherry-C1 (Clontech) with BsrGI and EcoRI, or into pmCherry-N1 (Clontech) with EcoRI and AgeI by ligation.

36i	F	R
N1	gcgcggaattcgccaccatggagcccaccttgccccgg	cgcgcaccggtccgctcagctcagccagactatccac
C1	gcgcgtgtacagcgagcccaccttgccccgg	cgcgcgaattcctacagctcagccagactatc

Table 2.5 36i Primers

2.1.5. LR Reaction

Gateway donor constructs were cloned into Gateway expression vectors using the LR clonase II (Invitrogen) according to manufacturers guidelines.

2.1.6. Transformation

Unless otherwise indicated, 100 µl DH5α were briefly thawed on ice before addition of plasmid or reaction to be transformed. Bacteria were incubated for 30 min on ice, before heat shock at 42 °C for 45 s. Bacteria were cooled on ice for minimum 2 min before addition of 500 µl LB media and 20 mM Glucose. Bacteria were shaken for 1 h at 37 °C before plating on LB agar plates with the required antibiotic, then left to form colonies overnight at 37 °C.

2.1.7. Plasmid DNA Purification

For minipreps single colonies were picked and grown in approximately 5 ml LB media in presence of the required selection antibiotic overnight at 37 °C shaking. DNA was purified from pelleted bacteria using the Zymogen Research ZR Plasmid Miniprep Classic kit (D4054), according to manufacturer's instructions. When more DNA was required, midipreps were done from 100 ml bacterial culture, using the

Invitrogen Midi kit (K210005). DNA concentrations were measured using a NanoDrop (PeqLab).

2.1.8. Glycerol Stock

Glycerol stocks were prepared from the same cultures as those for minipreps. 700 µl bacteria in LB media was combined with 300 µl glycerol, thoroughly mixed and frozen at -80 °C.

2.1.9. Sequencing

When necessary clones were sequenced by Source Bioscience (Berlin).

Sequencing Primers	Sequence	Binds
O19	TGCTCACATGTTCTTTCCTG	All Creator- before insert- F
O20	TGGATTTGTTCAGAACGCTC	All Creator- after insert- R
RE	CGA AGT TAT GGC GCG AGG G	Creator Expression- between tag and insert
M13F	TGT AAA ACG ACG GCC AGT	Gateway
M13R	CAG GAA ACA GCT ATG ACC	Gateway

Table 2.6 Primers used for sequencing

2.1.10. Agarose gel electrophoresis

Agarose gels of 0.8-1 % were prepared by dissolving agarose in TAE (40 mM Tris, 20 mM acetic acid, 1 mM Na_2EDTA). DNA samples were loaded in Orange G loading buffer (50 % Glycerol, 25 mM EDTA, 0.5 % Orange G). After running in TAE buffer, gels were incubated in a 0.025 mg/ml Ethidium Bromide bath for 10 min before imaging in a Transilluminator.

2.1.11. *In situ* hybridization

Specific fragments of the Arhgap36 gene were amplified from whole mouse E12.5 embryo cDNA using the following primers: GCATCTGTCAATGTTGTCCG and GGTGGCAAATTTGCCCTTCTTCC. The PCR product was then cloned into the pGEM-T Easy plasmid using T4 DNA ligase (Promega). *In vitro* transcription of the antisense probe was performed using the DIG-RNA labelling kit (Roche). Paraffin sections were rehydrated by successive incubations in decreasing concentrations of Ethanol before additional incubation in Xylol. Subsequently, the sections were post-fixed in 4 % PFA for 20 min and incubated in a 10 µg/ml Proteinase K solution for 8 min. The tissue was incubated with the RNA-probe overnight at 65 °C. Following

successive washing with SSC/Formamide and MABT, the sections were incubated in blocking reagent (Roche) and goat serum. The sections were then incubated with an alkaline-phosphatase-coupled against digoxigenin (DIG, Roche). After further washing with MABT and NTMT, NBT/ BCIP Purple (Roche) was used as a chromogenic substrate for the alkaline phosphatase (Boehringer) in order to detect the RNA probe. The sections were then mounted with Roti-Histokitt II (Roth) and imaged on a Leica DMI 6000B inverted microscope.

2.2. Cell Biology

2.2.1. Cell Lines

All cell lines were cultured at 37 °C with 5 % CO2, and split every 2-3 days at the indicated ratios. Cells were washed once with PBS (PAA) before incubation with Trypsin/EDTA (PAA) for the indicated times, followed by resuspension in the indicated media and replating. Penicillin/streptomycin (P/S) was purchased from PAA. All media were from Gibco.

a.

Cell Line	Origin	Species	Media	Additives
MDCK	Madin-Darby canine kidney II	Dog	MEM	10 % FBS, 1 % P/S
HEK293T	Human Embryonic Kidney	Human	DMEM	10 % FBS, 1 % P/S
HeLa	Cervical Cancer	Human	DMEM	10 % FBS, 1 % P/S
NIH-3T3	Fibroblast	Mouse	DMEM	10 % FBS, 1 % P/S
U2OS	Osteocarcoma	Human	DMEM	10 % FBS, 1 % P/S
MCD4	Collecting duct cells	Mouse	DMEM/ F12	10 % FBS, 10 µM dexamethasone
NGP	Neuroblastoma	Human	RPMI	10 % FBS, 1 % P/S
SK-N-BE(2)	Neuroblastoma	Human	DMEM/ F12	10 % FBS, 1 % P/S

b.

Cell Line	Splitting Density	Trypsinisation Time	DNA Transfection	RNA Transfection
MDCK	1:8	10-15 min	Effectene	-
HEK293T	1:8	3-5 min	PEI	RNAiMAX
HeLa	1:10	3-5 min	PEI	RNAiMAX
NIH-3T3	1:10	3-5 min	Lipofectamine 3000	
U2OS	1:5	3-5 min	Lipofectamine 3000	-
MCD4	1:4	3-5 min	PEI	
NGP	1:3	3 min	Lipofectamine 3000	RNAiMAX
SK-N-BE(2)	1:5	3-5 min	Lipofectamine 3000	RNAiMAX

Table 2.7 Cell Lines
The table shows the cell lines used within this thesis, how they were cultured and which reagents were used for transfection.

2.2.2. DNA Transfection

For live cell microscopy, cells were transfected the same day as they were seeded, a minimum of 3 h later, after cells had adhered. For immunofluorescence (IF) and other applications, cells were transfected the day after seeding, or for NGP cells two days after seeding.

Effectene (Qiagen): DNA and Enhancer were incubated together in Buffer EC for 5 min, before addition of Effectene for a further 10 min. The mixture was then vortexed for 10 s before adding to cells. Enhancer and Effectene were both vortexed before use, and used at a ratio of 3:1:1 (µl:µl:µg) with DNA. Medium on cells was changed to OptiMEM (Invitrogen) before transfection.

PEI: DNA and PEI were incubated together in OptiMEM at a ratio of 1:3 (µg:µl) for 15-60 min, before adding dropwise to cells. PEI (Polysciences Inc) was prepared by dissolving in water at 1 mg/ml pH 7 and sterile filtered before use.

Lipofectamine 3000 (Thermo): DNA and p3000 reagent were added together in OptiMEM and combined with Lipofectamine in OptiMEM at a ratio of 1:2:3 (DNA (µg): p3000 (µl): Lipofectamine(µl)). The mixture was incubated for 5 min before adding dropwise to cells. Medium on cells was changed to OptiMEM before transfection.

2.2.3. RNA Transfection

HEK293T cells were transfected one day after seeding in the absence of penicillin/streptomycin using Lipofectamine RNAiMAX (Invitrogen) and 40 nM final concentration siRNA according to manufacturer's guidelines. 48 h later cells were harvested. NGP cells were cultured for two days before transfection with 50 nM ARHGAP36 SMARTpool or individual oligos, also using Lipofectamine RNAiMAX. 24 h later cells were harvested. All oligos were purchased from Dharmacon, except for HRS which was custom synthesised.

Target	Species	No.	Sequence
Praja2	Human	J-006916-08	GAAGCACCCUAAACCUUGA
OTP		J-006916-07	AGACUGCUCUGGCCCAUUU
		J-006916-06	GCAGGAGGGUAUCAGACAA
		J-006916-05	GUUAGAUUCUGUACCAUUA
Stub1	Human	J-007201-10	UGGAAGAGUGCCAGCGAAA
OTP		J-007201-09	GAAGGAGGUUAUUGACGCA
		J-007201-08	GUGGAGGACUACUGAGGUU
		J-007201-07	CGCUGGUGGCCGUGUAUUA
Huwe1	Human	J-007185-10	UAACAUCAAUUGUCCACUU
OTP		J-007185-09	GAGCCCAGAUGACUAAGUA
		J-007185-08	GCAGUUGGCGGCUUUCUUA
		J-007185-07	GCUUUGGGCUGGCCUAAUA
ARHGAP36	Human	J-032590-12	GCGGGUCAGCUCCGAGAAA
OTP		J-032590-11	CCUCGGAGACGGACAUCGA
		J-032590-10	UAUGAGAUUUACCGGGAUU
		J-032590-09	GCAUGCAGAGAGAGCGCUA
HRS	Human	Sense	GUCAACGACAAGAACCCACdTdT
	Duplex	Anti-sense	dTdTCAGUUGCUGUUCUUGGGTG

Table 2.8 siRNA sequences

2.2.4. Virus Infection

Cells were infected with lentiviruses produced previously in the Pawson lab containing shRNA in a pLKO.1 vector and a puromycin selection cassette. The stuffer control virus contains the pLKO.1 plasmid containing a 1.9 kb stuffer sequence in place of the shRNA cassette. 24 h after infection puromycin was added at 2 µg/ml for SK-N-BE(2) and 0.5 µg/ml for NGP. Cells were then expanded in the presence of puromycin.

Virus Number	shRNA Sequence
A8	GATGACAATCAGAATGTGCAT
A9	GCTGTATCACACAAGACATTT
A10	CACACAAGACATTTGGCATTA
G11	GCAGAGATGTTTCTGTGTCAT
G12	CAACCGTATGACTTCCACTAA

Table 2.9 ARHGAP36 targeting shRNA sequences

2.2.5. Antibodies and Chemicals

Chemicals	Target	Source	Vehicle	Final Concentration
Bafilomycin	Lysosome	Cayman	DMSO	100 nM
Leupeptin	Lysosome	US Biological	Water	500 µM
Epoxomicin	Proteasome	Cayman	DMSO	Hek: 50 nM; MDCK: 100 nM
Cycloheximide	Protein Synthesis	Calbiochem	DMSO	Hek: 50 µg/ml; MDCK: 1 µg/ml
Forskolin	Adenyl Cyclase	Cayman	EtOH	10 µM
IBMX	Phosphodies terases	Cayman	EtOH	100 µM
SAG	Hh Pathway	Enzo	Water	0.2 µM
PKI	PKAC	Santa Cruz	DMSO	10 µM

Table 2.10 Inhibitors used within this thesis

Source	Species	Verified	IF	WB	IP	Order Number
Atlas	Rabbit	Y	1:200	1:500	~0.5 µg/ 1 mg protein	HPA002064
Thermo	Rabbit	Y	1:200	1:500	~1 µg/1 mg protein	PA5-31619
Sigma	Rabbit	-	1:100	1:500	-	SAB2102046
Millipore	Rabbit	-	1:100	1:500	-	07-2142
Abgent	Rabbit	-	1:100	1:500	-	AP16204b

Table 2.11 ARHGAP36 Antibodies

Antibody	Species	Source	Clone/Order Number	IF	WB	IP
EEA1	Rabbit	CST	3288	1:100	-	-
Rab7	Rabbit	CST	9367	1:100	-	-
GAPDH	Rabbit	CST	2118	-	1:10,000	-
GFP	Rabbit	AbCam	ab290	1:1000	1:10,000	0.5 µl
GFP	Chicken	AbCam	ab13970	1:1000	-	-
Flag	Mouse	Sigma	M2	1:500	1:5,000	-
His	Mouse	Sigma	H1029	-	1:500	1 µl
Ubiquitin	Mouse	Covance	P4G7	-	1:500	-
PKAC	Mouse	BD	610981	1:200	1:1000	-
PKAC	Rabbit	CST	4782	1:200	1:1000	-
pCREB	Rabbit	CST	9198	1:200	1:500	-
pSubstrate	Rabbit	CST	9624	-	1:1000	1 µl
RIa	Mouse	BD	610610	1:200	1:1000	-
RIb	Sheep	R&D	AF4177	-	1:500	
RIIa	Rabbit	Santa Cruz	sc-909	1:200	-	-
RIIa	Mouse	BD	612243	1:200	1:1000	
RIIb	Rabbit	Santa Cruz	sc-25424	1:200	-	-
RIIb	Mouse	BD	610626	1:200	1:1000	
AQP2	Rabbit	Enno Klussmann	H27	1:1000	-	-
ZO-1	Rat	Santa Cruz	sc33725	1:1000	-	-
HRS	Rabbit	Sylvie Urbe	958/3	1:500	1:1000	-
AMSH	Rabbit	Sylvie Urbe	850/3	1:500	1:500	-
Stub1	Rabbit	CST	2080	-	1:1000	-
Praja2	Rabbit	Bethyl	A302-991A	-	1:1000	-
GST	Mouse	CST	26H1	-	1:5000	-
Acetylated Tubulin	Mouse	Sigma	T6793	1:1000	-	-
Polaris	Goat	Acris	AP16448PU-N	1:100	-	-
Tubulin	Mouse	Sigma	DM1a, T6199	1:1000	1:10,000	-
β-catenin	Mouse	BD	610153	-	1:5,000	-
Vinculin	Mouse	Sigma	V9264	1:2000	-	-
Phalloidin-594	-	Biotium	CF594	1:200	-	-
Cell Tracker-647	-	Molecular Probes	C34565	250 nM	-	-

Table 2.12 Primary Antibodies

Alexa Fluor secondary antibodies for immunofluorescence were purchased from Molecular probes and used at 1:1000. 488, 555 and 647 conjugates were used. All HRP coupled antibodies for western blot were purchased from Biorad.

2.3. Microscopy

2.3.1. Immunofluorescence

Cells seeded on glass coverslips, were washed once with warm PBS containing calcium and magnesium (PBS++), before fixing with 4 % PFA in PBS for 10 min. Cells were washed 2 x 5 min with PBS between every further step. Cells were then permeabilised with 0.2 % Triton X-100/ 100 mM glycine in PBS for 10 min, and blocked for a minimum of 20 min in 3 % BSA in PBS. Primary antibodies were incubated in blocking solution for minimum 1 h at room temperature or at 4 °C over night. Alexa Fluor secondary antibodies were incubated for 30 min, also in blocking solution. Coverslips were mounted using ProLong Gold (Invitrogen). For experiments with Cell Tracker 647, cells were washed with PBS and incubated for 30 min with 250 nM Cell Tracker in serum free media, before fixing as normal.

2.3.2. Live Cell Imaging

Cells were seeded on MatTek dishes and transfected later the same day after having time to adhere. Transfected cells were imaged the following day.

2.3.3. Fluorescence microscopy

Confocal laser scanning microscopy was used for both live and fixed cells, and performed on a Fluoview 1000 confocal laser scanning microscope (Olympus) equipped with a UPLSAPO 60X/1.3 NA silicon immersion oil immersion lens. Images were taken with the following excitation (Ex) and emission (Em) settings: Hoechst Ex: 405 nm diode laser (50 mW) Em: 425-475 nm; mCerulean Ex: 440 nm diode laser (25 mW) Em: 460-500 nm; GFP, AlexaFluor488 Ex: Multi-Line Argon laser 488 nm (40 mW) Em: 500-545 nm; mCitrine, Venus Ex: Multi-Line Argon laser 515 nm (40 mW) Em: 530-545 nm; AlexaFluor555 Ex: 559 nm diode laser (20 mW) Em: 570-625 nm; mCherry Ex: 559 nm diode laser (20 mW) Em: 575-675 nm; AlexaFluor647 Ex: 635 nm diode laser (20 mW) Em: 655-755 nm.

2.3.4. AKAR FRET (with Markus Müller)

1.3 x 10^5 HEK293T cells were seeded per well on poly-L-lysine (0.01 %, Sigma) coated 12 well plates. The following day cells were transfected with 650 ng AKAR4-NES FRET sensor together with 150 ng Cherry tagged ARHGAP36 constructs or control. After 24 h transfection, cells were serum starved for 5 h, treated with 10 µM Forskolin and 100 µM IBMX for 30 min and subsequently imaged. Intensity-based

FRET ratio-imaging experiments were then performed on an inverted epifluorescence IX81 microscope (Olympus) equipped with a MT20 xenon-arc burner (Olympus) and an UPLSAPO air 10x/0.4 NA objective controlled by xcellence software (Olympus). Images were acquired with a Hamamatsu ImagEM Enhanced EM-CCD camera at a 16-bit depth. Donor and FRET-acceptor images were acquired with the following settings: 430/25 (excitation), zt442RDC (dichroic mirror) and emission changing between 483/32 (donor-channel) and 542/27 (FRET-acceptor-channel) using a filter wheel. Images were analysed with ImageJ. Images were background corrected and regions of interest were defined by AKAR4-Venus fluorescence channel. Average intensities of acceptor channel were divided by donor channel to calculate FRET efficiency.

2.3.5. Image Analysis (with Markus Müller)

Line scans to determine fluorescence intensity profiles were analysed using ImageJ software. Plot Profile analysis was used to create a graph of pixel intensity plotted against the distance along the line. To reduce noise, pixel intensity was averaged on a line width of 10 pixels. Intensity was then normalized to the lowest and the highest intensity within the selection. For analysis of protein level ratios of ARHGAP36 and PKAC in immunofluorescence images of NGP cells, automated cell segmentation was performed with CellProfiler software (Kamentsky *et al*, 2011) based on DAPI, CellTracker Deep Red and ARHGAP36 images. Average PKAC and ARHGAP36 intensities were measured in each cell outline. Each single cell intensity was normalised to the median intensity of all cells in each image. Pearson's sample correlation analysis was performed in OriginPro (OriginLab).

2.3.6. Cilia Formation

NIH-3T3 cells were seeded on coverslips, the following day they were starved for 48 h in serum free medium. Cells were transfected for the final 24 h before fixing. MDCK cells seeded on coverslips were grown for up to nine days in complete medium, and the media changed every day. Cells were then transfected for the final 24 h before fixing.

2.4. Biochemistry

2.4.1. Lysis

As HEK293T cells easily detach they were harvested by merely pipetting up and down in PBS++ on ice. Cells were then pelleted by spinning at 400 RCF for 5 min at 4˚C. Unless otherwise stated HEK293T cell pellets were lysed in NP40 (1 % NP40, 50 mM Tris-HCL pH 8, 150 mM NaCl,), with complete protease inhibitor cocktail (Roche) and 10 µM *N*-Ethylmaleimide (NEM, Sigma) for 20 min on ice. NGP cells were lysed directly in RIPA (50 mM Tris pH 7.4, 150 mM NaCl, 0.1 % SDS, 1 % NP40, 0.5 % Sodium deoxycholate) supplemented with complete protease inhibitor cocktail (Roche), 10 µM NEM. For Forskolin/IBMX stimulation experiments lysis buffer was also supplemented with PhosSTOP (Roche). All other cell lines were also lysed directly in RIPA. Lysates were then cleared by spinning at 18,000 RCF for 5 min at 4 ˚C. Cleared lysates were then transferred to new eppendorf tubes. Protein concentration was measured using the Precision Red Protein Assay (Cytoskeleton) according to manufacturers instructions. Absorbance was measured at 600nm.

2.4.2. Immunoprecipitation

HEK293T cells were transfected when 80 % confluent and harvested as above the following day. For Ubiquitin immunoprecipitations (IPs), His-Ubiquitin was always co-transfected for improved detection at the same ratio as the substrate protein, with less ARHGAP36. For a 10cm plate specifically 5:5:3 µg ratio of PKA:Ubiquitin:ARHGAP36 was used. Cleared lysates were added to either Flag-M2 affinity gel (Sigma), or Protein G Sepharose beads (Sigma) coupled with anti-GFP (ab290, Abcam) or anti-His (H1029, Sigma). After minimum 1 h rotation at 4 ˚C, beads were washed three times in lysis buffer and eluted with 2x Sample Buffer. To try to avoid antibodies becoming uncoupled from the beads, samples were incubated first at 37 °C for 20 min, then the supernatant was separated from the beads and boiled. Lysate samples were always saved and run together with the eluates to check for expression levels.

For endogenous ARHGAP36 IP NGP cells directly lysed in RIPA supplemented with EDTA-free complete protease inhibitor cocktail (Roche), 10 µM NEM, 5 mM $MgCl_2$ and 1 mM ADP were subjected to protein assay before IP. 4.5 mg protein was incubated for 1 h at 4 ˚C with 4 µg ARHGAP36 Thermo antibody or IgG control.

Beads were then added for 30 min, washed three times in lysis buffer and eluted with 2x Sample Buffer.

2.4.3. UbiCREST

The assay kit was purchased from Boston Biochem and the experiment carried out according to manufacturer's guidelines and as described previously (Hospenthal *et al*, 2015; Mevissen *et al*, 2013). Specifically, HEK293T cells were transiently transfected with PKAC-YFP, Flag-ARHGAP36 and His-Ubiquitin as for Ubiquitin IPs. Cells were lysed in the presence of 10 µM NEM. Lysates were subjected to one single GFP IP, which after washing, was then split and incubated with the DUBs for 45 min at 37 °C. Eluates were run on 12 % SDS-PAGE gels, and membranes probed with GFP and Ubiquitin antibodies.

2.4.4. Western Blotting

Boiled samples were separated on SDS-PAGE gels of varying percentage with a 4 % stacking gel. Gels were run first at 80 V then at up to 200 V until proteins were sufficiently separated, in SDS Running Buffer (100 mM Tris, 100 mM Hepes, 0.1 % SDS). Gels were then transferred onto 0.45 µm Nitrocellulose (Amersham) using the Wet Blot System (BioRad) for 90 min at 100 V in Wet Blot Transfer Buffer (25 mM Tris, 190 mM Glycine, 20 % Methanol). Membranes were then incubated with Ponceau Red to determine transfer efficiency. After washing with TBST (50mM Tris, 150mM NaCl, 0.01% Tween20), membranes were blocked with 5 % Milk Powder in TBST for approximately 1 h, before incubating with the primary antibody overnight at 4 °C. For phospho antibodies 1 % BSA/TBST was used for blocking. Membranes were then washed 3 x 5 min in TBST before incubation with HRP-coupled secondary antibodies for 1 h at RT. After washing 3 x 5 min in TBST membranes were then incubated with the LumiGlo Peroxide Substrate (CST) for 1 min. Films were exposed for varying times before developing.

2.4.5. Peptide Spots

Peptide spots were produced by automatic SPOT synthesis on Whatman 50 cellulose membranes using Fmoc (9-fluorenylmethyloxycarbonyl) chemistry with the AutoSpot-Robot ResPep-SL (Intavis Bioanalytical Instruments) as previously described (Hundsrucker *et al*, 2010). Fmoc-protected amino acids and derivatized cellulose-membranes (amino-modified acid-stable cellulose membrane with PEG-

spacer) were purchased from Intavis. Membranes were activated for 1 min in MeOH, washed 3 x 10 min in TBST followed by blocking for minimum 2 h in 3 % filtered BSA. Membranes were then incubated with 0.1 µg/µl GST-PKAC (Biovision) overnight at 4 °C. The next day membranes were washed 3 x 10 min in TBST, before primary antibody incubation with α-GST, for 2 h at RT. Membranes were then again washed before secondary antibody incubation for 1 h at RT, followed by final washing and developing as for western blotting.

2.4.6. Peptide Synthesis (Rudolf Volkmer)

36i and the corresponding scrambled control peptides were synthesised on a 433A peptide synthesiser (Applied Biosystems) on Rapp resin columns (Rapp Polymere, Tuebingen, Germany) using Fmoc (**N**-(9-fluorenyl)methoxycarbonyl) chemistry. The peptides were purified and analysed by high performance liquid chromatography on Polyencap A300 columns (Bischoff, Leonberg, Germany) and electrospray mass spectrometry (TSQ 700, Finnigan MAT, Bremen, Germany). The sequences of the peptides are:

36i: E-P-T-L-P-R-E-F-T-R-R-G-R-R-G-A-V-S-V-D-S-L-A-E-L

Scrambled: V-R-R-F-P-T-R-A-E-E-T-S-L-E-G-A-G-R-S-R-V-L-L-P-D

2.4.7. PepTag Assay (with Carolin Barth)

In order to assess PKA activity the Peptag Assay (Promega) was used as described previously (Christian *et al*, 2011). A1 Peptide (L-R-R-A-S-L-G) was incubated with or without 25 ng recombinant PKACα (Biovision) together with 10 µM scrambled, 36i or PKI peptides for 45 min shaking at 30 °C. The separation of phosphorylated and non-phosphorylated peptide was achieved by agarose gel (0.8 %) electrophoresis. PKI (5-24) peptide was purchased from Santa Cruz, the sequence is: TTYADFIASGRTGRRNAIHD. 36i and scrambled peptides were synthesised as described above.

2.5. Mass Spectrometry

2.5.1. Ubiquitin site identification (with Erik McShane)

For ubiquitin site identification HEK293T cells were cultured in SILAC DMEM (Life Technologies) containing 1% penicillin/streptomycin, and 10% dialysed FBS (Sigma-Aldrich) containing either heavy (Lys8 and Arg10, Cambridge isotope laboratories) or light (Lys0 and Arg0, Sigma-Aldrich) versions of amino acids, for a minimum five passages before being transiently transfected with PEI (Ong *et al*,

2002). Cells were harvested after 24 h transfection, lysed by sonicating in RIPA buffer (50 mM Tris HCl, pH 7.4, 150 mM NaCl, 0.25 % Na-deoxycholate, 1 mM EDTA) containing 0.1 % SDS, supplemented with NEM, DNAse and complete protease inhibitor cocktail (Roche). Lysates were subjected to IP using Flag-M2 affinity gel (Sigma). Heavy and light corresponding samples were mixed before the last washing step.

Proteins eluted in Guanidine-HCl were precipitated in ethanol over night at 4 °C as previously described (Sury *et al*, 2015). Proteins were spun down and ethanol decanted. Protein pellet was resuspended in 6 M urea and 2 M thiourea in 10 mM HEPES (pH 8). Proteins were denatured using DTT followed by alkylation of cysteines by 2-chloroacetamide (Nielsen *et al*, 2008). Proteins were digested by endoproteinase LysC and then diluted in 50 mM Ammonium bicarbonate (pH 8) in water before being further digested by trypsin over night at room temperature. Resulting peptide solution was desalted on stage tips by washing in 5 % acetonitrile and 0.1 % formic acid (Rappsilber *et al*, 2003). Samples were eluted in 80 % acetonitrile and 0.1 % formic acid and vacuum dried before being diluted in 5 % acetonitrile and 0.1 % formic acid. The peptides were separated on a 15 cm column packed in house with ReproSil-Pur 120 C18-AQ 3 µm resin (Dr. Maisch GmbH), using a 1 h linear gradient of increasing acetonitrile concentration with a flow rate of 250 nl/ min on a high pressure liquid chromatography (HPLC) system (ThermoScientific). Separated peptides were ionized using an electrospray ionization source (ThermoScientific) and analysed on Q Exactive mass spectrometer (ThermoScientific). The Orbitrap resolution was set to 70,000 (target value 3,000,000; maximum injection time of 20 ms) for full scans and 17,500 (maximum injection time 60 ms; target value 1,000,000) for MS/MS spectra. The system was run in a data dependent mode selecting the top 10 most intense ions for higher energy collision induced dissociation.

Raw files were analysed using the MaxQuant software 1.5.1.1 (Cox & Mann, 2008) using the default setting but with ‘Requantify’ and ‘match between runs’ activated. Lys8 and Arg10 were set as the heavy label. Ubiquitin leaves a signature GlyGly modification of Lysines (+114.0429 Da) after tryptic digestion. The GlyGly(K) modification, acetylation of protein N-termini and oxidation of methionine were set as variable modifications. C-terminal carbamidomethylation was set as a fixed modification. Trypsin/P was set as protease for the *in silico* digest of the Human Uniprot database (2014-01) in addition to a data base containing common

contaminants. The false discovery rate was set to 1 % both at the peptide and protein level and was estimated by in parallel matching the MS/MS spectra against a database contain the reversed sequences of the Uniprot database (Cox & Mann, 2008).

Plotting of the SILAC ratios was done using R version 2.15.1 (R Foundation for Statistical Computing, Vienna, Austria). Spectra were visualized using the MaxQuant viewer and figures were modified in Illustrator (Adobe).

2.5.2. Selected Reaction Monitoring (with Patrick Beaudette)

For Selected Reaction Monitoring (SRM) chain linkage identification, 1x 15 cm dish of HEK293T cells were used for each condition. Cells were lysed with NP40, and subjected to IP using GFP-Trap Beads (Chromotek) due to their ability to withstand harsh washing conditions, in order to elute only the GFP tagged protein itself. After 1 h rotating at 4 °C, beads were washed with 2 M Guanidine-HCl followed by water, then eluted by boiling in 2x SDS sample buffer. Eluates were run briefly on an SDS-PAGE gel followed by an in-gel digestion with trypsin. After a solid-phase extraction and desalting, peptides were eluted, lyophilized and reconstituted with a 0.1 % formic acid/ 3 % ACN buffer containing 100 fmol/µl of heavy tryptic peptide standards corresponding to all the different polyubiquitin linkage types (Mirzaei *et al*, 2010). Peptides were separated on a reversed-phase column (20 cm length, 75 µm ID, 3 µm Dr. Maisch C18) with a gradient from 3 to 36 % ACN in 38 min and SRM measurements performed using a Q-Trap 6500 (AB Sciex). The top two most intense transitions were selected and their peaks integrated with MultiQuant 3.0 software (AB Sciex). In parallel, the samples were measured in data-dependent acquisition mode using an Orbitrap Q-Exactive instrument (Thermo) with an on-line chromatography equivalent to what was described for the SRM analysis. The raw files were analysed with MaxQuant 1.5.2.8 and the signal intensity for PKAC used to normalize the SRM-MS data to account for variation between the IPs.

2.5.3. Identification of Stub1 as an ARHGAP36 interactor (with Erik McShane)

HEK293T cells transfected with YFP-ARHGAP36, were lysed with NP40 and subjected to regular GFP IP. Eluates were then separated by SDS-PAGE. Proteins in the SDS-PAGE gel were fixed by incubation in 50 % methanol and 10 % acetic acid solution. The gel was then stained with Coomassie blue using the Novex colloid blue stain Kit (Thermo Scientific) following the manufacturer's instructions. After the

gel was de-stained overnight, the unidentified band at approximately 35 kDa was cut out, then further cut into smaller pieces, and transferred to an Eppendorf tube. Proteins were then reduced, alkylated and digested “in-gel” as described previously (Shevchenko *et al*, 2007). In brief, gel pieces were washed by switching between 50 % ethanol in 50 mM ammoniumbicarbonate (ABC buffer) solution or just ABC buffer. Gel pieces were fully dehydrated in 100 % ethanol and then speed vacced. 10 mM DTT in ABC was then added and incubated at 56 °C for 1 h to reduce the proteins. After decanting the DTT solution, 55 mM iodoacetamide in ABC buffer was added to block free sulfhydryl groups. After 45 min the gel pieces were washed in ABC buffer before being dehydrated as described above. The proteins were digested by incubating the gel pieces with trypsin at 37 °C overnight. Peptides were eluted from the gel by sequentially adding 3 % trifluoracetic acid and 30 % acetonitrile followed by 100 % acetonitrile. The resulting peptide solution was vacuum dried to get rid of organic solvents before peptides were stored on StageTips as described above in section 2.5.1.

2.5.4. Global protein abundance measurements (iBAQ, with Patrick Beaudette and Erik McShane)

For iBAQ, NGP cells were harvested, pelleted and flash-frozen prior to precipitation of proteins with equal volumes of chloroform, methanol and water (Wessel & Flügge, 1984). Proteins were solubilized in 6 M urea/2 M thiourea buffer containing 10 mM HEPES and treated with benzonase to digest DNA and reduce viscosity. 50 µg lysate was subjected to reduction with TCEP (tris(2-carboxyethyl)phosphine) and alkylation with CAA (2-chloroacetamide) before digestion with trypsin. Peptides were extracted and desalted with a C18 StageTip prior to elution and reconstitution in 3 % ACN/0.1 % formic acid, followed by separation on a reversed-phase column (20 cm length, 75 µm ID, 3 µm Dr. Maisch C18) with a gradient from 5 to 45 % ACN in 120 min, while MS and MS/MS spectra were acquired in data-dependent mode on a Q-Exactive Plus interment (Thermo). Raw data files were then analysed with MaxQuant 1.5.2.8.

In order to calculate protein abundances we applied the ‘intensity based absolute quantification’ algorithm [iBAQ] (Schwanhäusser *et al*, 2011). In short, we first calculated the number of theoretically observable peptides per protein by *in silico* trypsin-digesting the Uniprot database. We then divided the protein intensities by the theoretical observable peptide count.

2.6. Statistics

An unpaired Student's T-test was used to evaluate statistical significance were required. Values are expressed as the mean ± s.e.m or s.d as indicated. Significance was set at the 95 % confidence level and ranked as * $p<0.05$, ** $p<0.01$, *** $p<0.001$.

Chapter 3. ARHGAP36 is a novel PKAC binding protein and pseudosubstrate inhibitor

3.1. Introduction

The starting point for my PhD thesis was a finding from a systematic screen carried out by my supervisor Oliver Rocks in the laboratory of Tony Pawson (Rocks and Pawson, manuscript in preparation). This screen set out to characterise the regulatory proteins of the Rho family GTPases. The interactome and localisation of all GAP and GEF proteins was analysed by mass spectrometry and imaging respectively. Proteins of significant interest were then selected for further extensive characterisation. One such protein was ARHGAP36, a novel GAP protein. Flag-tagged ARHGAP36 was found to interact with several proteins involved in PKA signalling, including the catalytic subunits of the kinase itself (PKACα and PKACβ). This alone is interesting: control of this pathway is mostly mediated through the regulatory subunits (which were not identified in the interactome) with few proteins binding directly to the catalytic subunits themselves. Rho GTPases and their regulatory proteins are known to be regulated by PKA phosphorylation (Tkachenko *et al*, 2011). In addition, many AKAP proteins have functions related to the cytoskeleton, and some of them are Rho related signalling proteins themselves (Klussmann *et al*, 2001; Wong & Scott, 2004). I was thus initially interested in the crosstalk of the Rho and PKA signalling pathways. In this chapter I aim to discuss the following questions:

- What is known about ARHGAP36?
- Do ARHGAP36 and PKAC interact?
- How do ARHGAP36 and PKAC interact?
- What is the nature of the interaction?

3.2. Results

3.2.1. ARHGAP36 Characterisation

ARHGAP36 is a relatively small GAP protein. Uniprot describes five isoforms, ranging in size between 46 and 61 kDa. These isoforms vary only in the very N-terminus and all share a Rho GAP domain and an arginine rich region (Figure. 3.1a). Isoform 1 contains an additional signal peptide, and is described in NCBI as a precursor. SignalP confirms the presence of a signal peptide and cleavage site (Petersen *et al*, 2011). ARHGAP36 is located between 131,058,242-131,089,883 on the forward strand of the X chromosome. ENSEMBL corroborates the existence of isoforms 1-4 at the transcript level (Figure 3.1b).

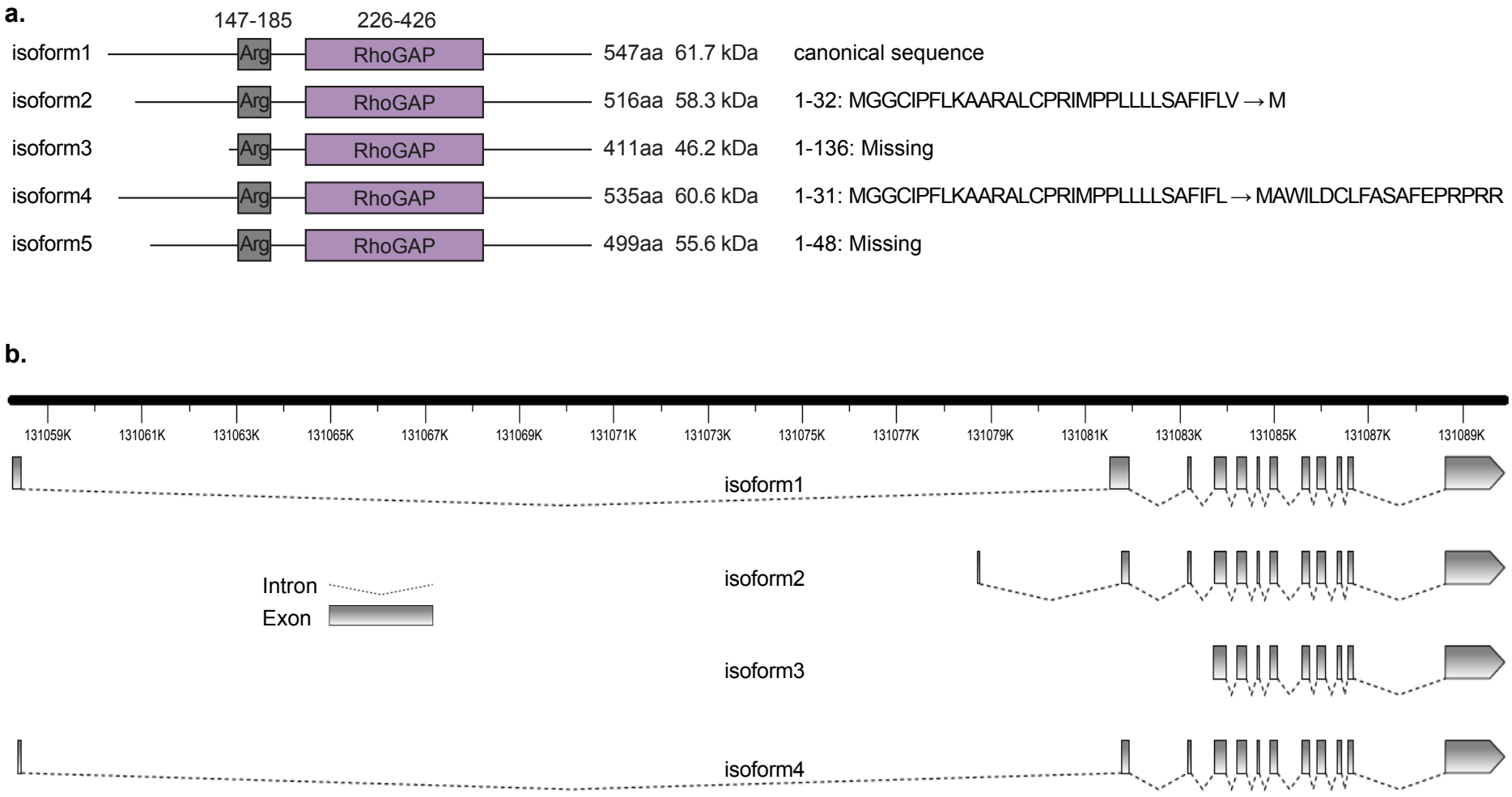

Figure 3.1 ARHGAP36 has five predicted isoforms Uniprot describes five ARHGAP36 isoforms, Q6ZR18 1-5, depicted in (**a**), four out of the five sequences are corroborated at the transcript level in Ensmbl and shown in the graphic in (**b**) created using Fancy Gene.

Upon overexpression, isoform 1 localised on cytoplasmic punctae, whilst Isoform 2 and the shortest isoform, 3, localised mostly to the plasma membrane in MDCK cells, as well as to some discrete cytoplasmic structures (Figure 3.2a). In hindsight, N-terminal tagging may have blocked cleavage of the signal peptide of Isoform 1, and C-terminally tagged constructs should have been tested for this isoform. However, as Rho GTPases signal from membranes, I focused on the interesting plasma membrane localisation of Isoform 2 and 3, which may be of functional relevance. I therefore set out to map the determinants for membrane localisation. I refer to isoform 2 of ARHGAP36 from here on, unless otherwise indicated.

3.2.1.1. ARHGAP36 membrane localisation is encoded by the arginine-rich region

I next generated a panel of ARHGAP36 expression constructs in order to delete discrete sections or to express them in isolation. All truncations were N-terminally tagged with either a CFP or YFP fluorophore. Interestingly deletion of the GAP domain had no effect on ARHGAP36 localisation, whereas the GAP domain alone appeared cytosolic (Figure 3.2b). Deletion of the N-terminus of ARHGAP36 rendered the protein cytosolic, whereas deletion of the C-terminus had no effect. Expression of the N-terminus alone was sufficient to localise ARHGAP36. The localisation requirements could be further pinpointed to the 36 amino acid arginine rich region. Expression of this region alone, ARHGAP36-ARG, or any construct containing it, resulted in localisation at the plasma membrane. Deletion of the arginine rich region in the context of the full-length protein was sufficient to render the protein cytosolic. Note the shorter expression constructs are not excluded from the nucleus.

3.2.1.2. ARHGAP36 localisation does not depend on the GAP domain

It was intriguing that the GAP domain did not contribute to ARHGAP36 membrane localisation. Overexpression of an active GAP protein may be expected to have an effect on the cytoskeleton due to perturbation of Rho GTPase activity. I therefore overexpressed ARHGAP36 and looked at effects on actin, microtubules and focal adhesions, visualised by phalloidin, tubulin and vinculin respectively. I saw no obvious effect on any of these markers in cells overexpressing YFP-ARHGAP36 (Figure 3.3). GAP proteins usually have a conserved ‘arginine finger’ which confers catalytic activity (Rittinger *et al*, 1997; Cherfils & Zeghouf, 2013), however ARHGAP36 has a threonine in place of this arginine (isoform 2: position 227).

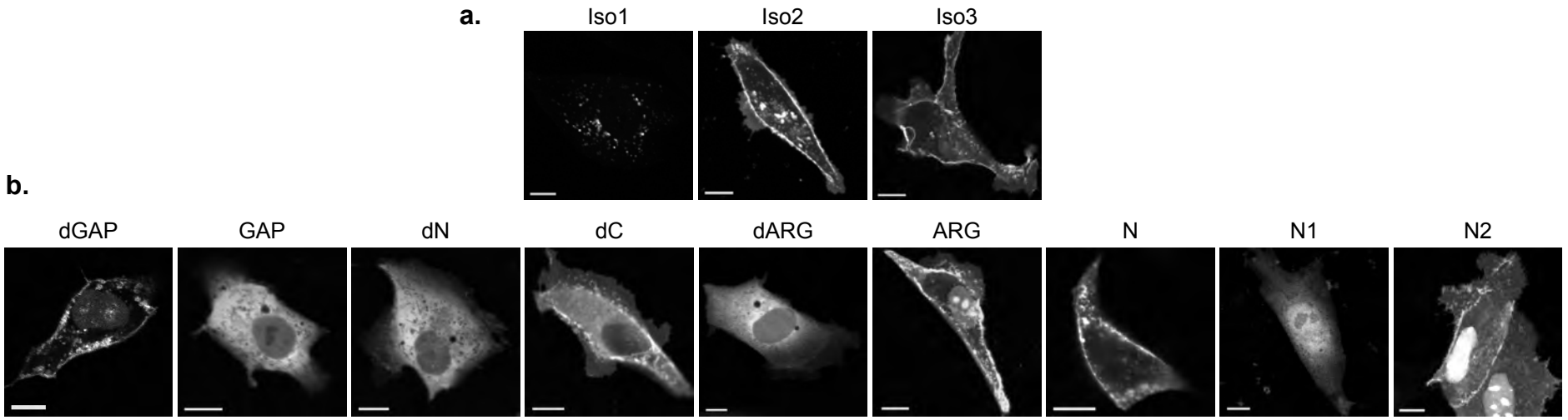

Construct	Boundaries	Localises
dGAP	1-194/396-516	Y
GAP	195-395	N
dN	195-516	N
dC	1-395	Y
dARG	1-117/155-516	N
ARG	118-154	Y
N	1-194	Y
N1	1-117	N
N2	118-194	Y

Figure 3.2 ARHGAP36 localises to the plasma membrane **(a)** Confocal live cell imaging micrographs of MDCK cells transiently transfected with CFP- or YFP- tagged ARGAP36 isoforms. Scale Bars: 10 µm. **(b)** As in (a) except cells transiently transfected with CFP- or YFP- tagged ARHGAP36 truncations based on Isoform 2. A comparison to Isoform 2 is shown, with construct boundaries indicated. Dashed line indicates deleted regions. All images are representative of both the CFP- and YFP- tagged forms, from three similar experiments.

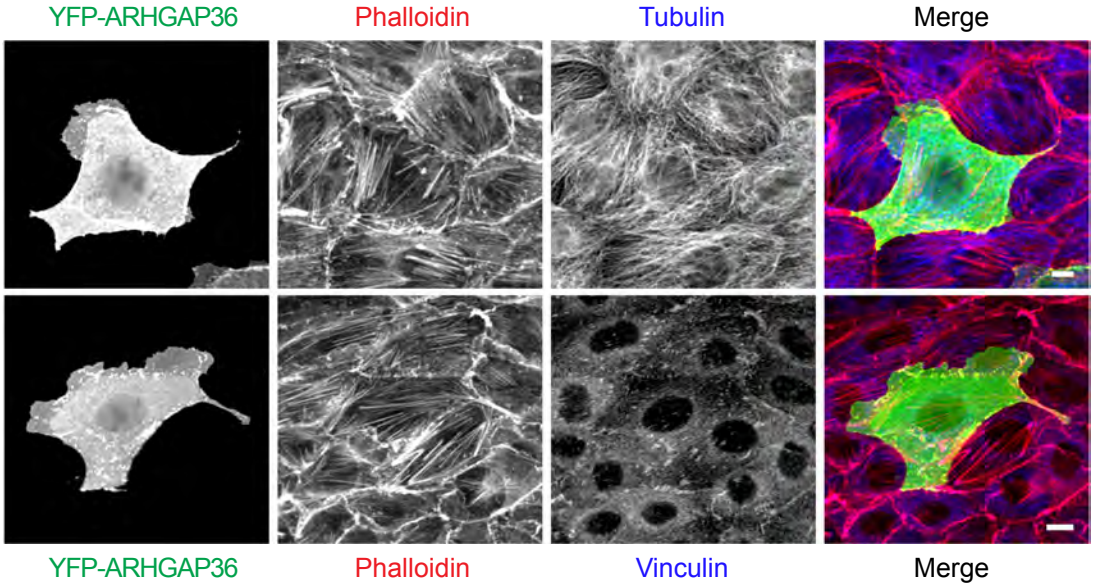

Figure 3.3 ARHGAP36 overexpression does not obviously affect the cytoskeleton. MDCK cells were transfected with YFP-ARHGAP36, then fixed the following day and subjected to immunofluorescence using antibodies against GFP, tubulin or vinculin, as well as Phalloidin-555.

Together with the lack of effect on the cytoskeleton, this led me to hypothesise that ARHGAP36 may not be an active GAP protein. Indeed, ARHGAP36 showed no activity toward RhoA, Cdc42 and Rac1, in an ongoing specificity screen using FRET activity sensors for these three GTPases (unpublished observation Markus Müller). However, specificity for one of the lesser-studied GTPases could not be ruled out.

3.2.1.3. ARHGAP36 localises to primary cilia

In 2014, a study by Rack and colleagues reported that ARHGAP36 overexpression caused massive Hh pathway activation (Rack *et al*, 2014). This activation was independent of Smoothened, and proposed to occur at the level of the Gli transcription factors, however, the mechanism by which ARHGAP36 achieved this was unclear. They also reported that ARHGAP36 localised to the primary cilium. Shh signalling requires a primary cilium: this organelle harbours the receptor Ptch and Gli proteins can be seen to translocate to the tip of the primary cilium upon pathway activation. Rack and colleagues showed that the N-terminus of mouse ARHGAP36, as well as human ARHGAP36-Iso3 localised at primary cilia in NIH-3T3 cells. I wanted to see whether I could confirm this result and if so, explore whether cilia localisation properties are the same as those required for membrane localisation. I thus established cilia formation protocols in both NIH-3T3 and MDCK cells. Most cells are capable of forming primary cilia upon growth arrest. For cilium formation in NIH-3T3 cells, I simply serum-starved the cells for 48 hours. In order to induce cilium formation in MDCK cells, I cultured the cells for up to 9 days in full media and changed the media daily. These cells are epithelial and must first polarize before they can form a cilium. Once the cells form a complete tightly packed epithelium, they start to become taller, differentiate basolateral and apical membrane domains, and form primary cilia. I identified cilia by immunostaining for acetylated Tubulin and Polaris (Ift88- Intraflagellar transport protein 88 homolog). Cilia formation was much more reproducible and showed higher penetrance in MDCK cells, with almost 100% of cells displaying cilia, and these were much longer and more identifiable than in NIH-3T3 cells. This is in agreement with published findings by others (Ott & Lippincott-Schwartz, 2012). In MDCK cells locating the cilium was obvious merely based on the acetylated tubulin stain, with no need for the Polaris co-stain. In these cells I could see clear localisation of both Isoform 2 and 3 at the primary cilium (Figure 3.4). As a negative control I used YFP to ensure the fluorophore or GFP staining did not by itself confer ciliary localisation.

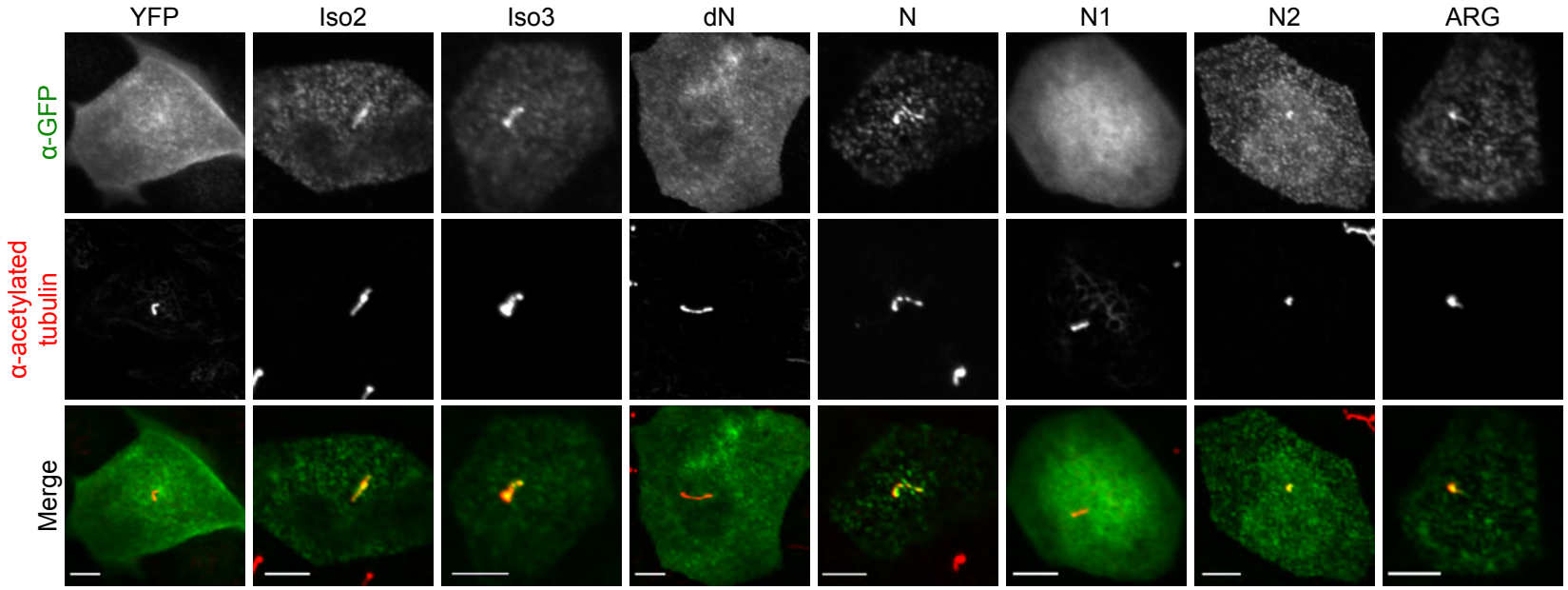

Figure 3.4 ARHGAP36 localises to primary cilia
MDCK cells were cultured on coverslips for seven days before transfection with the indicated constructs and fixation the following day. Cells were subjected to immunofluorescence with antibodies against GFP and acetylated tubulin. Scale bars: 5 μm. All constructs that localise to the plasma membrane also localise to cilia.

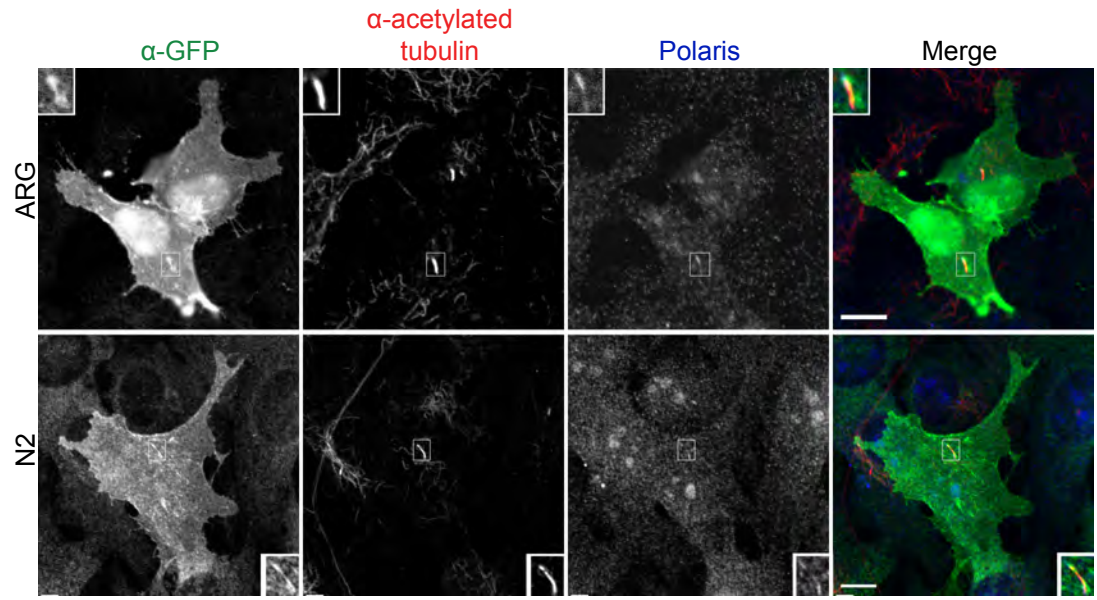

Figure 3.5 The arginine rich region is sufficient to target ARHGAP36 to the primary cilium NIH-3T3 cells were starved for 48 hours before fixing. 24 hours prior to fixation cells were transfected with the indicated constructs. Cells were subjected to immunofluorescence using antibodies against GFP, acetylated tubulin and polaris. Scale bars: 10 μm.

ARHGAP36-dN was unable to localise to the primary cilium, whereas the N-terminus alone was sufficient for localisation. I further mapped the localisation requirements to the ARG rich region, the same 36 amino acids that are required for membrane localisation (see Figure 3.2b).

NIH-3T3 cells have much more cytoplasmic acetylated tubulin, making it more difficult to identify the cilium. The Polaris staining was very weak and gave high background in these cells. In addition, the combination of transfected, ciliated cells was low, despite optimisation attempts. Transfecting ciliated cells is generally difficult, as in order to form cilia the cells need to differentiate and stop dividing, whereas many transfection reagents require cells to divide to ensure good expression. These cells are also notoriously difficult to transfect in the first place. I was able to show that ARHGAP36-ARG as well as the larger fragment encompassing the ARG region, ARHGAP36-N2, localised to the primary cilium (Figure 3.5). It is likely that full-length protein does localise to cilia, as in MDCK cells (Figure 3.4), however in NIH-3T3 cells only the shorter, more easily transfected constructs could be visualised there. Note that Rack and colleagues also only showed Isoform 3, the shortest variant, to localise on primary cilia in NIH3T3 cells (Rack *et al*, 2014).

Three different ARHGAP36 antibodies I was testing at the time also localised strikingly to the primary cilia. However, these antibodies had not yet been verified by knock down and it is also not clear whether ARHGAP36 is expressed in MDCK cells. It would be interesting to check whether ARHGAP36 is upregulated upon cilia formation and whether knocking down endogenous ARHGAP36 has an effect on cilium formation itself.

3.2.2. The ARHGAP36 interactome indicates a role in PKA signalling

Our interest in characterising ARHGAP36 stems from prior interactome data (Rocks & Pawson, manuscript in preparation). In that previous study, Flag-ARHGAP36 was overexpressed in HEK293T cells and interacting partners were identified by immunoprecipitation and subsequent mass spectrometry. Interestingly the PKA catalytic subunits, PKACα and PKACβ, were among the strongest hits. Other interactors identified were Praja2, the E3 ubiquitin ligase recently found to be an AKAP, which mediates ubiquitylation and proteasomal degradation of PKAR (Lignitto *et al*, 2011). Two other E3 ubiquitin ligases, Stub1 and Huwe1, were also

identified. I wanted to first confirm the interaction with PKAC, and then establish the nature of this interaction.

3.2.2.1. ARHGAP36 interacts with PKAC

In order to first confirm the interaction of ARHGAP36 with PKAC I performed co-immunoprecipitation (IP) experiments. I transiently overexpressed Flag-tagged ARHGAP36, or Flag-Cherry as a control, together with PKAC-YFP, in HEK293T cells for 24 hours. I then pulled down the Flag-tagged proteins using Flag-coupled beads and looked for interacting PKAC-YFP by western blotting. PKAC-YFP interacted strongly and specifically with Flag-ARHGAP36 (Figure 3.6a). I then wanted to know if ARHGAP36 could interact with endogenous PKAC. I pulled down overexpressed YFP-tagged ARHGAP36 or YFP-Cherry as a control from singly transfected HEK293T cells. Endogenous PKAC also interacted strongly and specifically with YFP-ARHGAP36 (Figure 3.6b).

3.2.2.2. ARHGAP36 relocalises PKAC

In MDCK cells PKAC-YFP is mostly cytosolic, with some Golgi localisation, presumably due to AKAP recruitment of PKA holoenzymes (Skroblin *et al*, 2010). In addition some aggregates can be seen that most likely result from overexpression (Figure 3.7a). Upon coexpression with ARHGAP36, PKAC is recruited and completely relocalises to the plasma membrane and to vesicles (Figure 3.7b).

3.2.2.3. Just 77 amino acids are required to recruit PKAC

I then wanted to map the determinants required for ARHGA36 recruitment of PKAC. To this end I utilised my mutation and deletion constructs previously designed to map ARHGAP36 localisation. Isoform 3, the shortest ARHGAP36 isoform, could also recruit PKAC (Figure 3.8). Deletion of the GAP domain had no effect on the ability of ARHGAP36 to recruit PKAC. Deletion of the N-terminus abolished the interaction, whereas the N-terminus alone was sufficient to recruit PKAC. From these imaging experiments it could not be ruled out that ARHGAP36 and PKAC interact in the cytosol, however IP experiments confirmed that the interaction site correlates with the ARHGAP36 membrane localisation determinants and lies within the N-terminus. PKAC-YFP did not interact with Flag-dN, whereas Flag-N did (Figure 3.9). ARGAP36-N2, encompassing just 77 amino acids, was sufficient to

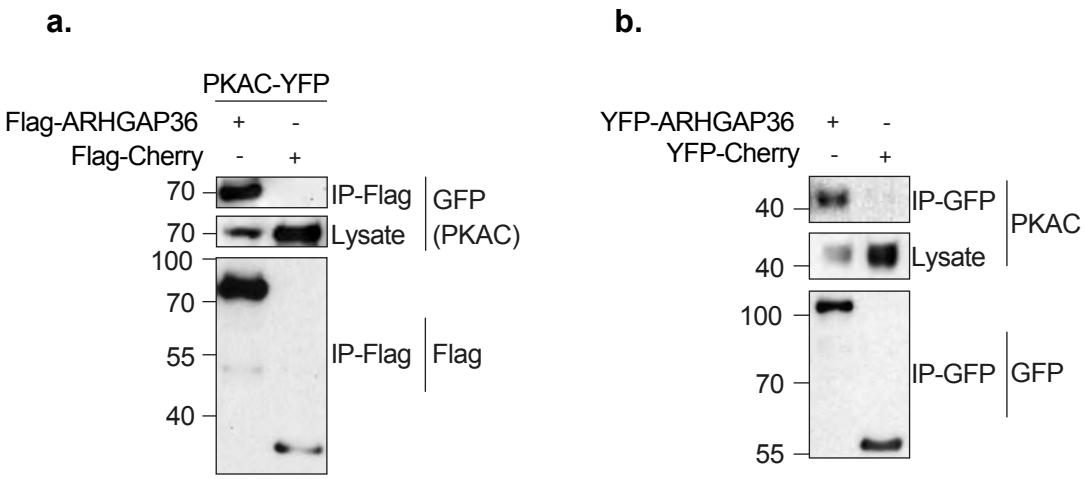

Figure 3.6 ARHGAP36 interacts with PKAC (a) HEK293T cells were transfected with PKAC-YFP and Flag-ARHGAP36 or a Flag-Cherry control. Lysates were subjected to IP using a Flag antibody, and immunoblotted with GFP or Flag antibodies. Blots representative of three similar experiments. **(b)** HEK293T cells were transfected with YFP-ARHGAP36 or a YFP-Cherry control. Lysates were subjected to IP using a GFP antibody, and immunoblotted with GFP or PKAC antibodies. Blots representative of three similar experiments.

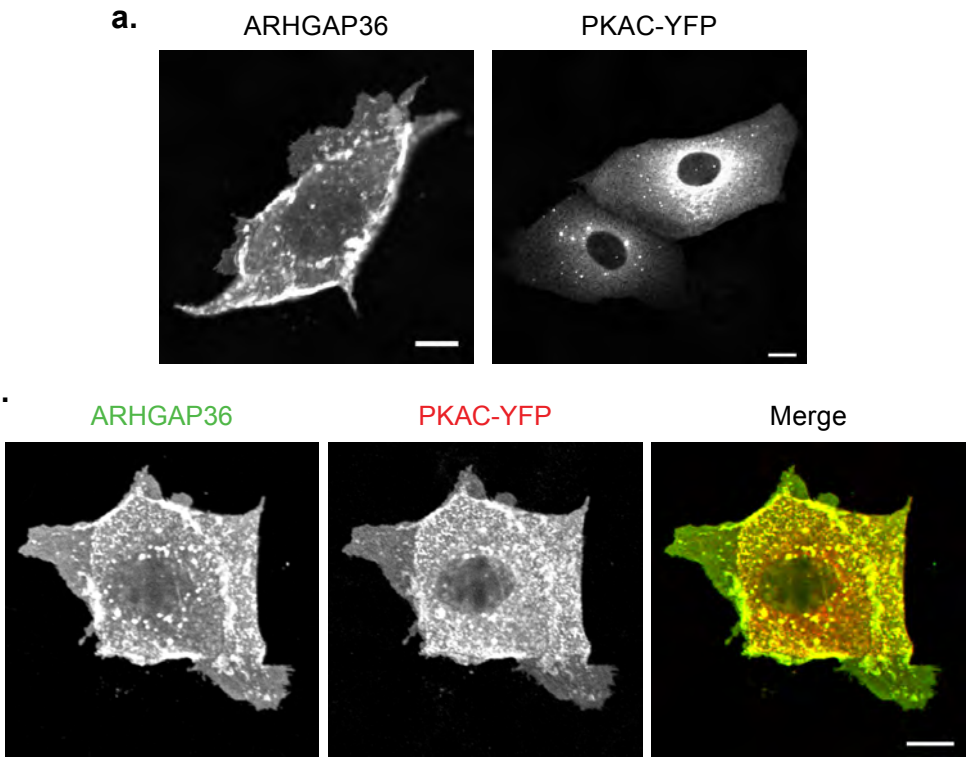

Figure 3.7 ARHGAP36 recruits PKAC to the plasma membrane and vesicles (a) MDCK cells transfected with PKAC-YFP or Flag-ARHGAP36, were fixed and stained with GFP or Flag antibodies. Images were collected by confocal microscopy. Scale bars: 10μM **(b)** As in (a) except cells were trasnfected with PKAC-YFP and Flag-ARHGAP36 together. Images representative of three independent experiments.

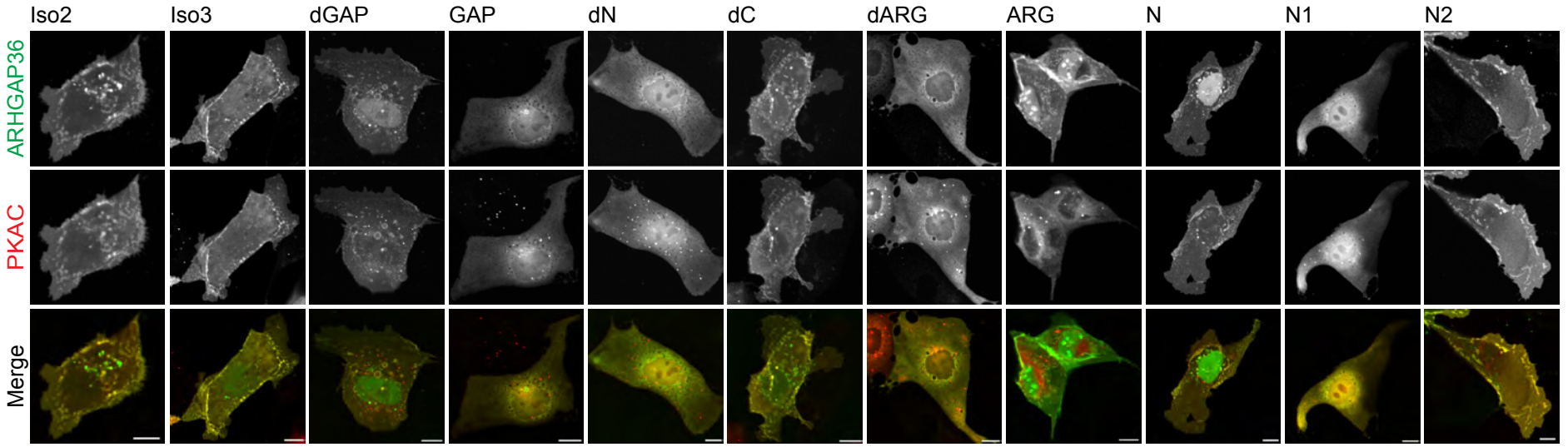

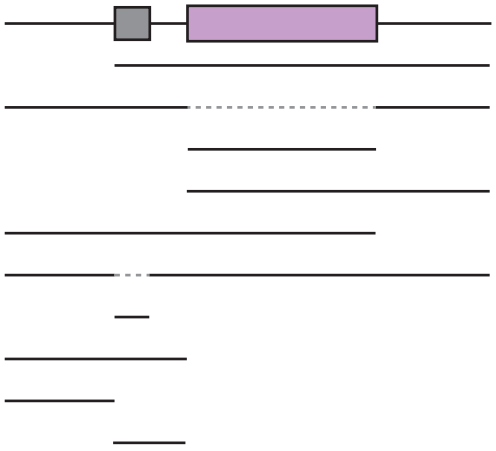

Construct	Boundaries	Localises	Recruits PKAC
Isoform3	118-516	Y	Y
dGAP	1-194/396-516	Y	Y
GAP	195-395	N	N
dN	195-516	N	N
dC	1-395	Y	Y
dARG	1-117/155-516	N	N
ARG	118-154	Y	N
N	1-194	Y	Y
N1	1-117	N	N
N2	118-194	Y	Y

Figure 3.8 Just 77 amino acids are required to recruit PKAC. Confocal live micrographs of MDCK cells transiently transfected with CFP-tagged ARGAP36 truncations together with PKAC-YFP. Images representative of three independent experiments. Scale Bars: 10 µm. All truncations are based on isoform 2 and are depicted below.

recruit PKAC (Figure 3.8). ARHGAP36-ARG was the only truncation that localised to membranes as the full-length ARHGAP36 but was unable to recruit PKAC.

3.2.2.4. ARHGAP36 contains an N-terminal pseudosubstrate domain

To further pinpoint the interaction site I used peptide-spotting experiments. 25 amino acid peptide spots were synthesised, with each spot shifted by five amino acids to provide overlap for the entire ARHGAP36 sequence. The spots were then incubated with purified GST-PKAC and interaction detected using a GST antibody as for western blotting (Figure 3.10a). One spot, B12, interacted most strongly. This spot spans part of the arginine rich region and the following 'linker' region, so called as it joins the arginine rich region to the GAP domain. This fits with my previous findings, as this sequence is located in the middle of ARHGAP36-N2, the minimal construct that could recruit PKAC. Further amino acid scanning experiments were performed, where each amino acid from the positive spot was in turn mutated to alanine or aspartic acid (Figure 3.10b). This revealed the requirement of two arginines, R153 and R154 for PKAC binding. The surrounding sequence (RRGAV) resembles that of the consensus motif (R-R-X-S/(A/G)-Y) for PKAC substrates/inhibitors found in the PKAR and PKI proteins. X is variable, Y a hydrophobic residue and S/(A/G) the phosphorylation/pseudophosphorylation site, respectively (Kemp *et al*, 1976; Taylor *et al*, 2012). This region of ARHGAP36 aligns perfectly with the pseudosubstrate inhibitor sites within PKAR and PKI (Figure 3.10c). I thus mutated three amino acids corresponding to R94, R95, V98 in PKAR, which had been shown to dock into the active site of PKAC (Buechler *et al*, 1993; Zhang *et al*, 2012)(Figure 3.11), to aspartic acid R153D/R154D/V157D (ARHGAP36-RRV). This mutation had no effect on ARHGAP36 localisation, however ARHGAP36-RRV could no longer recruit PKAC to membranes (Figure 3.12a). IP experiments confirmed that ARHGAP36-RRV could no longer interact with endogenous PKAC either (Figure 3.12b). Further analysis of the structure of PKAC in complex with PKAR, revealed three amino acids in the active site cleft of PKAC, critical for the interaction (Kim *et al*, 2005) (Figure 3.11). Mutation of these three amino acids E127A/E170A/E230A (PKAC-EEE) was enough to abolish PKAC recruitment by ARHGAP36 (Figure 3.12c). I thus identified point mutations on both proteins that abolish their interaction.

3.2.2.5. ARHGAP36 inhibits PKAC activity

As ARHGAP36 binds PKAC via a pseudosubstrate site, in the same manner as PKAR and the PKI proteins, I next asked if ARHGAP36 also inhibits PKAC. With

Figure 3.9 The N-terminus of ARHGAP36 mediates the interaction with PKAC. HEK293T cells were transfected with PKAC-YFP together with Flag-tagged wild-type ARHGAP36 (WT), dN, N or Flag-Cherry control. Lysates were immunoprecipitated using a GFP antibody, and immunoblotted with GFP or Flag antibodies.

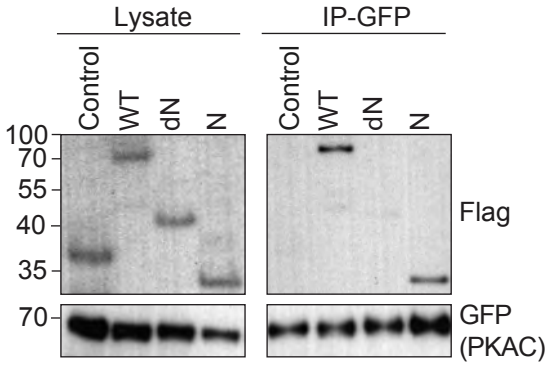

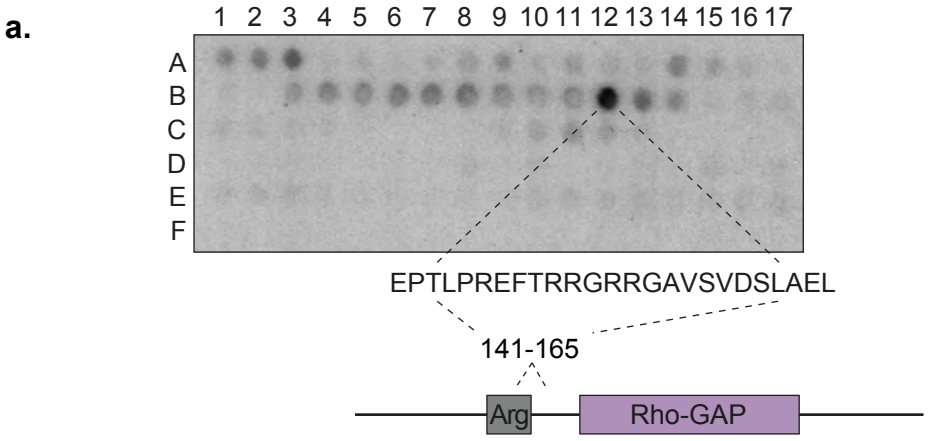

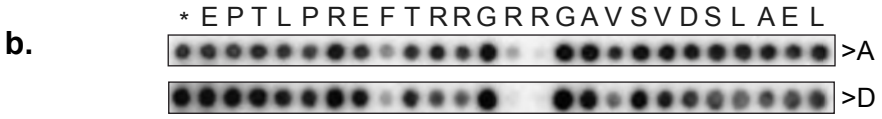

c.

```
hsARHGAP36:  FTRRGRRGAVSVDSLAE  :  164
hsPRKAR1A :  VKGRRRRGAISAEVYTE  :  107
hsPRKAR1B :  VKARRRRGGVSAEVYTE  :  107
hsPRKAR2A :  PSRFNRRVSVCAETYNP  :  107
hsPRKAR2B :  INRFTRRASVCAEAYNP  :  122
hsPKIa    :  SGRTGRRNAIHDILVSS  :   30
hsPKIb    :  SARAGRRNALPDIQSSA  :   37
hsPKIg    :  CDRTGRRNAVPDIQGDS  :   30
```

Figure 3.10 ARHGAP36 contains a PKA pseudosubstrate motif (a) Immobilised peptide 'spots'. Overlapping 25-mer peptides each shifted along by five amino acids in the entire ARHGAP36 sequence, were probed for interaction with GST-PKAC and immunoblotted using a GST antibody. The sequence of the spot with strongest interaction is shown. **(b)** Alanine and Aspartate scans of the spot indicated in (a) were treated the same as in (a). Asterisk indicates the control spot with the original sequence. **(c)** Alignment of human ARHGAP36 with the human isoforms of PRKAR and PKI revealing its pseudosubstrate motif RRxAY.

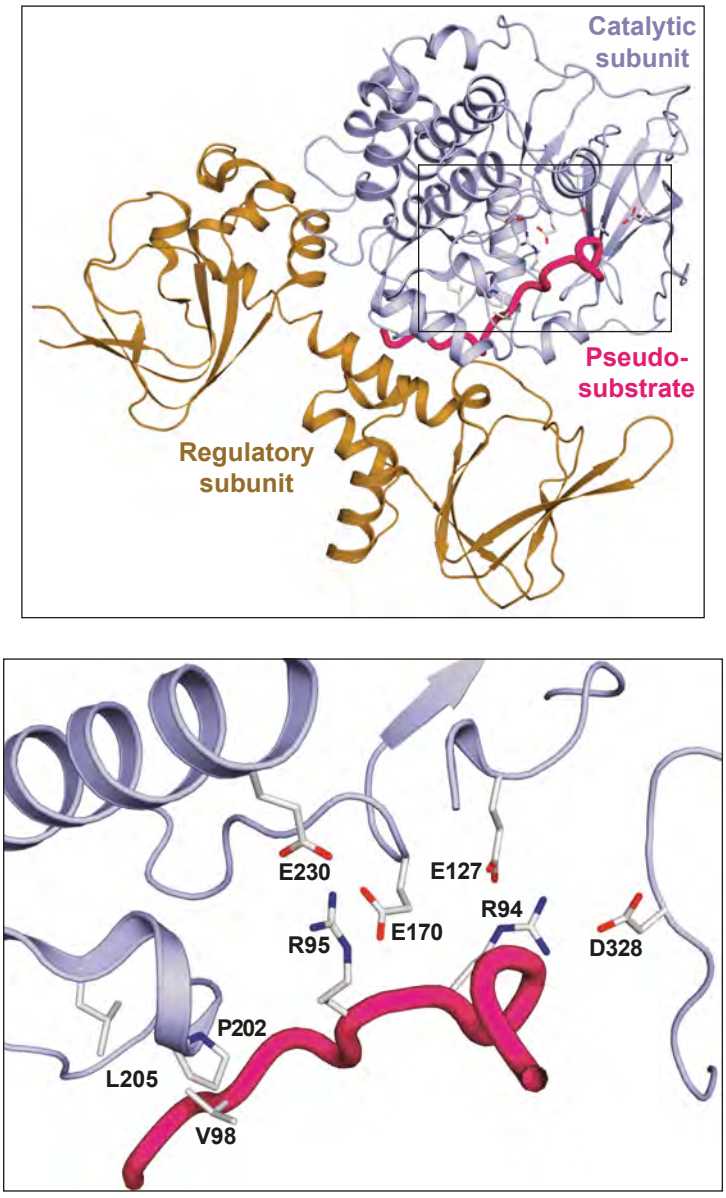

Figure 3.11 The PKA holoenzyme structure reveals critical residues for the pseudosubstrate interaction. Structure of the PKAC-PKARIIβ complex (in blue, sand, pdb 3TNP.pdb)(Zhang *et al*, 2012). The pseudo-substrate motif of the regulatory subunit is coloured in pink. The inset shows the three residues in the pseudosubstrate sequence (R94, R95, V98) that were mutated in the corresponding ARHGAP36 sequence, together with selected contacts in the catalytic subunit. **Figure created by Oliver Daumke (MDC).**

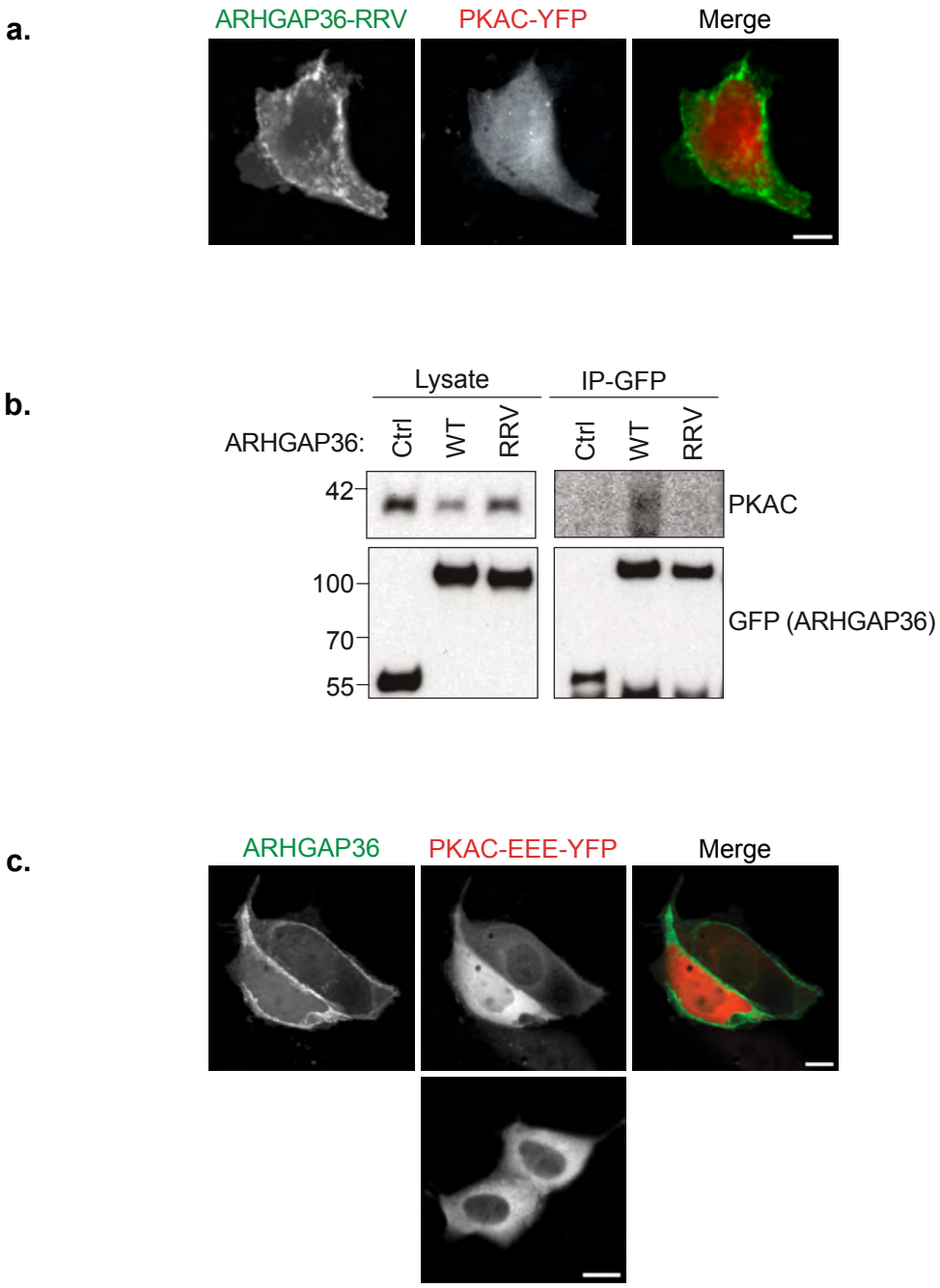

Figure 3.12 Point mutations on both proteins can abolish the interaction of ARHGAP36 and PKAC (a) Confocal live micrographs of MDCK cells coexpressing CFP-ARHGAP36-RRV and PKAC-YFP. Images representative of three similar experiments. **(b)** HEK293T cells were transfected with CFP-ARHGAP36, the RRV mutant or a CFP-Cherry control. Lysates were immunoprecipitated using a GFP antibody, and immunoblotted with GFP or PKAC antibodies. **(c)** Confocal live micrographs of MDCK cells expressing PKAC-YFP-EEE alone or together with CFP-ARHGAP36. Images representative of three similar experiments. Scale bars: 10 µm throughout.

help from Carolin Barth (AG Rocks, MDC), we first used an *in vitro* assay, which assesses the ability of purified PKAC to phosphorylate a substrate peptide (L-R-R-A-S-L-G). The peptide is then separated on an agarose gel, simply by its charge, as upon phosphorylation, modified residues become negatively charged. In the absence of purified PKAC, all the peptide is non-phosphorylated, whereas in the presence it is all phosphorylated. A scrambled peptide had no effect on phosphorylation, whereas the PKI (5-24) peptide could significantly inhibit phosphorylation. We then tested '36i', a 25 amino acid peptide comprising the pseudosubstrate motif, based on spot B12 from the peptide spot experiments. 36i could also significantly inhibit substrate phosphorylation (Figure 3.13a). I would of course have liked to do this experiment with full-length purified ARHGAP36, however my attempts to purify ARHGAP36 were unsuccessful as the protein was always insoluble.

I next wanted to know if full-length ARHGAP36 could inhibit PKAC *in vivo.* For this I used the AKAR4-NES FRET sensor. This is made up of cerulean and venus based (cpVE172) fluorophores, with a substrate site (LRRATLVD) and a FHA1 phospho-binding domain in between (Herbst *et al*, 2011; Depry *et al*, 2011) (Figure 3.13b). So when the substrate site is phosphorylated the FHA1 domain can bind and FRET can occur between the two fluorophores, which are brought closer together. There is also an additional nuclear export signal (NES), to ensure the sensor remains in the cytosol. I first attempted to measure the FRET efficiency of single cells before and after stimulation with forskolin, in order to see whether the sensor worked. However our microscopy set up at the time did not allow for constant perfusion of liquid, and therefore I had problems with losing focus upon addition of stimulants. Together with Markus Müller (AG Rocks, MDC) we then tried these experiments on a larger scale, assessing many stimulated cells at one time-point then comparing between conditions. We co-expressed mCherry tagged ARHGAP36 variants, or mCherry itself as a control, so that we could always normalise FRET measurements to the expression level of the constructs. Full-length ARHGAP36 and ARHGAP36-N2 could significantly reduce FRET activity, whereas ARHGAP36-RRV and ARHGAP36-dN had no effect (Figure 3.13c & d). Overexpressing constructs encoding 36i or full-length PKI also significantly reduced FRET activity. Together these experiments show that ARHGAP36 interacts directly with PKAC and inhibits its kinase activity via a pseudosubstrate domain.

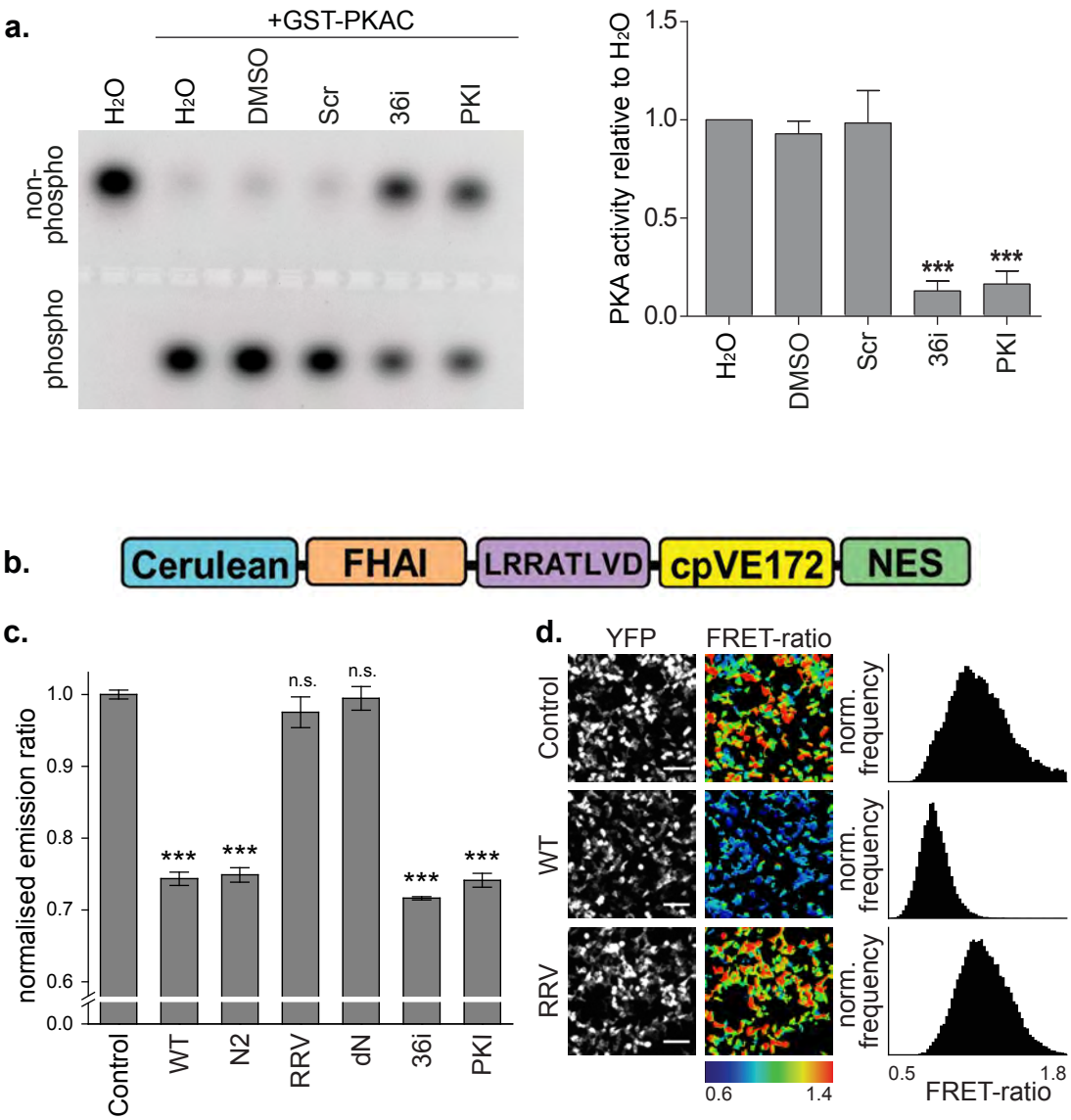

Figure 3.13 ARHGAP36 inhibits PKAC *in vitro* and *in vivo* (**a**) Recombinant PKAC α (25 ng) was incubated with 10 µM scrambled, 36i or PKI peptide, and its activity determined by its ability to phosphorylate the substrate peptide PepTag A1. Phosphorylated and non-phosphorylated peptide were separated by agarose electrophoresis, and densitometrically analysed. Representative gel shown. Recombinant PKACα activity is shown as the ratio of phosphorylated to non-phosphorylated peptide (mean of eight repeats +/- SEM, *** p<0.001 versus all three controls). **Figure contributed by Carolin Barth.** (**b**) Representation of AKAR4-NES FRET sensor (Herbst *et al*, 2011). (**c**) AKAR4-NES FRET sensor was expressed together with the indicated mCherry tagged constructs. Cells were serum starved for five hours, treated with 10 µM Forskolin and 100 µM IBMX for 30 min and subsequently imaged. Mean FRET emission ratio (acceptor/donor intensity) of three independent experiments normalised to control +/- s.d. *** p<0.001, n.s. not significant versus control and RRV (**d**) Representative images of HEK293T cells expressing AKAR4-NES FRET sensor together with the indicated mCherry tagged constructs. Cells were treated as in (c). Shown are YFP intensity images and pseudocoloured FRET ratio images (acceptor/donor intensity) reflecting the relative PKA activity levels. The histograms show the pixel distribution within the FRET emission ratio images. Scale bars: 100 µm. **Panels c-d contributed by Markus Müller.**

3.3. Discussion

Main Chapter Findings

- ARHGAP36 localises to the plasma membrane and the primary cilium via its arginine rich region.
- ARHGAP36 binds PKAC directly via a pseudosubstrate site, recruiting it to the plasma membrane
- ARHGAP36 inhibits PKAC activity *in vitro* and *in vivo*.

3.3.1. Non GAP functions of other GAP proteins

GEF and GAPs are diverse multidomain proteins that have numerous roles outside of regulating GTPase activity. ARHGAP36 may not be an active GAP protein. Other GAP proteins have already been shown to have functions independent of their GAP activity, even if they are still active. Overexpression of the GAP protein N-Chimaerin leads to lamellipodia and filopodia formation. Although this was shown to depend on Cdc42 and Rac1 activity, N-chimearin mutants lacking GAP activity could still cause the cellular phenotype (Kozma *et al*, 1996). Recently it was shown that ARHGAP30 regulates p53 acetylation in a Rho independent manner (Wang *et al*, 2014). Catalytic mutants still had the same effects. The shorter ARHGAP30 isoform could not affect p53 acetylation, pointing to a role of the Glutamine-rich domain contained only in the longer-isoform. The other domains of Rho proteins are thus important in mediating protein-protein interactions and thus their diverse roles. ARHGAP11A binds p53 and surprisingly this is actually via the GAP domain (Xu *et al*, 2013). ARHGAP11A promoted p53 function upon DNA damage, and there was no effect of mutating the catalytic arginine, showing the effect to be independent of Rho GTPase activation. Another Rho GAP family protein, OCRL, contains many other domains critical for its function, and mutation of this protein leads to Lowe syndrome and Dent disease (Mehta *et al*, 2014). OCRL is an inositol 5-phosphatase, and binding of a C-terminal ASH domain to Rab GTPases mediates its subcellular localisation and stimulates its phosphatase activity (Hyvola *et al*, 2006). Its GAP domain is actually catalytically inactive, however it is still thought to mediate binding to Rac1 and Cdc42 and rather act as an effector (Faucherre *et al*, 2003). Taken together this suggests that the GAP domain itself can also have functions independent of catalytic activity. The scaffolding roles of GAP proteins, even in context of GAP activity, contribute massively to their functions (Okada *et al*, 2011).

3.3.2. ARHGAP36 is a novel PKAC inhibitory protein

ARHGAP36 further extends the PKA regulatory repertoire. Regulation of this signalling pathway is mostly centred around PKAR, with much emphasis in the field on the role of AKAPs. ARHGAP36 interacts directly with PKAC via a pseudosubstrate motif that binds in the same manner as PKAR and the PKI proteins to the PKAC catalytic site. I thus conclude that binding would be at least in parts competitive. ARHGAP36 should thus be able to uncouple PKAC from upstream control via PKAR.

ARHGAP36 could act as a tonic suppressor of PKA to greatly reduce the sensitivity of certain cells to cAMP-releasing stimuli. It might also oppose basal PKA activity, particularly in situations with stoichiometric excess of free PKAC. Compensatory mechanisms have long been suggested to balance the relative expression levels of PKAR and PKAC, so that proper responsiveness of the PKA holoenzyme to cAMP is maintained (Hofmann *et al*, 1977; Amieux *et al*, 1997). ARHGAP36 may contribute to such a mechanism by providing additional buffering capacity.

3.3.3. Other pseudosubstrate Inhibitors of PKAC

Isothermal titration calorimetry (ITC) experiments performed by Stephan Grunwald (AG Daumke, MDC) also support that ARHGAP36 inhibits PKAC in a similar manner to the PKI proteins. He found similar high nanomolar binding constants for both 36i and PKI (5-24) peptides for purified His-PKAC. Most protein kinase inhibitors bind the ATP-binding site, and thus specificity is a problem (Murray, 2008). PKI and 36i block substrate binding and therefore are much more specific to PKA. I have thus identified a new pseudosubstrate peptide inhibitor which can be used to inhibit PKA *in vitro*, and possibly also *in vivo*.

It would be interesting to repeat these ITC experiments with full-length ARHGAP36 protein, and with a series of mutants, to establish if other parts of the protein can contribute to binding of PKAC. For PKI a phenylalanine located N-terminally to the pseudosubstrate motif contributes to binding affinity (Glass *et al*, 1989). Interestingly, the peptide spotting experiments did identify a possible role for F148 in PKAC binding (Figure 3.10b).

The PKI proteins have been implicated in nuclear export of PKAC (Fantozzi *et al*, 1992, 1994). They contain a nuclear export signal (NES) (Wen *et al*, 1995),

however, this is thought to be masked unless they are bound to PKAC (Dalton & Dewey, 2006). They can freely diffuse between the nucleus and cytoplasm, and upon binding active PKAC in the nucleus, the NES is uncovered and PKAC is translocated back to the cytoplasm. This is thought to then promote holoenzyme reformation. PKI thus participates in regulating the transcriptional response of PKA in the nucleus. ARHGAP36 is specifically targeted to the plasma membrane via its arginine rich region and can also recruit PKAC there. I would therefore hypothesise that ARHGAP36 rather regulates PKA activity at the plasma membrane. Similar to the role of PKI in the nucleus, ARHGAP36 could bind recently activated PKAC to ensure its timely inactivation in dynamic signalling events. ARHGAP36 would thus contribute to resetting the PKA pathway.

PKI is a rather small protein of only 75 amino acids. By comparison ARHGAP36 is much larger and thus the possibilities for protein-protein interaction and further functions are increased. The ARHGAP36 interactome contained many more interesting proteins. Although ARHGAP36 is not a canonical AKAP, as it interacts with PKAC rather than PKAR, it may still act as a scaffold to recruit other proteins that could further modulate PKA signalling.

The only other pseudosubstrate inhibitor of PKAC is PDE7A1, which actually contains two pseudosubstrate sites within its N-terminus (Han *et al*, 2006). It is also a phosphodiesterase, so can further regulate PKA activity by degrading cAMP.

3.3.4. ARHGAP36 in Hedgehog signalling and Medulloblastoma

Overexpressed ARHGAP36 has been shown to activate the Hh signalling pathway (Rack *et al*, 2014). Rack et al claimed that different parts of the protein had differential effects. Whereas the full-length protein activates Hh signalling, the N-terminus had an inhibitory effect on Gli activation. However they could not explain how either effect occurs. They did report that overexpressed full-length ARGAP36 could interact with overexpressed Sufu. Sufu is a negative regulator of Hh signalling, thought to bind the Gli proteins, and promote repressor formation. They did not explore how ARHGAP36 binds to Sufu or discuss how this could contribute to the observed effects on signalling. One theory would be that ARHGAP36 sequesters Sufu away from the Gli proteins, in order to promote their conversion into transcriptionally active forms.

In the absence of a Hh stimulus, the Gli proteins are ubiquitylated and, particularly in the case of Gli3, undergo partial proteolysis into repressor forms. This cleavage process is carefully regulated by multi-step phosphorylation by various kinases. PKA has been shown to directly phosphorylate the Gli proteins, in a priming event leading to further phosphorylation by GSK3β and CK1. This leads to βTRCP binding and subsequent ubiquitylation by the SCF E3 ligase complex, this mediates their partial cleavage into transcriptional repressors. PKA is thought to be a negative master regulator of the pathway. PKA knock out mice even phenocopy Ptch1 and Sufu knock outs in the developing embryo (Tuson *et al*, 2011). We thus hypothesised that ARHGAP36 mediates its effects via its inhibitory role on PKA. Maciej Czajkowski (AG Rocks) could show an increase in Gli transcript levels upon ARHGAP36 overexpression, as well as with ARHGAP36-N2, the minimal construct that binds and targets PKAC. More importantly ARHGAP36-RRV could no longer mediate an increase in Gli1 transcript levels. Therefore if the ARHGAP36 pseudosubstrate domain is mutated, and it can no longer bind and inhibit PKAC, it can no longer lead to Hh activation.

Rack et al also reported that ARHGAP36 was upregulated in medulloblastoma, the most common brain tumour in childhood. This disease is frequently associated with abnormal Hh signalling (Teglund & Toftgård, 2010). Medulloblastomas are normally split into four subtypes, with Type 2 being classified by upregulated Hh signalling (Kool *et al*, 2012). However ARHGAP36 was upregulated within subtypes 3 & 4, and its expression did not correlate with Gli1 or Ptch1 levels (Rack *et al*, 2014). They could show that isoforms 2, 3 and 5 were those found to be upregulated. This argues that these are the physiological (or pathophysiological) relevant isoforms. I have shown here that isoforms 2 and 3 bind PKAC. Isoform 5 is an intermediate version, its N-terminus starting between Isoforms 2 and 3. It contains no extra or different domains, and contains the pseudosubstrate motif, I would thus also expect isoform 5 to bind and inhibit PKAC. ARHGAP36 inhibition of PKAC thus provides a simple rationale for how Gli activation is achieved, and provides a mechanism by which ARHGAP36 could promote medulloblastoma formation. ARHGAP36 could also oppose PKAC in further disease contexts.

Unfortunately medulloblastoma cell lines are not thought to well represent the disease, otherwise this would have been an obvious choice to explore the role of endogenous ARHGAP36 on PKAC.

Chapter 4. ARHGAP36 mediates PKAC ubiquitylation and degradation via the endolysosomal pathway

4.1. Introduction

I consistently observed a dramatic decrease in PKAC protein levels upon overexpression of ARHGAP36. Loss of PKAC could be caused by either an effect at the transcriptional or post-translational level. However, I also observed a reduction of the over-expressed form, which is not under the control of the endogenous PKAC promoter. This points towards a post-translational regulatory mechanism such as degradation. The regulatory subunits are known to be degraded by the proteasome upon ubiquitylation by the E3-ligase Praja2 (Lignitto *et al*, 2011). Many activated kinases are ubiquitylated and degraded (Lu & Hunter, 2009; Liu *et al*, 2012), however thus far there is no known mechanism for ubiquitin-mediated PKAC degradation. In this chapter I aim to discuss the following questions:

- Does ARHGAP36 affect PKAC stability?
- How is PKAC degraded?
- Is PKAC ubiquitylated?
- What other proteins are involved?

4.2. Results

4.2.1. ARHGAP36 causes depletion of PKAC

Overexpression of ARHGAP36 in MDCK cells results in a striking loss of endogenous PKAC (Figure 4.1a, compare ARHGAP36 overexpressing cells with surrounding untransfected cells). In order to visualise an intermediate stage that may inform on the mechanism by which PKAC is degraded, I fixed cells after eight and 24 hours of transfection and monitored endogenous PKAC. At the eight hour timepoint, PKAC was concentrated on vesicles that colocalised with ARHGAP36, whilst it was completely lost after 24 hours of ARHGAP36 expression in the majority of transfected cells (Figure 4.1b). Overexpression of YFP had no effect on PKAC at either time-point. At first it was difficult to see this decrease in PKAC levels by western blotting, as only a small percentage of cells were transfected with ARHGAP36, but the entire cell population is assessed. Transfection efficiency thus had to be optimised first. HEK293T cells were used as they have the SV40 large T antigen for enhanced replication of DNA plasmids. Transfection of cells with PEI at high confluency (around 80%), resulted in transfection efficiency close to 100%. I always used YFP-tagged ARHGAP36 constructs, so efficiency could be easily judged by fluorescence microscopy before harvesting, and also later by western

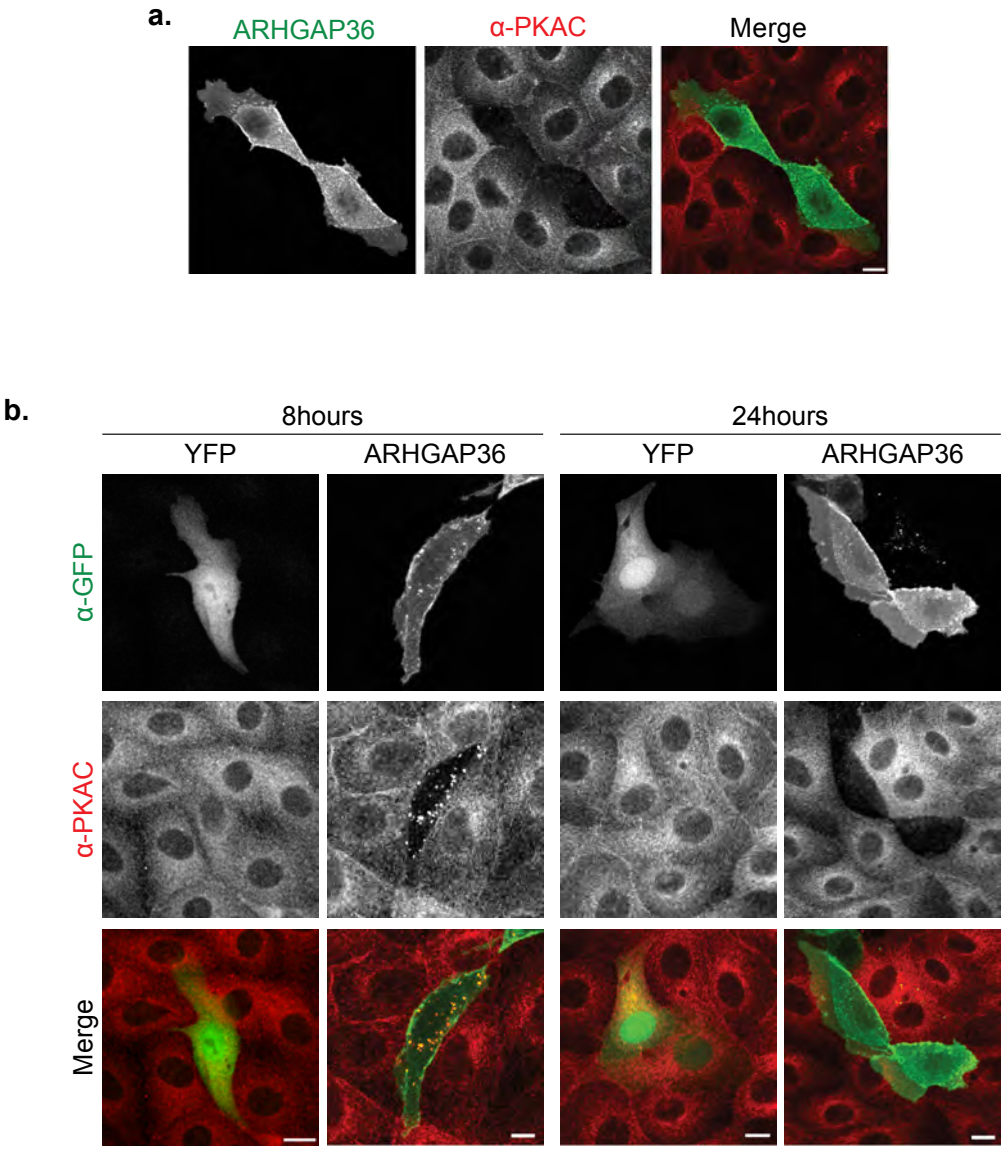

Figure 4.1 ARHGAP36 downregulates PKAC levels (**a**) MDCK cells were transfected with YFP-ARHGAP36. The next day cells were fixed and subjected to immunofluorescence using antibodies against PKAC and GFP. Images were collected by confocal microscopy. Scale bars: 10 μm. Images representative of three similar experiments (**b**) As in (a) except cells where also transfected with a YFP control were indicated and fixed after 8 or 24 hours. (**c**) HEK293T cells were transfected with YFP-ARHGAP36 or YFP-Cherry control for 24 hours. Lysates were immunoblotted with the indicated antibodies. Blots representative of three similar experiments.

blotting using an anti-GFP antibody. Once thus optimised, endogenous PKAC levels could also be seen by western blot (Figure 4.1c).

4.2.2. ARHGAP36 has no effect on PKAR

As most regulation of PKA signalling is mediated through PKAR, I first wanted to investigate if this effect on PKAC was secondary to an effect on PKAR. I performed the same experiments as for PKAC, overexpressing ARHGAP36 and assessing PKAR levels by IF in MDCK and by WB in HEK293T. ARHGAP36 had no effect on any PKAR subunit tested, either by IF or by WB (Figure 4.2a & b).

4.2.3. Pseudosubstrate binding is required but not sufficient to promote PKAC downregulation

I next hypothesised that degradation of PKAC may require binding of any pseudosubstrate, promoting its dissociation from the regulatory subunits and release from the protective holoenzyme setting. It is known that some components of protein complexes are much less stable in isolation. For example, ribosomal proteins are synthesised at a high rate and accumulate in the nucleus to allow for ready assembly of ribosomes when required. However most of these proteins do not become incorporated into the ribosome and any free ribosomal proteins are quickly degraded via the proteasome, in order to prevent over accumulation. Ribosomal proteins that do assemble into ribosomes become stable as components of the complex and have a much longer half-life (Lam *et al*, 2007). This is also true for subunits of the T Cell Antigen Receptor (TCR) that contain hydrophobic sequences recognised for degradation in the endoplasmic reticulum unless they are bound by other members of the complex (Bonifacino *et al*, 1990). It has also been shown for PKAR that RIα half live increases from three to 14 hours upon incorporation into the holoenzyme (Amieux *et al*, 1997). I thus overexpressed PKI, which binds PKAC in the same manner as ARHGAP36 in the substrate binding pocket, and assessed PKAC levels. Both N and C terminally tagged constructs were tested, as it is possible that the fluorophore could mask the pseudosubstrate site in this small protein. Neither N nor C terminally tagged PKI had an effect on PKAC levels (Figure 4.3a), arguing that down regulation of PKAC is a specific property of ARHGAP36. 36i expression, just 25aa comprising the ARHGAP36 pseudosubstrate motif, was equally unable to promote PKAC degradation (Figure 4.3b). I then questioned whether ARHGAP36 pseudosubstrate binding was even necessary to mediate PKAC-degradation. Perhaps binding of a secondary protein via a different site is

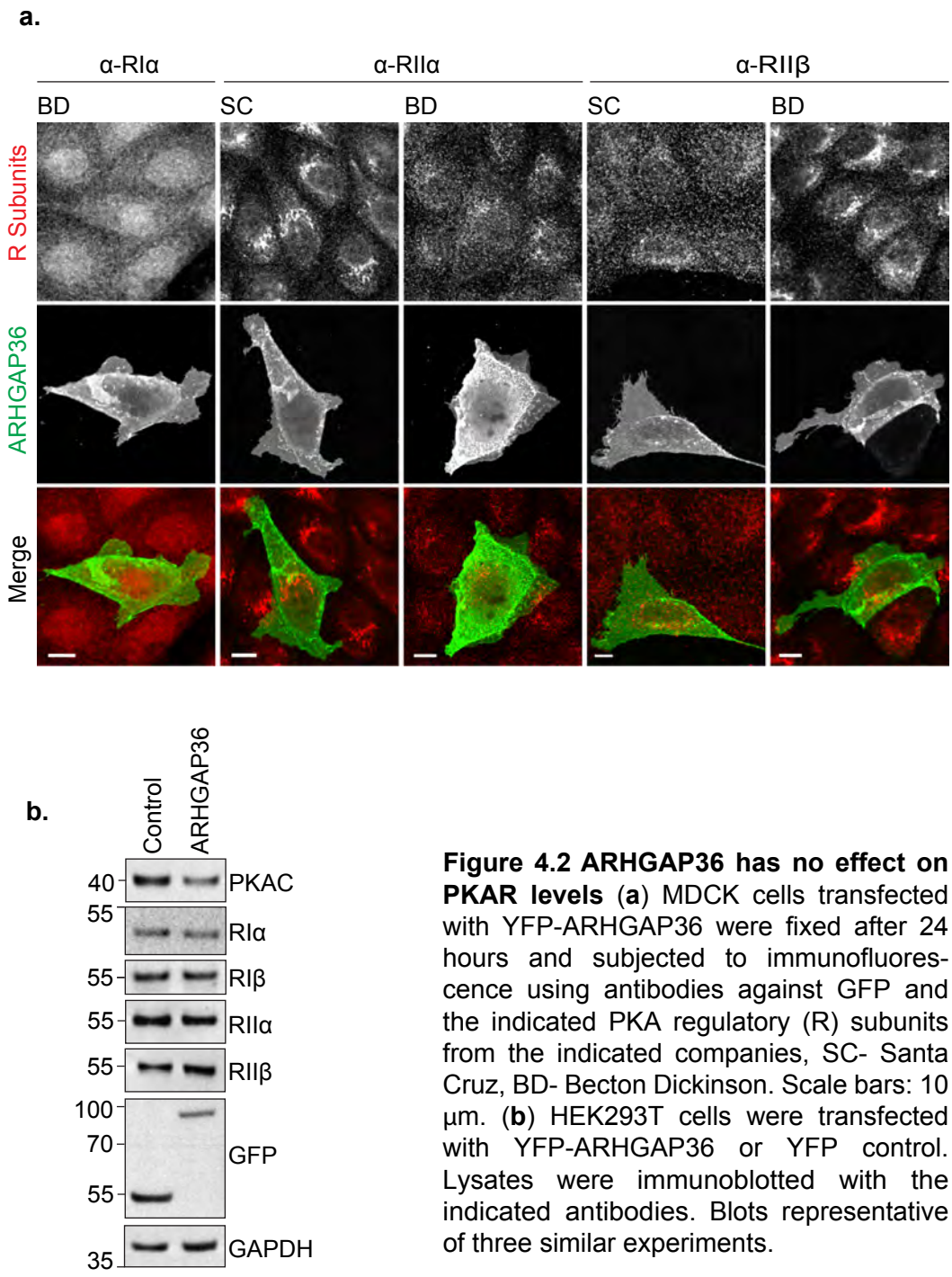

Figure 4.2 ARHGAP36 has no effect on PKAR levels (**a**) MDCK cells transfected with YFP-ARHGAP36 were fixed after 24 hours and subjected to immunofluorescence using antibodies against GFP and the indicated PKA regulatory (R) subunits from the indicated companies, SC- Santa Cruz, BD- Becton Dickinson. Scale bars: 10 µm. (**b**) HEK293T cells were transfected with YFP-ARHGAP36 or YFP control. Lysates were immunoblotted with the indicated antibodies. Blots representative of three similar experiments.

enough to catalyse this. However the RRV pseudosubstrate mutant, which varies from the WT ARHGAP36 by only three amino acids, could no longer cause degradation of PKAC (Figure 4.3c). This suggests a direct interaction via the pseudosubstrate domain is required but not sufficient to promote downregulation of PKAC.

4.2.4. ARHGAP36-N2, encompassing just 77 amino acids, can mediate PKAC degradation

I next set out to map the determinants in ARHGAP36 that are necessary and sufficient to promote downregulation of PKAC. ARHGAP36-N was able to promote down regulation of PKAC, and surprisingly so could ARHGAP36-N2, just 77 amino acids containing the pseudosubstrate domain. Otherwise all constructs that interact with PKAC could also cause its degradation (Figure 4.4, ARHGAP36-Iso3, -dGAP, -dC). This supports the fact that pseudosubstrate binding is absolutely required for degradation. ARHGAP36-ARG (aa118-154), which contains the two critical arginines but not the rest of the pseudosubstrate motif (^{153}-RRGAV-^{157}), can no longer cause PKAC degradation, despite the fact that it still localises similarly to full-length ARHGAP36.

4.2.5. ARHGAP36 induced PKAC degradation is rescued by lysosomal inhibitors

Most cytosolic proteins are degraded via the proteasome, therefore I tried to rescue PKAC degradation using proteasomal inhibitors such as MG132 and epoxomicin, but to no avail. The transient endosome-like vesicular PKAC staining observed prior to its degradation also pointed to a different mechanism. I next wanted to test the hypothesis that PKAC degradation occurs via the endolysosomal pathway, using inhibitors of the vacuolar ATPase that is responsible for lysosomal acidification and activation of lysosomal enzymes (Yoshimori *et al*, 1991). However, this was far from straight forward. In order to trigger PKAC degradation, I first needed to overexpress ARHGAP36, but as degradation is quite rapid, it was important to optimise the time window for treatment with inhibitors. I first tried transfecting and treating at the same time, however the proteasomal inhibitor MG132 and bafilomycin interfered with expression. The PEI transfection reagent works by allowing complexed DNA to bind membranes, be endocytosed and subsequently released into the cytoplasm (Boussif et al 1995). Bafilomycin has previously been shown to interfere with the progress of endocytosed material from early to late endosomes (Clague *et al*, 1994)

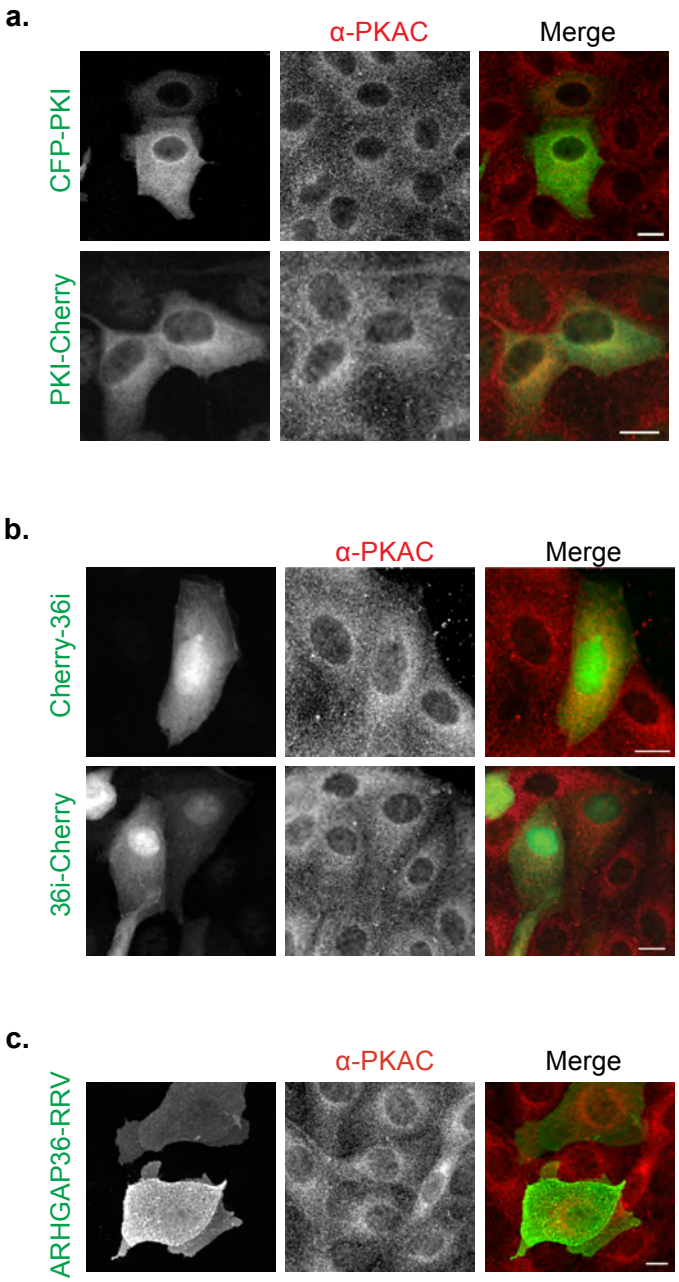

Figure 4.3 Pseudosubstrate binding alone is not sufficient to mediate PKAC degradation (**a**) MDCK cells transfected with CFP-PKI or PKI-cherry were fixed after 24 hours and subjected to immunofluorescence against PKAC. CFP-PKI signal was amplified using α-GFP. Images representative of three similar experiments. (**b**) The same as in (a) except cells were transfected with Cherry-36i or 36i-Cherry. 36i signal was not amplified using antibodies. Images representative of three similar experiments. (**c**) The same as in (a) except YFP-ARHGAP36-RRV was transfected. YFP-ARHGAP36-RRV signal was amplified with α-GFP. Images representative of three similar experiments. Scale bars: 10 μm throughout.

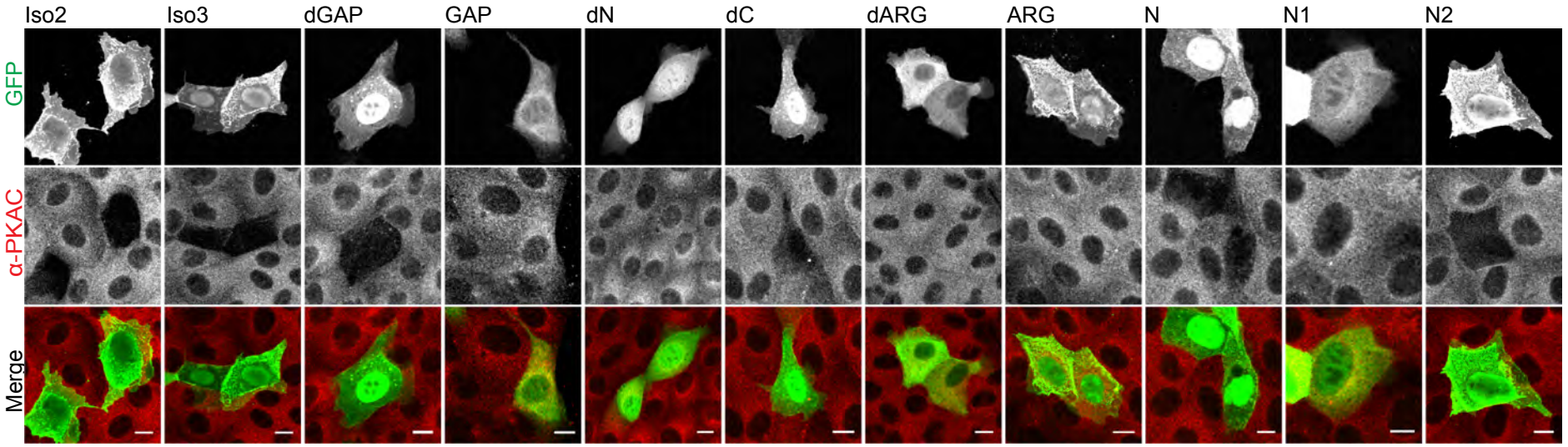

Figure 4.4 Only 77 amino acids, N2, are required for PKAC degradation MDCK cells were transfected with the indicated YFP-tagged ARHGAP36 truncation constructs for 24 hours before fixing. Cells were subjected to immunofluorescence with the indicated antibodies. Images were collected by confocal microscopy. Images representative of at least two similar experiments. Scale Bars: 10 μm. A summary of these truncations and those in Figure 4.3 is shown. Depicted is the structure compared to full-length ARHGAP36-Isoform2, whether they bind to PKAC and degrade it.

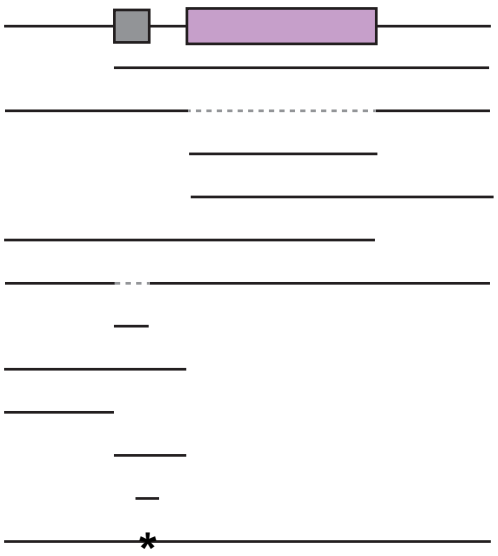

Construct	Boundaries	Binds	Degrades
Isoform3	118-516	Y	Y
dGAP	1-194/396-516	Y	Y
GAP	195-395	N	N
dN	195-516	N	N
dC	1-395	Y	Y
dARG	1-117/155-516	N	N
ARG	118-154	N	N
N	1-194	Y	Y
N1	1-117	N	N
N2	118-194	Y	Y
36i	141-165	Y	N
RRV	1-156 (R153D/R154D/V157D)	N	N

and may affect the release of DNA into the cytosol. Therefore I first had to wait after transfection to allow for proper ARHGAP36 expression, before an additional incubation with and without inhibitors. The second problem I encountered was that cells start to express ARHGAP36 at any point after transfection, thus after longer expression the ARHGAP36 transfected cells show quite heterogenous PKAC levels and localisation. By immunofluorescence microscopy, cells just starting to express ARHGAP36 present with the intermediate PKAC phenotype, which is also what a rescue may look like. In order to alleviate this confusing effect, I combined inhibitor treatment with cycloheximide (CHX), to also inhibit new protein synthesis. Cells can then no longer start to express ARHGAP36 during the inhibitor treatment, and are somewhat synchronised. PKAC levels should then be completely depleted in all ARHGAP36 transfected cells treated with CHX, therefore making the effect of inhibitors more obvious in comparison.

I co-overexpressed PKAC-Flag with YFP-cherry or YFP-ARHGAP36 in HEK293T cells for 12 hours. The following day I pre-treated the cells with epoxomicin or bafilomycin for 30 minutes prior to addition of CHX for a further six hours. In the absence of ARHGAP36 there was no effect of epoxomicin, bafilomycin or CHX on PKAC protein levels. This fits with previous observations that PKAC has a long half-life (T1/2 = 100 hours, (Schwanhäusser *et al*, 2011)). However in the presence of ARHGAP36, PKAC levels were much decreased, and a second higher molecular weight band became apparent. The addition of epoxomicin had no effect on PKAC, although the proteasomal substrate β-Catenin rapidly accumulated over the same timecourse (Figure 4.5a&b). In contrast, bafilomycin treatment partially restored PKAC levels.

The same effect on PKAC could be observed at the endogenous level by immunofluorescence in MDCK cells. Cells were first transfected with ARHGAP36 for eight hours, then pretreated with epoxomicin or bafilomycin for 30 minutes, before addition of CHX for a further eight hours. With the addition of CHX PKAC levels were clearly reduced in ARHGAP36 overexpressing cells. Bafilomycin, but not epoxomicin, caused a build up of PKAC on enlarged vesicles that colocalised with ARHGAP36 (Figure 4.5c).

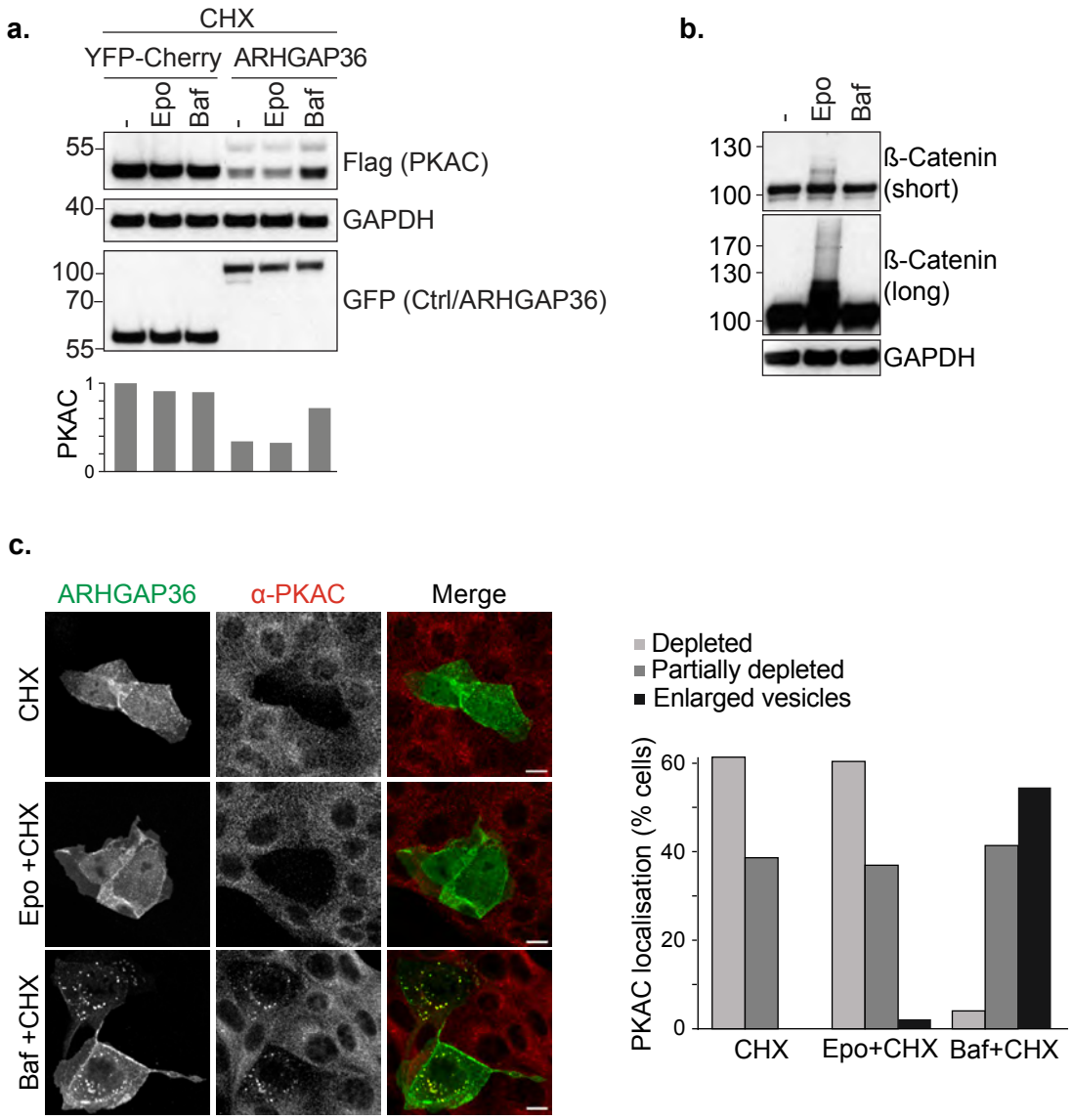

Figure 4.5 ARHGAP36 targets PKAC for lysosomal degradation (**a**) HEK293T cells were transfected with PKAC-Flag and YFP-ARHGAP36 or YFP-Cherry control as indicated. Before harvesting cells were pre-treated for 30 minutes with Epoxomicin (Epo, 50 nM) or Bafilomycin (Baf, 100 nM), before cycloheximide (CHX, 50 µg/ml) addition for a further six hours. Lysates were immunoblotted with the indicated antibodies. Flag-PKAC levels were densitometrically evaluated and normalised to the first lane shown. Blots representative of three independent experiments. (**b**) HEK293T cells were treated with Epoxomicin, Bafilomycin or DMSO vehicle control as in (a). Lysates were immunoblotted for the proteasomal substrate ß-Catenin. (**c**) MDCK cells were transfected with YFP-ARHGAP36 or YFP control for eight hours and, where indicated, were pre-treated for 30 minutes with Epoxomycin (100 nM) or Bafilomycin (100 nM), before cycloheximide (1 µg/ml) addition for a further eight hours. Cells were then fixed after a total of 16 hours transfection and subjected to immunofluorescence using antibodies against GFP and PKAC. Images were collected by confocal microscopy. Images representative of three independent experiments. Scale bars: 10 µm. The bar plot shows the percentage of YFP-ARHGAP36 transfected cells with the respective phenotype from a representative experiment, 100 cells counted per condition.

4.2.6. ARHGAP36 and PKAC colocalise along the endolysosomal pathway

In order to confirm PKAC is degraded in the lysosome I wanted to assess colocalisation with markers of the endolysosomal pathway. In U2OS cells overexpressed PKAC partially colocalised together with ARHGAP36 and the early endosomal marker EEA1, as well as with the MVB marker HRS (Figure 4.6a). In HeLa cells partial colocalisation could be seen with HRS, EEA1 and also with the late endosomal marker Rab7 (Figure 4.6b & c). Furthermore when HeLa cells were pretreated with bafilomycin for 30 mins and CHX for another six hours before fixing, PKAC-positive vesicles were affected in the same way as EEA1, with colocalisation becoming more pronounced. Before treatment both vesicle populations were diffusely distributed throughout the cell, whereas after treatment vesicles became more tubular and concentrated in the perinuclear region, in agreement with previous observations (Clague *et al*, 1994) (Figure 4.6c).

In MDCK cells endogenous PKAC partially colocalised together with ARHGAP36 and overexpressed HRS, as well as overexpressed LAMP-1, a lysosomal marker (Figure 4.7). Endogenous PKAC could also clearly be seen inside enlarged vesicles caused by the overexpression of Rab5-Q79L, a constitutively active GTPase variant (Stenmark *et al*, 1994). These experiments suggest that ARHGAP36 targets PKAC, a cytosolic protein, for endolysosomal degradation. The endolysosomal degradation pathway is usually reserved for transmembrane receptors. One other cytosolic kinase, GSK3 has been suggested to enter MVBs, but its fate is unknown as it does not seem to be subsequently degraded (Taelman *et al*, 2010). The absence of ubiquitin from this story caused much debate, as ubiquitylation of a cargo is generally thought to be required for its recognition by the ESCRT machinery and subsequent internalisation into MVBs (Metcalfe & Bienz, 2011). I thus wanted to explore whether PKAC is ubiquitylated and how this may be regulated by ARHGAP36.

4.2.7. ARHGAP36 mediates PKAC ubiquitylation

I first wanted to see if PKAC was ubiquitylated and whether the amount of ubiquitylated PKAC is increased in the presence of ARHGAP36. I pulled down PKAC-YFP in the presence or absence of Flag-ARHGAP36 and assessed its ubiquitylation status. I also cotransfected His tagged ubiquitin. In the presence of ARHGAP36, the amount of PKAC-YFP that was pulled down with anti-GFP appeared reduced and several higher molecular weight forms became apparent.

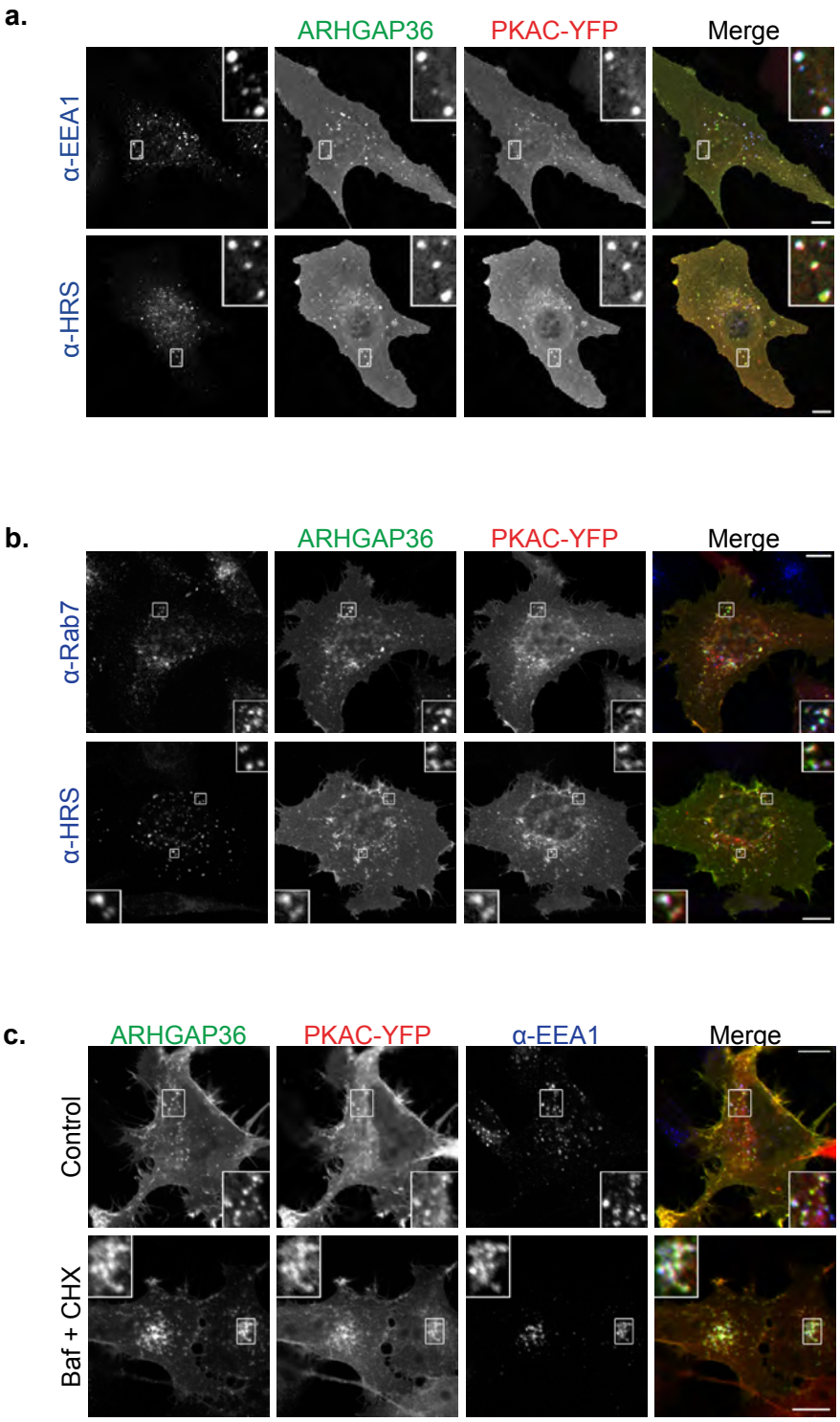

Figure 4.6 PKAC and ARHGAP36 partially colocalise with markers along the endocytic pathway (**a**) Confocal micrographs of U2OS cells transfected with PKAC-YFP and Flag-ARHGAP36. Cells were fixed and subjected to immunofluorescence using antibodies against GFP, Flag, EEA-1 and HRS. (**b**) As in (a) except HeLa cells were used, and cells were stained with antibodies against GFP, Flag, HRS and Rab7. (**c**) As in (b) except where indicated cells were pretreated for 30 min with 100 nM Bafilomycin (Baf), before addition of 1 µg/ml CHX for a further six hours before fixing. Cells were stained with antibodies against GFP, Flag and EEA-1. Scale bars: 10 µm throughout.

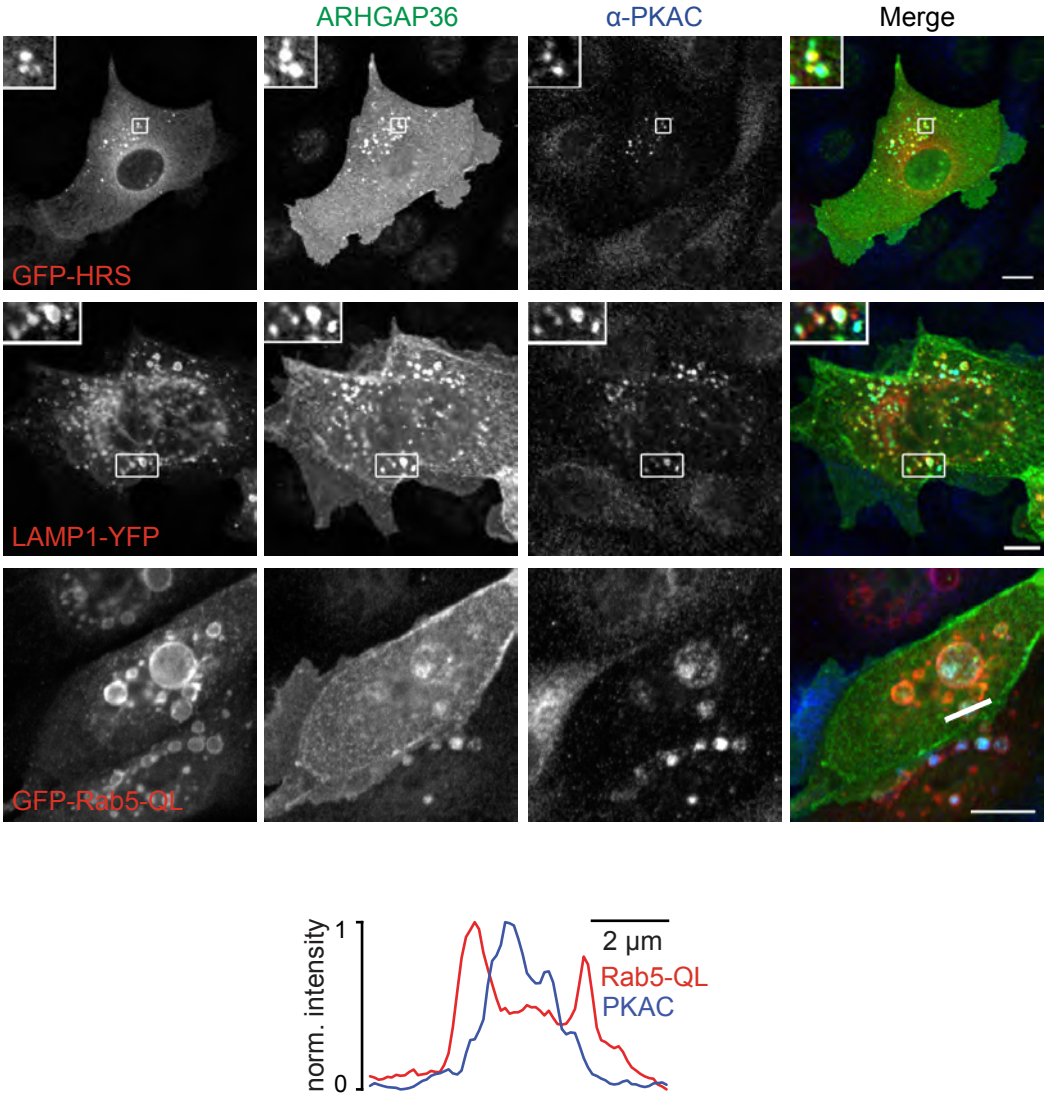

Figure 4.7 Endogenous PKAC colocalises with HRS, LAMP-1 and is enriched inside Rab5-Q79L vesicles. Confocal micrographs of MDCK cells transfected with Flag-ARHGAP36 together with GFP-HRS, LAMP1-YFP, or GFP-Rab5-QL. Cells were fixed and subjected to immunofluorescence using antibodies against GFP, Flag and PKAC. Scale bars: 10 µm. For Rab5-QL line scan fluorescence intensity profiles of the indicated area are shown below. In red Rab5-QL, in blue PKAC.

Probing the same immunoprecipitates with an anti-ubiquitin antibody, showed that a small amount of ubiquitin was present in the absence of ARHGAP36, however this was massively increased in the presence of ARHGAP36 (Figure 4.8a).

4.2.8. ARHGAP36 promotes PKAC ubiquitylation at a single lysine K285

In order to identify any ubiquitin sites on PKAC regulated by ARHGAP36, I designed SILAC-based mass spectrometry experiments, together with Erik McShane (AG Selbach, MDC). SILAC (Stable isotope labelling by amino acids in cell culture) involves culturing cells in media supplemented with heavy isotope labelled amino acids, specifically arginine and lysine, for a minimum of five passages, until these isotopes become incorporated into all newly synthesised proteins (Ong *et al*, 2002; Ong & Mann, 2007). Cell lysates derived from cells grown in 'light' or normal media, can then be mixed together 1:1 with 'heavy' labelled cells and subsequently subjected to tryptic digest for quantitation by mass spectrometry. As trypsin cleaves after arginines and lysines, each peptide should be efficiently labelled (Olsen *et al*, 2004). The relative intensity of heavy and light counterparts of each peptide then informs on the relative abundance of the parent protein in each condition. I labelled HEK293T cells with heavy or light media for a minimum of five passages, before transfecting cells with PKAC-Flag and YFP-ARHGAP36 or YFP-Cherry, so that PKAC would be differently labelled in the presence and absence of ARHGAP36. I lysed cells in RIPA, subjected proteins to Flag IP, then prior to the last washing step mixed heavy and light samples. After elution in 6M guanidine hydrochloride, samples were processed by Erik McShane. We found many PKAC peptides but only a single ubiquitin site, K285, identifiable by the additional isopeptide linked Gly-Gly remnant on the lysine side chain (Peng *et al*, 2003). This was also the only peptide to be regulated by ARHGAP36 (Figure 4.8b-d & Figure 4.9).

4.2.9. Lysine 285 is required for ARHGAP36-mediated PKAC poly-ubiquitylation

I next mutated this site to arginine, K285R, so it could no longer be ubiquitylated to see if PKAC could be stabilised. I pulled down YFP tagged PKAC-WT or PKAC-K285R in the presence and absence of Flag-ARHGAP36 and His-ubiquitin and assessed their ubiquitylation status. The lack of higher molecular weight bands with PKAC-K285R is immediately apparent, even upon probing with the GFP-antibody. The corresponding ubiquitin smear seemed to be completely lost with PKAC-K285R (Figure 4.10a). PKAC-K285R still bound to ARHGAP36, thus the lack of

a.

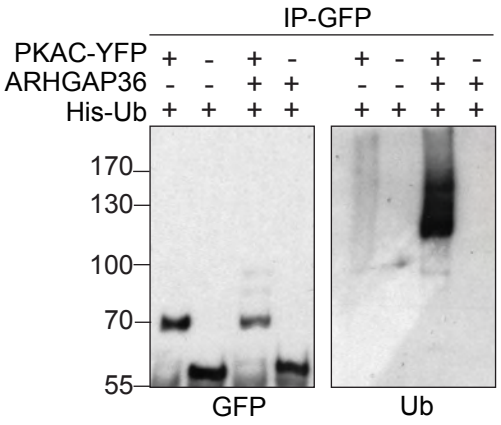

b.

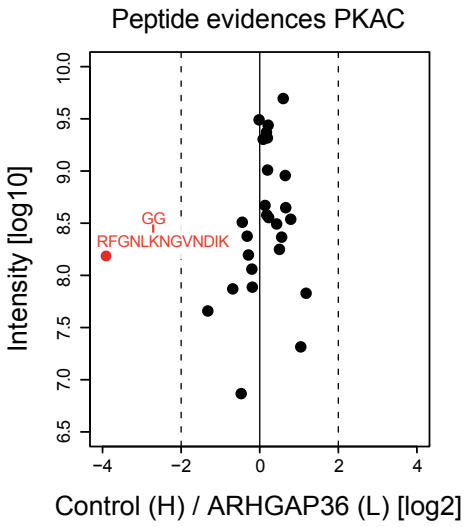

c.

Unique Peptides Identified:
RFGNLKNGVNDIK
ILQAVNFPFLVK
KWESPAQNTAHLDQFER
RILQAVNFPFLVK
WESPAQNTAHLDQFER
FPSHFSSDLK
VRFPSHFSSDLK
WFATTDWIAIYQR
DNSNLYMVMEYVPGGEMFSHLR
DNSNLYMVMEYVPGGEMFSHLRR
FYAAQIVLTFEYLHSLDLIYR
QIEHTLNEK
TLGTGSFGR
KVEAPFIPK
VEAPFIPK

d.

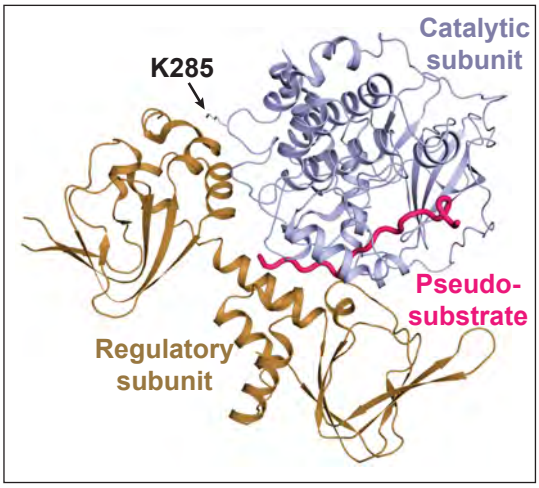

Figure 4.8 ARHGAP36 induces PKAC ubiquitylation (**a**) HEK293T cells were transfected with PKAC-YFP or YFP-Cherry control, Flag-ARHGAP36 and His-Ubiquitin as indicated. Lysates were subjected to GFP IP. Blots representative of three similar experiments (**b**) SILAC-labelled HEK293T cells were transfected with PKAC-Flag in the presence or absence of YFP-ARHGAP36. Lysates were subjected to Flag IP. Heavy/Light (H/L) ratio plot of the normalised peptide evidences matching PKAC. Only one peptide, highlighted in red, was upregulated in the presence of ARHGAP36 and this was the only ubiquitylated PKAC peptide identified. **Panel b courtesy of Erik McShane (AG Selbach, MDC)** (**c**) Sequences of unique peptides identified in (b). The underlined lysine in the top sequence is the ubiquitin modified K285. (**d**) Structure of the PKAC-PKARIIβ complex showing the position of K285 on PKAC that undergoes ubiquitylation. **Panel d courtesy of Oliver Daumke (MDC).**

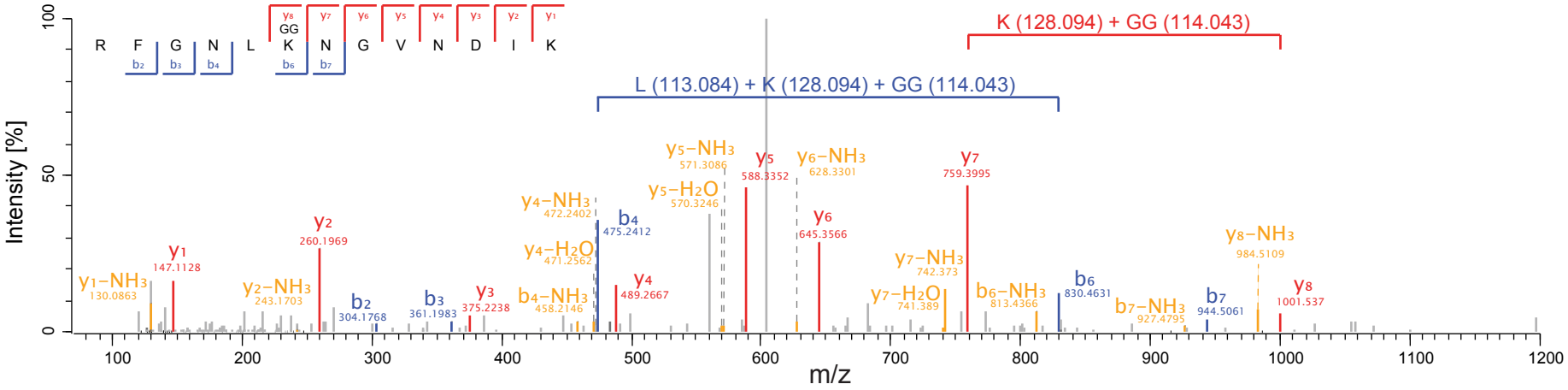

Figure 4.9 ARHGAP36 mediates PKAC ubiquitylation at K285
One out of two MS/MS spectra identifying the GlyGly modified peptide of PKAC. Amino acid sequence, modified amino acid and the corresponding ions are shown. The mass shift introduced by the ubiquitylation is annotated in both the b (blue) and y (red) series. **Figure kindly provided by Erik McShane.**

polyubiquitylation could not be attributed to a lack of binding to ARHGAP36. This was supported by inspection of the published holoenzyme structure, which shows that K285R is at a considerable distance from the pseudo/substrate binding domain (see Figure 4.8d). It also appears to be readily accessible, however a part of PKAR is missing from this structure that could possibly cover this site (Zhang *et al*, 2012). PKAC-WT was also pulled down via His-Ubiquitin IP and presented with multiple prominent higher molecular weight forms in the presence but not the absence ARHGAP36. In contrast, these high molecular weight species were not apparent for the K285R mutant. PKAC-K285R presence was much reduced in the His-Ubiquitin IP, to the level of PKAC-WT in absence of ARHGAP36 (Figure 4.10b). Note that PKAC-K285R does still appear to be mono-ubiquitylated (see Figure 4.10a, GFP IP, GFP blot, lane 4, arrow).

Direct binding to ARHGAP36 was required for PKAC ubiquitylation, as the pseudosubstrate mutant ARHGAP36-RRV, is unable to promote ubiquitylation of PKAC (Figure 4.10c).

4.2.10. PKAC-K285R is resistant to ARHGAP36 mediated degradation

CHX chase experiments showed that both PKAC-WT and PKAC-K285R are stable for at least nine hours, in agreement with previous data (Schwanhäusser *et al*, 2011). However when ARHGAP36 was co-transfected, PKAC-WT was turned over within three hours, whereas PKAC-K285R was stable throughout (Figure 4.10d). By IF, PKAC-WT was clearly lost in the presence of ARHGAP36 and CHX after six hours. Epoxomicin could not rescue this effect, but a build up of PKAC-positive vesicles could be seen with addition of either bafilomycin or the lysosomal protease inhibitor leupeptin. The polyubiquitylation deficient mutant PKAC-K285R was unaffected by either treatment and remained stable throughout (Figure 4.11). I thus conclude that polyubiquitylation of PKAC at K285 is absolutely required for ARHGAP36 mediated lysosomal degradation.

4.2.11. PKAC is decorated with K63-linked ubiquitin

Different ubiquitin chain linkages are known to be involved in different degradation or signalling pathways. While K48-linked ubiquitin chains normally target substrates to the proteasome, K63-linked chains have been implicated in lysosomal targeting (Komader and Rape 2012). I wanted to determine the ubiquitin chain linkages

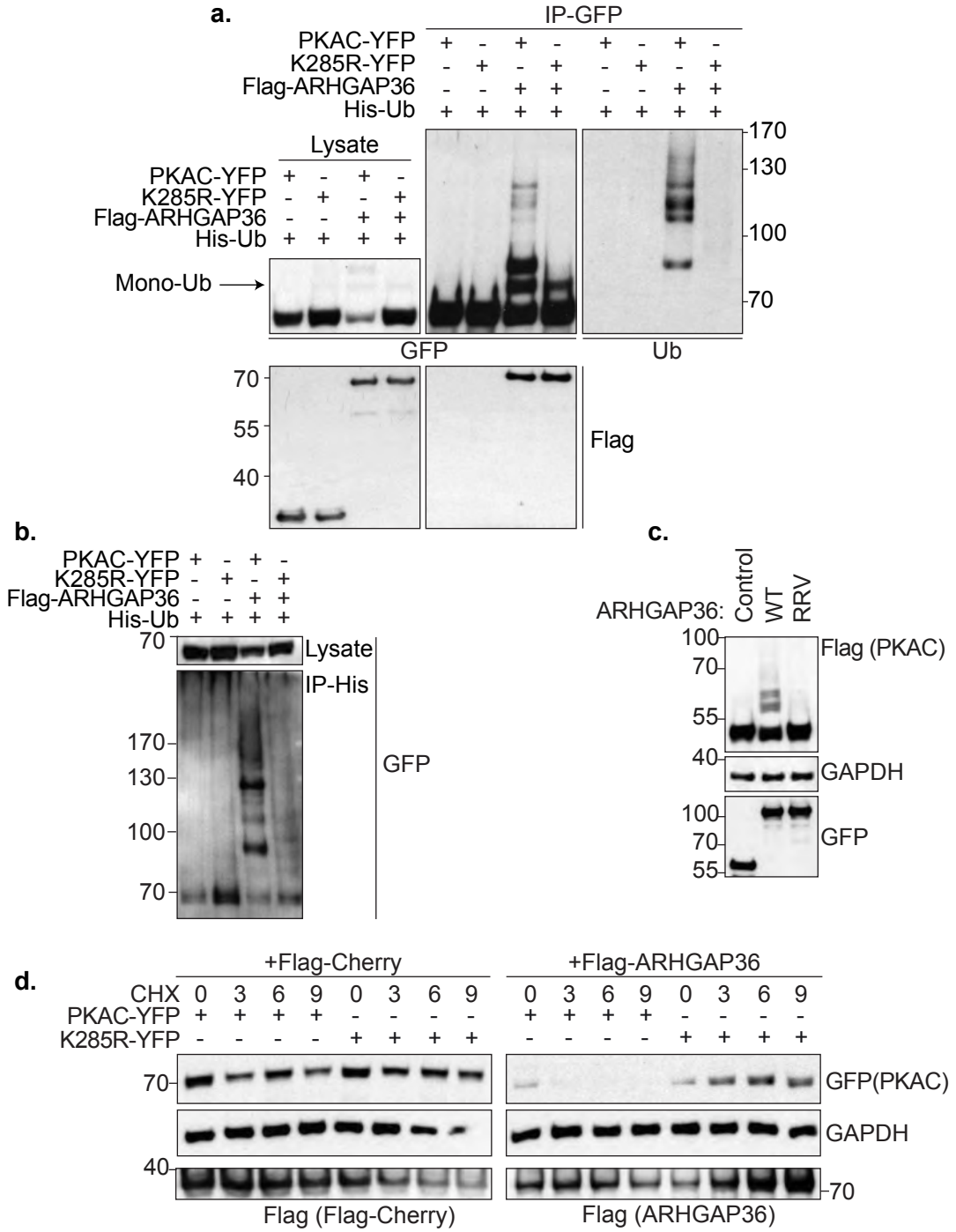

Figure 4.10 PKAC-K285R is resistant to ARHGAP36 induced polyubiquitylation and degradation (**b**) HEK293T cells were transfected with PKAC-YFP or K285R-YFP, Flag-ARHGAP36 or Flag-Cherry control, and His-Ubiquitin as indicated. Lysates were subjected to GFP IP. Blots representative of three independent experiments. (**b**) The same as in (a) except lysates were subjected to His IP and immunoblotted with anti-GFP. Blots representative of three independent experiments. (**c**) HEK293T cells were transfected with PKAC-Flag and CFP-ARHGAP36, the RRV mutant or CFP-Cherry control. Lysates were immunoblotted with the indicated antibodies. (**d**) HEK293T cells were transfected with PKAC-YFP or PKAC-K285R-YFP, and Flag-ARHGAP36 or Flag-Cherry control as indicated. 12 hours after transfection cells were treated with 50 µg/ml cycloheximide (CHX) and harvested at the indicated time points. Lysates were immunoblotted with indicated antibodies. Blots representative of three similar experiments.

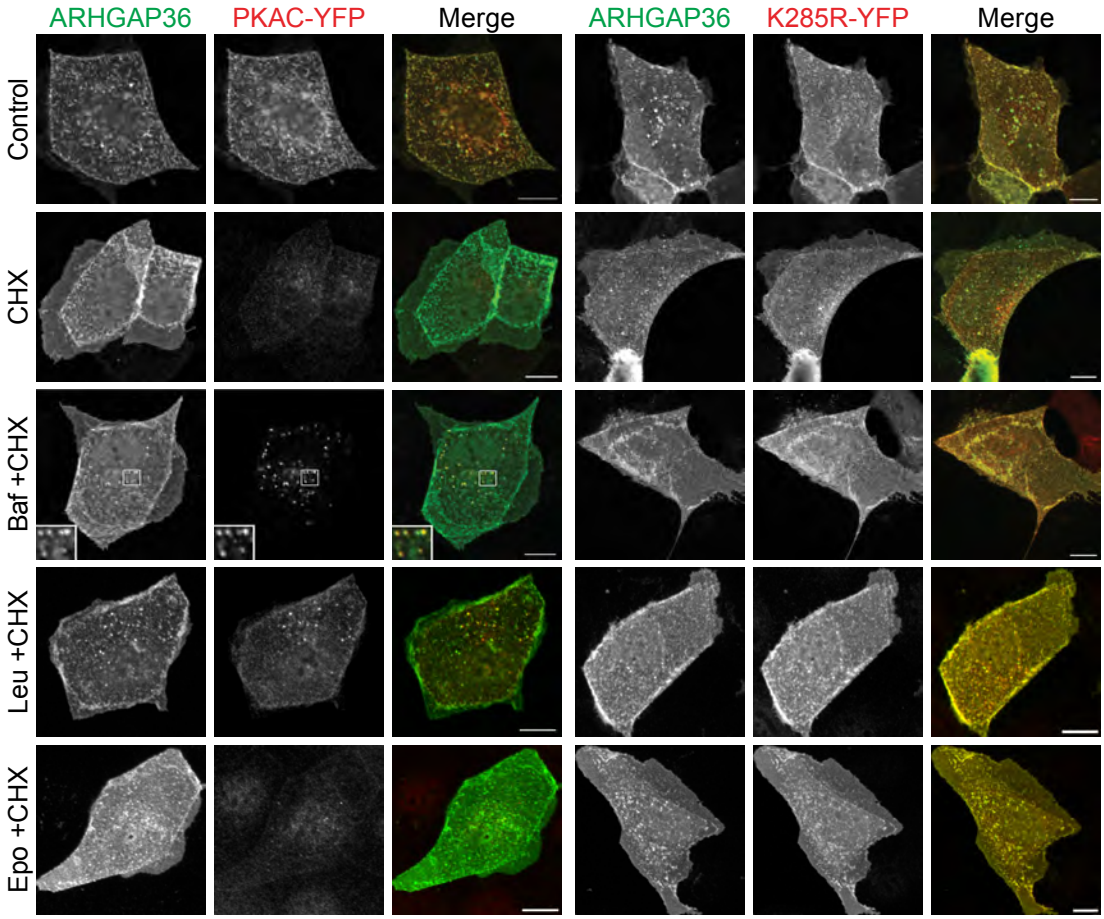

Figure 4.11 PKAC-WT is susceptible to CHX and degradation is rescued upon lysosomal inhibition, whereas PKAC-K285R is unaffected. Confocal micrographs of MDCK cells transfected with PKAC-YFP or PKAC-K285R-YFP and Flag-ARHGAP36. 12 hours after transfection, cells were pre-treated for 30 minutes with Bafilomycin (Baf,100 nM), Leupeptin (Leu, 500 µM) or Epoxomicin (Epo, 100 nM), before cycloheximide (CHX, 1 µg/ml) addition for a further five hours. Cells were fixed and subjected to immunofluorescence using antibodies against GFP and Flag. Images representative of three independent experiments. Scale bars: 10 µm.

attached to PKAC, especially as the ubiquitylation pattern consistently showed multiple discrete higher molecular weight bands. I first employed the UbiCREST assay developed in the lab of David Komander, which utilises the cleavage specificity of the DUBs to establish which linkages are within the chain (Mevissen *et al*, 2013; Hospenthal *et al*, 2015). After pulling down PKAC-YFP in the presence of Flag-ARHAGP36, the IP was split into aliquots and incubated with a panel of DUBs. USP2, a non linkage-specific DUB, reliably removed the whole smear, confirming this modification as ubiquitin (Figure 4.12a). None of the other DUBs were able to remove the entire smear, even after increasing the incubation time from the recommended 30 min to 45 min. However I consistently saw the appearance of a lower molecular weight species upon incubation with AMSH, a K63 chain editing DUB (McCullough *et al*, 2004, 2006; Komander *et al*, 2009b). This is most likely a mono-ubiquitylated species that would be resistant to AMSH. This partial cleavage may indicate the presence of complex mixed chains, which have also been implicated in lysosomal sorting (Boname *et al*, 2010). However, discussion with experts in the field revealed others had also experienced problems with DUB efficiency to completely remove chains from immunoprecipitated substrates (personal communication Anja Bremm, Buchmann Institute for Molecular Life Sciences, Frankfurt).

We then turned to Selected Reaction Monitoring mass spectrometry (SRM-MS) to try to quantitatively assess the type of ubiquitin chain linkages associated with PKAC. This utilises AQUA-peptides, as they allow Absolute QUAntification (Gerber *et al*, 2003; Kettenbach *et al*, 2011). These are heavy isotope labelled peptides corresponding to the digested forms of each of the possible ubiquitin chain linkages. These peptides are spiked as specific standards into the reaction at known amounts such that any ubiquitin linkages attached to the substrate can be accurately quantified (Mirzaei *et al*, 2010). I pulled down PKAC in the absence or presence of ARHGAP36 and washed under stringent conditions in order to get rid of any proteins that are non-covalently bound to PKAC and only detect PKAC-specific post-translational modifications. SRM-MS was then performed by Patrick Beaudette (AG Dittmar, MDC). In the absence of ARHGAP36, a small amount of K48-linked ubiquitin chains were detected. In the presence of ARHGAP36 there was no change in K48 levels, but a strong increase in K63 (Figure 4.12b). No other chain linkages were identified at significant levels. This confirms that PKAC is decorated with K63-linked ubiquitin chains and further supports that PKAC is degraded by the lysosome.

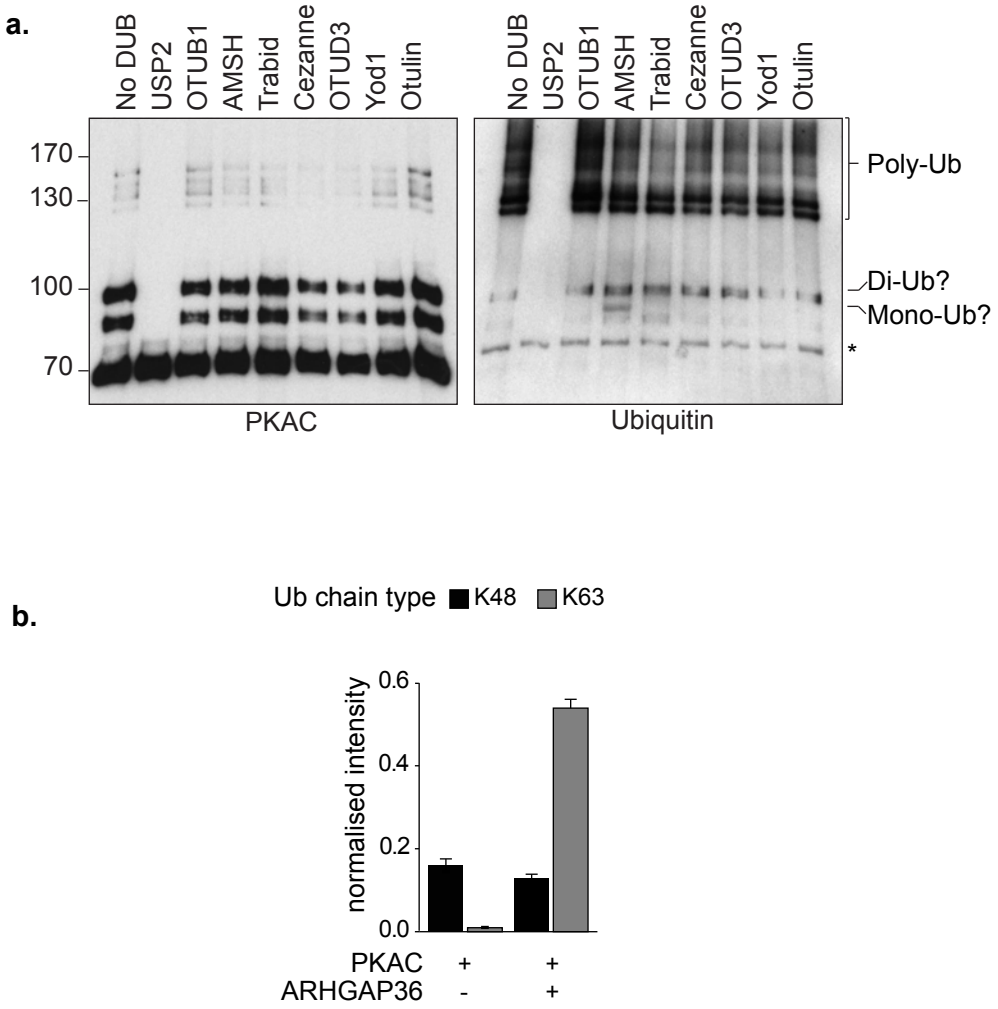

Figure 4.12 PKAC is decorated with K63 linked ubiquitin (**a**) HEK293T cells were transfected with His-Ubiquitin, PKAC-YFP and Flag-ARHGAP36. Lysates was subjected to a single GFP IP, then divided and incubated for 45 minutes at 37°C with the indicated DUB. Eluates were immunoblotted with antibodies against PKAC or Ubiquitin. Asterisk indicates background antibody band. Blots representative of three independent experiments. (**b**) HEK293T cells were transfected with PKAC-YFP in the presence or absence of Flag-ARHGAP36 and subjected to GFP IP followed by SRM-MS based relative quantitation of polyubiquitin linkage specific peptides. Data was normalised using the signal intensity of PKAC derived from a shotgun MS analysis of the same samples. Samples were measured in duplicate and the top two transitions used for quantitation. The error bars represent the standard deviation of the four calculated area ratios. **Panel b contributed by Patrick Beaudette (AG Dittmar, MDC).**

4.2.12. PKAC degradation requires the ESCRT pathway

Lysosomal targeting of ubiquitylated cargo relies on the ESCRT complexes. To provide further proof that PKAC is degraded at the lysosome, I wanted to assess the involvement of the ESCRT machinery. I first attempted to knock down the ESCRT-0 component HRS, however this proved difficult. In HEK293T cells I could only partially reduce HRS protein levels, despite attempting both single and double knock down protocols (Figure 4.13a). Knock down efficiency was better in HeLa cells, however transfection efficiency of ARHGAP36 plasmids was not sufficient to see a global decrease in PKAC levels. Instead I used Vps4, the AAA-ATPase that is involved in the recycling of ESCRT components in the final step when intraluminal vesicles pinch off into the MVB lumen (Williams & Urbé, 2007). I overexpressed Vps4-WT or the GTPase-deficient mutant, Vps4-E223Q (Bishop & Woodman, 2000; Sachse *et al*, 2004), and compared the turnover of PKAC-Flag over time. In the absence of ARHGAP36 neither Vps4-WT nor Vps4-EQ had an effect on PKAC-Flag. Upon cotransfection of ARHGAP36 and Vps4-WT, PKAC-Flag was readily degraded. In contrast, in Vps4-EQ cotransfected cells, PKAC-Flag still appeared to be ubiquitylated, however it was no longer degraded (Figure 4.13b). This suggests a role for the ESCRT machinery in ARHGAP36 induced PKAC degradation.

4.2.13. The ARHGAP36 interactome contains candidate E3 ligases

The original mass spectrometry screen that identified PKAC as an interactor of ARHGAP36 also turned up other hits. Three of them were ubiquitin E3 ligases: Praja2, Stub1 and Huwe1. We thought that it was conceivable that these could be the E3 ligases responsible for ubiquitylation of PKAC, with ARHGAP36 acting as a scaffold to bring substrate and ligase together. Praja2 is a RING E3 ligase (Yu *et al*, 2002), which is already known to ubiquitylate the PKA regulatory subunits, mediating their proteasomal degradation (Lignitto *et al*, 2011). Stub1, aka CHIP, is a small (35kDa) U-box domain containing E3, while Huwe1 is a very large (481kDa) HECT domain containing E3.

4.2.14. E3 overexpression does not affect PKAC levels

YFP-expression constructs for each ligase were overexpressed in MDCK cells to assess localisation of the encoded proteins. All E3s appeared mostly cytosolic with no apparent distinctive intracellular structures (Figure 4.14a). I next wanted to assess if ARHGAP36 could recruit any of the E3 ligases, however there was no change in E3 localisation upon co-expression of ARHGAP36 (Figure 4.14b). I then

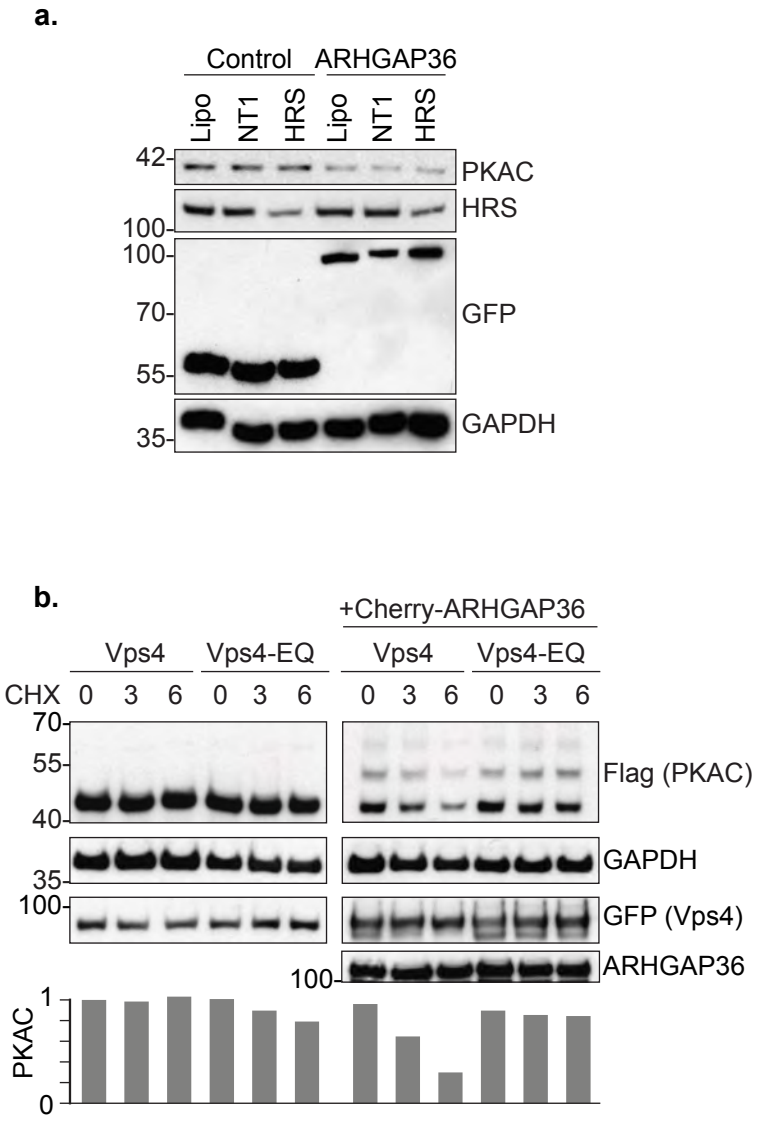

Figure 4.13 ARHGAP36 induced PKAC degradation requires Vps4 (**a**) HEK293T cells were transfected with 40 nM HRS siRNA the day after seeding. At 48 hours cells were transfected with YFP-ARHGAP36 or YFP-Cherry control. Cells were harvested 72 hours after knock down. Lysates were immunoblotted with the indicated antibodies. Lipo: reagent only control. NT1: non-targeting oligo control. (**b**) HEK293T cells were transfected with GFP-Vps4-WT or GFP-Vps4-EQ, PKAC-Flag and Cherry-ARHGAP36 or Cherry control as indicated. Cells were treated with cycloheximide (CHX, 50 µg/ml) and harvested at the indicated time points. Lysates were immunoblotted with the indicated antibodies. PKAC-Flag levels were densitometrically evaluated and normalised to the amount present in the first lane of each gel. Blots representative of three independent experiments.

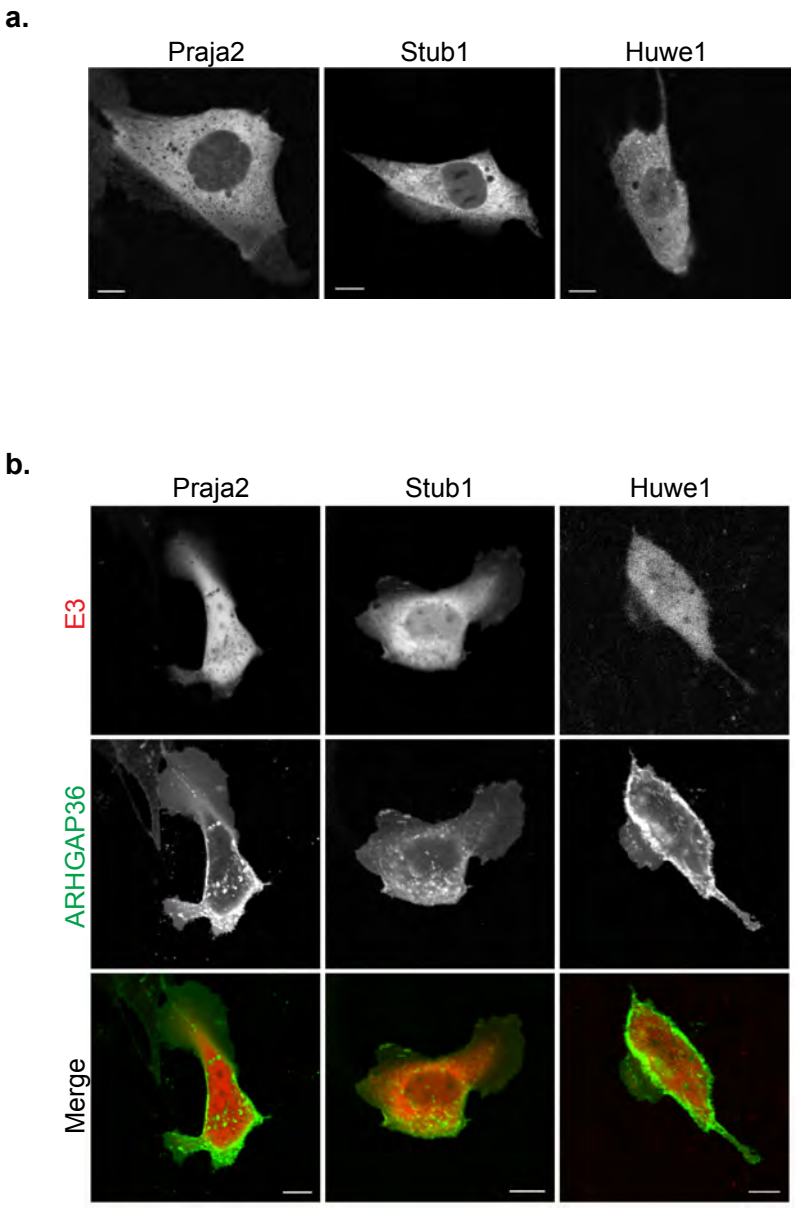

Figure 4.14 ARHGAP36 has no effect on the localisation of its E3 ligase interactors (**a**) YFP-tagged E3 ligases were overexpressed in MDCK cells and images collected by live cell confocal microscopy. (**b**) YFP-tagged E3 ligases were co-expressed with CFP-ARHGAP36 in MDCK cells and images collected by live cell confocal microscopy. Scale bars: 10 μm.

wanted to see if any of the E3 ligases could cause PKAC degradation, however overexpression did not have any effect on endogenous PKAC levels, or localisation, by IF (Figure 4.15a). After eight hours of ARHGAP36 expression, endogenous PKAC is still present and co-localises with ARHGAP36 on vesicles (Figure 4.1b) I co-overexpressed the E3 ligases for this length of time, to see if they could increase the degradation rate of PKAC. PKAC was still found on vesicles, with no change in comparison to cells cotransfected with ARHGAP36 and a control plasmid (Figure 4.15b). Huwe1 expression was problematic throughout, due to its large size it was hard to express and transfection efficiency was low. Therefore solid conclusions could not be drawn for this E3. Huwe1 is also listed in the CRAPome, a mass spectrometry database collating commonly identified background proteins (Mellacheruvu *et al*, 2013). It was found in 17% of experiments, suggesting this hit could be unspecific. For this reason, as well as difficulties working with a protein of this size, the other E3s were prioritised.

4.2.15. E3 knockdown does not affect PKAC levels

Having established that overexpression of the E3 ligases had no effect on PKAC levels, I next sought to knock them down to see if PKAC levels could be stabilised. Praja2 and Stub1 were knocked down using a smart pool comprised of four oligos for 48 hours with a single hit in HEK293T cells. Praja2 and Stub1 knock down were confirmed at the protein level via antibody staining. There was no effect on PKAC levels upon either E3 knock down. Co-expression of ARHGAP36 for the last 24 hours of knock down consistently caused a decrease in PKAC levels independent of the presence of either ligase (Figure 4.16a). I then knocked down Praja2 and Stub1 together, to see if they could compensate for each other. However simultaneous knock down of both Praja2 and Stub1 had no effect on PKAC, even when ARHGAP36 was overexpressed (Figure 4.16b). Huwe1 was also knocked down alone and in combination with Praja2 and Stub1. Although its knock down was not verified by antibody staining, initial experiments revealed no alteration in PKAC levels, even in the presence of ARHGAP36. Interestingly ARHGAP36 overexpression promoted a decrease in Stub1 levels.

4.2.16. Stub1 and Praja2 interact with ARHGAP36

In order to at least confirm the interaction of Praja2 and Stub1 with ARHGAP36, I performed immunoprecipitation experiments. ARHGAP36 was able to pull down both Praja2 and Stub1 (Figure 4.17a). Conversely, Stub1 could pull down both

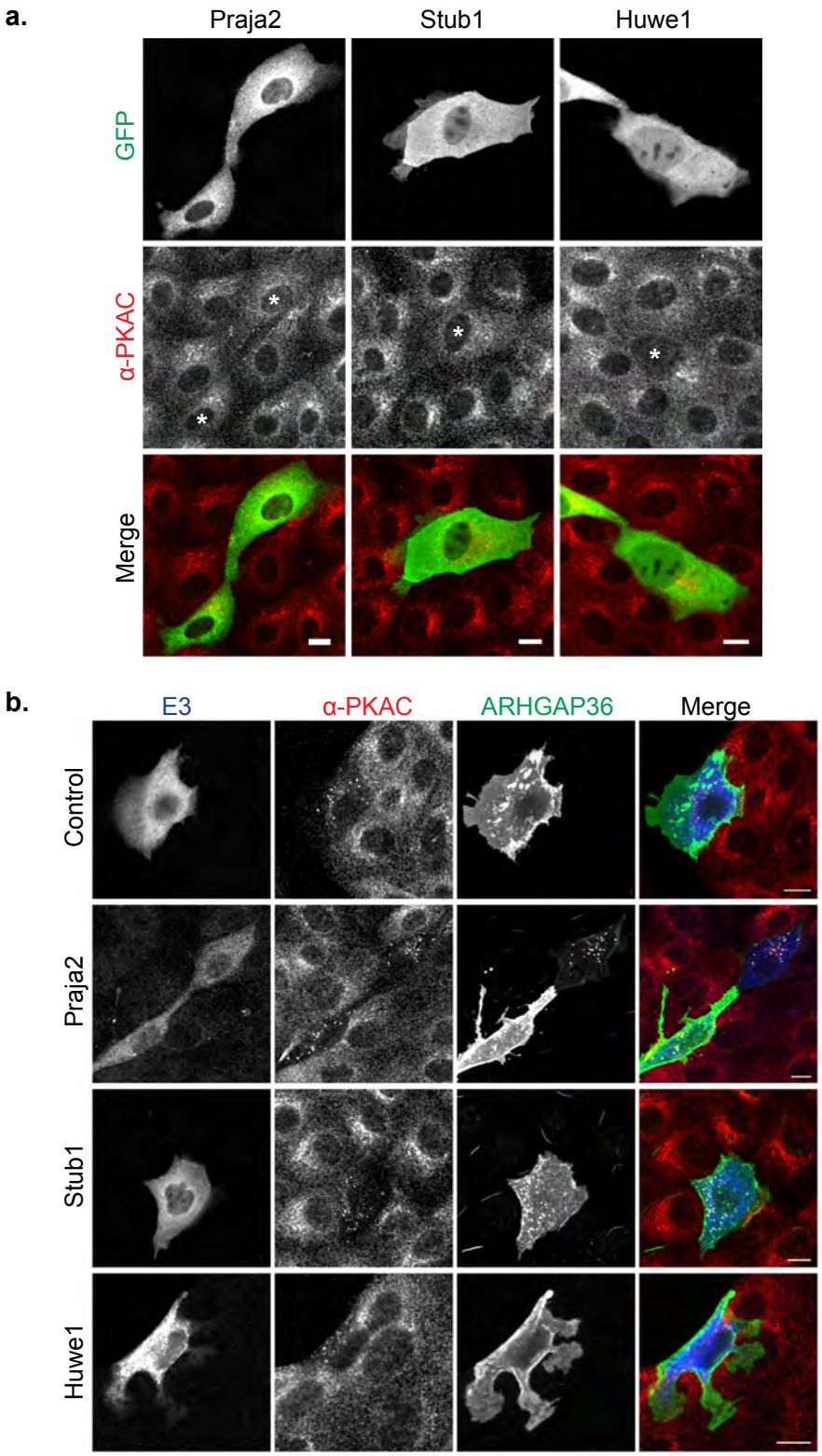

Figure 4.15 E3 interactor overexpression has no effect on PKAC levels, even in the presence of ARHGAP36 (**a**) YFP-tagged E3 ligases were overexpressed in MDCK cells. After 24 hours cells were fixed and subjected to immunoflouresence using antibodies against GFP and PKAC. Asterisk in PKAC channel indicates E3 transfected cells. (**b**) YFP-tagged E3 ligases were co-expressed with Flag-ARHGAP36 in MDCK cells. After eight hours the cells were fixed and subjected to immunofluorescence using antibodies against GFP, ARHGAP36 and PKAC. Scale bars: 10 μm.

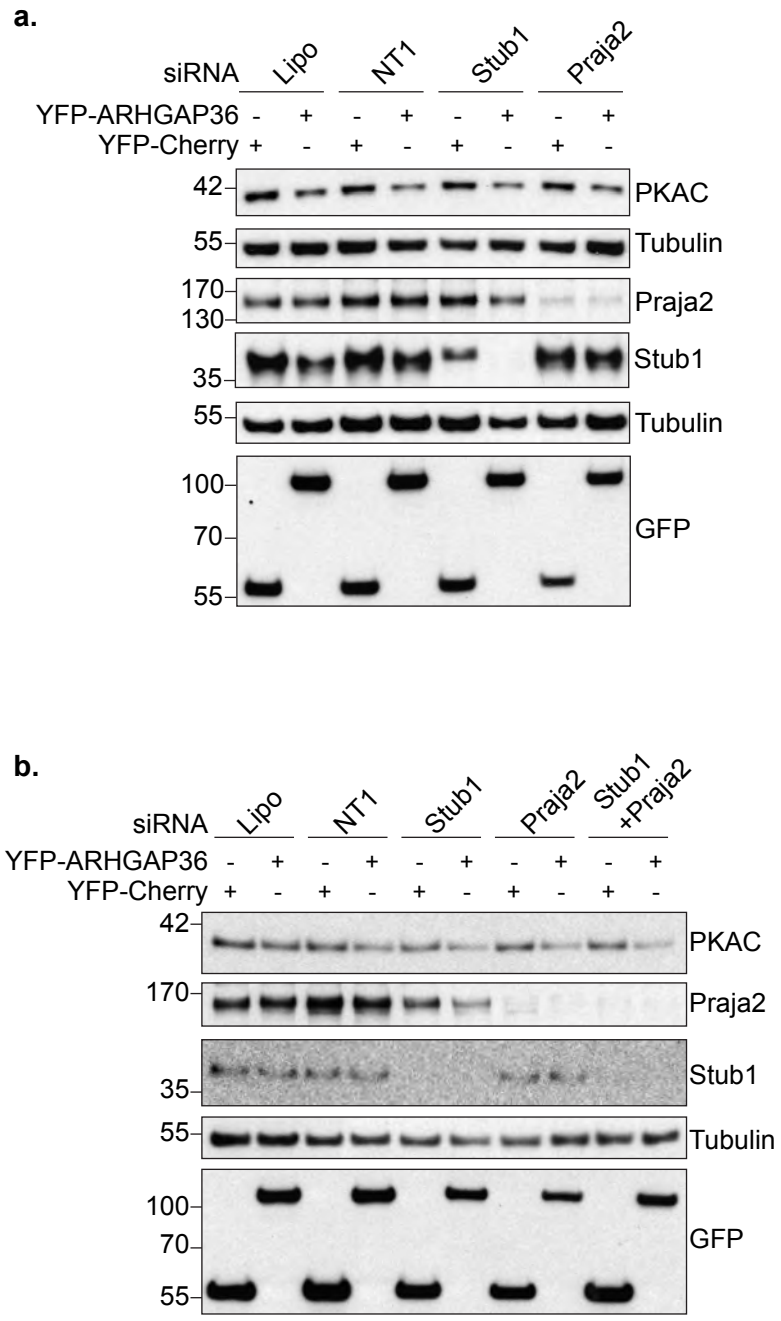

Figure 4.16 Knockdown of Praja2 or Stub1 has no effect on ARHGAP36 mediated PKAC degradation (**a**) HEK293T cells were transfected using Lipofectamine RNAiMAX with 40 nM siRNA SMARTpools against Praja2, Stub1, the control oligo NT1, or the reagent alone (Lipo). After 24hours cells were transfected with YFP-ARHGAP36 or YFP-Cherry using PEI. After a further 24 hours cells were harvested, yielding a 48 hour total knockdown. Lysates were probed with the indicated antibodies. (**b**) As in (a) except where indicated, cells were treated with 40 nM each Stub1 and Praja2 together.

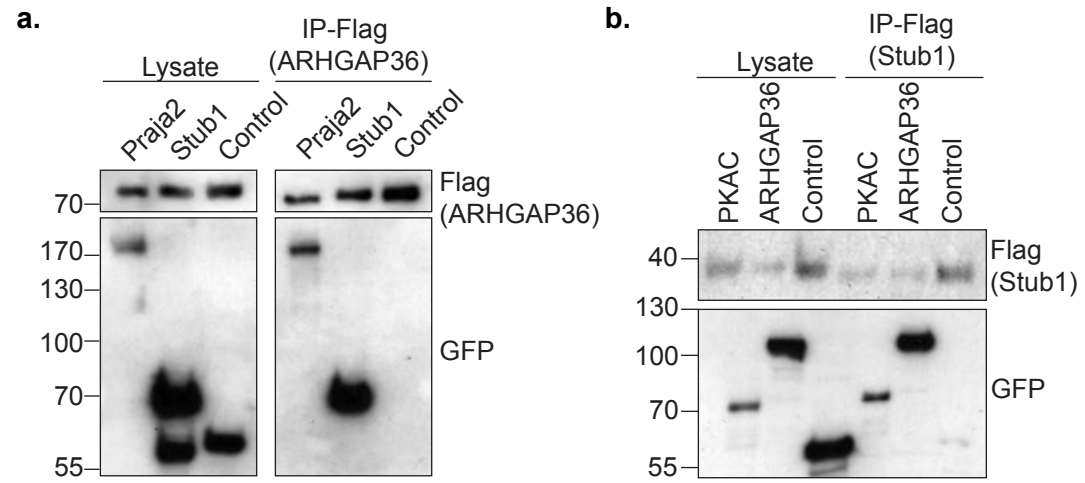

Figure 4.17 ARHGAP36 interacts with Praja2 and Stub1 (**a**) HEK293T cells were transfected with Flag-ARHGAP36 together with YFP-Praja2, YFP-Stub1 or YFP-Cherry control. Lysates were subjected to Flag IP and immunoblotted with antibodies against Flag and GFP. (**b**) As in (a) except cells were transfected with Flag-Stub1 together with PKAC-YFP, YFP-ARHGAP36 or YFP-Cherry control.

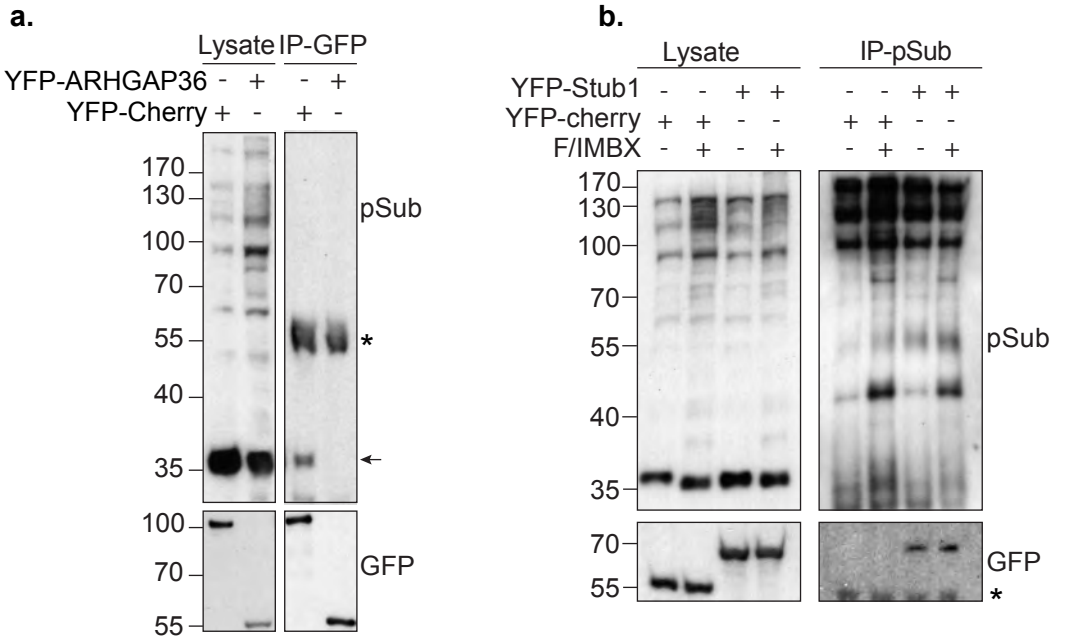

Figure 4.18 Stub1 is a PKA substrate (**a**) HEK293T cells were transfected with YFP-ARHGAP36 or a YFP-Cherry control. Lysates were subjected to GFP IP and immunoblotted with PKA p-Substrate and GFP antibodies. Arrow indicates the band which was subsequently identified as Stub1. Asterisk indicates the heavy chain of the antibody used for IP. (**b**) HEK293T cells were transiently transfected with YFP-Stub1 or a YFP-Cherry control. 24hours after transfection, cells were stimulated with 10 μM Forskolin and 100 μM IBMX for 20 mins, before harvesting. Lysates were subjected to IP using a PKA p-Substrate antibody and immunoblotted with antibodies against p-Substrate and GFP. Asterisk indicates the heavy chain of the antibody used for IP.

cotransfected ARHGAP36 and PKAC (Figure 4.17b). PKAC is already known to interact at least indirectly with Praja2 via PKAR (Lignitto *et al*, 2011). The interaction of ARHGAP36 with Praja2 and Stub1 was thus confirmed, however the nature of these interactions is still unclear.

4.2.17. Stub1 is a possible PKA substrate

Immunoblotting of an YFP-ARHGAP36 IP with a PKA phospho-substrate antibody suggested that one particular substrate was consistently pulled down with ARHGAP36 (Figure 4.18a). To identify this protein of around 35 kDa, the YFP-ARHGAP36 IP was repeated, the eluate run on a gel, stained and the band cut out and analysed by mass spectrometry by Erik McShane (AG Selbach, MDC). The top hit was none other than Stub1. PKA phosphorylation site prediction software turned up three candidate sites, two of which had also been identified in phosphosite. GFP-Stub1 could also be pulled down with the PKA p-Substrate antibody (Figure 4.18b).

4.3. Discussion

Main Chapter Findings

- ARHGAP36 mediates PKAC degradation
- Unusually for a cytosolic protein, PKAC degradation occurs at the lysosome
- ARHGAP36 mediates K63 linked ubiquitylation of PKAC at a single site, K285

4.3.1. Monoubiquitylation vs Polyubiquitylation

ARHGAP36 promotes ubiquitylation of a single site on PKAC, K285. Mutation of this site to arginine, K285R, stabilises PKAC completely and abolishes its polyubiquitylation. PKAC-K285R still appears to be mono-ubiquitylated, however this does not lead to its degradation. Further mass spectrometric analysis of PKAC-K285R in the presence of ARHGAP36 did identify another ubiquitin site, K279. However, ubiquitylation at this site was only present on the mutant protein, and was much less abundant than at K285 in PKAC-WT. This could be an attempt of the E3 ligase to compensate, by ubiquitylating the next closest lysine, upon mutation of the primary site. This mono-ubiquitylation is however not sufficient to trigger downregulation of PKAC. Interestingly, it has previously been shown for EGFR that monoubiquitylation is sufficient for initial internalisation, but polyubiquitylation is

required for further endosomal sorting and lysosomal degradation (Huang *et al*, 2013).

4.3.2. K63 linked ubiquitylation

I have shown that ARHGAP36 mediates K63 linked ubiquitylation of PKAC. This chain linkage is already widely implicated in endolysosomal trafficking (Duncan *et al*, 2006; Lauwers *et al*, 2009; Erpapazoglou *et al*, 2012). The UbiCREST assay may implicate the presence of more complex mixed chains (e.g. K63 and K11-linked chains), which have previously been implicated in endolysosomal targeting (Boname *et al*, 2010). However, as others also experienced problems with immounoprecipitated substrates, and the SRM data only identified an increase in K63 linked chains upon ARHGAP36 co-expression, this would rather argue for an exclusive role of this chain linkage. Further experiments would be needed to clarify this point.

4.3.3. ARHGAP36 inclusion in MVBs

Some overexpressed ARHGAP36 appears to translocate inside Rab5-Q79L enlarged endosomes together with endogenous PKAC. However, the majority of the protein does not appear to be degraded, as it was stable throughout CHX chase experiments as assessed by WB (Figure 4.10d & 4.13b) and IF (Figure 4.11). The ubiquitin E3 ligase and multi subunit adaptor protein c-Cbl has also been seen inside MVBs. It ubiquitylates EGFR and has been proposed to remain associated with its substrate along its endocytic journey (de Melker *et al*, 2001). The ESCRT-I protein Tsg101 is a well-known marker for internal vesicles, and is even thought to be co-degraded with cargo as a possible feedback mechanism to limit receptor degradation (Malerød *et al*, 2011).

4.3.4. E3 ligase identification

The E3 ligase involved in ARHGAP36-mediated ubiquitylation of PKAC has yet to be identified. Since I have not found any evidence for an involvement of Praja2 in this process, I would argue for completely different mechanisms of degradation for PKAR and PKAC. Their degradation is spatially separated, PKAC in the lysosome, and PKAR in the proteasome, and this seems to involve different sets of proteins. As there are over 600 E3 ligases, identifying the E3 responsible for PKAC ubiquitylation will be a daunting task. Stub1 does not seem to control PKAC stability,

however it appears to be phosphorylated by PKAC and is itself downregulated by ARHGAP36. Phosphorylation of Stub1 by PKAC will need to be further confirmed, as the phospho-substrate antibody used for IP can potentially also recognise Akt and PKC substrates, albeit to a lesser extent. Regardless of the kinase, it would be interesting to see if there is an effect of this modification on Stub1 function. Further experiments would also be required to establish how ARHGAP36 affects Stub1 stability. For both Praja2 and Stub1 it would be interesting to know how they bind to ARHGAP36, and whether simultaneous binding to PKAC is possible.

4.3.5. Cross Regulation of PKAC and PKAR levels

It has previously been shown indirectly that in a wide variety of tissues PKAC and PKAR subunit proteins are present at approximately the same levels (Hofmann *et al*, 1977). Safeguarding mechanisms to ensure proper responsiveness of the holoenzyme to cAMP have thus long been hypothesised. In S49 mutant cell lines that lack PKAC, the PKAR subunits were shown to be much less stable (Steinberg & Agard, 1981a). It could also be shown that much less PKAR subunits are synthesised in these cells. Conversely, in wild type S49 cells that do express PKAC, kinase activation was shown to stimulate PKAR synthesis (Steinberg & Agard, 1981b). Thus active free PKAC can lead to an increase in PKAR. It was later confirmed that PKARIα transcription is indeed stimulated by cAMP (Solberg *et al*, 1997). In cells where PKAC is exogenously overexpressed, a corresponding increase in PKAR is also observed (Uhler & McKnight, 1987). Furthermore, PKARIβ and PKARIIβ knock out mice both show a compensatory increase in PKARIα levels (Amieux *et al*, 1997). ARHGAP36 may provide additional buffering capacity in situations of PKAC excess.

4.3.6. PKAR degradation

PKA signalling is known to play a critical role in synaptic plasticity. This requires sustained signalling through PKAC (Sweatt & Kandel, 1989). The ubiquitin-proteasome system has long been implicated in this mechanism through the degradation of PKAR. This shifts the balance of the R/C ratio and leads to persistent and eventually autonomous PKAC activation, despite basal cAMP levels (Greenberg *et al*; Hegde *et al*, 1993; Chain *et al*, 1995, 1999). Recently Praja2, a neuronal E3 ligase, was shown to mediate PKAR ubiquitylation and proteasomal degradation (Lignitto *et al*, 2011). Praja2 is an AKAP, which binds PKAR via an amphipathic a-helix located N-terminally from its RING domain. Praja2 is also a PKA

substrate, and phosphorylation is thought to increase its catalytic activity. Praja2 thus mediates a positive feed forward loop. Elevation of cAMP-levels causes dissociation of the holoenzyme, thus activation of PKAC, which phosphorylates Praja2, which in turn ubiquitylates PKAR. PKAR degradation thus leads to an increase in free and active PKAC. Lignitto and co-authors could show that siRNA knockdown of Praja2 in rat brain leads to decreased p-CREB levels upon stimulation. They further demonstrated that Praja2 knockdown affects long-term potentiation in the rat brain. ARHGAP36 could be involved in resetting the pathway in the brain.

4.3.7. Hints at PKAC degradation in the literature

Whereas many protein kinases are ubiquitylated and degraded upon activation (Lu & Hunter, 2009; Liu *et al*, 2012), this is the first proposed mechanism for ubiquitin-dependent turnover of PKAC. PKAC is intrinsically active, with its activity regulated by binding to PKAR. Therefore it was mostly thought that PKA signalling is reset through holoenzyme reassociation.

Loss of PKAC upon prolonged stimulation was first observed for a porcine kidney cell line (Hemmings, 1986). In this case the loss of PKAC was strongly accentuated upon IBMX addition, which inhibits phosphodiesterase activity. This argues that normally cAMP would be degraded over short periods, so the holoenzyme can reassociate. Then mechanisms may need to come into play to degrade any remaining free PKAC left over at longer time points. ARHGAP36 could be involved in such a mechanism.

It has been shown in thyroid follicular cells that under constant hormone stimulation the PKA pathway becomes unresponsive, and CREB-dependent transcriptional activation ceases. Over shorter periods this was shown to be due to dephosphorylation of CREB at Ser-133, however after longer periods of sustained activation phosphatase inhibitors were unable to rescue this effect. It was claimed that this was due to a loss of PKAC, however the quality of western blotting was questionable (Armstrong *et al*, 1995). Loss of PKAC with constant stimulation was also seen over time in a growth hormone producing pituitary cell line, however this was assessed indirectly via PKI-binding assays (Richardson *et al*, 1990a). Nevertheless ARHGAP36 may play a role in such a hormone-induced refractory period.

One recent paper implicated a cell-type specific role of the Regγ (PSME3) proteasome activator in regulating PKAC stability (Liu *et al*, 2014). It had previously been described that Regγ could mediate ubiquitin and ATP independent degradation of SRC-3 and p21 (Li *et al*, 2006, 2007). PKAC was shown to be more abundant and stable in Regγ knock out cells. I saw no effect of proteasome inhibitors on ARHGAP36 induced PKAC degradation.

4.3.8. Kinase inhibition by endolysosomal inclusion

Surprisingly for a cytosolic protein, ARHGAP36 targets PKAC not to the proteasome, but to the endolysosomal pathway. One other cytosolic kinase, GSK3, has also been seen to enter MVBs, however it is not subsequently degraded by the endolysosomal system (Taelman *et al*, 2010). GSK3ß is a central component of the destruction complex in the canonical Wnt signalling pathway (Wu & Pan, 2010). In the absence of a Wnt stimulus, GSK3ß together with CK1 takes part in the sequential phosphorylation of β-catenin, which as a result is recognised by the $SCF^{ßTRCP}$ ubiquitin-ligase, ubiquitylated and degraded at the proteasome (MacDonald *et al*, 2009). Upon pathway activation, β-catenin ubiquitylation is prevented, so that newly synthesised beta-catenin can accumulate and drive target gene expression in the nucleus. GSK3ß inactivation is critical for this. Taelman and colleagues claimed that when the activated Frizzled receptor and its co-receptor LRP5/6 become endocytosed, GSK3 that is bound to the cytoplasmic tail of LRP5/6 becomes internalised into MVBs. They used cryoimmunoelectron microscopy to show convincingly that some GSK3 is located inside MVBs upon Wnt stimulation. They could also show that accumulation of β-catenin and Wnt pathway activation requires HRS and Vps4, implying a role for the ESCRT machinery. However they did not show or discuss a role for ubiquitin in this process, although the ESCRT pathway, and particularly HRS are known to specifically recognise ubiquitylated cargo for translocation into the internal vesicles of MVBs. The authors thus proposed that GSK3 may be actively sequestered in the endolysosomal pathway without providing evidence for downregulation of this critical kinase. This paper led to much discussion in the field (Metcalfe & Bienz, 2011).

In contrast to this story, I have shown that PKAC is ubiquitylated, providing a mechanism by which it can engage with the ESCRT machinery. I have also shown that this process requires active Vps4, suggesting a role for the ESCRT pathway.

Furthermore, unlike GSK3, ARHGAP36-mediated translocation of PKAC into the endolysosomal pathway results in its degradation.

Interestingly GSK3 is also thought to be inhibited by pseudosubstrate binding of LRP6 (Cselenyi *et al*, 2008; Mi *et al*, 2006; Piao *et al*, 2008; Wu *et al*, 2009). Thus parallels can be drawn with PKAC, which is subjected to bimodal inhibition by ARHGAP36. Pseudosubstrate binding ensures immediate inhibition of the kinase, and internalisation into MVBs ensures this inhibition is sustained, as the kinase can no longer access its substrates. For PKAC, degradation is the final step. One could argue that this may turn out to be a general mechanism for long-term signal termination of cytosolic signalling proteins.

The Taelman paper implies that entry into the endolysosomal pathway could be facilitated by any membrane associated interaction partner that itself is sorted into the endocytic pathway. ARHGAP36 could thus mediate PKAC endolysosomal sorting as it independently localises to the plasma membrane and also to vesicular structures. I have shown that the ARHGAP36 arginine rich region is sufficient to target ARHGAP36 to membranes (Figure 3.2). The positively charged arginines could hydrostatically associate with the negatively charged plasma membrane. A polylysine charged region plays a role in KRas4b association with the membrane (Hancock *et al*, 1990; Jang *et al*, 2015), and basic regions in ESCRT-III proteins are thought to mediate binding to endosomal membranes (Williams & Urbé, 2007). Isoform 1 of ARHGAP36 contains a signal peptide, however this could also be a transmembrane protein. More investigation will be required to determine this, and whether it is of physiological relevance. It is also tempting to speculate whether ARHAGP36 could play a more general role in endocytic sorting.

4.3.9. Global or local degradation?

From my experiments with overexpressed ARHGAP36, all cellular PKAC was degraded, however this may not be the case in the endogenous context. A pool of PKAC may be turned over, for example at the membrane or within the primary cilia, in response to acute upregulation or stabilisation of ARHGAP36. This could be coupled to specific GPCR receptor stimulation within this space. Alternatively PKAC degradation could also take place in a constitutive manner in order to decrease sensitivity of cells to cAMP, leading to a tonic suppression of the pathway wherever ARHGAP36 is expressed.

Chapter 5. ARHGAP36 is a suppressor of PKA signalling

5.1. Introduction

ARHGAP36 has a dramatic inhibitory effect on PKA, firstly by direct inhibition and secondly by promoting its degradation. One would expect that as a result of this, signalling downstream of PKA is abolished. In this chapter I will aim to answer the following questions:

- Does ARHGAP36 expression affect PKA signalling outputs?
- Where is ARHGAP36 expressed?
- Does ARHGAP36 regulate PKAC in an endogenous setting?

5.2. Results

5.2.1. ARHGAP36 abolishes CREB phosphorylation

PKA phosphorylation controls many cellular processes. The transcriptional effects of PKA are partially mediated through the cAMP response element binding protein (CREB). This transcription factor is activated upon phosphorylation by PKA (Gonzalez & Montminy, 1989). Upon activation, CREB binds CRE sequences and activates transcription of target genes. CREB activation in the nucleus can be easily assessed by monitoring its phosphorylation status using phospho-specific antibodies. I transfected MDCK cells in OptiMEM with YFP-ARHGAP36 or YFP as a control. In unstimulated cells, there was hardly any phospho-CREB (p-CREB) signal in untransfected cells or those transfected with either construct (Figure 5.1a). Upon stimulation with 10 μM Forskolin and 100 μM IBMX for 20 min, all untransfected cell nuclei became positive for p-CREB staining. The same was true for YFP-transfected cells, however YFP-ARHGAP36 transfected cells remained p-CREB negative (Figure 5.1b). I counted the p-CREB positive nuclei of transfected cells and could show that ARHGAP36 causes more than a 90% reduction in CREB activation (Figure 5.1c). Overexpression of 36i, the 25 amino acids comprising the pseudosubstrate motif, also effectively inhibited CREB phosphorylation (Figure 5.2). Both N- and C-terminally tagged constructs were tested, as it is possible that the fluorophore could mask the pseudosubstrate site in this small protein. Both were found to be equally effective. CREB inhibition could thus be attributed to the pseudosubstrate binding and direct inhibition of PKAC, since 36i does not trigger PKAC downregulation. Both N- and C -terminally tagged PKI constructs could also inhibit CREB phosphorylation, serving as a positive control for inhibition of this PKA-dependant process. Importantly, the pseudosubstrate mutant ARHGAP36-RRV,

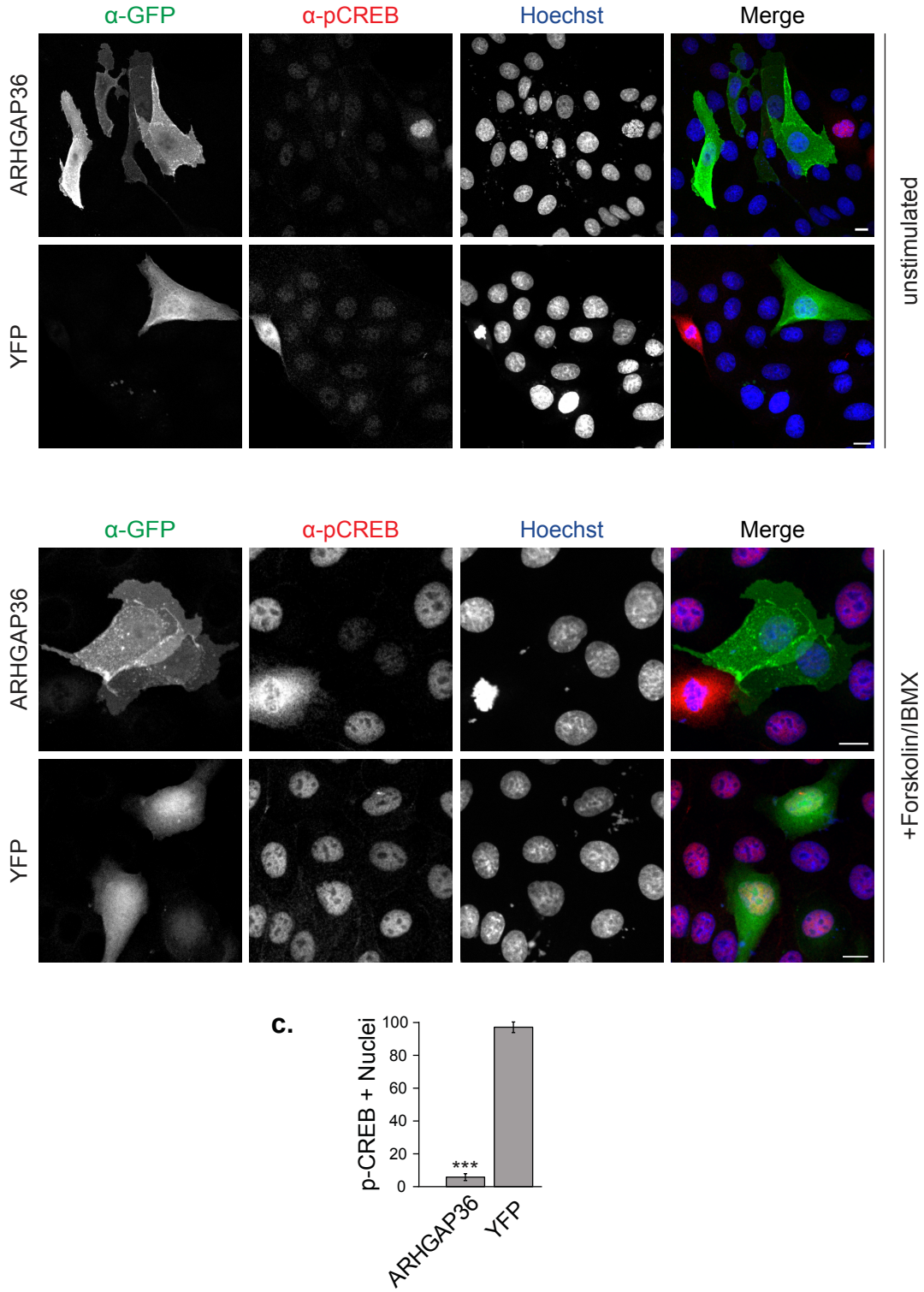

Figure 5.1 ARHGAP36 inhibits CREB phosphorylation (**a**) MDCK cells expressing YFP-ARHGAP36 or YFP control in OptiMEM were fixed without any stimulation and subjected to immunofluorescence using antibodies against GFP and phospho-CREB. Images were collected by confocal microscopy. Images representative of three independent experiments. Scale bars: 10 μm. (**b**) As in (a) except cells were treated with 10 μM Forskolin and 100 μM IBMX for 20 minutes before fixation. (**c**) Quantitative analysis of nuclear phospho-CREB staining in cells expressing the indicated constructs as in (b) (n>100 for each of three independent experiments, shown as mean ±s.d. *** p<0.001).

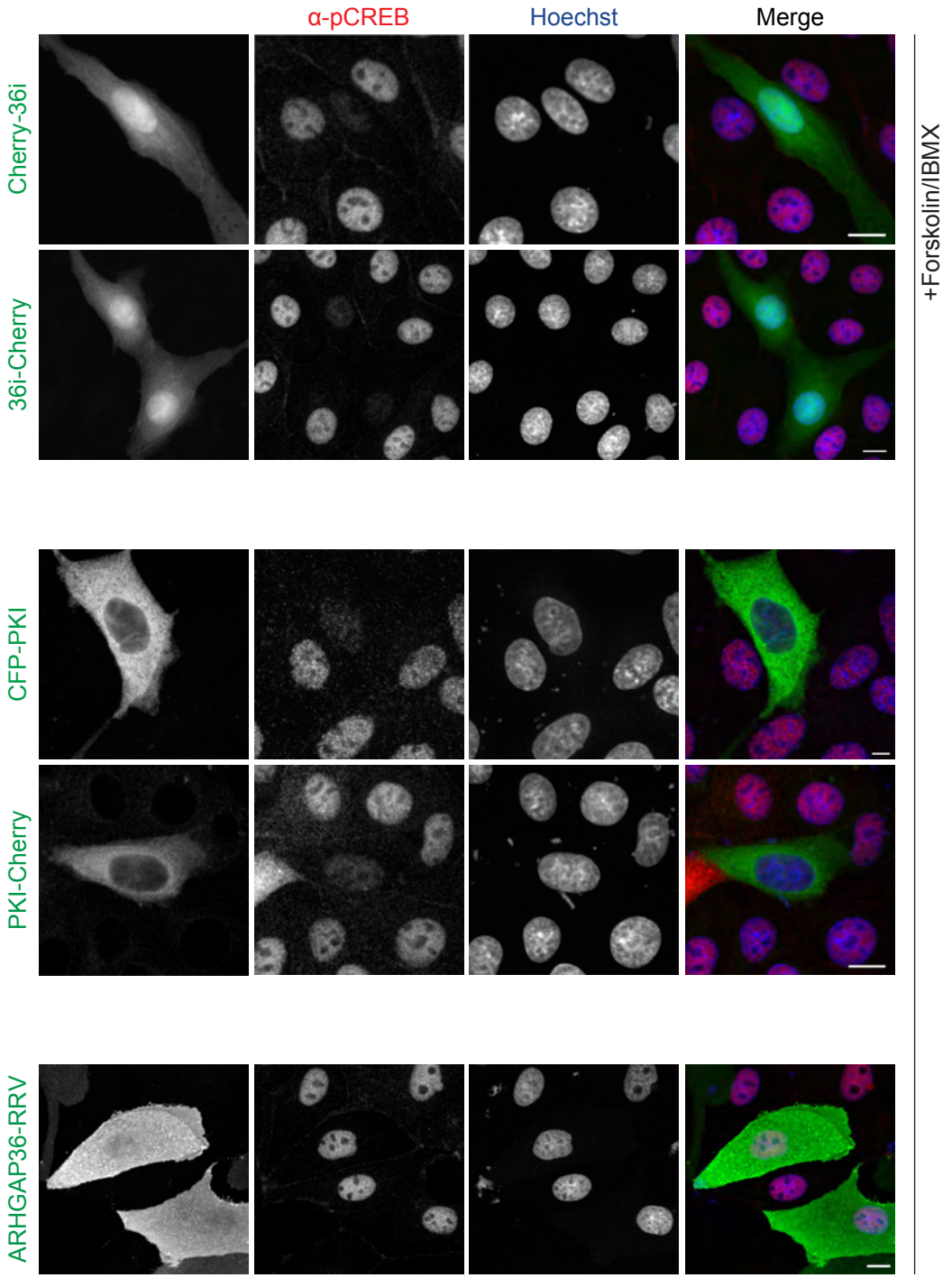

Figure 5.2 ARHGAP36 inhibits CREB phosphorylation via the pseudo-substrate motif MDCK cells expressing Cherry-36i, 36i-Cherry, CFP-PKI, PKI-Cherry or CFP-ARHGAP36-RRV in OptiMEM were treated with 10 µM Forskolin and 100 µM IBMX for 20 minutes, fixed and subjected to immunofluorescence using an antibody against phospho-CREB, and for CFP constructs signal was amplified using a GFP antibody. Images were collected by confocal microscopy. Scale bars: 10 µm.

which cannot interact with nor inhibit PKAC, was unable to suppress CREB phosphorylation.

5.2.2. ARHGAP36 inhibits AQP2 trafficking

Trafficking of the water channel aquaporin-2 (AQP2) is also a PKA dependant process. This occurs in the collecting duct cells of the kidney and is an important process for water homeostasis. Under basal conditions AQP2 is located on vesicles in the cytoplasm. However, upon vasopressin stimulus and cAMP production, activated PKA phosphorylates AQP2 (Katsura *et al*, 1997; Fushimi *et al*, 1997). This mediates the translocation and insertion of AQP2 into the plasma membrane, where it can affect water reabsorption. Using a mouse kidney collecting duct cell line, MCD4, which stably expresses AQP2 (Iolascon *et al*, 2007), I could assess the effect of ARHGAP36 on AQP2 translocation. I transfected MCD4 cells overnight in OptiMEM with YFP-ARHGAP36 or a YFP control plasmid. Cells were then fixed and stained for GFP and AQP2, as well as for the tight junction marker ZO-1 in order to identify the cell membrane. In unstimulated cells, AQP2 was indeed localised mainly to vesicles in the cytoplasm and did not colocalise with ZO-1 (Figure 5.3a). When cells were stimulated prior to fixation with 10 μM Forskolin and 100 μM IBMX for 20 min, a portion of AQP2 relocalised to the plasma membrane. YFP transfection had no effect on AQP2 translocation, whereas in YFP-ARHGAP36 expressing cells, AQP2 remained on vesicles in the cytoplasm (Figure 5.3b). This could be clearly shown by the lack of colocalisation with ZO-1, which is also depicted as a line-scan intensity plot in Figure 5.3b. In contrast, clear colocalisation of AQP2 and ZO-1 could be seen in YFP-expressing cells.

5.2.3. ARHGAP36 expression is largely restricted to embryonic skeletal muscle

With such an extreme effect on PKAC itself, as well as signalling downstream, we hypothesised that ARHGAP36 expression must be tightly regulated both spatially and perhaps temporally throughout development. In order to address this question I designed an *in situ* hybridisation probe, to recognise *Arhgap36* mouse mRNA. At that time we did not have a validated antibody.

I initially tested my probe on sections from E14 and E16 mice. I saw a striking expression in the tongue, the diaphragm, and the intercostal muscles (Figure 5.4). In discussion with experts, we realised that *Arhgap36* mRNA was present in all

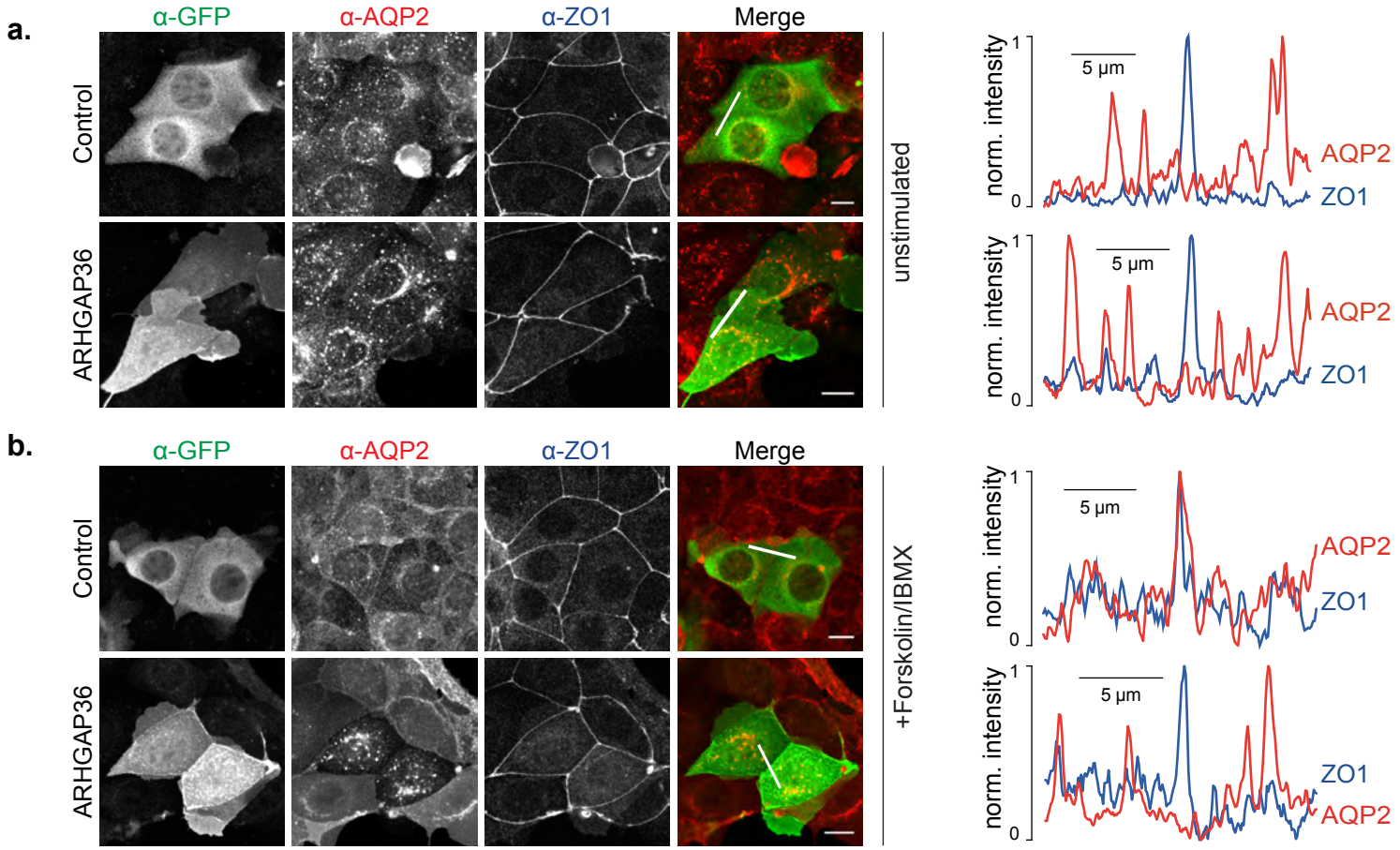

Figure 5.3 ARHGAP36 inhibits AQP2 trafficking (**a**) MCD4 cells stably expressing Aquaporin2 (AQP2) were transfected with YFP-ARHGAP36 or YFP control in OptiMEM. 24 hours post-transfection, without any stimulation, cells were fixed and subjected to immunofluorescence using antibodies against GFP, AQP2 and the tight junction protein ZO-1, to visualise the plasma membrane at cell-cell contact sites. Images were collected by confocal microscopy. Scale bars: 10 µm. Line scan fluorescence intensity profiles are shown on the right. In red: AQP2, in blue: ZO-1. Images representative of three similar experiments. (**b**) As in (a) except cells were treated with 10 µM Forskolin for 20 minutes before fixing.

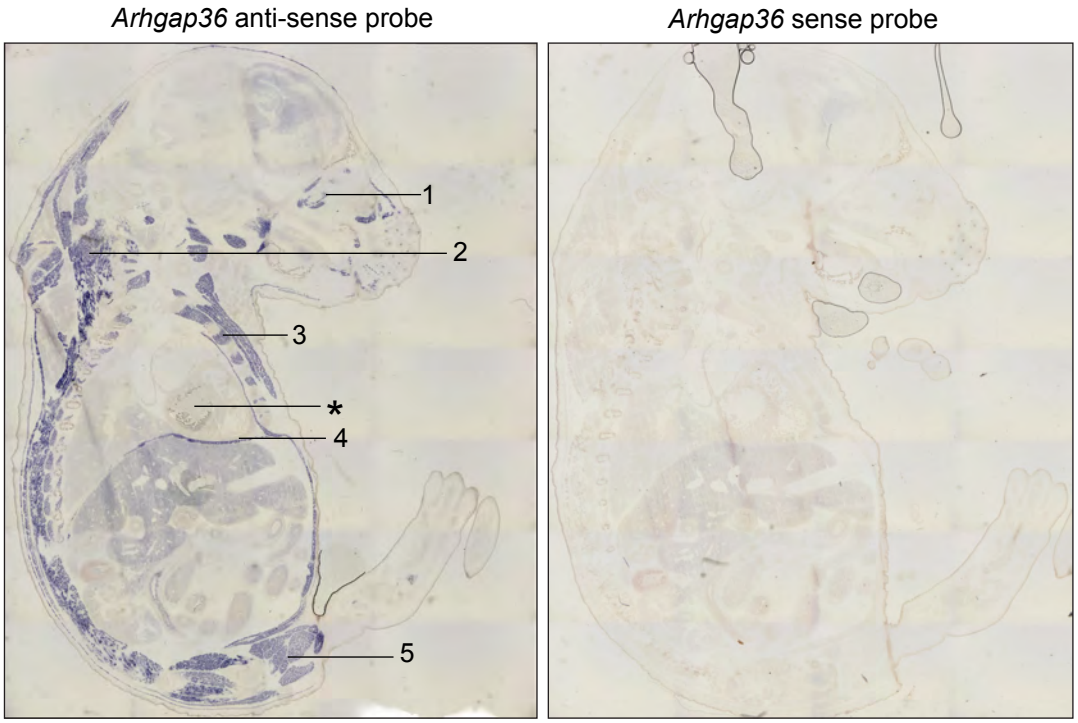

Figure 5.4 *Arhgap36* is expressed in embryonic skeletal muscle. *In situ* hybridization using an *Arhgap36*-specific probe on wild-type E14 mice. Left panel anti-sense probe, right panel negative control using sense probe. Positive blue staining can be seen in: 1- extraocular muscles, 2- back muscles, 3- intercostal muscles, 4-diaphragm, 5- muscles of the hindlimb. Note that the heart (*), a cardiac muscle, is not positively stained.

skeletal muscles. Upon seeing such strong expression in skeletal muscle, I wanted to use the C2C12 muscle cell line as a model, however no Arhgap36 mRNA could be detected. As these cells are derived from adult mouse muscle fibres, I wondered whether Arhgap36 is actually still expressed in adult muscle. In collaboration with Nora Mecklenburg (AG Hammes-Lewin, MDC) and Maciej Czajkowski (AG Rocks, MDC) *Arhgap36* expression was surveyed across the developmental stages. These expression data suggest that *Arhgap36* is present in skeletal muscle from formation, up until birth. Expression starts as early as E10 in the somites, however is quickly lost after birth, and completely gone at P2 (Figure 5.5).

5.2.4. ARHGAP36 is absent from commonly used cell lines

The restricted expression pattern explains why we had failed to detect Arhgap36 mRNA by qRT-PCR in a number of commonly used cell lines, such as those used in this thesis so far. I then queried disease databases and found that ARHGAP36 was upregulated in neuroblastoma cell lines (nextbio.com), and even identified as part of a neuroblastoma signature (Lee *et al*, 2014). qRT-PCR revealed a substantial increase in mRNA levels in SK-N-BE(2) cells, and an even greater increase in NGP cells (25 and approximately 3000 fold respectively compared to HeLa cells, Maciej Czajkowski, AG Rocks, unpublished data). Both of these cell lines are derived from human neuroblastoma. I then wanted to confirm ARHGAP36 expression at the protein level. I ran 10 µg of protein lysate from NGP and SK-N-BE(2) cells, as well as HeLa, HEK293T and U2OS for comparison, and assessed expression by WB with a commercial ARHGAP36 antibody. I detected a strong band at the relevant size only in NGP cells (Figure 5.6a). This band between 40 and 50 kDa could correspond to human Isoform 3, which is predicted to have a MW of 46 kDa. I have already confirmed that Isoform 3 can both interact with PKAC and cause its degradation (Figure 3.8 and 4.4).

5.2.5. ARHGAP36 is expressed in neuroblastoma cells

I next attempted to knock down ARHGAP36 in NGP cells using siRNA in order to first confirm the specificity of the antibody. Cells were cultured for 48 hours before transfection with Lipofectamine RNAiMAX, NT1 or a smart pool comprising four oligos targeting ARHGAP36. 24 hours after siRNA transfection, cells were lysed directly in the well with RIPA buffer. Western blotting revealed that the ARHGAP36 band at 46 kDa is specific, as it is reduced upon treatment with siRNA (Figure 5.6b). When I ran much more SK-N-BE(2) protein I could also see an ARHGAP36 band at

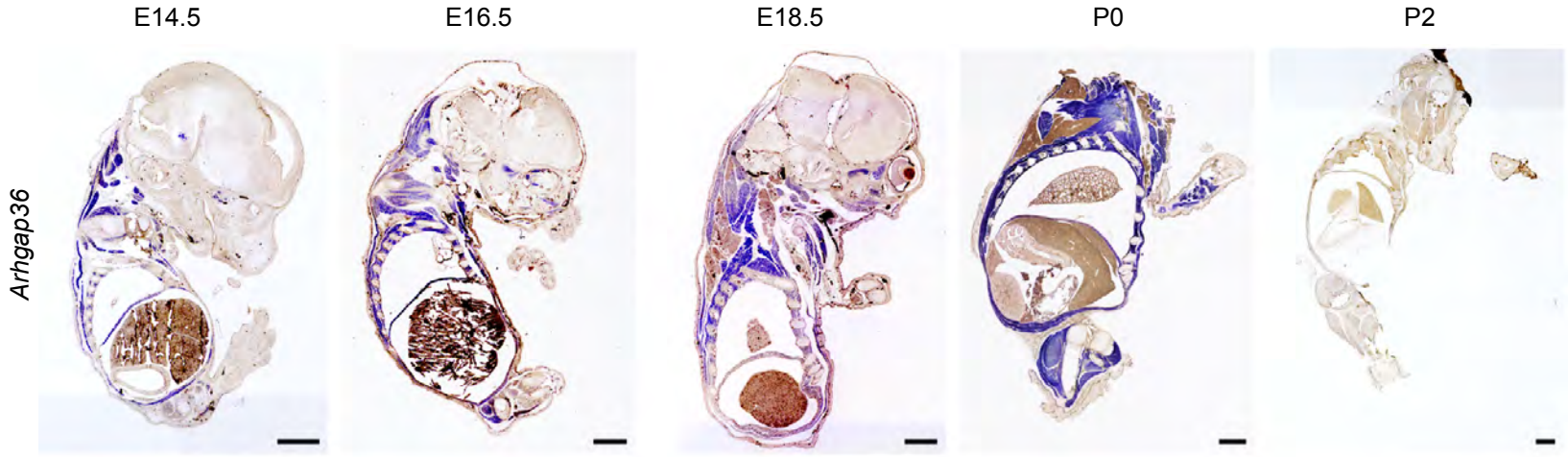

Figure 5.5 *Arhgap36* expression is developmentally regulated.
In situ hybridization using an *Arhgap36*-specific probe on wild-type mice at the indicated developmental stages. Blue indicates positive *Arhgap36* staining. Images are representative of the expression in at least three different embryos for each time point. Scale bars: 1 mm. **Figure contributed by Maciej Czajkowski (AG Rocks, MDC) and Nora Mecklenberg (AG Hammes, MDC).**

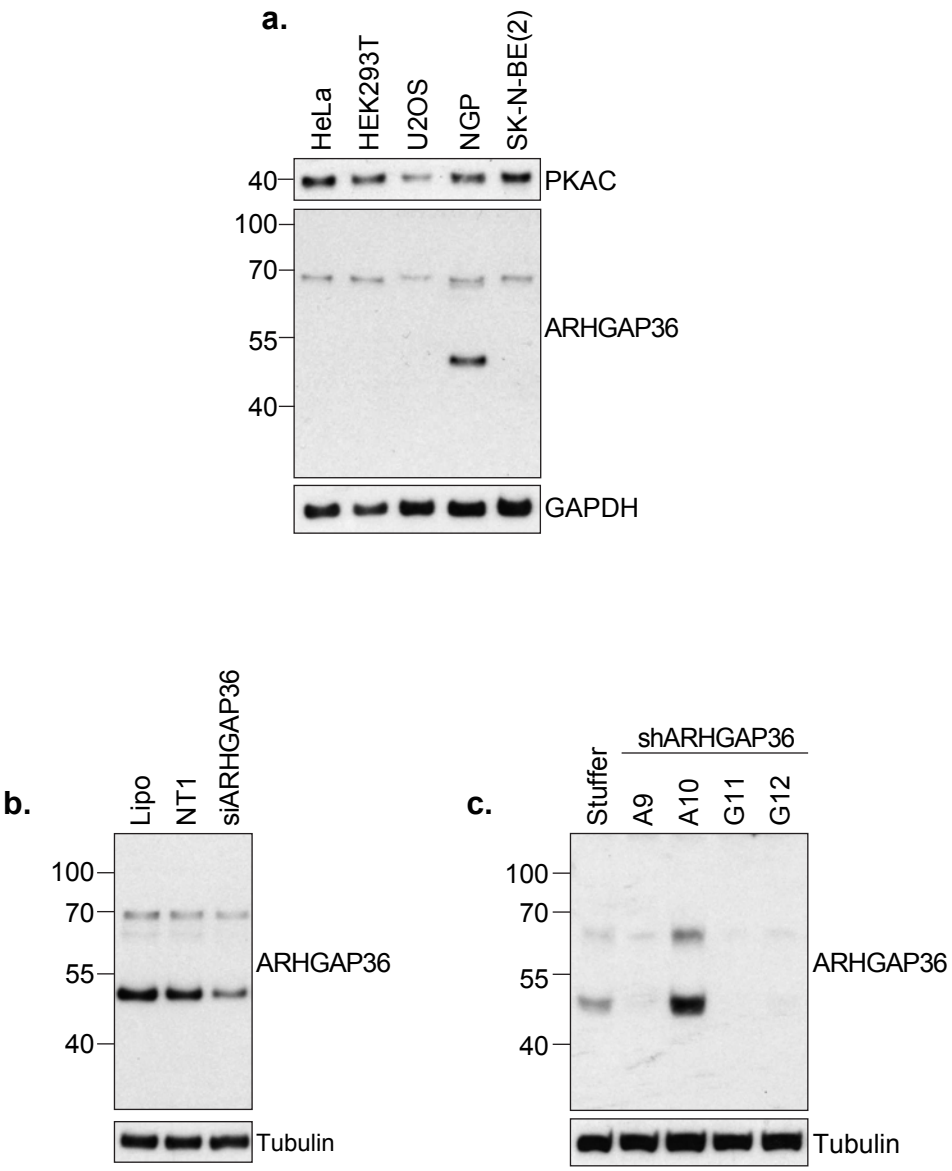

Figure 5.6 ARHGAP36 is expressed in neuroblastoma cells (**a**) 10 µg lysate of the indicated cell lines were immunoblotted with the indicated antibodies. A band at the right size, 46 kDa, corresponding to isoform 3 of ARHGAP36, was only obsereved in NGP cells. (**b**) ARHGAP36 was knocked down using an siRNA SMARTpool in NGP cells for 24 hours. Lipo: reagent only control, NT1: non-targeting oligo control. 10 µg lysate was immunoblotted with the indicated antibodies. (**c**) ARHGAP36 was stably knocked down in SK-N-BE(2) cells using lentiviral infection of shRNA. Stuffer: control. A9, A10, G11, G12: ARHGAP36 shRNA. 20 µg lysate was immunoblotted with the indicated antibodies. All blots representative of three similar experiments.

46 kDa. I therefore also attempted to knock down ARHGAP36 using siRNA in SK-N-BE(2) cells, however there was no obvious effect. I then set out to create stable ARHGAP36 knockdown cell lines using lentiviral infection of ARHGAP36 targeting shRNAs. Cells were infected with viruses one day after seeding, and the following day 2 µg/µl puromycin was added to select for cells which had integrated the viral plasmid. Cells were then expanded in the presence of puromycin. As a control I infected cells with a virus containing a random stuffer sequence as opposed to ARHGAP36 shRNA. These cells have therefore undergone the same procedure as ARHGAP36 knock down cells, namely viral infection, followed by puromycin selection. I could demonstrate knockdown of the 46 kDa band with 3 out of 4 ARHGAP36 shRNAs (Figure 5.6c). ARHGAP36 is thus also expressed in SK-N-BE(2) cells, albeit at much lower levels. I therefore focused on NGP cells to characterise the role of endogenous ARHGAP36.

5.2.6. ARHGAP36 and PKAC are expressed at equimolar levels in NGP cells

I next conducted a snapshot analysis of the NGP proteome with the help of Erik McShane (AG Selbach, MDC) and Patrick Beaudette (AG Dittmar, MDC). Intensity based absolute quantitation (iBAQ, Schwanhäusser *et al*, 2011) was used to compare protein levels of ARHGAP36 to PKAC and other components of the pathway. This technique divides the protein intensity, derived from the sum of all peptide intensities, by the number of theoretically observable peptides, derived from an *in silico* trypsin digest of the proteome. For absolute quantitation, protein standards must be spiked in at known amounts, to create a standard curve, however without this it is still possible to compare protein levels to one another. PKACα was the majorly expressed catalytic isoform, and was expressed in approximately equimolar levels to ARHGAP36 (Figure 5.7a). PKACβ was expressed at much lower levels such that the pooled total of catalytic subunits was approximately equal to ARHGAP36 (Figure 5.7b & c). ARHGAP36 is thus present at sufficiently high levels to theoretically form a 1:1 complex with PKAC.

The predominantly expressed R subunit was R1α, which was 3 fold more highly expressed than ARHGAP36. R2α was expressed at only slightly higher levels than ARHGAP36, whereas R2β was expressed at a much lower level. Finally, no peptides were detected for R1β. The sum total of PKAR subunits was 4.4 fold that of ARHGAP36 (Figure 5.7c). We did not detect PKI.

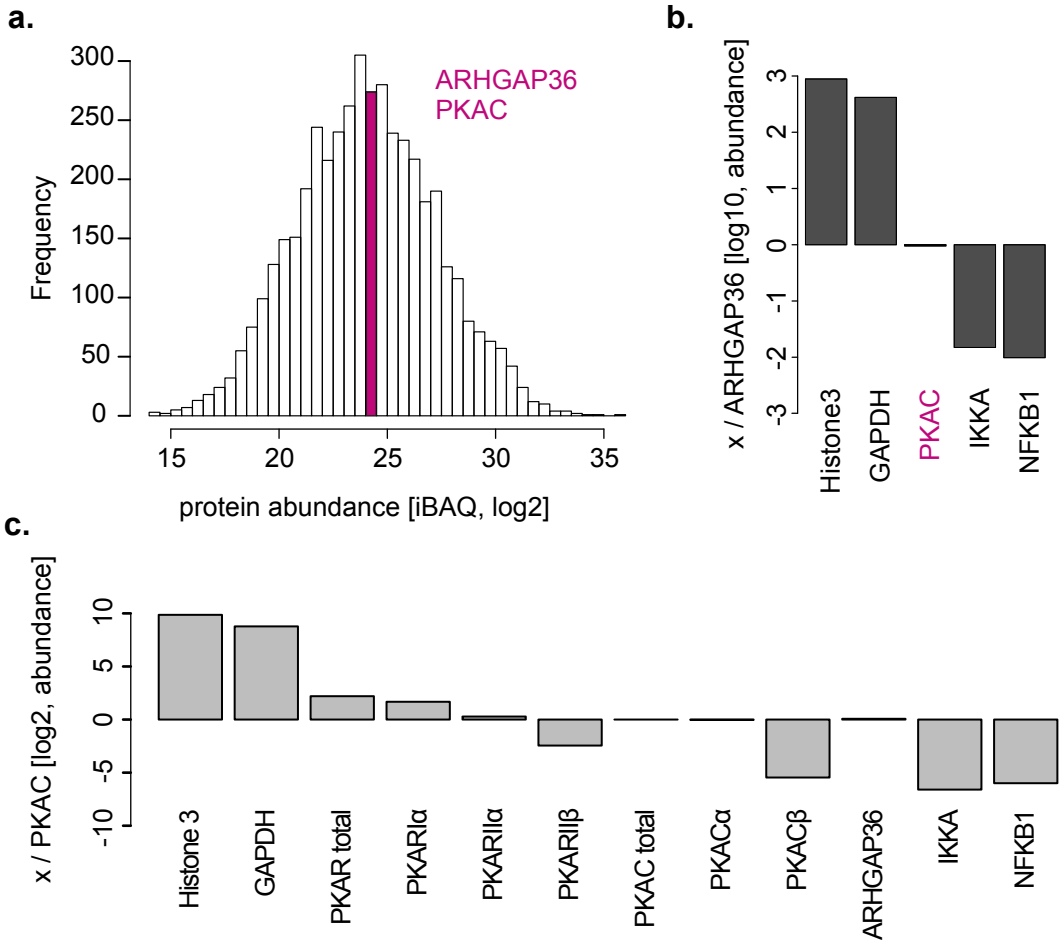

Figure 5.7 ARHGAP36 and PKAC are expressed at equimolar levels in NGP cells (**a**) Histogram displaying the distribution of the relative abundance of all measured proteins. ARHGAP36 and PKAC are found within the same bin (pink). (**b**) Bar plot of log 10 abundance of the indicated proteins relative to ARHGAP36. GAPDH and PKAC are expressed in a 437 fold and 0.95 fold abundance relative to ARHGAP36, respectively. PKAC is the summed total of PKACα and PKACβ. (**c**) Bar plot of log 2 abundance of the indicated proteins relative to PKAC total, the summed total of PKACα and PKACβ. PKAR is the summed total of RIα, RIIα and RIIβ. **Figures kindly provided by Erik McShane (AG Selbach, MDC).**

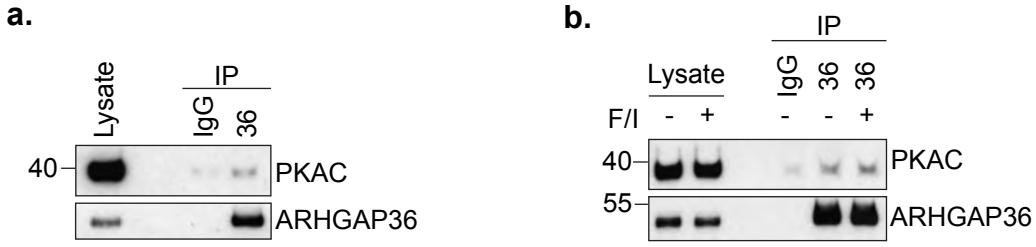

Figure 5.8 Endogenous PKAC interacts with endogenous ARHGAP36 (**a**) NGP cell lysates were immunoprecipitated with an ARHGAP36 antibody or an IgG rabbit control. Seperate gels were immunoblotted for ARHGAP36 or PKAC. 25% less lysate and eluate were run for ARHGAP36 than for PKAC. Blots representative of three similar experiments. (**b**) As in (a) except where indicated cells were stimulated for 30 min with 10 µM Forskolin and 100 µM IBMX (F/I).

5.2.7. Endogenous ARHGAP36 interacts with endogenous PKAC

After confirming the presence of ARHGAP36 and PKAC in NGP cells, the next step was to see if endogenous ARHGAP36 regulates endogenous PKAC in these cells. First I attempted to co-immunoprecipitate ARHGAP36 and PKAC. I supplemented my RIPA lysis buffer with ADP and $MgCl_2$ as nucleotide and metal ion presence was shown to be critical for pseudosubstrate binding to PKAC (Herberg & Taylor, 1993). 15 cm dishes of NGP cells were scraped directly in 500 µl RIPA buffer in order to concentrate lysates as much as possible. 4.5 mg NGP lysates were incubated first with 4 µg ARHGAP36 antibody or IgG rabbit control for one hour at 4 °C, before addition of beads for a further 30 min. I could pull down endogenous PKAC with endogenous ARHGAP36 (Figure 5.8a), proving that this interaction does happen at the endogenous level *in vivo*. Interestingly stimulation of cells with 10 µM Forskolin and 100 µM IBMX for 30 minutes prior to harvesting did not increase the amount of PKAC pulled down with ARHGAP36 (Figure 5.8b).

5.2.8. ARHGAP36 knockdown leads to an increase in PKAC protein levels and activity in NGP cells

I then wanted to see whether ARHGAP36 knock down had an effect on PKAC stability or activity. I knocked down ARHGAP36 for 24 hours and stimulated cells with 10 µM Forskolin and 100 µM IBMX for 30 minutes prior to harvesting directly in RIPA. Lysis buffer was supplemented with phosSTOP to specifically inhibit cellular phosphatases and ensure any effects on phosphorylation were captured. Knock down of ARHGAP36 led to a reproducible and significant increase in PKAC levels (37%) and also activity, as seen by an increase in pCREB levels (78%) (Figure 5.9a). ARHGAP36 knock down and similar, albeit overall weaker effects on PKAC and p-CREB levels could also be seen when deconvoluting the SMARTpool into individual oligos (Figure 5.9b). Out of the 4 oligos (9-12), oligo 11 was clearly not as effective at knocking down ARHGAP36, and thus had a lesser effect on PKAC and p-CREB. The extent of ARHGAP36 knockdown negatively correlates with PKAC and p-CREB levels, as determined by the Pearson's sample correlation coefficient. I also created NGP cell lines with stable knock down of ARHGAP36 using lentiviral infection of shRNA, as for SK-N-BE(2). Using these cells I could further show a reproducible and significant increase in CREB phosphorylation upon knockdown, even in the absence of stimulus, with two different viruses (Figure 5.9c 68% and 107%). However, I did not see a clear effect on PKAC levels, which may be accounted for by compensatory mechanisms in the stable cell line setting. As

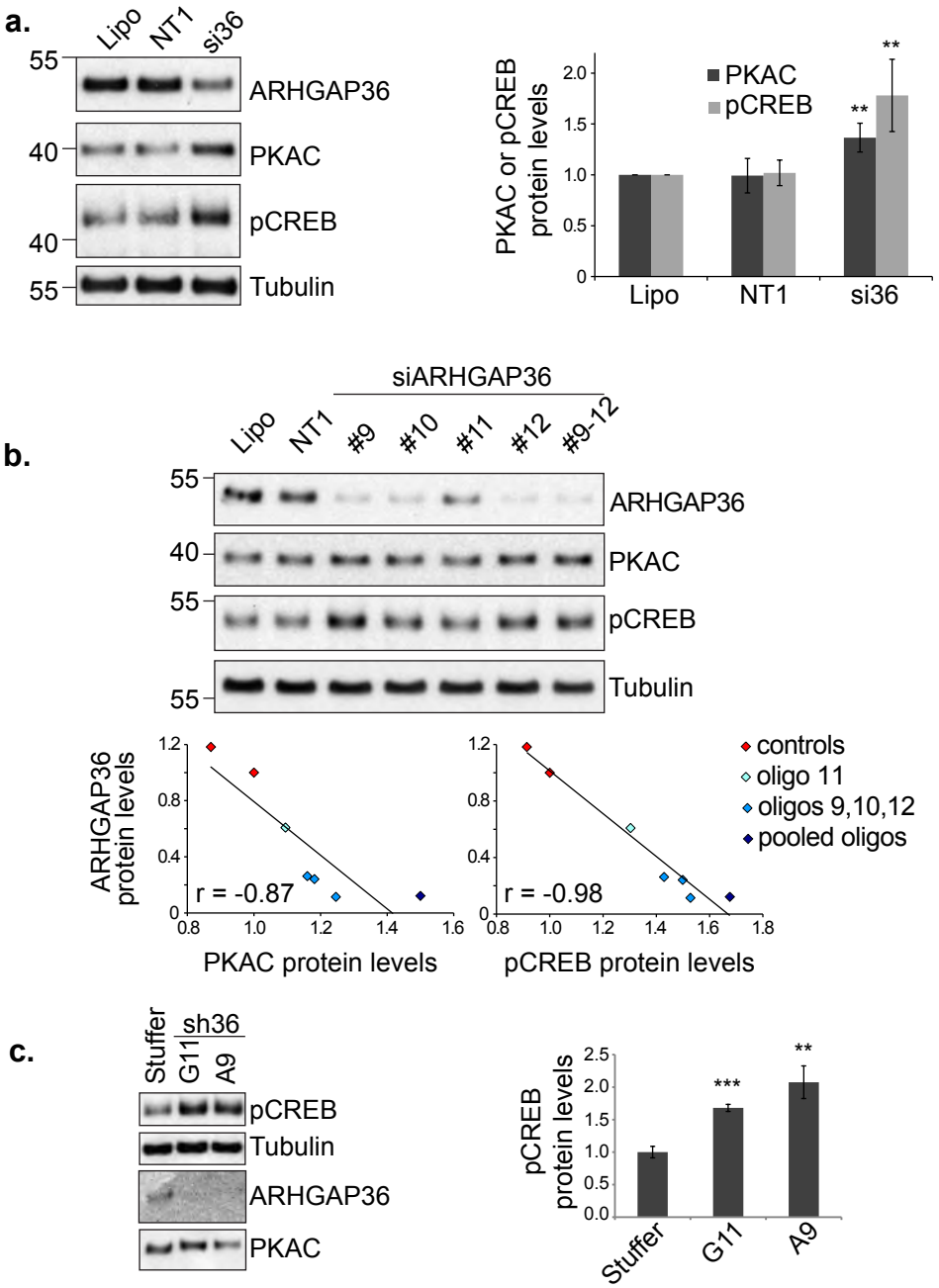

Figure 5.9 ARHGAP36 antagonises PKAC in an endogenous setting (**a**) NGP cells were treated with an siRNA SMARTpool against ARHGAP36 for 24 hours. Cells were stimulated with 10 µM Forskolin and 100 µM IBMX before harvesting. Lysates were immunoblotted with the indicated antibodies. Lipo: reagent only control. NT1: non-targeting oligo control. Bands were densitometrically evaluated, normalised first to tubulin then to Lipo. Mean of five independent experiments +/- s.d. ** p<0.01 compared to NT1. (**b**) As in (a) except cells were treated with both individual and pooled oligos against ARHGAP36. Bands were densitometrically evaluated, normalised first to tubulin then to NT1. Scatter plot shows pCREB or PKAC values plotted against ARHGAP36 values. Linear regression analysis indicates a negatively correlated distribution (Pearson's sample correlation coefficient, PKAC: r = -0.87, pCREB: r = -0.98). (**c**) ARHGAP36 was stably knocked down in NGP cells using lentiviral infection of shRNA. Stuffer: control. A9, G11: ARHGAP36 shRNA. Lysates were immunoblotted with the indicated antibodies. Bands were densitometrically evaluated, normalised first to tubulin then to Stuffer. Mean of three independent experiments +/- s.d. ** p<0.01 or *** p<0.001 compared to Stuffer.

discussed in Chapter 4, manipulation of PKAC or PKAR levels commonly leads to a corresponding increase or decrease in the other protein (Steinberg & Agard, 1981a, 1981b; Uhler & McKnight, 1987).

5.2.9. ARHGAP36 and PKAC expression levels are negatively correlated in NGP cells

Immunofluorescence of wild-type NGP cells showed that endogenous ARHGAP36 localised like the overexpressed protein, to the plasma membrane, and also some vesicular structures (Figure 5.10a). Upon siRNA knockdown of ARHGAP36, this antibody staining was partially reduced, confirming specificity of the ARHGAP36 antibody also for immunofluorescence. At steady state however, ARHGAP36 expression appeared to be heterogeneous in this non-clonal cell line, with protein levels varying dramatically from cell to cell. Interestingly where ARHGAP36 levels where high, PKAC levels were low (Figure 5.10b). Together with Markus Müller (AG Rocks, MDC) I was able to quantify this effect, by utilising cell tracker (Molecular Probes), a dye that can freely pass into cells, but once taken up is converted into a product that can no longer escape. This allowed individual cells to be segmented and their levels of ARHGAP36 and PKAC quantitated. The ratio of PKAC to ARHGAP36 could then be represented (Figure 5.10b pseudo-coloured image). The levels of ARHGAP36 and PKAC were plotted against each other and showed a negative correlation (Figure 5.10b scatter plot, Pearson's coefficient: -0.296). By immunofluorescence microscopy, SK-N-BE(2) cells also appeared to have heterogeneous ARHGAP36 expression levels. However the majority of cells showed just background nuclear staining. A very small number of cells exhibited a significant ARHGAP36 signal (less than 1%), which was associated predominantly with vesicles and accumulated on structures in the perinuclear region (Figure 5.11).

5.2.10. ARHGAP36 and PKAC colocalise inside Rab5QL vesicles

We could not see any convincing colocalisation between endogenous ARHGAP36 and PKAC. This is not surprising as the two proteins show negative correlation and I have shown that ARHGAP36 causes the efficient degradation of interacting PKAC. I thus overexpressed GFP-Rab5-Q79L, in order to induce enlarged endosomes and hopefully trap some PKAC before it is degraded. I could indeed see endogenous PKAC inside these enlarged endosomes, colocalising together with ARHGAP36 (Figure 5.12). I had expected to perhaps see ARHGAP36 only on the outer membrane of Rab5-QL in endosomes, however some ARHGAP36 was also present

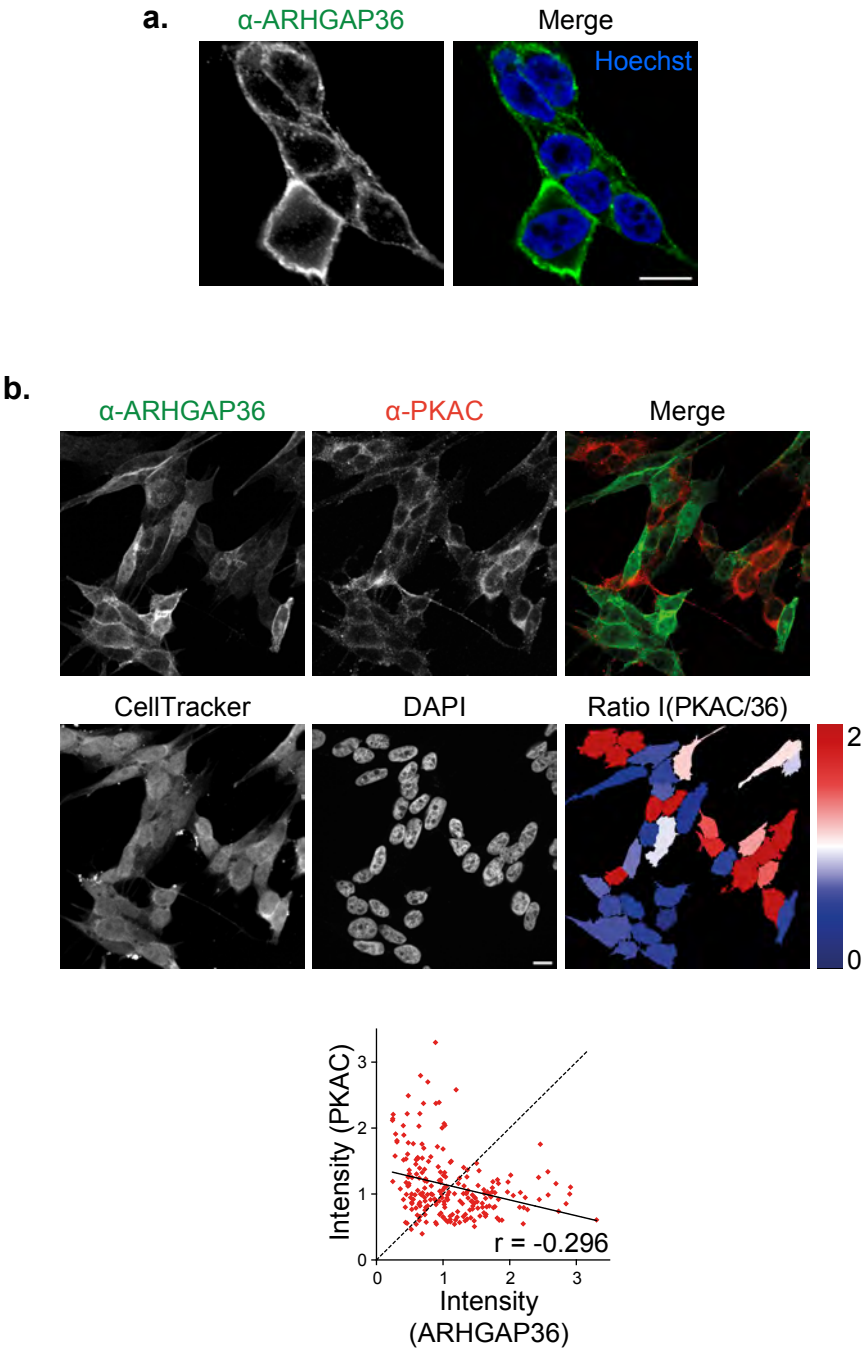

Figure 5.10 ARHGAP36 and PKAC levels are negatively correlated in NGP cells (**a**) Confocal micrographs of NGP cells subjected to immunofluorescence using an antibody against ARHGAP36. Scale bar: 10 µm. (**b**) Confocal micrographs of Cell Tracker Deep Red treated NGP cells that were subjected to immunofluorescence using antibodies against ARHGAP36 and PKAC. Images representative of three similar experiments. Cells were segmented and the ratio of average PKAC over ARHGAP36 fluorescence intensity of single cells is shown in the pseudocolour image. Scale bar: 10 µm. The scatterplot shows the normalised single cell average intensity of PKAC plotted against ARHGAP36 (red dots, n=225 cells). Linear regression analysis (continuous line) indicates a negatively correlated distribution (Pearson's sample correlation coefficient r = -0.296). Dashed line indicates theoretical maximal positive correlation (r = 1). Image analysis was performed with the help of Markus Müller.

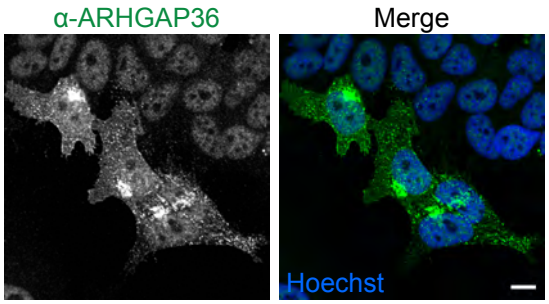

Figure 5.11 ARHGAP36 levels are heterogeneous in SK-N-BE(2) cells Confocal micrographs of SK-N-BE(2) cells subjected to immunofluorescence using an antibody against ARHGAP36. Scale bar: 10 μm.

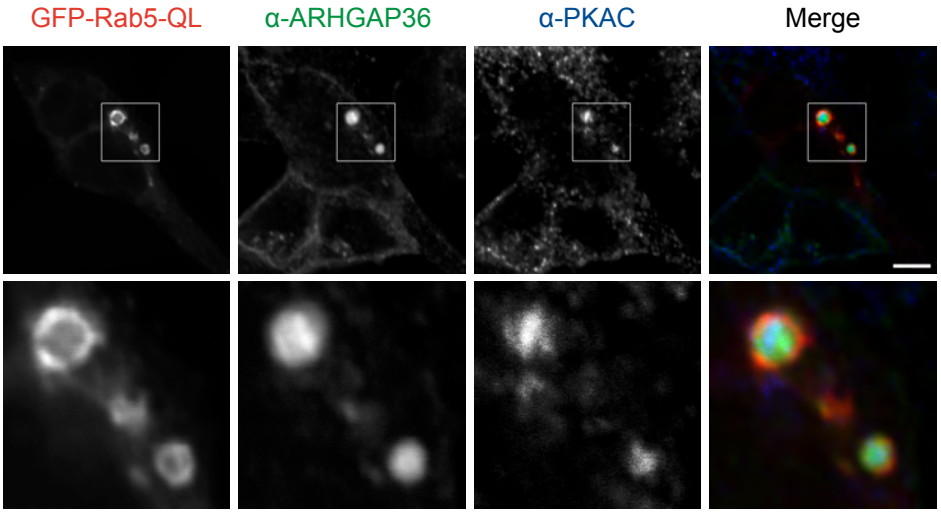

Figure 5.12 ARHGAP36 and PKAC colocalise inside Rab5-QL induced vesicles. Confocal micrographs of NGP cells transfected with GFP-Rab5-QL. Cells were fixed and subjected to immunofluorescence using antibodies against GFP, ARHGAP36 and PKAC. Images representative of three similar experiments. Scale bar: 5 μm

inside. In Chapter 4 I had already observed overexpressed ARHGAP36 inside these enlarged endosomes together with endogenous PKAC. However whereas PKAC was only localised inside, ARHGAP36 was still present on the outer membrane of the vesicles, as well as elsewhere in the cell (Figure 4.7). CHX chase experiments had also shown that overexpressed ARHGAP36 protein levels do not change with CHX treatment, in the same time that overexpressed PKAC is efficiently degraded (Figure 4.10d). It would be interesting to repeat the CHX chase experiments in NGP cells looking at both endogenous ARHGAP36 and PKAC. This would help to establish whether a subpopulation of ARHGAP36 is degraded together with PKAC. A precedence for this has already been discussed above with respect to the E3 ligase Cbl and the ESCRT-I component Tsg101 which become internalised into MVBs together with cargo (de Melker *et al*, 2001; Malerød *et al*, 2011).

5.3. Discussion

Main Chapter Findings

- ARHGAP36 suppresses PKA signalling
- ARHGAP36 expression is tissue specific and developmentally regulated
- ARHGAP36 is expressed in neuroblastoma cell lines
- Endogenous ARHGAP36 controls endogenous PKAC activity and stability

5.3.1. ARHGAP36 supresses a wide range of PKA signalling responses

I have shown that PKA signalling responses are suppressed in the presence of ARHGAP36. CREB is the main mediator of the PKA transcriptional response, and is ubiquitously expressed. AQP2 trafficking is a more specific process that takes place in the collecting duct cells of the kidney. I have also described in Chapter 3 how Hedgehog signalling is activated in the presence of ARHGAP36, as PKA is a negative master regulator of this pathway. ARHGAP36 can thus oppose PKA signalling in a wide variety of contexts. These are just three examples, however I hypothesise that ARHGAP36 could antagonise PKAC wherever it is expressed.

5.3.2. Arhgap36 expression is developmentally regulated

We found that *Arhgap36* is regulated during development and specifically found in embryonic skeletal muscle. Previous work also indicated developmental regulation of Arhgap36. Rack and colleagues assayed whole embryos at E7, E10, E15 and E17, and found increasing *Arhgap36* mRNA levels throughout the developmental

stages. When looking at specific adult tissues they also observed no expression except in the spinal cord and to a lesser extent the brain.

5.3.3. ARHGAP36 in skeletal muscle

Myogenesis involves specification of embryonic precursors into myoblasts, which then differentiate and finally fuse into multinucleate myotubes. This process is controlled by four transcription factors. Three of the four, MyoD, Myf5 and Myr4 are determination factors, whereas Myogenin is a differentiation factor (Buckingham & Rigby, 2014). Myogenin thus controls the conversion of myoblasts into myofibres.

A study comparing differences in wild-type versus myogenin knock-out mice, found that Arhgap36 expression is massively reduced in the absence of this transcription factor (Davie *et al*, 2007). In fact Arhgap36 was one of the most downregulated genes in the entire screen. They could further confirm that Arhgap36, at the time only known as RIKEN1100001E04, was expressed in the same fibres as myogenin in the tongue of embryonic wild-type mice. They could also show myogenin and MyoD bound to the *Arhgap36* sequence upstream of the transcription initiation site. They further hypothesised the presence of another possible binding site within the first intron.

We carried out preliminary experiments to see if *Arhgap36* expression is reinitiated upon injury. Together with the lab of Simone Spuler (ECRC, Berlin) we tried regeneration experiments, where adult mouse *tibialis anterior* muscle was injected with cholera toxin, or DMSO as a control, in order to wound the muscle and initiate the wound-healing program. *Arhgap36* presence was assessed by *in situ* hybridisation 3, 6 and 12 days after injection. We saw no upregulation of *Arhgap36* upon wound healing and muscle regeneration. This is surprising as the same gene program controls the activation of satellite cells and their differentiation into new muscle fibres (Montarras *et al*, 2013). ARHGAP36 can be found repeatedly upregulated in biopsies obtained from myopathy patients or probands after muscle exercise (NCBI GEO profiles). It will be interesting to reassess the role of ARHGAP36 in muscle regeneration in future gene-targeting studies.

5.3.4. ARHGAP36 in neuroblastoma

Neuroblastoma is a rare childhood cancer of neuroendocrine origin. It is an extremely heterogenous disease, with diverse outcomes: tumours can metastasise

or even spontaneously regress (Cheung & Dyer, 2013). It is thus thought that many cases are never even detected (Brodeur & Bagatell, 2014). It is derived from neural crest cells, and is mostly diagnosed associated with the adrenal gland. Approximately 22% of tumours have amplified MYCN and 8-10% ALK1, but apart from this there is a lack of candidates for targeted treatment.

Neuroblastoma cell lines are known to contain heterogenous cell populations (Thiele, 1998). This is thought to be due to the fact that the tumours originally derive from multi-potent neural crest progenitors. Cells were characterised as having mainly neuronal or melanocytic properties, two neural crest derivative cell types. Some studies have aimed to isolate these different cell types from mixed populations, however these cells have been shown to have the capacity to spontaneously differentiate and change phenotype (Biedler *et al*, 1978; Ciccarone *et al*, 1989). It could be of interest to characterize the properties of cells with high ARHGAP36 levels, to determine if they are more neuronal or have properties of other neural crest cell derivatives.

NGP cells were isolated from the lung after treatment, but the original site of the tumour was unknown (Brodeur & Goldstein, 1976). The SK-N-BE(2) line was isolated from bone marrow after treatment, its original site is also unknown. Interestingly another cell line, SK-N-BE(1), was isolated from the same patient just 5 months earlier before treatment (Biedler *et al*, 1978). It would be interesting to compare the number of ARHGAP36 expressing cells in these two lines. A number of these paired lines exist.

ARHGAP36 was identified as an interactor of CLN5 in a mass spectrometry screen in SH-SY5Y cells (Scifo *et al*, 2013). These cells are a neuronal type subclone of the SKNSH neuroblastoma cell line. CLN5 (ceroid lipofuscinosis neuronal protein 5) is a lysosomal protein that has been implicated in endocytic sorting (Mamo *et al*, 2012). CLN5 mutations lead to a variant of neuronal ceroid lipoduscinoses (NCL) (Savukoski *et al*, 1998). Most of these mutations were found to abolish the lysosomal localisation of CLN5 (Isosomppi *et al*, 2002; Schmiedt *et al*, 2010). As ARHGAP36 mediates the endolysosomal degradation of PKAC in neuroblastoma cells, this interaction is of particular interest.

5.3.5. Competitive binding?

We previously hypothesised that ARHGAP36 binds PKAC in the same manner as PKI and thus would not be able to compete for PKAC binding in the holoenzyme setting. In this case one would expect to see increased binding between ARHGAP36 and PKAC upon pathway activation, when PKAC is released by PKAR. However, this was not the case. Stimulation of NGP cells with forskolin did not increase the interaction (Figure 5.8). It could be that PKA activity in these cells is uncoupled from cAMP. Indeed, in initial western blotting experiments, stimulation did not lead to a major increase in phosphorylation of substrates compared to basal levels. However, another possibility is that ARHGAP36 could compete with PKAR for binding. ARHGAP36 could potentially bind to the holoenzyme via an alternate site in order to displace PKAR and facilitate pseudosubstrate binding. In this case binding may be independent of cellular cAMP levels. Further experiments would be required to determine if ARHGAP36 has the potential to bind PKAR. The ARHGAP36-RRV pseudosubstrate mutant that no longer binds PKAC will be useful in establishing this.

5.3.6. Bimodal antagonism

It is hard to dissect the inhibitory and degradative properties of ARHGAP36, as one leads to the other, and if PKA is absent it obviously cannot be active. However, I could see that expression of ARHGAP36-36i, which contains the pseudosubstrate domain but cannot trigger PKAC degradation, was sufficient to inhibit CREB activation. In NGP cells I saw an increase in PKAC protein levels upon ARHGAP36 knock down, arguing that ARHGAP36 also mediates PKAC degradation here. It would be interesting to knock down the E3 ligases identified in the interactome in NGP cells and assess if PKAC protein levels are affected. Our mass spectrometry data demonstrated that Stub1 and Huwe1 are indeed expressed in NGP cells, however Praja2, a supposedly neuronal specific gene, was not detected and thus is not within the top 4518 abundantly expressed proteins.

It is of course possible that the degradative properties of ARHGAP36 could be uncoupled from PKAC inhibition dependent on the cell-type or the signalling state of the cell. In response to low levels of EGF stimulus, EGFR is thought to be mostly recycled back to the plasma membrane, whereas in response to high levels of EGF it is degraded in the lysosome (Sigismund *et al*, 2008). The same principle could apply for ARHGAP36 regulation of PKAC. Pseudosubstrate binding alone could

mediate short-term inhibition in response to low-level stimulus, whereas degradation may only take place upon high level or repetitive exposure to stimulus. In general, degradation could be responsible for a tonic suppression of the pathway, whereas pseudosubstrate binding alone may mediate acute reversible inhibition.

Chapter 6. Discussion

6.1. Summary

In this thesis I have shown that ARHGAP36 binds the PKA catalytic subunit directly and inhibits it via a pseudosubstrate motif. Furthermore, ARHGAP36 binding leads to depletion of PKAC levels. ARHGAP36 mediates K63 linked polyubiquitylation of PKAC at a single site, K285. Unexpectedly for a cytosolic protein PKAC is then degraded via the endolysosomal system in a Vps4 dependent manner. ARHGAP36 can thus drastically suppress PKA signalling in a wide variety of settings. With such a striking effect on a ubiquitous pathway it is not surprising that ARHGAP36 expression is extremely restricted. I observed it only in embryonic skeletal muscles. It is, however, upregulated in neuroblastoma cells, where I could show that it modulates PKAC activity and stability in an endogenous setting.

6.2. Open Mechanistic Questions

I will discuss here some of the outstanding questions from my work. One of the key points raised throughout these sections is how the interaction between ARHGAP36 and PKAC is regulated.

6.2.1. Why is PKAC not degraded by the proteasome?

PKAC degradation is mediated via the endolysosomal pathway, and not by the proteasome which is unusual for a cytosolic protein. It is possible that PKAC is not amenable to unfolding by the AAA-ATPases of the proteasomal regulatory particle, which is a prerequisite for entry into the core particle and thus degradation (Finley *et al*, 2016). Interestingly, PKAC has been implicated in phosphorylation of regulatory particle proteasomal subunits, which leads to enhanced proteasome activity (Zhang *et al*, 2007; Lokireddy *et al*, 2015). PKAC may thus be unsusceptible to proteasomal degradation in order to allow it to phosphorylate proteasomal subunits and stimulate their activity without itself being degraded. I found that PKAC is decorated with K63 linked chains. As well as mediating endolysosomal trafficking, this may ensure it is not degraded by the proteasome. All the DUBs associated with the proteasome have the ability to cleave K63 linked chains, and thus rescue substrates from degradation (Jacobson *et al*, 2009). Endosomal ubiquitin receptor binding of K63-linked chains has also been argued to block proteins modified with this linkage from proteasomal ubiquitin receptor binding and thus shield them from proteasomal degradation (Nathan *et al*, 2013).

In contrast to PKAC, PKAR is degraded by the proteasome. In the regulation of synaptic plasticity, PKAR degradation facilitates an alteration in the R/C ratio and thus an increase in PKAC activity (Greenberg *et al*, 1987; Sweatt & Kandel, 1989). The spatial separation of PKAR and PKAC degradation may be important in such mechanisms, by ensuring that PKAC is not co-degraded. Endolysosomal degradation of PKAC could also be a mechanism to degrade only the fraction of cellular PKAC that is localised together with ARHGAP36 at the plasma membrane or on endosomes. This could help to further compartmentalise PKA signalling responses, and ensure timely inactivation of PKAC in this context. This would also ensure that inactivation and degradation of PKA in one part of the cell, does not lead to a loss of activity at other subcellular localisations.

6.2.2. Lysosomal degradation of cytosolic kinases: a more general mechanism?

Other cytosolic kinases are also known to be degraded by the lysosome, however they take different routes to reach this destination. PKAC is trafficked along the endocytic pathway before arriving at the lysosome. In contrast, Src and Ret, both non-receptor tyrosine kinases, have been shown to be sequestered into autophagosomes which then fuse with lysosomes (Sandilands *et al*, 2011, 2012). This has so far been shown to be ubiquitin independent. This process occurs in response to the loss of their binding partner focal adhesion kinase (FAK), a signalling hub at focal adhesions, which would normally anchor them there. Autophagy of Src and Ret is thought to be a mechanism that promotes cancer cell survival by allowing cells to cope with FAK loss and the subsequent increase in these untethered kinases. This has been termed ‘signalophagy’: autophagy of signalling proteins (Khaminets *et al*, 2016). The identification here that PKAC is also degraded in the lysosome, albeit in a process that depends on ubiquitin and the ESCRT-machinery, may suggest that lysosomal degradation of cytosolic signalling proteins is a more general way to achieve long-term signal termination. This is a well-established mechanism for transmembrane receptor tyrosine kinases, such as the Epidermal Growth Factor Receptor (EGFR) (Lu & Hunter, 2009; Liu *et al*, 2012). Like PKAC, GSK3β is also sequestered by the endosomal pathway into MVBs, although it is not thought to be subsequently degraded (Taelman *et al*, 2010). However, this still results in protection of cytosolic substrates from GSK3β phosphorylation.

6.2.3. What are the roles of the uncharacterised regions of ARHGAP36?

Just 25 amino acids were required for pseudosubstrate inhibition of PKAC (36i), and 77 amino acids for its degradation (ARHGAP36-N2). I have therefore only characterised the function of a small part of ARHGAP36. It will be interesting to find out what the rest of the protein contributes. In this respect the GAP domain is particularly interesting as it may still mediate binding to Rho proteins, even if it is catalytically inactive, and thus serve to integrate Rho and PKA signalling pathways. The Rho GAP family protein OCRL contains a catalytically inactive GAP domain, but still binds to Rac1 and Cdc42, and is rather thought to act as a Rho effector protein (Faucherre *et al*, 2003; Mehta *et al*, 2014). It is possible that binding of ARHGAP36 to Rho-family members either blocks or stimulates PKAC binding, thus adding another layer of regulation to the interaction.

6.2.4. Can ARHGAP36 compete with PKAR for PKAC binding?

It still needs to be determined if ARHGAP36 can compete with PKAR for binding to PKAC, or whether it merely binds to free PKAC in the same manner as PKI. Another part of ARHGAP36 may be involved in binding to PKAR and mediate its displacement from the PKAC catalytic site. If ARHGAP36 cannot compete with PKAR for PKAC binding, then inhibition and degradation is thus coupled to cAMP levels, as PKAC is only released from PKAR upon cAMP binding. This would constitute another incidence where activation of a kinase is coupled to its degradation (Lu & Hunter, 2009; Liu *et al*, 2012). It would be interesting to see if ARHGAP36 itself is reactive to other cellular stimuli.

6.2.5. Which E3 ligase mediates PKAC ubiquitylation, and is recruitment and thus degradation regulated?

This is the first description of ubiquitin-mediated degradation of PKAC. The E3 ligase mediating PKAC ubiquitylation has still to be identified. As there are over 600 E3 ligases, this will be a daunting task. ARHGAP36 interacts with multiple E3 ligases, that were identified in an unbiased fashion, however I have so far not obtained any evidence that Praja2, Stub1 or Huwe1 are involved in the degradation of PKAC. Perhaps ARHGAP36 recruitment of an E3 ligase is also regulated, such that ubiquitylation and degradation of PKAC is only initiated upon high or repeated exposure to stimulus. There is already precedence for such degradation of PKAC in the literature. Constant stimulation of thyroid follicular cells, growth-hormone producing pituitary cells and porcine kidney cells all led to an eventual decrease in

PKAC protein levels (Hemmings, 1986; Armstrong *et al*, 1995; Richardson *et al*, 1990a). ARHGAP36 could thus be involved in a hormone-induced refractory period. Alternatively this could occur in a constitutive manner, to completely suppress PKA signalling wherever ARHGAP36 is expressed. The inhibitory and degradative properties of ARHAGP36 may be differentially regulated, and possibly segregated, dependent on the cell type.

6.3. Physiological Relevance and future perspectives

6.3.1. ARHGAP36 and the cAMP-PKA axis during development

6.3.1.1. PKA in Myogenesis

A role for PKA has been implicated at multiple stages of myogenesis (Knight & Kothary, 2011). It was found that PKA phosphorylation of CREB, stimulated by non-canonical Wnt signalling, led to the initial expression of the myogenic transcription factors (Chen *et al*, 2005). It is not clear whether this is direct, however Myf5 contains a CRE element, as does Pax3, a transcription factor further upstream of the myogenic programme. ARHGAP36 expression is under the control of myogenic transcription factors (Davie *et al*, 2007). PKA activity itself may thus indirectly lead to ARHGAP36 expression. The interplay of Shh and Wnt signals regulates the specification of the dermomyotome, which gives rise to the myotome and myogenic progenitors, from the somites. Wnt regulation of PKA signalling thus provides a mechanism of how Wnt could also antagonize Shh signalling (Pourquié, 2005).

Later in myogenesis the role of PKA in differentiation of myoblasts is unclear, with some studies claiming it inhibits myoblast fusion and others claiming it enhances it (Winter *et al*, 1993; Mukai & Hashimoto, 2008; Knight & Kothary, 2011). cAMP levels are thought to drop dramatically after myoblast fusion (Siow *et al*, 2002). Older studies focused mainly on CREB activation and transcription downstream of PKAC, however it is now becoming apparent that PKAC has many different roles throughout the cell. It is thus conceivable that PKA may have differential activities within the same cell. PKAC is clearly dynamically regulated throughout myogenesis. It will be interesting to explore exactly how ARHGAP36 contributes to its activity profile during muscle development.

It has also been hypothesised that PKAC and PKAR levels and lifetimes vary between myoblasts and myotubes. PKAC is supposedly longer lived in myoblasts than myotubes, whereas for PKAR it is the opposite (Lorimer *et al*, 1987; Lorimer & Sanwal, 1989). The lifetimes of both subunits decrease in myoblasts upon cAMP stimulation. It will be extremely interesting to explore the role of ARHGAP36 in regulating PKAC stability throughout myogenesis.

6.3.1.2. Dissecting the role and cellular localisation of ARHGAP36 in development

The restricted embryonic expression of ARHGAP36 made it extremely difficult to investigate the role of endogenous ARHGAP36. The generation of knock-out (KO) mice will facilitate this. Cell lines derived from Arhgap36 KO mice will allow the comparison of PKAC activity, levels and turnover between KO and wild-type cells. Analysing the phenotypes of Arhgap36 mutant mice will also facilitate pinpointing when and where Arhgap36 expression is important in myogenesis. The plan is to generate and assess both skeletal muscle specific and complete knockouts.

Non-myogenic associated phenotypes of the complete KO will also help to ascertain whether Arhgap36 is expressed in further discrete tissues that I may have missed thus far. We are also developing antibodies to recognise mouse Arhgap36 for this purpose. This will allow us to assess the specific subcellular localisation of Arhgap36 wherever it is expressed. Ultimately, these approaches will help to establish whether Arhgap36 acts in a local or global manner to inhibit and degrade PKAC.

I described in Chapter 3 that ARHGAP36 can localise to the primary cilium (Figure 3.4 & 5). It will be interesting to see if this is the case during muscle development. It was recently shown that primary cilia are dynamically regulated during myogenesis (Fu *et al*, 2014). Interfering with cilia formation inhibits myogenic differentiation and instead promotes proliferation. Fu and colleagues also showed that these cilia contribute to Hh signalling in myoblasts. Cell lines derived from Arhgap36 KO mice will allow us to assess whether Arhgap36 plays a role in cilia formation and maintenance. We will also be able to explore whether Arhgap36 enables Hh signalling via PKAC inhibition in this context. PKAC is generally thought to be localised at the basal body (Tuson *et al*, 2011), however it was recently detected within the cilium itself (Mick *et al*, 2015). Furthermore, overexpression of a cilia-

targeted PKI caused a reduction in Gli3 repressor processing, indicating a role for PKAC within the cilium (Mick *et al*, 2015). As ARHGAP36 can localise to the cilium independently, it could be a physiological and dynamic regulator of PKAC within cilia.

Maciej Czajkowski (AG Rocks, MDC) has already started to generate complete KO mice. So far only heterozygous females have been born, suggesting that deletion in males of the one and only copy of *Arhgap36*, encoded on the X-chromosome, is embryonically lethal.

6.3.2. ARHGAP36 and the cAMP-PKA axis in oncogenesis

6.3.2.1. ARHGAP36 upregulation in cancer

ARHGAP36 is upregulated in neuroblastoma (nextbio.com) and was identified as part of a neuroblastoma signature (Lee *et al*, 2014). I could show in Chapter 5 that ARHGAP36 is expressed in neuroblastoma cells, and it can modulate both PKAC activity and stability in an endogenous setting. ARHGAP36 has also very recently been shown to be upregulated in pheochromocytoma (Croisé *et al*, 2016). This tumour arises from the chromaffin cells of the adrenal medulla. It is interestingly also of neural crest origin, and has similarities to neuroblastoma in its genetic landscape (Castro-Vega *et al*, 2016). It will be interesting to see if ARHGAP36 is also upregulated in other cancers of neural crest origin, such as melanoma, glioma and glioblastoma. As described in Chapter 3, ARHGAP36 was also found upregulated in a subset of medullablastoma.

6.3.2.2. The diverse roles of PKAC in cancer

As in normal physiology, PKAC plays complicated and sometimes seemingly opposing roles in cancer biology. PKAC has been identified as both an oncogene and tumour suppressor in a variety of malignancies (Sapio *et al*, 2014).

Much attention has been given recently to the discovery that activating mutations of PKAC result in tumours of the adrenal cortex leading to Cushing's syndrome (Beuschlein *et al*, 2014; Cao *et al*, 2014; Goh *et al*, 2014; Sato *et al*, 2014). These mutations are thought to inhibit PKAR binding. A fusion protein of PKAC has also been described in fibrolamellar hepatocellular carcinoma (FL-HCC) (Honeyman *et al*, 2014). PKAC is fused to the C-terminus of the molecular chaperone DNAJB1.

PKAC retains kinase activity and is overproduced under the control of the DNAJB1 promoter. In both cases signalling is thus uncontrolled. There were conflicting reports on whether the DNAJB1-PKAC fusion also retained PKAR binding (Honeyman *et al*, 2014; Cheung *et al*, 2015). It would be interesting to see if these mutant proteins can still bind ARHGAP36, as Cao and colleagues claimed PKI could still inhibit activity of the PKAC Leu206 mutant. Peptides based on ARHGAP36 may be an option for targeted therapy to inhibit this mutant PKAC.

GPCR coupled $G\alpha_S$ signalling through PKA is thought to be tumour suppressive in medulloblastoma (He *et al*, 2014). This supports our hypothesis that the reason ARHGAP36 is upregulated in medulloblastoma is that it oncogenically activates Hedgehog signalling via inhibition of PKAC.

The $G\alpha_S$-PKA axis is also thought to act as a tumour suppressor pathway in basal-cell carcinoma (Iglesias-Bartolome *et al*, 2015). It was even shown that PKI is oncogenic in this context: transgenic mice expressing PKI in the epidermis rapidly develop skin lesions. We would thus expect ARHGAP36 to have a similar, if not a more extreme phenotype. It would be interesting to see if ARHGAP36 is upregulated in this cancer. Iglesias-Bartolome and colleagues showed that $G\alpha_S$ mediated activation of PKA normally leads to Shh pathway inhibition, as well as Hippo pathway inhibition. PKA has recently been implicated in regulating Hippo signalling (Kim *et al*, 2013; Yu *et al*, 2013). This is yet another pathway where ARHGAP36 could modulate the tumour suppressive function of PKAC.

Most recently PKA has been in the spotlight for regulating mesenchymal to epithelial transition (MET) in a number of cancer cell lines (Pattabiraman *et al*, 2016). This is partially via phosphorylation and activation of PHF2, a histone demethylase, which derepresses genes required for the epithelial state. Importantly PKA-induced MET renders cells much more susceptible to chemotherapeutics and dramatically reduces their potential to metastasise and initiate secondary tumours. The PKA pathway has thus had a recent revival as a potential drug target in cancer. It would be interesting to know if ARHGAP36 can contribute to epithelial to mesenchymal transition (EMT) via suppression of PKA signalling. Tumour-initiating cells with mesenchymal properties may be more likely to express ARHGAP36 in order to suppress PKAC and the epithelial state. The study from Pattabiraman and colleagues also highlights the importance of heterogeneity within tumour cell populations. It further identifies PKAC transcriptional signatures that can be utilised

as a readout for future studies, such as an increase in E-Cadherin and a decrease in EMT-inducing transcription factors Snail, Twist1 and Zeb1 (Pattabiraman *et al*, 2016). It will be interesting to see whether ARHGAP36 upregulation in cancer negatively correlates with this signature, and vice versa.

Dependent on the tissue setting and signalling context in which PKA functions, aberrant ARHGAP36 expression could have either tumour suppressive or oncogenic roles. In terms of targeting oncogenic PKA signalling, ARHGAP36 as a pseudosubstrate inhibitor should be very specific for PKA as opposed to other kinases. Its bimodal inhibitory mechanism also indicates it could be a much more potent suppressor of PKA than PKI, which is only a transient inhibitor of activity. Dissecting the role of ARHGAP36 and its interplay with PKAC will allow further understanding of the context-specific roles of PKA signalling, and its impact in both development and disease.

References

Agarraberes FA, Terlecky SR & Dice JF (1997) An intralysosomal hsp70 is required for a selective pathway of lysosomal protein degradation. *J. Cell Biol.* **137:** 825–34

Aguilera M, Oliveros M, Martínez-Padrón M, Barbas JA & Ferrús A (2000) Ariadne-1: a vital Drosophila gene is required in development and defines a new conserved family of ring-finger proteins. *Genetics* **155:** 1231–44

Ajiro K, Shibata K & Nishikawa Y (1990) Subtype-specific cyclic AMP-dependent histone H1 phosphorylation at the differentiation of mouse neuroblastoma cells. *J. Biol. Chem.* **265:** 6494–500

Al-Hakim AK, Zagorska A, Chapman L, Deak M, Peggie M & Alessi DR (2008) Control of AMPK-related kinases by USP9X and atypical Lys(29)/Lys(33)-linked polyubiquitin chains. *Biochem. J.* **411:** 249–60

Alenghat FJ, Tytell JD, Thodeti CK, Derrien A & Ingber DE (2009) Mechanical control of cAMP signaling through integrins is mediated by the heterotrimeric Galphas protein. *J. Cell. Biochem.* **106:** 529–38

Altarejos JY & Montminy M (2011) CREB and the CRTC co-activators: sensors for hormonal and metabolic signals. *Nat. Rev. Mol. Cell Biol.* **12:** 141–51

Amieux PS, Cummings DE, Motamed K, Brandon EP, Wailes LA, Le K, Idzerda RL & McKnight GS (1997) Compensatory regulation of RIalpha protein levels in protein kinase A mutant mice. *J. Biol. Chem.* **272:** 3993–8

Arakane F, King SR, Du Y, Kallen CB, Walsh LP, Watari H, Stocco DM & Strauss JF (1997) Phosphorylation of steroidogenic acute regulatory protein (StAR) modulates its steroidogenic activity. *J. Biol. Chem.* **272:** 32656–62

Armstrong R, Wen W, Meinkoth J, Taylor S & Montminy M (1995) A refractory phase in cyclic AMP-responsive transcription requires down regulation of protein kinase A. *Mol. Cell. Biol.* **15:** 1826–32

Arndt V, Dick N, Tawo R, Dreiseidler M, Wenzel D, Hesse M, Fürst DO, Saftig P, Saint R, Fleischmann BK, Hoch M & Höhfeld J (2010) Chaperone-Assisted Selective Autophagy Is Essential for Muscle Maintenance. *Curr. Biol.* **20:** 143–148

Artemenko IP, Zhao D, Hales DB, Hales KH & Jefcoate CR (2001) Mitochondrial processing of newly synthesized steroidogenic acute regulatory protein (StAR), but not total StAR, mediates cholesterol transfer to cytochrome P450 side chain cleavage enzyme in adrenal cells. *J. Biol. Chem.* **276:** 46583–96

Asao H, Sasaki Y, Arita T, Tanaka N, Endo K, Kasai H, Takeshita T, Endo Y, Fujita T & Sugamura K (1997) Hrs is associated with STAM, a signal-transducing adaptor molecule. Its suppressive effect on cytokine-induced cell growth. *J. Biol. Chem.* **272:** 32785–91

Bache KG, Brech A, Mehlum A & Stenmark H (2003) Hrs regulates multivesicular body formation via ESCRT recruitment to endosomes. *J. Cell Biol.* **162:** 435–42

Bachmann VA, Riml A, Huber RG, Baillie GS, Liedl KR, Valovka T & Stefan E (2013)

Reciprocal regulation of PKA and Rac signaling. *Proc. Natl. Acad. Sci. U. S. A.* **110:** 8531–6

Baker RT & Board PG (1991) The human ubiquitin-52 amino acid fusion protein gene shares several structural features with mammalian ribosomal protein genes. *Nucleic Acids Res.* **19:** 1035–40

Barzi M, Kostrz D, Menendez A & Pons S (2011) Sonic Hedgehog-induced proliferation requires specific Gα inhibitory proteins. *J. Biol. Chem.* **286:** 8067–74

Bastidas AC, Deal MS, Steichen JM, Keshwani MM, Guo Y & Taylor SS (2012) Role of N-terminal myristylation in the structure and regulation of cAMP-dependent protein kinase. *J. Mol. Biol.* **422:** 215–29

Beachy PA, Karhadkar SS & Berman DM (2004) Tissue repair and stem cell renewal in carcinogenesis. *Nature* **432:** 324–31

Beebe SJ, Oyen O, Sandberg M, Frøysa A, Hansson V & Jahnsen T (1990) Molecular cloning of a tissue-specific protein kinase (C gamma) from human testis--representing a third isoform for the catalytic subunit of cAMP-dependent protein kinase. *Mol. Endocrinol.* **4:** 465–75

Beuschlein F, Fassnacht M, Assié G, Calebiro D, Stratakis C a, Osswald A, Ronchi CL, Wieland T, Sbiera S, Faucz FR, Schaak K, Schmittfull A, Schwarzmayr T, Barreau O, Vezzosi D, Rizk-Rabin M, Zabel U, Szarek E, Salpea P, Forlino A, et al (2014) Constitutive activation of PKA catalytic subunit in adrenal Cushing's syndrome. *N. Engl. J. Med.* **370:** 1019–28

Biedler JL, Roffler-Tarlov S, Schachner M & Freedman LS (1978) Multiple neurotransmitter synthesis by human neuroblastoma cell lines and clones. *Cancer Res.* **38:** 3751–7

Bingol B, Tea JS, Phu L, Reichelt M, Bakalarski CE, Song Q, Foreman O, Kirkpatrick DS & Sheng M (2014) The mitochondrial deubiquitinase USP30 opposes parkin-mediated mitophagy. *Nature* **510:** 370–5

Bishop N & Woodman P (2000) ATPase-defective mammalian VPS4 localizes to aberrant endosomes and impairs cholesterol trafficking. *Mol. Biol. Cell* **11:** 227–39

Boname JM, Thomas M, Stagg HR, Xu P, Peng J & Lehner PJ (2010) Efficient internalization of MHC I requires lysine-11 and lysine-63 mixed linkage polyubiquitin chains. *Traffic* **11:** 210–20

Bonifacino JS, Cosson P & Klausner RD (1990) Colocalized transmembrane determinants for ER degradation and subunit assembly explain the intracellular fate of TCR chains. *Cell* **63:** 503–13

Bos JL, Rehmann H & Wittinghofer A (2007) GEFs and GAPs: critical elements in the control of small G proteins. *Cell* **129:** 865–77

Bradbury AW, Carter DC, Miller WR, Cho-Chung YS & Clair T (1994) Protein kinase A (PK-A) regulatory subunit expression in colorectal cancer and related mucosa. *Br. J. Cancer* **69:** 738–42

Braun T & Dods RF (1975) Development of a Mn-2+-sensitive, 'soluble' adenylate cyclase in

rat testis. *Proc. Natl. Acad. Sci. U. S. A.* **72:** 1097–101

Bremm A, Freund SM V & Komander D (2010) Lys11-linked ubiquitin chains adopt compact conformations and are preferentially hydrolyzed by the deubiquitinase Cezanne. *Nat. Struct. Mol. Biol.* **17:** 939–47

Brodeur GM & Bagatell R (2014) Mechanisms of neuroblastoma regression. *Nat. Rev. Clin. Oncol.* **11:** 704–713

Brodeur GM & Goldstein MN (1976) Histochemical demonstration of an increase in acetylcholinesterase in established lines of human and mouse neuroblastomas by nerve growth factor. *Cytobios* **16:** 133–8

Buck J, Sinclair ML, Schapal L, Cann MJ & Levin LR (1999) Cytosolic adenylyl cyclase defines a unique signaling molecule in mammals. *Proc. Natl. Acad. Sci. U. S. A.* **96:** 79–84

Buckingham M & Rigby PWJ (2014) Gene regulatory networks and transcriptional mechanisms that control myogenesis. *Dev. Cell* **28:** 225–38

Buechler YJ, Herberg FW & Taylor SS (1993) Regulation-defective mutants of type I cAMP-dependent protein kinase. Consequences of replacing arginine 94 and arginine 95. *J. Biol. Chem.* **268:** 16495–503

Burnett G & Kennedy EP (1954) The enzymatic phosphorylation of proteins. *J. Biol. Chem.* **211:** 969–80

Cao Y, He M, Gao Z, Peng Y, Li Y, Li L, Zhou W, Li X, Zhong X, Lei Y, Su T, Wang H, Jiang Y, Yang L, Wei W, Yang X, Jiang X, Liu L, He J, Ye J, et al (2014) Activating Hotspot L205R Mutation in PRKACA and Adrenal Cushing's Syndrome. *Science (80-.).***:** 1249480

Cardozo T & Pagano M (2004) The SCF ubiquitin ligase: insights into a molecular machine. *Nat. Rev. Mol. Cell Biol.* **5:** 739–51

Castro-Vega LJ, Lepoutre-Lussey C, Gimenez-Roqueplo A-P & Favier J (2016) Rethinking pheochromocytomas and paragangliomas from a genomic perspective. *Oncogene* **35:** 1080–1089

Chain DG, Casadio A, Schacher S, Hegde AN, Valbrun M, Yamamoto N, Goldberg AL, Bartsch D, Kandel ER & Schwartz JH (1999) Mechanisms for generating the autonomous cAMP-dependent protein kinase required for long-term facilitation in Aplysia. *Neuron* **22:** 147–56

Chain DG, Hegde AN, Yamamoto N, Liu-Marsh B & Schwartz JH (1995) Persistent activation of cAMP-dependent protein kinase by regulated proteolysis suggests a neuron-specific function of the ubiquitin system in Aplysia. *J. Neurosci.* **15:** 7592–603

Chastagner P, Israël A & Brou C (2006) Itch/AIP4 mediates Deltex degradation through the formation of K29-linked polyubiquitin chains. *EMBO Rep.* **7:** 1147–53

Chaturvedi D, Cohen MS, Taunton J & Patel TB (2009) The PKARIalpha subunit of protein kinase A modulates the activation of p90RSK1 and its function. *J. Biol. Chem.* **284:** 23670–81

Chaturvedi D, Poppleton HM, Stringfield T, Barbier A & Patel TB (2006) Subcellular localization and biological actions of activated RSK1 are determined by its interactions with subunits of cyclic AMP-dependent protein kinase. *Mol. Cell. Biol.* **26:** 4586–600

Chen AE, Ginty DD & Fan C-M (2005) Protein kinase A signalling via CREB controls myogenesis induced by Wnt proteins. *Nature* **433:** 317–22

Chen X & Walters KJ (2015) Structural plasticity allows UCH37 to be primed by RPN13 or locked down by INO80G. *Mol. Cell* **57:** 767–8

Chen Y, Cann MJ, Litvin TN, Iourgenko V, Sinclair ML, Levin LR & Buck J (2000) Soluble adenylyl cyclase as an evolutionarily conserved bicarbonate sensor. *Science* **289:** 625–8

Chen Y, Cardinaux JR, Goodman RH & Smolik SM (1999) Mutants of cubitus interruptus that are independent of PKA regulation are independent of hedgehog signaling. *Development* **126:** 3607–16

Chen Y, Gallaher N, Goodman RH & Smolik SM (1998) Protein kinase A directly regulates the activity and proteolysis of cubitus interruptus. *Proc. Natl. Acad. Sci. U. S. A.* **95:** 2349–54

Chen Y, Harry A, Li J, Smit MJ, Bai X, Magnusson R, Pieroni JP, Weng G & Iyengar R (1997) Adenylyl cyclase 6 is selectively regulated by protein kinase A phosphorylation in a region involved in Galphas stimulation. *Proc. Natl. Acad. Sci. U. S. A.* **94:** 14100–4

Chen Y & Jiang J (2013) Decoding the phosphorylation code in Hedgehog signal transduction. *Cell Res.* **23:** 186–200

Chen Y, Yue S, Xie L, Pu X, Jin T & Cheng SY (2011) Dual Phosphorylation of suppressor of fused (Sufu) by PKA and GSK3beta regulates its stability and localization in the primary cilium. *J. Biol. Chem.* **286:** 13502–11

Cherfils J & Zeghouf M (2013) Regulation of small GTPases by GEFs, GAPs, and GDIs. *Physiol. Rev.* **93:** 269–309

Cheung J, Ginter C, Cassidy M, Franklin MC, Rudolph MJ, Robine N, Darnell RB & Hendrickson WA (2015) Structural insights into mis-regulation of protein kinase A in human tumors. *Proc. Natl. Acad. Sci. U. S. A.* **112:** 1374–9

Cheung N-K V & Dyer M a (2013) Neuroblastoma: developmental biology, cancer genomics and immunotherapy. *Nat. Rev. Cancer* **13:** 397–411

Chiang HL & Dice JF (1988) Peptide sequences that target proteins for enhanced degradation during serum withdrawal. *J. Biol. Chem.* **263:** 6797–805

Chiang HL, Terlecky SR, Plant CP & Dice JF (1989) A role for a 70-kilodalton heat shock protein in lysosomal degradation of intracellular proteins. *Science* **246:** 382–5

Chiaruttini N, Redondo-Morata L, Colom A, Humbert F, Lenz M, Scheuring S & Roux A (2015) Relaxation of Loaded ESCRT-III Spiral Springs Drives Membrane Deformation. *Cell* **163:** 866–79

Cho-Chung YS, Nesterova M, Pepe S, Lee GR, Noguchi K, Srivastava RK, Srivastava AR, Alper O, Park YG & Lee YN (1999) Antisense DNA-targeting protein kinase A-RIA

subunit: a novel approach to cancer treatment. *Front. Biosci.* **4:** D898–907

Cho-Chung YS & Nesterova M V (2005) Tumor reversion: protein kinase A isozyme switching. *Ann. N. Y. Acad. Sci.* **1058:** 76–86

Cho-Chung YS, Pepe S, Clair T, Budillon A & Nesterova M (1995) cAMP-dependent protein kinase: role in normal and malignant growth. *Crit. Rev. Oncol. Hematol.* **21:** 33–61

Christian F, Szaszák M, Friedl S, Drewianka S, Lorenz D, Goncalves A, Furkert J, Vargas C, Schmieder P, Götz F, Zühlke K, Moutty M, Göttert H, Joshi M, Reif B, Haase H, Morano I, Grossmann S, Klukovits A, Verli J, et al (2011) Small molecule AKAP-protein kinase A (PKA) interaction disruptors that activate PKA interfere with compartmentalized cAMP signaling in cardiac myocytes. *J. Biol. Chem.* **286:** 9079–96

Ciccarone V, Spengler BA, Meyers MB, Biedler JL & Ross RA (1989) Phenotypic diversification in human neuroblastoma cells: expression of distinct neural crest lineages. *Cancer Res.* **49:** 219–25

Ciechanover A (2005) Proteolysis: from the lysosome to ubiquitin and the proteasome. *Nat. Rev. Mol. Cell Biol.* **6:** 79–87

Ciechanover A, Elias S, Heller H & Hershko A (1982) 'Covalent affinity' purification of ubiquitin-activating enzyme. *J. Biol. Chem.* **257:** 2537–42

Ciechanover A, Heller H, Katz-Etzion R & Hershko A (1981) Activation of the heat-stable polypeptide of the ATP-dependent proteolytic system. *Proc. Natl. Acad. Sci. U. S. A.* **78:** 761–5

Clague MJ (2002) Membrane transport: a coat for ubiquitin. *Curr. Biol.* **12:** R529–31

Clague MJ, Barsukov I, Coulson JM, Liu H, Rigden DJ & Urbé S (2013) Deubiquitylases from genes to organism. *Physiol. Rev.* **93:** 1289–315

Clague MJ, Liu H & Urbé S (2012) Governance of Endocytic Trafficking and Signaling by Reversible Ubiquitylation. *Dev. Cell* **23:** 457–467

Clague MJ & Urbé S (2006) Endocytosis: the DUB version. *Trends Cell Biol.* **16:** 551–9

Clague MJ & Urbé S (2010) Ubiquitin: same molecule, different degradation pathways. *Cell* **143:** 682–5

Clague MJ, Urbé S, Aniento F & Gruenberg J (1994) Vacuolar ATPase activity is required for endosomal carrier vesicle formation. *J. Biol. Chem.* **269:** 21–4

Clark BJ, Ranganathan V & Combs R (2001) Steroidogenic acute regulatory protein expression is dependent upon post-translational effects of cAMP-dependent protein kinase A. *Mol. Cell. Endocrinol.* **173:** 183–92

Clark BJ, Wells J, King SR & Stocco DM (1994) The purification, cloning, and expression of a novel luteinizing hormone-induced mitochondrial protein in MA-10 mouse Leydig tumor cells. Characterization of the steroidogenic acute regulatory protein (StAR). *J. Biol. Chem.* **269:** 28314–22

Cohen P (2000) The regulation of protein function by multisite phosphorylation--a 25 year update. *Trends Biochem. Sci.* **25:** 596–601

Colwill K, Wells CD, Elder K, Goudreault M, Hersi K, Kulkarni S, Hardy WR, Pawson T &

Morin GB (2006) Modification of the Creator recombination system for proteomics applications--improved expression by addition of splice sites. *BMC Biotechnol.* **6:** 13

Comb M, Birnberg NC, Seasholtz A, Herbert E & Goodman HM (1986) A cyclic AMP- and phorbol ester-inducible DNA element. *Nature* **323:** 353–6

Conti M & Beavo J (2007) Biochemistry and physiology of cyclic nucleotide phosphodiesterases: essential components in cyclic nucleotide signaling. *Annu. Rev. Biochem.* **76:** 481–511

Conze DB, Wu C-J, Thomas JA, Landstrom A & Ashwell JD (2008) Lys63-linked polyubiquitination of IRAK-1 is required for interleukin-1 receptor- and toll-like receptor-mediated NF-kappaB activation. *Mol. Cell. Biol.* **28:** 3538–47

Cook WJ, Jeffrey LC, Kasperek E & Pickart CM (1994) Structure of tetraubiquitin shows how multiubiquitin chains can be formed. *J. Mol. Biol.* **236:** 601–9

Corbin JD, Keely SL & Park CR (1975) The distribution and dissociation of cyclic adenosine 3':5'-monophosphate-dependent protein kinases in adipose, cardiac, and other tissues. *J. Biol. Chem.* **250:** 218–25

Correa R, Salpea P & Stratakis CA (2015) Carney complex: an update. *Eur. J. Endocrinol.* **173:** M85–97

Costa M, Manen CA & Russell DH (1975) In vivo activation of cAMP-dependent protein kinase by aminophylline and 1-methyl, 3-isobutylxanthine. *Biochem. Biophys. Res. Commun.* **65:** 75–81

Cox J & Mann M (2008) MaxQuant enables high peptide identification rates, individualized p.p.b.-range mass accuracies and proteome-wide protein quantification. *Nat. Biotechnol.* **26:** 1367–72

Croisé P, Houy S, Gand M, Lanoix J, Calco V, Tryoen-Tóth P, Brunaud L, Lomazzi S, Paramithiotis E, Chelsky D, Ory S & Gasman S (2016) Cdc42 and Rac1 activity is reduced in human pheochromocytoma and correlates with FARP1 and ARHGEF1 expression. *Endocr. Relat. Cancer.* **23:** 281-93

Cselenyi CS, Jernigan KK, Tahinci E, Thorne CA, Lee LA & Lee E (2008) LRP6 transduces a canonical Wnt signal independently of Axin degradation by inhibiting GSK3's phosphorylation of beta-catenin. *Proc. Natl. Acad. Sci. U. S. A.* **105:** 8032–7

Cuervo AM & Dice JF (1996) A receptor for the selective uptake and degradation of proteins by lysosomes. *Science* **273:** 501–3

Daaka Y, Luttrell LM & Lefkowitz RJ (1997) Switching of the coupling of the beta2-adrenergic receptor to different G proteins by protein kinase A. *Nature* **390:** 88–91

Dai P, Akimaru H, Tanaka Y, Maekawa T, Nakafuku M & Ishii S (1999) Sonic Hedgehog-induced activation of the Gli1 promoter is mediated by GLI3. *J. Biol. Chem.* **274:** 8143–52

Dalton GD & Dewey WL (2006) Protein kinase inhibitor peptide (PKI): a family of endogenous neuropeptides that modulate neuronal cAMP-dependent protein kinase function. *Neuropeptides* **40:** 23–34

Dammer EB, Na CH, Xu P, Seyfried NT, Duong DM, Cheng D, Gearing M, Rees H, Lah JJ, Levey AI, Rush J & Peng J (2011) Polyubiquitin linkage profiles in three models of proteolytic stress suggest the etiology of Alzheimer disease. *J. Biol. Chem.* **286:** 10457–65

David Y, Ternette N, Edelmann MJ, Ziv T, Gayer B, Sertchook R, Dadon Y, Kessler BM & Navon A (2011) E3 ligases determine ubiquitination site and conjugate type by enforcing specificity on E2 enzymes. *J. Biol. Chem.* **286:** 44104–15

Davie JK, Cho J-H, Meadows E, Flynn JM, Knapp JR & Klein WH (2007) Target gene selectivity of the myogenic basic helix-loop-helix transcription factor myogenin in embryonic muscle. *Dev. Biol.* **311:** 650–64

Deen PM & Knoers N V (1998) Vasopressin type-2 receptor and aquaporin-2 water channel mutants in nephrogenic diabetes insipidus. *Am. J. Med. Sci.* **316:** 300–9

Dell'Acqua ML, Faux MC, Thorburn J, Thorburn A & Scott JD (1998) Membrane-targeting sequences on AKAP79 bind phosphatidylinositol-4, 5-bisphosphate. *EMBO J.* **17:** 2246–60

DeManno DA, Cottom JE, Kline MP, Peters CA, Maizels ET & Hunzicker-Dunn M (1999) Follicle-stimulating hormone promotes histone H3 phosphorylation on serine-10. *Mol. Endocrinol.* **13:** 91–105

Depry C, Allen MD & Zhang J (2011) Visualization of PKA activity in plasma membrane microdomains. *Mol. Biosyst.* **7:** 52–8

Dikic I, Wakatsuki S & Walters KJ (2009) Ubiquitin-binding domains - from structures to functions. *Nat. Rev. Mol. Cell Biol.* **10:** 659–671

Diviani D, Abuin L, Cotecchia S & Pansier L (2004) Anchoring of both PKA and 14-3-3 inhibits the Rho-GEF activity of the AKAP-Lbc signaling complex. *EMBO J.* **23:** 2811–20

Diviani D, Baisamy L & Appert-Collin A (2006) AKAP-Lbc: a molecular scaffold for the integration of cyclic AMP and Rho transduction pathways. *Eur. J. Cell Biol.* **85:** 603–10

Diviani D, Langeberg LK, Doxsey SJ & Scott JD (2000) Pericentrin anchors protein kinase A at the centrosome through a newly identified RII-binding domain. *Curr. Biol.* **10:** 417–20

Diviani D, Soderling J & Scott JD (2001) AKAP-Lbc anchors protein kinase A and nucleates Galpha 12-selective Rho-mediated stress fiber formation. *J. Biol. Chem.* **276:** 44247–57

Duncan LM, Piper S, Dodd RB, Saville MK, Sanderson CM, Luzio JP & Lehner PJ (2006) Lysine-63-linked ubiquitination is required for endolysosomal degradation of class I molecules. *EMBO J.* **25:** 1635–45

Durcan TM & Fon EA (2015) The three 'P's of mitophagy: PARKIN, PINK1, and post-translational modifications. *Genes Dev.* **29:** 989–99

Durcan TM, Tang MY, Pérusse JR, Dashti EA, Aguileta MA, McLelland G-L, Gros P, Shaler TA, Faubert D, Coulombe B & Fon EA (2014) USP8 regulates mitophagy by removing K6-linked ubiquitin conjugates from parkin. *EMBO J.* **33:** 2473–91

De Duve C, Gianetto R, Appelmanns F & Wattieux R (1953) Enzymic content of the mitochondria fraction. *Nature* **172:** 1143–4

De Duve C & Wattiaux R (1966) Functions of lysosomes. *Annu. Rev. Physiol.* **28:** 435–92

Eisenhaber B, Chumak N, Eisenhaber F & Hauser M-T (2007) The ring between ring fingers (RBR) protein family. *Genome Biol.* **8:** 209

Ellerbroek SM, Wennerberg K & Burridge K (2003) Serine phosphorylation negatively regulates RhoA in vivo. *J. Biol. Chem.* **278:** 19023–31

Epstein LF & Orme-Johnson NR (1991) Regulation of steroid hormone biosynthesis. Identification of precursors of a phosphoprotein targeted to the mitochondrion in stimulated rat adrenal cortex cells. *J. Biol. Chem.* **266:** 19739–45

Erpapazoglou Z, Dhaoui M, Pantazopoulou M, Giordano F, Mari M, Léon S, Raposo G, Reggiori F & Haguenauer-Tsapis R (2012) A dual role for K63-linked ubiquitin chains in multivesicular body biogenesis and cargo sorting. *Mol. Biol. Cell* **23:** 2170–83

Etlinger JD & Goldberg AL (1977) A soluble ATP-dependent proteolytic system responsible for the degradation of abnormal proteins in reticulocytes. *Proc. Natl. Acad. Sci. U. S. A.* **74:** 54–8

Faesen AC, Luna-Vargas MPA, Geurink PP, Clerici M, Merkx R, van Dijk WJ, Hameed DS, El Oualid F, Ovaa H & Sixma TK (2011) The differential modulation of USP activity by internal regulatory domains, interactors and eight ubiquitin chain types. *Chem. Biol.* **18:** 1550–61

Fantozzi DA, Harootunian AT, Wen W, Taylor SS, Feramisco JR, Tsien RY & Meinkoth JL (1994) Thermostable inhibitor of cAMP-dependent protein kinase enhances the rate of export of the kinase catalytic subunit from the nucleus. *J. Biol. Chem.* **269:** 2676–86

Fantozzi DA, Taylor SS, Howard PW, Maurer RA, Feramisco JR & Meinkoth JL (1992) Effect of the thermostable protein kinase inhibitor on intracellular localization of the catalytic subunit of cAMP-dependent protein kinase. *J. Biol. Chem.* **267:** 16824–8

Faucherre A, Desbois P, Satre V, Lunardi J, Dorseuil O & Gacon G (2003) Lowe syndrome protein OCRL1 interacts with Rac GTPase in the trans-Golgi network. *Hum. Mol. Genet.* **12:** 2449–56

Finley D (2009) Recognition and processing of ubiquitin-protein conjugates by the proteasome. *Annu. Rev. Biochem.* **78:** 477–513

Finley D, Chen X & Walters KJ (2016) Gates, Channels, and Switches: Elements of the Proteasome Machine. *Trends Biochem. Sci.* **41:** 77–93

Forget M-A, Desrosiers RR, Gingras D & Béliveau R (2002) Phosphorylation states of Cdc42 and RhoA regulate their interactions with Rho GDP dissociation inhibitor and their extraction from biological membranes. *Biochem. J.* **361:** 243–54

Fu W, Asp P, Canter B & Dynlacht BD (2014) Primary cilia control hedgehog signaling during muscle differentiation and are deregulated in rhabdomyosarcoma. *Proc. Natl. Acad. Sci. U. S. A.***:** 1–6

Fushimi K, Sasaki S & Marumo F (1997) Phosphorylation of serine 256 is required for

cAMP-dependent regulatory exocytosis of the aquaporin-2 water channel. *J. Biol. Chem.* **272:** 14800–4

Gaffarogullari EC, Masterson LR, Metcalfe EE, Traaseth NJ, Balatri E, Musa MM, Mullen D, Distefano MD & Veglia G (2011) A myristoyl/phosphoserine switch controls cAMP-dependent protein kinase association to membranes. *J. Mol. Biol.* **411:** 823–36

Gangal M, Clifford T, Deich J, Cheng X, Taylor SS & Johnson DA (1999) Mobilization of the A-kinase N-myristate through an isoform-specific intermolecular switch. *Proc. Natl. Acad. Sci. U. S. A.* **96:** 12394–9

Gao N, Asamitsu K, Hibi Y, Ueno T & Okamoto T (2008) AKIP1 enhances NF-kappaB-dependent gene expression by promoting the nuclear retention and phosphorylation of p65. *J. Biol. Chem.* **283:** 7834–43

Gao X, Chaturvedi D & Patel TB (2010) p90 ribosomal S6 kinase 1 (RSK1) and the catalytic subunit of protein kinase A (PKA) compete for binding the pseudosubstrate region of PKAR1alpha: role in the regulation of PKA and RSK1 activities. *J. Biol. Chem.* **285:** 6970–9

Gao X, Chaturvedi D & Patel TB (2012) Localization and retention of p90 ribosomal S6 kinase 1 in the nucleus: implications for its function. *Mol. Biol. Cell* **23:** 503–515

Gao X & Patel TB (2009) Regulation of protein kinase A activity by p90 ribosomal S6 kinase 1. *J. Biol. Chem.* **284:** 33070–8

Garcia-Mata R, Boulter E & Burridge K (2011) The 'invisible hand': regulation of RHO GTPases by RHOGDIs. *Nat. Rev. Mol. Cell Biol.* **12:** 493–504

Geetha T, Jiang J & Wooten MW (2005) Lysine 63 polyubiquitination of the nerve growth factor receptor TrkA directs internalization and signaling. *Mol. Cell* **20:** 301–12

Geisler S, Holmström KM, Skujat D, Fiesel FC, Rothfuss OC, Kahle PJ & Springer W (2010) PINK1/Parkin-mediated mitophagy is dependent on VDAC1 and p62/SQSTM1. *Nat. Cell Biol.* **12:** 119–31

Gerber SA, Rush J, Stemman O, Kirschner MW & Gygi SP (2003) Absolute quantification of proteins and phosphoproteins from cell lysates by tandem MS. *Proc. Natl. Acad. Sci. U. S. A.* **100:** 6940–5

Ghil S, Choi J-M, Kim S-S, Lee Y-D, Liao Y, Birnbaumer L & Suh-Kim H (2006) Compartmentalization of protein kinase A signaling by the heterotrimeric G protein Go. *Proc. Natl. Acad. Sci. U. S. A.* **103:** 19158–63

Gillingham AK & Munro S (2000) The PACT domain, a conserved centrosomal targeting motif in the coiled-coil proteins AKAP450 and pericentrin. *EMBO Rep.* **1:** 524–9

Gillooly DJ, Morrow IC, Lindsay M, Gould R, Bryant NJ, Gaullier JM, Parton RG & Stenmark H (2000) Localization of phosphatidylinositol 3-phosphate in yeast and mammalian cells. *EMBO J.* **19:** 4577–88

Gilman AG (1987) G proteins: transducers of receptor-generated signals. *Annu. Rev. Biochem.* **56:** 615–49

Glass DB, Lundquist LJ, Katz BM & Walsh DA (1989) Protein kinase inhibitor-(6-22)-amide

peptide analogs with standard and nonstandard amino acid substitutions for phenylalanine 10. Inhibition of cAMP-dependent protein kinase. *J. Biol. Chem.* **264:** 14579–84

Gloerich M & Bos JL (2010) Epac: defining a new mechanism for cAMP action. *Annu. Rev. Pharmacol. Toxicol.* **50:** 355–75

Goh G, Scholl UI, Healy JM, Choi M, Prasad ML, Nelson-Williams C, Kuntsman JW, Korah R, Suttorp A-C, Dietrich D, Haase M, Willenberg HS, Stålberg P, Hellman P, Akerström G, Björklund P, Carling T & Lifton RP (2014) Recurrent activating mutation in PRKACA in cortisol-producing adrenal tumors. *Nat. Genet.***:** 1–6

Goldberg AL (2012) Development of proteasome inhibitors as research tools and cancer drugs. *J. Cell Biol.* **199:** 583–8

Goldfinger LE, Han J, Kiosses WB, Howe AK & Ginsberg MH (2003) Spatial restriction of alpha4 integrin phosphorylation regulates lamellipodial stability and alpha4beta1-dependent cell migration. *J. Cell Biol.* **162:** 731–41

Gonzalez GA & Montminy MR (1989) Cyclic AMP stimulates somatostatin gene transcription by phosphorylation of CREB at serine 133. *Cell* **59:** 675–80

Greenberg SM, Castellucci VF, Bayley H & Schwartz JH A molecular mechanism for long-term sensitization in Aplysia. *Nature* **329:** 62–5

Greene EL, Horvath AD, Nesterova M, Giatzakis C, Bossis I & Stratakis CA (2008) In vitro functional studies of naturally occurring pathogenic PRKAR1A mutations that are not subject to nonsense mRNA decay. *Hum. Mutat.* **29:** 633–9

Hagiwara M, Alberts A, Brindle P, Meinkoth J, Feramisco J, Deng T, Karin M, Shenolikar S & Montminy M (1992) Transcriptional attenuation following cAMP induction requires PP-1-mediated dephosphorylation of CREB. *Cell* **70:** 105–13

Haider M & Segal HL (1972) Some characteristics of the alanine aminotransferase- and arginase-inactivating system of lysosomes. *Arch. Biochem. Biophys.* **148:** 228–37

Hall A (1998) Rho GTPases and the Actin Cytoskeleton. *Science (80-.).* **279:** 509–514

Halls ML & Cooper DMF (2011) Regulation by Ca2+-signaling pathways of adenylyl cyclases. *Cold Spring Harb. Perspect. Biol.* **3:** a004143

Han J, Liu S, Rose DM, Schlaepfer DD, McDonald H & Ginsberg MH (2001) Phosphorylation of the integrin alpha 4 cytoplasmic domain regulates paxillin binding. *J. Biol. Chem.* **276:** 40903–9

Han P, Sonati P, Rubin C & Michaeli T (2006) PDE7A1, a cAMP-specific phosphodiesterase, inhibits cAMP-dependent protein kinase by a direct interaction with C. *J. Biol. Chem.* **281:** 15050–7

Hancock JF, Paterson H & Marshall CJ (1990) A polybasic domain or palmitoylation is required in addition to the CAAX motif to localize p21ras to the plasma membrane. *Cell* **63:** 133–9

Harburger DS & Calderwood DA (2009) Integrin signalling at a glance. *J. Cell Sci.* **122:** 159–63

Hassink GC, Zhao B, Sompallae R, Altun M, Gastaldello S, Zinin N V, Masucci MG & Lindsten K (2009) The ER-resident ubiquitin-specific protease 19 participates in the UPR and rescues ERAD substrates. *EMBO Rep.* **10:** 755–61

Hatipoglu BA (2012) Cushing's syndrome. *J. Surg. Oncol.* **106:** 565–71

He X, Zhang L, Chen Y, Remke M, Shih D, Lu F, Wang H, Deng Y, Yu Y, Xia Y, Wu X, Ramaswamy V, Hu T, Wang F, Zhou W, Burns DK, Kim SH, Kool M, Pfister SM, Weinstein LS, et al (2014) The G protein α subunit Gαs is a tumor suppressor in Sonic hedgehog-driven medulloblastoma. *Nat. Med.* **20:** 1035–42

Heasman SJ & Ridley AJ (2008) Mammalian Rho GTPases: new insights into their functions from in vivo studies. *Nat. Rev. Mol. Cell Biol.* **9:** 690–701

Hegde AN, Goldberg AL & Schwartz JH (1993) Regulatory subunits of cAMP-dependent protein kinases are degraded after conjugation to ubiquitin: a molecular mechanism underlying long-term synaptic plasticity. *Proc. Natl. Acad. Sci. U. S. A.* **90:** 7436–40

Hemmings BA (1986) cAMP mediated proteolysis of the catalytic subunit of cAMP-dependent protein kinase. *FEBS Lett.* **196:** 126–30

Henne WM, Buchkovich NJ, Zhao Y & Emr SD (2012) The endosomal sorting complex ESCRT-II mediates the assembly and architecture of ESCRT-III helices. *Cell* **151:** 356–71

Herberg FW & Taylor SS (1993) Physiological inhibitors of the catalytic subunit of cAMP-dependent protein kinase: effect of MgATP on protein-protein interactions. *Biochemistry* **32:** 14015–22

Herbst KJ, Allen MD & Zhang J (2011) Spatiotemporally regulated protein kinase A activity is a critical regulator of growth factor-stimulated extracellular signal-regulated kinase signaling in PC12 cells. *Mol. Cell. Biol.* **31:** 4063–75

Heride C, Urbé S & Clague MJ (2014) Ubiquitin code assembly and disassembly. *Curr. Biol.* **24:** R215–20

Hershko A, Ciechanover A, Heller H, Haas AL & Rose IA (1980) Proposed role of ATP in protein breakdown: conjugation of protein with multiple chains of the polypeptide of ATP-dependent proteolysis. *Proc. Natl. Acad. Sci. U. S. A.* **77:** 1783–6

Hershko A, Heller H, Elias S & Ciechanover A (1983) Components of ubiquitin-protein ligase system. Resolution, affinity purification, and role in protein breakdown. *J. Biol. Chem.* **258:** 8206–14

Hofmann F, Bechtel PJ & Krebs EG (1977) Concentrations of cyclic AMP-dependent protein kinase subunits in various tissues. *J. Biol. Chem.* **252:** 1441–7

Honeyman JN, Simon EP, Robine N, Chiaroni-Clarke R, Darcy DG, Lim IIP, Gleason CE, Murphy JM, Rosenberg BR, Teegan L, Takacs CN, Botero S, Belote R, Germer S, Emde A-K, Vacic V, Bhanot U, LaQuaglia MP & Simon SM (2014) Detection of a recurrent DNAJB1-PRKACA chimeric transcript in fibrolamellar hepatocellular carcinoma. *Science* **343:** 1010–4

Hong Y-H, Ahn H-C, Lim J, Kim H-M, Ji H-Y, Lee S, Kim J-H, Park EY, Song HK & Lee B-J

(2009) Identification of a novel ubiquitin binding site of STAM1 VHS domain by NMR spectroscopy. *FEBS Lett.* **583:** 287–92

Horvath A, Boikos S, Giatzakis C, Robinson-White A, Groussin L, Griffin KJ, Stein E, Levine E, Delimpasi G, Hsiao HP, Keil M, Heyerdahl S, Matyakhina L, Libè R, Fratticci A, Kirschner LS, Cramer K, Gaillard RC, Bertagna X, Carney JA, et al (2006) A genome-wide scan identifies mutations in the gene encoding phosphodiesterase 11A4 (PDE11A) in individuals with adrenocortical hyperplasia. *Nat. Genet.* **38:** 794–800

Horvath A, Mericq V & Stratakis CA (2008) Mutation in PDE8B, a cyclic AMP-specific phosphodiesterase in adrenal hyperplasia. *N. Engl. J. Med.* **358:** 750–2

Hospenthal MK, Mevissen TET & Komander D (2015) Deubiquitinase-based analysis of ubiquitin chain architecture using Ubiquitin Chain Restriction (UbiCRest). *Nat. Protoc.* **10:** 349–61

Hough R, Pratt G & Rechsteiner M (1986) Ubiquitin-lysozyme conjugates. Identification and characterization of an ATP-dependent protease from rabbit reticulocyte lysates. *J. Biol. Chem.* **261:** 2400–8

Hough R & Rechsteiner M (1986) Ubiquitin-lysozyme conjugates. Purification and susceptibility to proteolysis. *J. Biol. Chem.* **261:** 2391–9

Houslay MD (2010) Underpinning compartmentalised cAMP signalling through targeted cAMP breakdown. *Trends Biochem. Sci.* **35:** 91–100

Howe AK (2011) Cross-talk between calcium and protein kinase A in the regulation of cell migration. *Curr. Opin. Cell Biol.* **23:** 554–61

Howe AK, Baldor LC & Hogan BP (2005) Spatial regulation of the cAMP-dependent protein kinase during chemotactic cell migration. *Proc. Natl. Acad. Sci. U. S. A.* **102:** 14320–5

Howe AK & Juliano RL (2000) Regulation of anchorage-dependent signal transduction by protein kinase A and p21-activated kinase. *Nat. Cell Biol.* **2:** 593–600

Huang F, Kirkpatrick D, Jiang X, Gygi S & Sorkin A (2006) Differential regulation of EGF receptor internalization and degradation by multiubiquitination within the kinase domain. *Mol. Cell* **21:** 737–48

Huang F, Zeng X, Kim W, Balasubramani M, Fortian A, Gygi SP, Yates NA & Sorkin A (2013) Lysine 63-linked polyubiquitination is required for EGF receptor degradation. *Proc. Natl. Acad. Sci. U. S. A.* **110:** 15722–7

Huang H, Jeon M-S, Liao L, Yang C, Elly C, Yates JR & Liu Y-C (2010) K33-linked polyubiquitination of T cell receptor-zeta regulates proteolysis-independent T cell signaling. *Immunity* **33:** 60–70

Hui C-C & Angers S (2011) Gli proteins in development and disease. *Annu. Rev. Cell Dev. Biol.* **27:** 513–37

Humke EW, Dorn K V, Milenkovic L, Scott MP & Rohatgi R (2010) The output of Hedgehog signaling is controlled by the dynamic association between Suppressor of Fused and the Gli proteins. *Genes Dev.* **24:** 670–82

Hundsrucker C, Skroblin P, Christian F, Zenn H-M, Popara V, Joshi M, Eichhorst J, Wiesner

B, Herberg FW, Reif B, Rosenthal W & Klussmann E (2010) Glycogen synthase kinase 3beta interaction protein functions as an A-kinase anchoring protein. *J. Biol. Chem.* **285:** 5507–21

Hurley JH (1999) Structure, mechanism, and regulation of mammalian adenylyl cyclase. *J. Biol. Chem.* **274:** 7599–602

Hurley JH & Hanson PI (2010) Membrane budding and scission by the ESCRT machinery: it's all in the neck. *Nat. Rev. Mol. Cell Biol.* **11:** 556–66

Hurley JH & Stenmark H (2011) Molecular mechanisms of ubiquitin-dependent membrane traffic. *Annu. Rev. Biophys.* **40:** 119–42

Husnjak K & Dikic I (2012) Ubiquitin-Binding Proteins: Decoders of Ubiquitin-Mediated Cellular Functions. *Annu. Rev. Biochem.* **81:** 291–322

Husnjak K, Elsasser S, Zhang N, Chen X, Randles L, Shi Y, Hofmann K, Walters KJ, Finley D & Dikic I (2008) Proteasome subunit Rpn13 is a novel ubiquitin receptor. *Nature* **453:** 481–8

Hyvola N, Diao A, McKenzie E, Skippen A, Cockcroft S & Lowe M (2006) Membrane targeting and activation of the Lowe syndrome protein OCRL1 by rab GTPases. *EMBO J.* **25:** 3750–61

Iglesias-Bartolome R, Torres D, Marone R, Feng X, Martin D, Simaan M, Chen M, Weinstein LS, Taylor SS, Molinolo AA & Gutkind JS (2015) Inactivation of a Gα(s)-PKA tumour suppressor pathway in skin stem cells initiates basal-cell carcinogenesis. *Nat. Cell Biol.* **17:** 793–803

Iolascon A, Aglio V, Tamma G, D'Apolito M, Addabbo F, Procino G, Simonetti MC, Montini G, Gesualdo L, Debler EW, Svelto M & Valenti G (2007) Characterization of two novel missense mutations in the AQP2 gene causing nephrogenic diabetes insipidus. *Nephron. Physiol.* **105:** p33–41

Isosomppi J, Vesa J, Jalanko A & Peltonen L (2002) Lysosomal localization of the neuronal ceroid lipofuscinosis CLN5 protein. *Hum. Mol. Genet.* **11:** 885–91

Iwai K & Tokunaga F (2009) Linear polyubiquitination: a new regulator of NF-kappaB activation. *EMBO Rep.* **10:** 706–13

Iwami G, Kawabe J, Ebina T, Cannon PJ, Homcy CJ & Ishikawa Y (1995) Regulation of adenylyl cyclase by protein kinase A. *J. Biol. Chem.* **270:** 12481–4

Jacobson AD, Zhang N-Y, Xu P, Han K-J, Noone S, Peng J & Liu C-W (2009) The lysine 48 and lysine 63 ubiquitin conjugates are processed differently by the 26 s proteasome. *J. Biol. Chem.* **284:** 35485–94

Jang H, Abraham SJ, Chavan TS, Hitchinson B, Khavrutskii L, Tarasova NI, Nussinov R & Gaponenko V (2015) Mechanisms of membrane binding of small GTPase K-Ras4B farnesylated hypervariable region. *J. Biol. Chem.* **290:** 9465–77

Jarnaess E, Stokka AJ, Kvissel A-K, Skålhegg BS, Torgersen KM, Scott JD, Carlson CR & Taskén K (2009) Splicing factor arginine/serine-rich 17A (SFRS17A) is an A-kinase anchoring protein that targets protein kinase A to splicing factor compartments. *J. Biol.*

Chem. **284:** 35154–64

Jiang J & Hui C-C (2008) Hedgehog signaling in development and cancer. *Dev. Cell* **15:** 801–12

Jin J, Smith FD, Stark C, Wells CD, Fawcett JP, Kulkarni S, Metalnikov P, O'Donnell P, Taylor P, Taylor L, Zougman A, Woodgett JR, Langeberg LK, Scott JD & Pawson T (2004) Proteomic, functional, and domain-based analysis of in vivo 14-3-3 binding proteins involved in cytoskeletal regulation and cellular organization. *Curr. Biol.* **14:** 1436–50

Jin L, Williamson A, Banerjee S, Philipp I & Rape M (2008) Mechanism of ubiquitin-chain formation by the human anaphase-promoting complex. *Cell* **133:** 653–65

Jo I, Ward DT, Baum MA, Scott JD, Coghlan VM, Hammond TG & Harris HW (2001) AQP2 is a substrate for endogenous PP2B activity within an inner medullary AKAP-signaling complex. *Am. J. Physiol. Renal Physiol.* **281:** F958–65

Johannessen M, Delghandi MP & Moens U (2004) What turns CREB on? *Cell. Signal.* **16:** 1211–27

Johnson LN & Lewis RJ (2001) Structural basis for control by phosphorylation. *Chem. Rev.* **101:** 2209–42

Johnston CA & Siderovski DP (2007) Receptor-mediated activation of heterotrimeric G-proteins: current structural insights. *Mol. Pharmacol.* **72:** 219–30

Kaiser SE, Riley BE, Shaler TA, Trevino RS, Becker CH, Schulman H & Kopito RR (2011) Protein standard absolute quantification (PSAQ) method for the measurement of cellular ubiquitin pools. *Nat. Methods* **8:** 691–6

Kamentsky L, Jones TR, Fraser A, Bray M-A, Logan DJ, Madden KL, Ljosa V, Rueden C, Eliceiri KW & Carpenter AE (2011) Improved structure, function and compatibility for CellProfiler: modular high-throughput image analysis software. *Bioinformatics* **27:** 1179–80

Katsura T, Gustafson CE, Ausiello DA & Brown D (1997) Protein kinase A phosphorylation is involved in regulated exocytosis of aquaporin-2 in transfected LLC-PK1 cells. *Am. J. Physiol.* **272:** F817–22

Kaushik S & Cuervo AM (2012) Chaperone-mediated autophagy: a unique way to enter the lysosome world. *Trends Cell Biol.* **22:** 407–17

Kee BL, Arias J & Montminy MR (1996) Adaptor-mediated recruitment of RNA polymerase II to a signal-dependent activator. *J. Biol. Chem.* **271:** 2373–5

Keely SL (1977) Activation of cAMP-dependent protein kinase without a corresponding increase in phosphorylase activity. *Res. Commun. Chem. Pathol. Pharmacol.* **18:** 283–90

Kemp BE, Benjamini E & Krebs EG (1976) Synthetic hexapeptide substrates and inhibitors of 3':5'-cyclic AMP-dependent protein kinase. *Proc. Natl. Acad. Sci. U. S. A.* **73:** 1038–42

Keshwani MM, Klammt C, von Daake S, Ma Y, Kornev AP, Choe S, Insel PA & Taylor SS

(2012) Cotranslational cis-phosphorylation of the COOH-terminal tail is a key priming step in the maturation of cAMP-dependent protein kinase. *Proc. Natl. Acad. Sci. U. S. A.* **109:** E1221–9

Kettenbach AN, Rush J & Gerber SA (2011) Absolute quantification of protein and post-translational modification abundance with stable isotope-labeled synthetic peptides. *Nat. Protoc.* **6:** 175–86

Khaminets A, Behl C & Dikic I (2016) Ubiquitin-Dependent And Independent Signals In Selective Autophagy. *Trends Cell Biol.* **26:** 6–16

Kim C, Xuong N-H & Taylor SS (2005) Crystal structure of a complex between the catalytic and regulatory (RIalpha) subunits of PKA. *Science* **307:** 690–6

Kim HC & Huibregtse JM (2009) Polyubiquitination by HECT E3s and the determinants of chain type specificity. *Mol. Cell. Biol.* **29:** 3307–18

Kim M, Kim M, Lee S, Kuninaka S, Saya H, Lee H, Lee S & Lim D-S (2013) cAMP/PKA signalling reinforces the LATS-YAP pathway to fully suppress YAP in response to actin cytoskeletal changes. *EMBO J.* **32:** 1543–55

Kimura Y, Yashiroda H, Kudo T, Koitabashi S, Murata S, Kakizuka A & Tanaka K (2009) An inhibitor of a deubiquitinating enzyme regulates ubiquitin homeostasis. *Cell* **137:** 549–59

Kirkin V, McEwan DG, Novak I & Dikic I (2009) A role for ubiquitin in selective autophagy. *Mol. Cell* **34:** 259–69

Kirschner LS, Carney JA, Pack SD, Taymans SE, Giatzakis C, Cho YS, Cho-Chung YS & Stratakis CA (2000) Mutations of the gene encoding the protein kinase A type I-alpha regulatory subunit in patients with the Carney complex. *Nat. Genet.* **26:** 89–92

Klionsky DJ (2005) Autophagy. *Curr. Biol.* **15:** R282–3

Klionsky DJ, Cregg JM, Dunn WA, Emr SD, Sakai Y, Sandoval I V, Sibirny A, Subramani S, Thumm M, Veenhuis M & Ohsumi Y (2003) A unified nomenclature for yeast autophagy-related genes. *Dev. Cell* **5:** 539–45

Klionsky DJ & Schulman BA (2014) Dynamic regulation of macroautophagy by distinctive ubiquitin-like proteins. *Nat. Struct. Mol. Biol.* **21:** 336–45

Klussmann E, Edemir B, Pepperle B, Tamma G, Henn V, Klauschenz E, Hundsrucker C, Maric K & Rosenthal W (2001) Ht31: the first protein kinase A anchoring protein to integrate protein kinase A and Rho signaling. *FEBS Lett.* **507:** 264–8

Klussmann E, Maric K, Wiesner B, Beyermann M & Rosenthal W (1999) Protein kinase A anchoring proteins are required for vasopressin-mediated translocation of aquaporin-2 into cell membranes of renal principal cells. *J. Biol. Chem.* **274:** 4934–8

Knight JD & Kothary R (2011) The myogenic kinome: protein kinases critical to mammalian skeletal myogenesis. *Skelet. Muscle* **1:** 29

Komander D, Clague MJ & Urbé S (2009a) Breaking the chains: structure and function of the deubiquitinases. *Nat. Rev. Mol. Cell Biol.* **10:** 550–563

Komander D & Rape M (2012) The ubiquitin code. *Annu. Rev. Biochem.* **81:** 203–29

Komander D, Reyes-Turcu F, Licchesi JDF, Odenwaelder P, Wilkinson KD & Barford D (2009b) Molecular discrimination of structurally equivalent Lys 63-linked and linear polyubiquitin chains. *EMBO Rep.* **10:** 466–73

Kool M, Korshunov A, Remke M, Jones DTW, Schlanstein M, Northcott PA, Cho Y-J, Koster J, Schouten-van Meeteren A, van Vuurden D, Clifford SC, Pietsch T, von Bueren AO, Rutkowski S, McCabe M, Collins VP, Bäcklund ML, Haberler C, Bourdeaut F, Delattre O, et al (2012) Molecular subgroups of medulloblastoma: an international meta-analysis of transcriptome, genetic aberrations, and clinical data of WNT, SHH, Group 3, and Group 4 medulloblastomas. *Acta Neuropathol.* **123:** 473–84

Kozma R, Ahmed S, Best A & Lim L (1996) The GTPase-activating protein n-chimaerin cooperates with Rac1 and Cdc42Hs to induce the formation of lamellipodia and filopodia. *Mol. Cell. Biol.* **16:** 5069–80

Krebs EG & Fischer EH (1956) The phosphorylase b to a converting enzyme of rabbit skeletal muscle. *Biochim. Biophys. Acta* **20:** 150–7

Krupinski J, Coussen F, Bakalyar HA, Tang WJ, Feinstein PG, Orth K, Slaughter C, Reed RR & Gilman AG (1989) Adenylyl cyclase amino acid sequence: possible channel- or transporter-like structure. *Science* **244:** 1558–64

Kulathu Y & Komander D (2012) Atypical ubiquitylation - the unexplored world of polyubiquitin beyond Lys48 and Lys63 linkages. *Nat. Rev. Mol. Cell Biol.* **13:** 508–23

Kunz JB, Schwarz H & Mayer A (2004) Determination of four sequential stages during microautophagy in vitro. *J. Biol. Chem.* **279:** 9987–96

Kvissel A-K, Ørstavik S, Eikvar S, Brede G, Jahnsen T, Collas P, Akusjärvi G & Skålhegg BS (2007) Involvement of the catalytic subunit of protein kinase A and of HA95 in pre-mRNA splicing. *Exp. Cell Res.* **313:** 2795–809

Lam YW, Lamond AI, Mann M & Andersen JS (2007) Analysis of nucleolar protein dynamics reveals the nuclear degradation of ribosomal proteins. *Curr. Biol.* **17:** 749–60

Lang P, Gesbert F, Delespine-Carmagnat M, Stancou R, Pouchelet M & Bertoglio J (1996) Protein kinase A phosphorylation of RhoA mediates the morphological and functional effects of cyclic AMP in cytotoxic lymphocytes. *EMBO J.* **15:** 510–9

Langan TA (1969) Phosphorylation of liver histone following the administration of glucagon and insulin. *Proc. Natl. Acad. Sci. U. S. A.* **64:** 1276–83

Lauwers E, Jacob C & André B (2009) K63-linked ubiquitin chains as a specific signal for protein sorting into the multivesicular body pathway. *J. Cell Biol.* **185:** 493–502

Lawler OA, Miggin SM & Kinsella BT (2001) Protein kinase A-mediated phosphorylation of serine 357 of the mouse prostacyclin receptor regulates its coupling to G(s)-, to G(i)-, and to G(q)-coupled effector signaling. *J. Biol. Chem.* **276:** 33596–607

Lazarou M, Sliter DA, Kane LA, Sarraf SA, Wang C, Burman JL, Sideris DP, Fogel AI & Youle RJ (2015) The ubiquitin kinase PINK1 recruits autophagy receptors to induce mitophagy. *Nature* **524:** 309–14

Lee MJ, Lee B-H, Hanna J, King RW & Finley D (2011) Trimming of ubiquitin chains by

proteasome-associated deubiquitinating enzymes. *Mol. Cell. Proteomics* **10:** R110.003871

Lee S, Rahnenführer J, Lang M, De Preter K, Mestdagh P, Koster J, Versteeg R, Stallings RL, Varesio L, Asgharzadeh S, Schulte JH, Fielitz K, Schwermer M, Morik K & Schramm A (2014) Robust selection of cancer survival signatures from high-throughput genomic data using two-fold subsampling. *PLoS One* **9:** e108818

Li M, Brooks CL, Wu-Baer F, Chen D, Baer R & Gu W (2003) Mono- versus polyubiquitination: differential control of p53 fate by Mdm2. *Science* **302:** 1972–5

Li S, Chen Y, Shi Q, Yue T, Wang B & Jiang J (2012) Hedgehog-regulated ubiquitination controls smoothened trafficking and cell surface expression in Drosophila. *PLoS Biol.* **10:** e1001239

Li W, Bengtson MH, Ulbrich A, Matsuda A, Reddy VA, Orth A, Chanda SK, Batalov S & Joazeiro CAP (2008) Genome-wide and functional annotation of human E3 ubiquitin ligases identifies MULAN, a mitochondrial E3 that regulates the organelle's dynamics and signaling. *PLoS One* **3:** e1487

Li X, Amazit L, Long W, Lonard DM, Monaco JJ & O'Malley BW (2007) Ubiquitin- and ATP-independent proteolytic turnover of p21 by the REGgamma-proteasome pathway. *Mol. Cell* **26:** 831–42

Li X, Lonard DM, Jung SY, Malovannaya A, Feng Q, Qin J, Tsai SY, Tsai M-J & O'Malley BW (2006) The SRC-3/AIB1 coactivator is degraded in a ubiquitin- and ATP-independent manner by the REGgamma proteasome. *Cell* **124:** 381–92

Liang J-R, Martinez A, Lane JD, Mayor U, Clague MJ & Urbé S (2015) USP30 deubiquitylates mitochondrial Parkin substrates and restricts apoptotic cell death. *EMBO Rep.* **16:** 618–27

Libby P & Goldberg AL (1978) Leupeptin, a protease inhibitor, decreases protein degradation in normal and diseased muscles. *Science* **199:** 534–6

Lignitto L, Carlucci A, Sepe M, Stefan E, Cuomo O, Nisticò R, Scorziello A, Savoia C, Garbi C, Annunziato L & Feliciello A (2011) Control of PKA stability and signalling by the RING ligase praja2. *Nat. Cell Biol.* **13:** 412–22

Lim CJ, Han J, Yousefi N, Ma Y, Amieux PS, McKnight GS, Taylor SS & Ginsberg MH (2007) Alpha4 integrins are type I cAMP-dependent protein kinase-anchoring proteins. *Nat. Cell Biol.* **9:** 415–421

Lim CJ, Kain KH, Tkachenko E, Goldfinger LE, Gutierrez E, Allen MD, Groisman A, Zhang J & Ginsberg MH (2008) Integrin-mediated protein kinase A activation at the leading edge of migrating cells. *Mol. Biol. Cell* **19:** 4930–41

Liu H, Urbé S & Clague MJ (2012) Selective protein degradation in cell signalling. *Semin. Cell Dev. Biol.* **23:** 509–14

Liu S, Lai L, Zuo Q, Dai F, Wu L, Wang Y, Zhou Q, Liu J, Liu J, Li L, Lin Q, Creighton CJ, Costello MG, Huang S, Jia C, Liao L, Luo H, Fu J, Liu M, Yi Z, et al (2014) PKA turnover by the REGγ-proteasome modulates FoxO1 cellular activity and VEGF-

induced angiogenesis. *J. Mol. Cell. Cardiol.* **72:** 28–38

Lloyd TE, Atkinson R, Wu MN, Zhou Y, Pennetta G & Bellen HJ (2002) Hrs regulates endosome membrane invagination and tyrosine kinase receptor signaling in Drosophila. *Cell* **108:** 261–9

Lodish M & Stratakis CA (2016) A genetic and molecular update on adrenocortical causes of Cushing syndrome. *Nat. Rev. Endocrinol.* **12:** 255–262

Logue JS, Whiting JL & Scott JD (2011a) Sequestering Rac with PKA confers cAMP control of cytoskeletal remodeling. *Small GTPases* **2:** 173–176

Logue JS, Whiting JL, Tunquist B, Langeberg LK & Scott JD (2011b) Anchored protein kinase A recruitment of active Rac GTPase. *J. Biol. Chem.* **286:** 22113–21

Loilome W, Juntana S, Namwat N, Bhudhisawasdi V, Puapairoj A, Sripa B, Miwa M, Saya H, Riggins GJ & Yongvanit P (2011) PRKAR1A is overexpressed and represents a possible therapeutic target in human cholangiocarcinoma. *Int. J. cancer* **129:** 34–44

Lokireddy S, Kukushkin NV & Goldberg AL (2015) cAMP-induced phosphorylation of 26S proteasomes on Rpn6/PSMD11 enhances their activity and the degradation of misfolded proteins. *Proc. Natl. Acad. Sci. U. S. A.* **112:** E7176–85

Lorimer IA, Mason ME & Sanwal BD (1987) Levels of type I cAMP-dependent protein kinase regulatory subunit are regulated by changes in turnover rate during skeletal myogenesis. *J. Biol. Chem.* **262:** 17200–5

Lorimer IA & Sanwal BD (1989) Regulation of cyclic AMP-dependent protein kinase levels during skeletal myogenesis. *Biochem. J.* **264:** 305–8

Lu Q, Hope LW, Brasch M, Reinhard C & Cohen SN (2003) TSG101 interaction with HRS mediates endosomal trafficking and receptor down-regulation. *Proc. Natl. Acad. Sci. U. S. A.* **100:** 7626–31

Lu Z & Hunter T (2009) Degradation of activated protein kinases by ubiquitination. *Annu. Rev. Biochem.* **78:** 435–75

Luzio JP, Gray SR & Bright NA (2010) Endosome-lysosome fusion. *Biochem. Soc. Trans.* **38:** 1413–6

MacDonald BT, Tamai K & He X (2009) Wnt/beta-catenin signaling: components, mechanisms, and diseases. *Dev. Cell* **17:** 9–26

MacDonald E, Urbé S & Clague MJ (2014) USP8 controls the trafficking and sorting of lysosomal enzymes. *Traffic* **15:** 879–88

Machacek M, Hodgson L, Welch C, Elliott H, Pertz O, Nalbant P, Abell A, Johnson GL, Hahn KM & Danuser G (2009) Coordination of Rho GTPase activities during cell protrusion. *Nature* **461:** 99–103

Machesky LM & Insall RH (1998) Scar1 and the related Wiskott-Aldrich syndrome protein, WASP, regulate the actin cytoskeleton through the Arp2/3 complex. *Curr. Biol.* **8:** 1347–56

Malbon CC, Tao J & Wang H (2004) AKAPs (A-kinase anchoring proteins) and molecules that compose their G-protein-coupled receptor signalling complexes. *Biochem. J.* **379:**

1–9

Malerød L, Pedersen NM, Sem Wegner CE, Lobert VH, Leithe E, Brech A, Rivedal E, Liestøl K & Stenmark H (2011) Cargo-dependent degradation of ESCRT-I as a feedback mechanism to modulate endosomal sorting. *Traffic* **12:** 1211–26

Mamo A, Jules F, Dumaresq-Doiron K, Costantino S & Lefrancois S (2012) The role of ceroid lipofuscinosis neuronal protein 5 (CLN5) in endosomal sorting. *Mol. Cell. Biol.* **32:** 1855–66

Manna PR, Stetson CL, Slominski AT & Pruitt K (2015) Role of the steroidogenic acute regulatory protein in health and disease. *Endocrine* **51:** 7–21

Manning G, Whyte DB, Martinez R, Hunter T & Sudarsanam S (2002) The protein kinase complement of the human genome. *Science* **298:** 1912–34

Mantovani G, Bondioni S, Lania AG, Rodolfo M, Peverelli E, Polentarutti N, Veliz Rodriguez T, Ferrero S, Bosari S, Beck-Peccoz P & Spada A (2008) High expression of PKA regulatory subunit 1A protein is related to proliferation of human melanoma cells. *Oncogene* **27:** 1834–43

Marzella L, Ahlberg J & Glaumann H (1981) Autophagy, heterophagy, microautophagy and crinophagy as the means for intracellular degradation. *Virchows Arch. B. Cell Pathol. Incl. Mol. Pathol.* **36:** 219–34

Matsumoto ML, Wickliffe KE, Dong KC, Yu C, Bosanac I, Bustos D, Phu L, Kirkpatrick DS, Hymowitz SG, Rape M, Kelley RF & Dixit VM (2010) K11-linked polyubiquitination in cell cycle control revealed by a K11 linkage-specific antibody. *Mol. Cell* **39:** 477–84

Mazzucchelli C & Sassone-Corsi P (1999) The inducible cyclic adenosine monophosphate early repressor (ICER) in the pituitary intermediate lobe: role in the stress response. *Mol. Cell. Endocrinol.* **155:** 101–13

McCullough J, Clague MJ & Urbé S (2004) AMSH is an endosome-associated ubiquitin isopeptidase. *J. Cell Biol.* **166:** 487–92

McCullough J, Row PE, Lorenzo O, Doherty M, Beynon R, Clague MJ & Urbé S (2006) Activation of the endosome-associated ubiquitin isopeptidase AMSH by STAM, a component of the multivesicular body-sorting machinery. *Curr. Biol.* **16:** 160–5

McDaid HM, Cairns MT, Atkinson RJ, McAleer S, Harkin DP, Gilmore P & Johnston PG (1999) Increased expression of the RIalpha subunit of the cAMP-dependent protein kinase A is associated with advanced stage ovarian cancer. *Br. J. Cancer* **79:** 933–9

Mehta ZB, Pietka G & Lowe M (2014) The cellular and physiological functions of the Lowe syndrome protein OCRL1. *Traffic* **15:** 471–87

de Melker AA, van der Horst G, Calafat J, Jansen H & Borst J (2001) c-Cbl ubiquitinates the EGF receptor at the plasma membrane and remains receptor associated throughout the endocytic route. *J. Cell Sci.* **114:** 2167–78

Mellacheruvu D, Wright Z, Couzens AL, Lambert J-P, St-Denis NA, Li T, Miteva Y V, Hauri S, Sardiu ME, Low TY, Halim VA, Bagshaw RD, Hubner NC, Al-Hakim A, Bouchard A, Faubert D, Fermin D, Dunham WH, Goudreault M, Lin Z-Y, et al (2013) The

CRAPome: a contaminant repository for affinity purification-mass spectrometry data. *Nat. Methods* **10:** 730–6

Metcalfe C & Bienz M (2011) Inhibition of GSK3 by Wnt signalling--two contrasting models. *J. Cell Sci.* **124:** 3537–44

Metzger H & Lindner E (1981) The positive inotropic-acting forskolin, a potent adenylate cyclase activator. *Arzneimittelforschung.* **31:** 1248–50

Metzger MB, Pruneda JN, Klevit RE & Weissman AM (2014) RING-type E3 ligases: master manipulators of E2 ubiquitin-conjugating enzymes and ubiquitination. *Biochim. Biophys. Acta* **1843:** 47–60

Mevissen TET, Hospenthal MK, Geurink PP, Elliott PR, Akutsu M, Arnaudo N, Ekkebus R, Kulathu Y, Wauer T, El Oualid F, Freund SM V, Ovaa H & Komander D (2013) OTU deubiquitinases reveal mechanisms of linkage specificity and enable ubiquitin chain restriction analysis. *Cell* **154:** 169–84

Mi K, Dolan PJ & Johnson GVW (2006) The low density lipoprotein receptor-related protein 6 interacts with glycogen synthase kinase 3 and attenuates activity. *J. Biol. Chem.* **281:** 4787–94

Mick DU, Rodrigues RB, Leib RD, Adams CM, Chien AS, Gygi SP & Nachury M V. (2015) Proteomics of Primary Cilia by Proximity Labeling. *Dev. Cell* **35:** 497–512

Miki H, Suetsugu S & Takenawa T (1998) WAVE, a novel WASP-family protein involved in actin reorganization induced by Rac. *EMBO J.* **17:** 6932–41

Miller WR (2002) Regulatory subunits of PKA and breast cancer. *Ann. N. Y. Acad. Sci.* **968:** 37–48

Mirzaei H, Rogers RS, Grimes B, Eng J, Aderem A & Aebersold R (2010) Characterizing the connectivity of poly-ubiquitin chains by selected reaction monitoring mass spectrometry. *Mol. Biosyst.* **6:** 2004–14

Mizuno E, Kawahata K, Kato M, Kitamura N & Komada M (2003) STAM proteins bind ubiquitinated proteins on the early endosome via the VHS domain and ubiquitin-interacting motif. *Mol. Biol. Cell* **14:** 3675–89

Mizushima N, Yoshimori T & Ohsumi Y (2011) The role of Atg proteins in autophagosome formation. *Annu. Rev. Cell Dev. Biol.* **27:** 107–32

Molina CA, Foulkes NS, Lalli E & Sassone-Corsi P (1993) Inducibility and negative autoregulation of CREM: an alternative promoter directs the expression of ICER, an early response repressor. *Cell* **75:** 875–86

Montarras D, L'honoré A & Buckingham M (2013) Lying low but ready for action: the quiescent muscle satellite cell. *FEBS J.* **280:** 4036–50

Montminy MR, Sevarino KA, Wagner JA, Mandel G & Goodman RH (1986) Identification of a cyclic-AMP-responsive element within the rat somatostatin gene. *Proc. Natl. Acad. Sci. U. S. A.* **83:** 6682–6

Morris JR & Solomon E (2004) BRCA1 : BARD1 induces the formation of conjugated ubiquitin structures, dependent on K6 of ubiquitin, in cells during DNA replication and

repair. *Hum. Mol. Genet.* **13:** 807–17

Mukai A & Hashimoto N (2008) Localized cyclic AMP-dependent protein kinase activity is required for myogenic cell fusion. *Exp. Cell Res.* **314:** 387–97

Mukhopadhyay S, Wen X, Ratti N, Loktev A, Rangell L, Scales SJ & Jackson PK (2013) The ciliary G-protein-coupled receptor Gpr161 negatively regulates the sonic hedgehog pathway via cAMP signaling. *Cell* **152:** 210–223

Murray AJ (2008) Pharmacological PKA inhibition: all may not be what it seems. *Sci. Signal.* **1:** re4

Nakamura N & Hirose S (2008) Regulation of mitochondrial morphology by USP30, a deubiquitinating enzyme present in the mitochondrial outer membrane. *Mol. Biol. Cell* **19:** 1903–11

Nathan JA, Kim HT, Ting L, Gygi SP & Goldberg AL (2013) Why do cellular proteins linked to K63-polyubiquitin chains not associate with proteasomes? *EMBO J.* **32:** 552–65

Nedvetsky PI, Tamma G, Beulshausen S, Valenti G, Rosenthal W & Klussmann E (2009) Regulation of aquaporin-2 trafficking. *Handb. Exp. Pharmacol.***:** 133–57

Nesterova M & Cho-Chung YS (1995) A single-injection protein kinase A-directed antisense treatment to inhibit tumour growth. *Nat. Med.* **1:** 528–33

Nesterova M, Noguchi K, Park YG, Lee YN & Cho-Chung YS (2000) Compensatory stabilization of RIIbeta protein, cell cycle deregulation, and growth arrest in colon and prostate carcinoma cells by antisense-directed down-regulation of protein kinase A RIalpha protein. *Clin. Cancer Res.* **6:** 3434–41

Nesterova M, Yokozaki H, McDuffie E & Cho-Chung YS (1996) Overexpression of RII beta regulatory subunit of protein kinase A in human colon carcinoma cell induces growth arrest and phenotypic changes that are abolished by site-directed mutation of RII beta. *Eur. J. Biochem.* **235:** 486–94

Nielsen ML, Vermeulen M, Bonaldi T, Cox J, Moroder L & Mann M (2008) Iodoacetamide-induced artifact mimics ubiquitination in mass spectrometry. *Nat. Methods* **5:** 459–60

Niewiadomski P, Kong J, Ahrends R, Ma Y, Humke E, Khan S, Teruel M, Novitch B & Rohatgi R (2014) Gli protein activity is controlled by multisite phosphorylation in vertebrate hedgehog signaling. *Cell Rep.* **6:** 168–181

van Nocker S, Sadis S, Rubin DM, Glickman M, Fu H, Coux O, Wefes I, Finley D & Vierstra RD (1996) The multiubiquitin-chain-binding protein Mcb1 is a component of the 26S proteasome in Saccharomyces cerevisiae and plays a nonessential, substrate-specific role in protein turnover. *Mol. Cell. Biol.* **16:** 6020–8

O'Hayre M, Vázquez-Prado J, Kufareva I, Stawiski EW, Handel TM, Seshagiri S & Gutkind JS (2013) The emerging mutational landscape of G proteins and G-protein-coupled receptors in cancer. *Nat. Rev. Cancer* **13:** 412–24

Ogden SK, Fei DL, Schilling NS, Ahmed YF, Hwa J & Robbins DJ (2008) G protein Galphai functions immediately downstream of Smoothened in Hedgehog signalling. *Nature* **456:** 967–70

Okada H, Uezu A, Mason FM, Soderblom EJ, Moseley MA & Soderling SH (2011) SH3 domain-based phototrapping in living cells reveals Rho family GAP signaling complexes. *Sci. Signal.* **4:** rs13

Olsen J V, Ong S-E & Mann M (2004) Trypsin cleaves exclusively C-terminal to arginine and lysine residues. *Mol. Cell. Proteomics* **3:** 608–14

Omori K & Kotera J (2007) Overview of PDEs and their regulation. *Circ. Res.* **100:** 309–27

Ong S-E, Blagoev B, Kratchmarova I, Kristensen DB, Steen H, Pandey A & Mann M (2002) Stable isotope labeling by amino acids in cell culture, SILAC, as a simple and accurate approach to expression proteomics. *Mol. Cell. Proteomics* **1:** 376–86

Ong S-E & Mann M (2007) Stable isotope labeling by amino acids in cell culture for quantitative proteomics. *Methods Mol. Biol.* **359:** 37–52

Ordureau A, Heo J-M, Duda DM, Paulo JA, Olszewski JL, Yanishevski D, Rinehart J, Schulman BA & Harper JW (2015) Defining roles of PARKIN and ubiquitin phosphorylation by PINK1 in mitochondrial quality control using a ubiquitin replacement strategy. *Proc. Natl. Acad. Sci. U. S. A.* **112:** 6637–42

Ørstavik S, Reinton N, Frengen E, Langeland BT, Jahnsen T & Skålhegg BS (2001) Identification of novel splice variants of the human catalytic subunit Cbeta of cAMP-dependent protein kinase. *Eur. J. Biochem.* **268:** 5066–73

Ott C & Lippincott-Schwartz J (2012) Visualization of live primary cilia dynamics using fluorescence microscopy. *Curr. Protoc. Cell Biol.* **Chapter 4:** Unit 4.26

Pal K, Hwang S-H, Somatilaka B, Badgandi H, Jackson PK, DeFea K & Mukhopadhyay S (2016) Smoothened determines β-arrestin-mediated removal of the G protein-coupled receptor Gpr161 from the primary cilium. *J. Cell Biol.* **212:** 861–75

Pan Y, Wang C & Wang B (2009) Phosphorylation of Gli2 by protein kinase A is required for Gli2 processing and degradation and the Sonic Hedgehog-regulated mouse development. *Dev. Biol.* **326:** 177–89

Pattabiraman DR, Bierie B, Kober KI, Thiru P, Krall J a., Zill C, Reinhardt F, Tam WL & Weinberg R a. (2016) Activation of PKA leads to mesenchymal-to-epithelial transition and loss of tumor-initiating ability. *Science (80-.).* **351:** aad3680–aad3680

Paulucci-Holthauzen A a, Vergara L a, Bellot LJ, Canton D, Scott JD & O'Connor KL (2009) Spatial distribution of protein kinase A activity during cell migration is mediated by A-kinase anchoring protein AKAP Lbc. *J. Biol. Chem.* **284:** 5956–67

Pearce LR, Komander D & Alessi DR (2010) The nuts and bolts of AGC protein kinases. *Nat. Rev. Mol. Cell Biol.* **11:** 9–22

Peng J, Schwartz D, Elias JE, Thoreen CC, Cheng D, Marsischky G, Roelofs J, Finley D & Gygi SP (2003) A proteomics approach to understanding protein ubiquitination. *Nat. Biotechnol.* **21:** 921–6

Petersen TN, Brunak S, von Heijne G & Nielsen H (2011) SignalP 4.0: discriminating signal peptides from transmembrane regions. *Nat. Methods* **8:** 785–6

Petroski MD & Deshaies RJ (2005) Function and regulation of cullin-RING ubiquitin ligases.

Nat. Rev. Mol. Cell Biol. **6:** 9–20

Piao S, Lee S-H, Kim H, Yum S, Stamos JL, Xu Y, Lee S-J, Lee J, Oh S, Han J-K, Park B-J, Weis WI & Ha N-C (2008) Direct inhibition of GSK3beta by the phosphorylated cytoplasmic domain of LRP6 in Wnt/beta-catenin signaling. *PLoS One* **3:** e4046

Pickart CM & Eddins MJ (2004) Ubiquitin: structures, functions, mechanisms. *Biochim. Biophys. Acta* **1695:** 55–72

Pierce KL, Premont RT & Lefkowitz RJ (2002) Seven-transmembrane receptors. *Nat. Rev. Mol. Cell Biol.* **3:** 639–50

Poole B, Ohkuma S & Warburton MJ (1977) The accumulation of weakly basic substances in lysosomes and the inhibition of intracellular protein degradation. *Acta Biol. Med. Ger.* **36:** 1777–88

Pourquié O (2005) Signal transduction: a new canon. *Nature* **433:** 208–9

Prag G, Watson H, Kim YC, Beach BM, Ghirlando R, Hummer G, Bonifacino JS & Hurley JH (2007) The Vps27/Hse1 complex is a GAT domain-based scaffold for ubiquitin-dependent sorting. *Dev. Cell* **12:** 973–86

Qiao J, Holian O, Lee B-S, Huang F, Zhang J & Lum H (2008) Phosphorylation of GTP dissociation inhibitor by PKA negatively regulates RhoA. *Am. J. Physiol. Cell Physiol.* **295:** C1161–8

Qiu X-B, Ouyang S-Y, Li C-J, Miao S, Wang L & Goldberg AL (2006) hRpn13/ADRM1/GP110 is a novel proteasome subunit that binds the deubiquitinating enzyme, UCH37. *EMBO J.* **25:** 5742–53

Rabinovitz M & Fisher JM (1964) Characteristics Of The Inhibition Of Hemoglobin Synthesis In Rabbit Reticulocytes By Threo-Alpha-Amino-Beta-Chlorobutyric Acid. *Biochim. Biophys. Acta* **91:** 313–22

Rack PG, Ni J, Payumo AY, Nguyen V, Crapster JA, Hovestadt V, Kool M, Jones DTW, Mich JK, Firestone AJ, Pfister SM, Cho Y-J & Chen JK (2014) Arhgap36-dependent activation of Gli transcription factors. *Proc. Natl. Acad. Sci. U. S. A.* **111:** 11061–6

Raftopoulou M & Hall A (2004) Cell migration: Rho GTPases lead the way. *Dev. Biol.* **265:** 23–32

Raiborg C, Bache KG, Gillooly DJ, Madshus IH, Stang E & Stenmark H (2002) Hrs sorts ubiquitinated proteins into clathrin-coated microdomains of early endosomes. *Nat. Cell Biol.* **4:** 394–8

Raiborg C, Bremnes B, Mehlum A, Gillooly DJ, D'Arrigo A, Stang E & Stenmark H (2001) FYVE and coiled-coil domains determine the specific localisation of Hrs to early endosomes. *J. Cell Sci.* **114:** 2255–63

Ramachandran J, Tsubokawa M & Gohil K (1987) Corticotropin receptors. *Ann. N. Y. Acad. Sci.* **512:** 415–25

Ranieri N, Thérond PP & Ruel L (2014) Switch of PKA substrates from Cubitus interruptus to Smoothened in the Hedgehog signalosome complex. *Nat. Commun.* **5:** 5034

Rannels SR, Cobb CE, Landiss LR & Corbin JD (1985) The regulatory subunit monomer of

cAMP-dependent protein kinase retains the salient kinetic properties of the native dimeric subunit. *J. Biol. Chem.* **260:** 3423–30

Rappsilber J, Ishihama Y & Mann M (2003) Stop and go extraction tips for matrix-assisted laser desorption/ionization, nanoelectrospray, and LC/MS sample pretreatment in proteomics. *Anal. Chem.* **75:** 663–70

Razani B & Lisanti MP (2001) Two distinct caveolin-1 domains mediate the functional interaction of caveolin-1 with protein kinase A. *Am. J. Physiol. Cell Physiol.* **281:** C1241–50

Razani B, Rubin CS & Lisanti MP (1999) Regulation of cAMP-mediated signal transduction via interaction of caveolins with the catalytic subunit of protein kinase A. *J. Biol. Chem.* **274:** 26353–60

Reggiori F & Klionsky DJ (2002) Autophagy in the eukaryotic cell. *Eukaryot. Cell* **1:** 11–21

Reimann EM, Brostrom CO, Corbin JD, King CA & Krebs EG (1971) Separation of regulatory and catalytic subunits of the cyclic 3',5'-adenosine monophosphate-dependent protein kinase(s) of rabbit skeletal muscle. *Biochem. Biophys. Res. Commun.* **42:** 187–94

Ren X & Hurley JH (2010) VHS domains of ESCRT-0 cooperate in high-avidity binding to polyubiquitinated cargo. *EMBO J.* **29:** 1045–54

Richardson JM, Howard P, Massa JS & Maurer RA (1990a) Post-transcriptional regulation of cAMP-dependent protein kinase activity by cAMP in GH3 pituitary tumor cells. Evidence for increased degradation of catalytic subunit in the presence of cAMP. *J. Biol. Chem.* **265:** 13635–40

Richardson M, Massa S & Maurer A (1990b) Post-transcriptional Regulation of CAMP-dependent Activity by CAMP in GH3 Pituitary Tumor Cells Protein Kinase. **265:** 13635–13640

Ridley AJ (2001) Rho GTPases and cell migration. *J. Cell Sci.* **114:** 2713–22

Ridley AJ & Hall A (1992) The small GTP-binding protein rho regulates the assembly of focal adhesions and actin stress fibers in response to growth factors. *Cell* **70:** 389–99

Riobo NA, Saucy B, Dilizio C & Manning DR (2006) Activation of heterotrimeric G proteins by Smoothened. *Proc. Natl. Acad. Sci. U. S. A.* **103:** 12607–12

Rittinger K, Walker PA, Eccleston JF, Nurmahomed K, Owen D, Laue E, Gamblin SJ & Smerdon SJ (1997) Crystal structure of a small G protein in complex with the GTPase-activating protein rhoGAP. *Nature* **388:** 693–7

Robinson-Steiner AM, Beebe SJ, Rannels SR & Corbin JD (1984) Microheterogeneity of type II cAMP-dependent protein kinase in various mammalian species and tissues. *J. Biol. Chem.* **259:** 10596–605

de Rooij J, Zwartkruis FJ, Verheijen MH, Cool RH, Nijman SM, Wittinghofer A & Bos JL (1998) Epac is a Rap1 guanine-nucleotide-exchange factor directly activated by cyclic AMP. *Nature* **396:** 474–7

Rossman KL, Der CJ & Sondek J (2005) GEF means go: turning on RHO GTPases with

guanine nucleotide-exchange factors. *Nat. Rev. Mol. Cell Biol.* **6:** 167–180

Row PE, Liu H, Hayes S, Welchman R, Charalabous P, Hofmann K, Clague MJ, Sanderson CM & Urbé S (2007) The MIT domain of UBPY constitutes a CHMP binding and endosomal localization signal required for efficient epidermal growth factor receptor degradation. *J. Biol. Chem.* **282:** 30929–37

Row PE, Prior IA, McCullough J, Clague MJ & Urbé S (2006) The ubiquitin isopeptidase UBPY regulates endosomal ubiquitin dynamics and is essential for receptor down-regulation. *J. Biol. Chem.* **281:** 12618–24

Sachse M, Strous GJ & Klumperman J (2004) ATPase-deficient hVPS4 impairs formation of internal endosomal vesicles and stabilizes bilayered clathrin coats on endosomal vacuoles. *J. Cell Sci.* **117:** 1699–708

Sahtoe DD, van Dijk WJ, El Oualid F, Ekkebus R, Ovaa H & Sixma TK (2015) Mechanism of UCH-L5 activation and inhibition by DEUBAD domains in RPN13 and INO80G. *Mol. Cell* **57:** 887–900

Sahu R, Kaushik S, Clement CC, Cannizzo ES, Scharf B, Follenzi A, Potolicchio I, Nieves E, Cuervo AM & Santambrogio L (2011) Microautophagy of cytosolic proteins by late endosomes. *Dev. Cell* **20:** 131–9

Salpea P & Stratakis CA (2014) Carney complex and McCune Albright syndrome: an overview of clinical manifestations and human molecular genetics. *Mol. Cell. Endocrinol.* **386:** 85–91

Salvador N, Aguado C, Horst M & Knecht E (2000) Import of a cytosolic protein into lysosomes by chaperone-mediated autophagy depends on its folding state. *J. Biol. Chem.* **275:** 27447–56

Sample V, DiPilato LM, Yang JH, Ni Q, Saucerman JJ & Zhang J (2012) Regulation of nuclear PKA revealed by spatiotemporal manipulation of cyclic AMP. *Nat. Chem. Biol.* **8:** 375–82

Sandilands E, Serrels B, McEwan DG, Morton JP, Macagno JP, McLeod K, Stevens C, Brunton VG, Langdon WY, Vidal M, Sansom OJ, Dikic I, Wilkinson S & Frame MC (2011) Autophagic targeting of Src promotes cancer cell survival following reduced FAK signalling. *Nat. Cell Biol.* **14:** 51–60

Sandilands E, Serrels B, Wilkinson S & Frame MC (2012) Src-dependent autophagic degradation of Ret in FAK-signalling-defective cancer cells. *EMBO Rep.* **13:** 733–40

Sapio L, Maiolo F Di, Illiano M, Esposito A, Chiosi E, Spina A & Naviglio S (2014) Targeting Protein Kinase A In Cancer Therapy : An Update. **:** 843–855

Sastri M, Barraclough DM, Carmichael PT & Taylor SS (2005) A-kinase-interacting protein localizes protein kinase A in the nucleus. *Proc. Natl. Acad. Sci. U. S. A.* **102:** 349–54

Sato Y, Maekawa S, Ishii R, Sanada M, Morikawa T, Shiraishi Y, Yoshida K, Nagata Y, Sato-Otsubo A, Yoshizato T, Suzuki H, Shiozawa Y, Kataoka K, Kon A, Aoki K, Chiba K, Tanaka H, Kume H, Miyano S, Fukayama M, et al (2014) Recurrent somatic mutations underlie corticotropin-independent Cushing's syndrome. *Science* **344:** 917–

20

Savukoski M, Klockars T, Holmberg V, Santavuori P, Lander ES & Peltonen L (1998) CLN5, a novel gene encoding a putative transmembrane protein mutated in Finnish variant late infantile neuronal ceroid lipofuscinosis. *Nat. Genet.* **19:** 286–8

Schiebel K, Winkelmann M, Mertz A, Xu X, Page DC, Weil D, Petit C & Rappold GA (1997) Abnormal XY interchange between a novel isolated protein kinase gene, PRKY, and its homologue, PRKX, accounts for one third of all (Y+)XX males and (Y-)XY females. *Hum. Mol. Genet.* **6:** 1985–9

Schmiedt M-L, Bessa C, Heine C, Ribeiro MG, Jalanko A & Kyttälä A (2010) The neuronal ceroid lipofuscinosis protein CLN5: new insights into cellular maturation, transport, and consequences of mutations. *Hum. Mutat.* **31:** 356–65

Schneider DL (1981) ATP-dependent acidification of intact and disrupted lysosomes. Evidence for an ATP-driven proton pump. *J. Biol. Chem.* **256:** 3858–64

Schoenheimer R, Ratner S & Rittenberg D (1939) The Process Of Continuous Deamination And Reamination Of Amino Acids In The Proteins Of Normal Animals. *Science* **89:** 272–3

Schrier RW (2011) Use of diuretics in heart failure and cirrhosis. *Semin. Nephrol.* **31:** 503–12

Schwanhäusser B, Busse D, Li N, Dittmar G, Schuchhardt J, Wolf J, Chen W & Selbach M (2011) Global quantification of mammalian gene expression control. *Nature* **473:** 337–42

Scifo E, Szwajda A, Debski J, Uusi-Rauva K, Kesti T, Dadlez M, Gingras AC, Tyynel?? J, Baumann MH, Jalanko A & Lalowski M (2013) Drafting the CLN3 protein interactome in SH-SY5Y human neuroblastoma cells: A label-free quantitative proteomics approach. *J. Proteome Res.* **12:** 2101–2115

Scott D, Oldham NJ, Strachan J, Searle MS & Layfield R (2015) Ubiquitin-binding domains: mechanisms of ubiquitin recognition and use as tools to investigate ubiquitin-modified proteomes. *Proteomics* **15:** 844–61

Scott JD, Fischer EH, Demaille JG & Krebs EG (1985) Identification of an inhibitory region of the heat-stable protein inhibitor of the cAMP-dependent protein kinase. *Proc. Natl. Acad. Sci. U. S. A.* **82:** 4379–83

Shabb JB (2001) Physiological substrates of cAMP-dependent protein kinase. *Chem. Rev.* **101:** 2381–411

Shao D & Lazar MA (1999) Modulating nuclear receptor function: may the phos be with you. *J. Clin. Invest.* **103:** 1617–8

Shevchenko A, Tomas H, Havli\[sbreve] J, Olsen J V & Mann M (2007) In-gel digestion for mass spectrometric characterization of proteins and proteomes. *Nat. Protoc.* **1:** 2856–2860

Shi Y, Chen X, Elsasser S, Stocks BB, Tian G, Lee B-H, Shi Y, Zhang N, de Poot SAH, Tuebing F, Sun S, Vannoy J, Tarasov SG, Engen JR, Finley D & Walters KJ (2016)

Rpn1 provides adjacent receptor sites for substrate binding and deubiquitination by the proteasome. *Science* **351:**

Short JM, Wynshaw-Boris A, Short HP & Hanson RW (1986) Characterization of the phosphoenolpyruvate carboxykinase (GTP) promoter-regulatory region. II. Identification of cAMP and glucocorticoid regulatory domains. *J. Biol. Chem.* **261:** 9721–6

Sigismund S, Argenzio E, Tosoni D, Cavallaro E, Polo S & Di Fiore PP (2008) Clathrin-mediated internalization is essential for sustained EGFR signaling but dispensable for degradation. *Dev. Cell* **15:** 209–19

Simpson ER & Waterman MR (1988) Regulation of the synthesis of steroidogenic enzymes in adrenal cortical cells by ACTH. *Annu. Rev. Physiol.* **50:** 427–40

Siow NL, Choi RCY, Cheng AWM, Jiang JXS, Wan DCC, Zhu SQ & Tsim KWK (2002) A cyclic AMP-dependent pathway regulates the expression of acetylcholinesterase during myogenic differentiation of C2C12 cells. *J. Biol. Chem.* **277:** 36129–36

Skalhegg BS & Tasken K (2000) Specificity in the cAMP/PKA signaling pathway. Differential expression,regulation, and subcellular localization of subunits of PKA. *Front. Biosci.* **5:** D678–93

Skroblin P, Grossmann S, Schäfer G, Rosenthal W & Klussmann E (2010) Mechanisms of protein kinase A anchoring. *Int. Rev. Cell Mol. Biol.* **283:** 235–330

Soderling SH, Binns KL, Wayman GA, Davee SM, Ong SH, Pawson T & Scott JD (2002) The WRP component of the WAVE-1 complex attenuates Rac-mediated signalling. *Nat. Cell Biol.* **4:** 970–5

Solberg R, Sandberg M, Natarajan V, Torjesen PA, Hansson V, Jahnsen T & Taskén K (1997) The human gene for the regulatory subunit RI alpha of cyclic adenosine 3', 5'-monophosphate-dependent protein kinase: two distinct promoters provide differential regulation of alternately spliced messenger ribonucleic acids. *Endocrinology* **138:** 169–81

Song L & Rape M (2010) Regulated degradation of spindle assembly factors by the anaphase-promoting complex. *Mol. Cell* **38:** 369–82

Songyang Z, Blechner S, Hoagland N, Hoekstra MF, Piwnica-Worms H & Cantley LC (1994) Use of an oriented peptide library to determine the optimal substrates of protein kinases. *Curr. Biol.* **4:** 973–82

Steegborn C, Litvin TN, Levin LR, Buck J & Wu H (2005) Bicarbonate activation of adenylyl cyclase via promotion of catalytic active site closure and metal recruitment. *Nat. Struct. Mol. Biol.* **12:** 32–7

Stefan E, Wiesner B, Baillie GS, Mollajew R, Henn V, Lorenz D, Furkert J, Santamaria K, Nedvetsky P, Hundsrucker C, Beyermann M, Krause E, Pohl P, Gall I, MacIntyre AN, Bachmann S, Houslay MD, Rosenthal W & Klussmann E (2007) Compartmentalization of cAMP-dependent signaling by phosphodiesterase-4D is involved in the regulation of vasopressin-mediated water reabsorption in renal principal cells. *J. Am. Soc. Nephrol.* **18:** 199–212

Steichen JM, Iyer GH, Li S, Saldanha SA, Deal MS, Woods VL & Taylor SS (2010) Global consequences of activation loop phosphorylation on protein kinase A. *J. Biol. Chem.* **285:** 3825–32

Steichen JM, Kuchinskas M, Keshwani MM, Yang J, Adams JA & Taylor SS (2012) Structural basis for the regulation of protein kinase A by activation loop phosphorylation. *J. Biol. Chem.* **287:** 14672–80

Steinberg RA & Agard DA (1981a) Turnover of regulatory subunit of cyclic AMP-dependent protein kinase in S49 mouse lymphoma cells. Regulation by catalytic subunit and analogs of cyclic AMP. *J. Biol. Chem.* **256:** 10731–4

Steinberg RA & Agard DA (1981b) Studies on the phosphorylation and synthesis of type I regulatory subunit of cyclic AMP-dependent protein kinase in intact S49 mouse lymphoma cells. *J. Biol. Chem.* **256:** 11356–64

Stenmark H, Parton RG, Steele-Mortimer O, Lütcke A, Gruenberg J & Zerial M (1994) Inhibition of rab5 GTPase activity stimulates membrane fusion in endocytosis. *EMBO J.* **13:** 1287–96

Stolz A, Ernst A & Dikic I (2014) Cargo recognition and trafficking in selective autophagy. *Nat. Cell Biol.* **16:** 495–501

Strausberg RL, Feingold EA, Grouse LH, Derge JG, Klausner RD, Collins FS, Wagner L, Shenmen CM, Schuler GD, Altschul SF, Zeeberg B, Buetow KH, Schaefer CF, Bhat NK, Hopkins RF, Jordan H, Moore T, Max SI, Wang J, Hsieh F, et al (2002) Generation and initial analysis of more than 15,000 full-length human and mouse cDNA sequences. *Proc. Natl. Acad. Sci. U. S. A.* **99:** 16899–903

Sunahara RK & Taussig R (2002) Isoforms of mammalian adenylyl cyclase: multiplicities of signaling. *Mol. Interv.* **2:** 168–84

Sury MD, McShane E, Hernandez-Miranda LR, Birchmeier C & Selbach M (2015) Quantitative proteomics reveals dynamic interaction of c-Jun N-terminal kinase (JNK) with RNA transport granule proteins splicing factor proline- and glutamine-rich (Sfpq) and non-POU domain-containing octamer-binding protein (Nono) during neuronal differ. *Mol. Cell. Proteomics* **14:** 50–65

Sutherland EW & Rall TW (1958) Fractionation and characterization of a cyclic adenine ribonucleotide formed by tissue particles. *J. Biol. Chem.* **232:** 1077–91

Sweatt JD & Kandel ER (1989) Persistent and transcriptionally-dependent increase in protein phosphorylation in long-term facilitation of Aplysia sensory neurons. *Nature* **339:** 51–4

Taelman VF, Dobrowolski R, Plouhinec J-L, Fuentealba LC, Vorwald PP, Gumper I, Sabatini DD & De Robertis EM (2010) Wnt signaling requires sequestration of glycogen synthase kinase 3 inside multivesicular endosomes. *Cell* **143:** 1136–48

Tan JMM, Wong ESP, Kirkpatrick DS, Pletnikova O, Ko HS, Tay S-P, Ho MWL, Troncoso J, Gygi SP, Lee MK, Dawson VL, Dawson TM & Lim K-L (2008) Lysine 63-linked ubiquitination promotes the formation and autophagic clearance of protein inclusions

associated with neurodegenerative diseases. *Hum. Mol. Genet.* **17:** 431–9

Tanaka K, Waxman L & Goldberg AL (1983) ATP serves two distinct roles in protein degradation in reticulocytes, one requiring and one independent of ubiquitin. *J. Cell Biol.* **96:** 1580–5

Tang WJ & Gilman AG (1991) Type-specific regulation of adenylyl cyclase by G protein beta gamma subunits. *Science* **254:** 1500–3

Taylor SS, Ilouz R, Zhang P & Kornev AP (2012) Assembly of allosteric macromolecular switches: lessons from PKA. *Nat. Rev. Mol. Cell Biol.* **13:** 646–58

Tcherkezian J & Lamarche-Vane N (2007) Current knowledge of the large RhoGAP family of proteins. *Biol. Cell* **99:** 67–86

Teglund S & Toftgård R (2010) Hedgehog beyond medulloblastoma and basal cell carcinoma. *Biochim. Biophys. Acta* **1805:** 181–208

Teis D, Saksena S & Emr SD (2008) Ordered assembly of the ESCRT-III complex on endosomes is required to sequester cargo during MVB formation. *Dev. Cell* **15:** 578–89

Tempé D, Casas M, Karaz S, Blanchet-Tournier M-F & Concordet J-P (2006) Multisite protein kinase A and glycogen synthase kinase 3beta phosphorylation leads to Gli3 ubiquitination by SCFbetaTrCP. *Mol. Cell. Biol.* **26:** 4316–26

Theurkauf WE & Vallee RB (1982) Molecular characterization of the cAMP-dependent protein kinase bound to microtubule-associated protein 2. *J. Biol. Chem.* **257:** 3284–90

Thiele CJ (1998) Neuroblastoma Cell Lines

Thorne C, Eccles RL, Coulson JM, Urbé S & Clague MJ (2011) Isoform-specific localization of the deubiquitinase USP33 to the Golgi apparatus. *Traffic* **12:** 1563–74

Thorslund T, Ripplinger A, Hoffmann S, Wild T, Uckelmann M, Villumsen B, Narita T, Sixma TK, Choudhary C, Bekker-Jensen S & Mailand N (2015) Histone H1 couples initiation and amplification of ubiquitin signalling after DNA damage. *Nature* **527:** 389–93

Thrower JS, Hoffman L, Rechsteiner M & Pickart CM (2000) Recognition of the polyubiquitin proteolytic signal. *EMBO J.* **19:** 94–102

Tian L, Holmgren RA & Matouschek A (2005) A conserved processing mechanism regulates the activity of transcription factors Cubitus interruptus and NF-κB. *Nat. Struct. Mol. Biol.* **12:** 1045–1053

Tkachenko E, Sabouri-Ghomi M, Pertz O, Kim C, Gutierrez E, Machacek M, Groisman A, Danuser G & Ginsberg MH (2011) Protein kinase A governs a RhoA-RhoGDI protrusion-retraction pacemaker in migrating cells. *Nat. Cell Biol.* **13:** 660–7

Tokunaga F, Sakata S, Saeki Y, Satomi Y, Kirisako T, Kamei K, Nakagawa T, Kato M, Murata S, Yamaoka S, Yamamoto M, Akira S, Takao T, Tanaka K & Iwai K (2009) Involvement of linear polyubiquitylation of NEMO in NF-kappaB activation. *Nat. Cell Biol.* **11:** 123–32

Trotter KW, Fraser ID, Scott GK, Stutts MJ, Scott JD & Milgram SL (1999) Alternative splicing regulates the subcellular localization of A-kinase anchoring protein 18 isoforms. *J. Cell Biol.* **147:** 1481–92

Tukachinsky H, Lopez L V & Salic A (2010) A mechanism for vertebrate Hedgehog signaling: recruitment to cilia and dissociation of SuFu-Gli protein complexes. *J. Cell Biol.* **191:** 415–28

Tuson M, He M & Anderson K V. (2011) Protein kinase A acts at the basal body of the primary cilium to prevent Gli2 activation and ventralization of the mouse neural tube. *Development* **138:** 4921–4930

Ubersax JA & Ferrell JE (2007) Mechanisms of specificity in protein phosphorylation. *Nat. Rev. Mol. Cell Biol.* **8:** 530–41

Uhler MD, Chrivia JC & McKnight GS (1986) Evidence for a second isoform of the catalytic subunit of cAMP-dependent protein kinase. *J. Biol. Chem.* **261:** 15360–3

Uhler MD & McKnight GS (1987) Expression of cDNAs for two isoforms of the catalytic subunit of cAMP-dependent protein kinase. *J. Biol. Chem.* **262:** 15202–7

Ulbricht A & Höhfeld J (2013) Tension-induced autophagy: May the chaperone be with you. *Autophagy* **9:** 920–922

Urbé S, Liu H, Hayes SD, Heride C, Rigden DJ & Clague MJ (2012) Systematic survey of deubiquitinase localization identifies USP21 as a regulator of centrosome- and microtubule-associated functions. *Mol. Biol. Cell* **23:** 1095–103

Urbé S, Sachse M, Row PE, Preisinger C, Barr FA, Strous G, Klumperman J & Clague MJ (2003) The UIM domain of Hrs couples receptor sorting to vesicle formation. *J. Cell Sci.* **116:** 4169–79

Vallee RB, DiBartolomeis MJ & Theurkauf WE (1981) A protein kinase bound to the projection portion of MAP 2 (microtubule-associated protein 2). *J. Cell Biol.* **90:** 568–76

VanderLinden RT, Hemmis CW, Schmitt B, Ndoja A, Whitby FG, Robinson H, Cohen RE, Yao T & Hill CP (2015) Structural basis for the activation and inhibition of the UCH37 deubiquitylase. *Mol. Cell* **57:** 901–11

Vanhaesebroeck B, Guillermet-Guibert J, Graupera M & Bilanges B (2010) The emerging mechanisms of isoform-specific PI3K signalling. *Nat. Rev. Mol. Cell Biol.* **11:** 329–41

Vega FM & Ridley AJ (2008) Rho GTPases in cancer cell biology. *FEBS Lett.* **582:** 2093–101

Vijay-Kumar S, Bugg CE & Cook WJ (1987) Structure of ubiquitin refined at 1.8 A resolution. *J. Mol. Biol.* **194:** 531–44

Vina-Vilaseca A & Sorkin A (2010) Lysine 63-linked polyubiquitination of the dopamine transporter requires WW3 and WW4 domains of Nedd4-2 and UBE2D ubiquitin-conjugating enzymes. *J. Biol. Chem.* **285:** 7645–56

Vo N & Goodman RH (2001) CREB-binding protein and p300 in transcriptional regulation. *J. Biol. Chem.* **276:** 13505–8

Voges D, Zwickl P & Baumeister W (1999) The 26S proteasome: a molecular machine designed for controlled proteolysis. *Annu. Rev. Biochem.* **68:** 1015–68

Wadzinski BE, Wheat WH, Jaspers S, Peruski LF, Lickteig RL, Johnson GL & Klemm DJ (1993) Nuclear protein phosphatase 2A dephosphorylates protein kinase A-

phosphorylated CREB and regulates CREB transcriptional stimulation. *Mol. Cell. Biol.* **13:** 2822–34

Walsh DA, Perkins JP & Krebs EG (1968) An adenosine 3',5'-monophosphate-dependant protein kinase from rabbit skeletal muscle. *J. Biol. Chem.* **243:** 3763–5

Wang B, Fallon JF & Beachy PA (2000) Hedgehog-regulated processing of Gli3 produces an anterior/posterior repressor gradient in the developing vertebrate limb. *Cell* **100:** 423–34

Wang B & Li Y (2006) Evidence for the direct involvement of {beta}TrCP in Gli3 protein processing. *Proc. Natl. Acad. Sci. U. S. A.* **103:** 33–8

Wang G, Wang B & Jiang J (1999) Protein kinase A antagonizes Hedgehog signaling by regulating both the activator and repressor forms of Cubitus interruptus. *Genes Dev.* **13:** 2828–37

Wang J, Qian J, Hu Y, Kong X, Chen H, Shi Q, Jiang L, Wu C, Zou W, Chen Y, Xu J & Fang J-Y (2014) ArhGAP30 promotes p53 acetylation and function in colorectal cancer. *Nat. Commun.* **5:** 4735

Wartosch L, Bright NA & Luzio JP (2015) Lysosomes. *Curr. Biol.* **25:** R315–6

Wei Y, Yu L, Bowen J, Gorovsky MA & Allis CD (1999) Phosphorylation of histone H3 is required for proper chromosome condensation and segregation. *Cell* **97:** 99–109

Weinstein LS, Shenker A, Gejman P V, Merino MJ, Friedman E & Spiegel AM (1991) Activating mutations of the stimulatory G protein in the McCune-Albright syndrome. *N. Engl. J. Med.* **325:** 1688–95

Wen W, Taylor SS & Meinkoth JL (1995) The expression and intracellular distribution of the heat-stable protein kinase inhibitor is cell cycle regulated. *J. Biol. Chem.* **270:** 2041–6

Wenzel DM, Lissounov A, Brzovic PS & Klevit RE (2011) UBCH7 reactivity profile reveals parkin and HHARI to be RING/HECT hybrids. *Nature* **474:** 105–8

Wessel D & Flügge UI (1984) A method for the quantitative recovery of protein in dilute solution in the presence of detergents and lipids. *Anal. Biochem.* **138:** 141–3

Westphal RS, Soderling SH, Alto NM, Langeberg LK & Scott JD (2000) Scar/WAVE-1, a Wiskott-Aldrich syndrome protein, assembles an actin-associated multi-kinase scaffold. *EMBO J.* **19:** 4589–600

Wiborg O, Pedersen MS, Wind A, Berglund LE, Marcker KA & Vuust J (1985) The human ubiquitin multigene family: some genes contain multiple directly repeated ubiquitin coding sequences. *EMBO J.* **4:** 755–9

Williams RL & Urbé S (2007) The emerging shape of the ESCRT machinery. *Nat. Rev. Mol. Cell Biol.* **8:** 355–68

Williamson A, Wickliffe KE, Mellone BG, Song L, Karpen GH & Rape M (2009) Identification of a physiological E2 module for the human anaphase-promoting complex. *Proc. Natl. Acad. Sci. U. S. A.* **106:** 18213–8

Winklhofer KF (2014) Parkin and mitochondrial quality control: toward assembling the puzzle. *Trends Cell Biol.* **24:** 332–41

Winter B, Braun T & Arnold HH (1993) cAMP-dependent protein kinase represses myogenic differentiation and the activity of the muscle-specific helix-loop-helix transcription factors Myf-5 and MyoD. *J. Biol. Chem.* **268:** 9869–78

Wollert T & Hurley JH (2010) Molecular mechanism of multivesicular body biogenesis by ESCRT complexes. *Nature* **464:** 864–9

Wollert T, Wunder C, Lippincott-Schwartz J & Hurley JH (2009) Membrane scission by the ESCRT-III complex. *Nature* **458:** 172–7

Wong W & Scott JD (2004) AKAP signalling complexes: focal points in space and time. *Nat. Rev. Mol. Cell Biol.* **5:** 959–70

Wu D & Pan W (2010) GSK3: a multifaceted kinase in Wnt signaling. *Trends Biochem. Sci.* **35:** 161–168

Wu G, Huang H, Garcia Abreu J & He X (2009) Inhibition of GSK3 phosphorylation of beta-catenin via phosphorylated PPPSPXS motifs of Wnt coreceptor LRP6. *PLoS One* **4:** e4926

Xia R, Jia H, Fan J, Liu Y & Jia J (2012) USP8 promotes smoothened signaling by preventing its ubiquitination and changing its subcellular localization. *PLoS Biol.* **10:** e1001238

Xu J, Zhou X, Wang J, Li Z, Kong X, Qian J, Hu Y & Fang J-Y (2013) RhoGAPs attenuate cell proliferation by direct interaction with p53 tetramerization domain. *Cell Rep.* **3:** 1526–38

Yang Z & Klionsky DJ (2010) Eaten alive: a history of macroautophagy. *Nat. Cell Biol.* **12:** 814–22

Yao T & Cohen RE (2002) A cryptic protease couples deubiquitination and degradation by the proteasome. *Nature* **419:** 403–7

Yonemoto W, McGlone ML & Taylor SS (1993) N-myristylation of the catalytic subunit of cAMP-dependent protein kinase conveys structural stability. *J. Biol. Chem.* **268:** 2348–52

Yoshimori T, Yamamoto A, Moriyama Y, Futai M & Tashiro Y (1991) Bafilomycin A1, a specific inhibitor of vacuolar-type H(+)-ATPase, inhibits acidification and protein degradation in lysosomes of cultured cells. *J. Biol. Chem.* **266:** 17707–12

Yu F-X, Zhang Y, Park HW, Jewell JL, Chen Q, Deng Y, Pan D, Taylor SS, Lai Z-C & Guan K-L (2013) Protein kinase A activates the Hippo pathway to modulate cell proliferation and differentiation. *Genes Dev.* **27:** 1223–32

Yu P, Chen Y, Tagle DA & Cai T (2002) PJA1, encoding a RING-H2 finger ubiquitin ligase, is a novel human X chromosome gene abundantly expressed in brain. *Genomics* **79:** 869–74

Yuan W-C, Lee Y-R, Lin S-Y, Chang L-Y, Tan YP, Hung C-C, Kuo J-C, Liu C-H, Lin M-Y, Xu M, Chen ZJ & Chen R-H (2014) K33-Linked Polyubiquitination of Coronin 7 by Cul3-KLHL20 Ubiquitin E3 Ligase Regulates Protein Trafficking. *Mol. Cell* **54:** 586–600

Yue S, Chen Y & Cheng SY (2009) Hedgehog signaling promotes the degradation of tumor

suppressor Sufu through the ubiquitin-proteasome pathway. *Oncogene* **28:** 492–9

Zaccolo M & Pozzan T (2002) Discrete microdomains with high concentration of cAMP in stimulated rat neonatal cardiac myocytes. *Science* **295:** 1711–5

Zamborlini A, Usami Y, Radoshitzky SR, Popova E, Palu G & Göttlinger H (2006) Release of autoinhibition converts ESCRT-III components into potent inhibitors of HIV-1 budding. *Proc. Natl. Acad. Sci. U. S. A.* **103:** 19140–5

Zhang F, Hu Y, Huang P, Toleman CA, Paterson AJ & Kudlow JE (2007) Proteasome function is regulated by cyclic AMP-dependent protein kinase through phosphorylation of Rpt6. *J. Biol. Chem.* **282:** 22460–71

Zhang P, Smith-Nguyen E V, Keshwani MM, Deal MS, Kornev AP & Taylor SS (2012) Structure and allostery of the PKA RIIβ tetrameric holoenzyme. *Science* **335:** 712–6

Zhong H, SuYang H, Erdjument-Bromage H, Tempst P & Ghosh S (1997) The transcriptional activity of NF-kappaB is regulated by the IkappaB-associated PKAc subunit through a cyclic AMP-independent mechanism. *Cell* **89:** 413–24

Zimmermann B, Chiorini JA, Ma Y, Kotin RM & Herberg FW (1999) PrKX is a novel catalytic subunit of the cAMP-dependent protein kinase regulated by the regulatory subunit type I. *J. Biol. Chem.* **274:** 5370–8

Zippin JH, Farrell J, Huron D, Kamenetsky M, Hess KC, Fischman DA, Levin LR & Buck J (2004) Bicarbonate-responsive 'soluble' adenylyl cyclase defines a nuclear cAMP microdomain. *J. Cell Biol.* **164:** 527–34